Development of the Zinc-Chlorine Battery for Utility Applications

EM-1051, Parts 1-3
Research Project 226-3

Interim Report, April 1979
Work Period January 1, 1977– March 31, 1978

Prepared by

ENERGY DEVELOPMENT ASSOCIATES
A Gulf + Western Company
1100 W. Whitcomb Avenue
Madison Heights, Michigan 48071

Prepared for

Electric Power Research Institute
3412 Hillview Avenue
Palo Alto, California 94304

EPRI Project Manager
J. Birk
Fossil Fuel and Advanced Systems Division

ORDERING INFORMATION

Requests for copies of this report should be directed to Research Reports Center (RRC), Box 10090, Palo Alto, CA 94303, (415) 961-9043. There is no charge for reports requested by EPRI member utilities and affiliates, contributing nonmembers, U.S. utility associations, U.S. government agencies (federal, state, and local), media, and foreign organizations with which EPRI has an information exchange agreement. On request, RRC will send a catalog of EPRI reports.

NOTICE

Prepared by
Energy Development Associates
Madison Heights, Michigan

ABSTRACT

The zinc-chlorine battery system is presently under development as a peak-shaving energy-storage device for the electric-utility industry. The technical feasibility of this battery system for the peak-shaving application was confirmed in an earlier program, RP226-1. A subsequent program, RP226-2, resulted in: (a) a successful demonstration of an 18-kWh breadboard system; and (b) preparation of two conceptual designs of a 100-MWh (20MW) zine-chlorine battery plant. Cost analyses for the two conceptual designs indicated that these battery plants, located at utility substations, would be highly competitive with combustion turbines from an electricity-cost standpoint. The two principal thrusts of this follow-on program, Phase I of RP226-3, were: (1) preparation and analysis of a new 100-MWh plant design; and (2) design, fabrication, and initial testing of a 45-Wh battery module--the basic unit of the new 100-MWh plant design. Development programs on electrode research, electrolyte optimization, cell design, battery-performance verification, and low-cost materials and processes were conducted in support of these objectives.

A new conceptual design of a 100-MWh battery plant located at a utility substation was prepared. This design, designated Mark 4, is based on the concept of fully-integrated zinc-chlorine hydrate battery modules, i.e. each module contains not only the battery stack but also chlorine-hydrate formation, storage, and decomposition equipment. The battery plant comprises thirty-six independent strings--each string consisting of 44 series-connected 66-kWh battery modules. A conceptual manufacturing plan for a production rate of 100 battery modules per day was prepared. The installed cost of the 100-MWh battery plant was estimated to be $26/kWh plus $91/kW (1977 $). The safety, environmental, and legal aspects of siting 100-MWh zinc-chlorine battery plants at substations in residential areas were also analyzed. The Mark 4 design is judged to be optimal in the areas of performance, safety, and manufacturability, while comparing favorably in cost and reliability to earlier designs.

The Mark 4 module prototype was designed, fabricated, assembled, and tested during Phase I. The 45-kWh module, which performed well as a system, delivered in excess of the design level for dc energy output. However, the efficiency, at 50%, was lower than the design target of 63%. The two major contributors to the reduced efficiency

have been identified. Both of these design-related problems will be addressed during the refurbishing of the battery module which is planned for Phase II of RP226-3.

The significant accomplishments in the development program during Phase I are as follows: (1) qualification of porous graphites--the chlorine-electrode material--and plastics which meet the cost criteria for commercialization; (2) development of an in-situ technique for chlorine-electrode activation which shortens the time required from ten or more days to a matter of hours; (3) invention of a dendrite-inhibiting additive which will result in higher-efficiency lower-cost battery stacks; (4) understanding the major cause of significant levels of hydrogen evolution in battery systems, e.g., the 18-kWh battery of RP226-2; and (5) demonstration of 500 charge-discharge cycles--20-25% of the commercialization target--on a 1.7-kWh system without performance deterioration.

EPRI PERSPECTIVE

PROJECT DESCRIPTION

EPRI, DOE and EDA are engaged in a closely coordinated major program to develop a zinc-chlorine battery for utility energy storage. The EPRI portion of this program is to provide the necessary technology base; the goal of the DOE-sponsored portion of the program is to design and construct a 5-MWh battery for BEST facility testing. The EPRI-sponsored work is covered in a 39-month, $7.6 million contract initiated in January, 1977; the costs are equally shared by EDA and EPRI. The DOE portion is covered in a separate 33-month, $11.5 million contract with EDA initiated in January, 1979. This report reviews progress of the EPRI-EDA contract for the period from January, 1977 through March, 1978.

PROJECT OBJECTIVE

The ultimate objective of this effort is the commercialization of battery energy storage systems for utility application. A major objective was to build and test a 45-kWh module. This module is the basic building block of a battery energy storage system. Further objectives were to develop the components and subsystems for this module. In addition, work to demonstrate cycle-life potential, to identify failure mechanisms, and to ascertain the economic viability of the technology has continued.

PROJECT RESULTS

The scale-up hardware from a 20-kWh breadboard system (late-1976) to a 45-kWh fully-integrated battery module (early-1978) was accomplished. However, the performance of the first 45-kWh module was low; energy efficiency was only about 50% compared to a design goal of 63%. This problem is receiving major attention in the present phase of the project. Recent results of cell tests suggest that the problem can be resolved. Four more 45-kWh modules will be tested in 1979. Performance of these will give us insight into the status of the technology and the likelihood of technical success.

Before a 5-kWh battery prototype can be fabricated and tested in the BEST facility, several questions need to be answered and some major problems remain to be solved.

These include the demonstration of (1) adequate performance and life using low-cost chlorine electrodes, (2) zinc electrodes having improved-capacity and greater reliability, and (3) reliable and durable 50-kWh battery modules. In addition, adequate safety of commercial battery systems must be assured, as these batteries may be sited at substations in residential areas. These needs are now being addressed as part of the DOE and EPRI programs at EDA.

The zinc-chlorine system continues to be a strong contender for use as an energy-storage system for electric utilities. However, problems continue to make this a difficult effort and commercial hardware is likely to be 5-10 years away.

James R. Birk, Project Manager
Fossil Fuel and Advanced Systems Division

ACKNOWLEDGMENTS

Energy Development Associates

P. Symons
C. Warde
P. Carr

F. Baker
H. Catherino
C. Chi
M. Hammond
G. Henriksen

H. Bjorkman
W. Coughlin
A. Laethem
A. Stein
C. Whittlesey

D. Aller
C. Blevins
A. Chu
C. Flenniken
P. Racenis
G. Sussman
P. Tylutki

Wayne State University

J. Jorné
J. Kim
D. Kralik

Purdue University

W. Leidenfrost
J. Loveley
B. Korenic

CONTENTS

SUMMARY

In the last five years, battery systems have been under intensive review as potential peak-shaving devices for the electric-utility industry. Storage of off-peak electric energy in batteries and the availability of this energy during periods of peak-power demand would permit more efficient utilization of baseload generating capacity. In common with other energy-storage options, batteries would confer substantial spinning-reserve and system-regulation benefits because of their operating characteristics. The modular construction of battery systems offers the prospect of locating these systems at utility substations in order to meet the specific needs of a local industrial, commercial, or residential market. In addition, peak-shaving battery systems would permit the conservation of natural gas or oil which would otherwise be consumed by turbine peaking units. A 1977 assessment by EPRI suggests that oil consumption in the U.S. would be reduced in the year 2000 by ten million to one-hundred million barrels per year for total installed capacities of 18-50GW.

Since mid-1974, Energy Development Associates (EDA) and the Electric Power Research Institute (EPRI) have jointly funded a research, development, and engineering program at EDA to develop a zinc-chlorine hydrate battery for utility peak-shaving. The technical feasibility of the zinc-chlorine battery system was demonstrated in RP226-1. Successful scale-up from the 1kWh level to a 18kWh system was achieved in RP226-2, in which the economic attractiveness of the zinc-chlorine system was also analyzed. This report presents the work performed in the first fifteen months -- Phase I -- of a thirty-nine month, three-phase program, designated RP226-3. The major objective of this program was to provide a background of research, development, and engineering activities for an additional program which was negotiated during 1977-78, which would lead to the design, fabrication, installation, and testing of a zinc-chlorine battery system in the Battery Energy Storage Test (BEST) Facility in the early 1980's. Expenditures during the Phase I segment of the program were $2,400,000, with EDA and EPRI each supplying 50% of the total.

CONCEPTUAL DESIGNS OF A 100MWh ZINC-CHLORINE BATTERY PLANT, considered to be a typical size in ultimate utility use, have been prepared and analyzed in each phase of the EPRI-EDA program. This was done in order to ensure the relevance of the concurrent development programs and battery scale-up activities. EPRI has indicated that three primary criteria must be met in order for a 100MWh battery plant to be acceptable to the electric-utility industry. These criteria are:

- Installed cost: <$25/kWh + $75/kW (1977 $)
- Overall plant efficiency: >65% (ac to ac)
- Minimum siting restrictions

Feedback from electric-utility, EPRI, and U.S. Department of Energy (DoE) representatives, as well as internal EDA studies indicated that earlier plant designs could be criticized on all three grounds. To meet these criticisms, a design was proposed which was based on the use of a smaller battery module. An artist's rendition of this design, designated Mark 4, is shown in Figure 1. The battery portion of the plant consists of thirty-six racks -- each rack containing forty-four 66kWh modules. To simplify busing, a pair of racks are connected to form two electrical strings. Thus, there are thirty-six 2.9MWh dc strings in the battery plant, each with its individual disconnect. The associated power-conditioning and refrigeration subsystem are shown in the background.

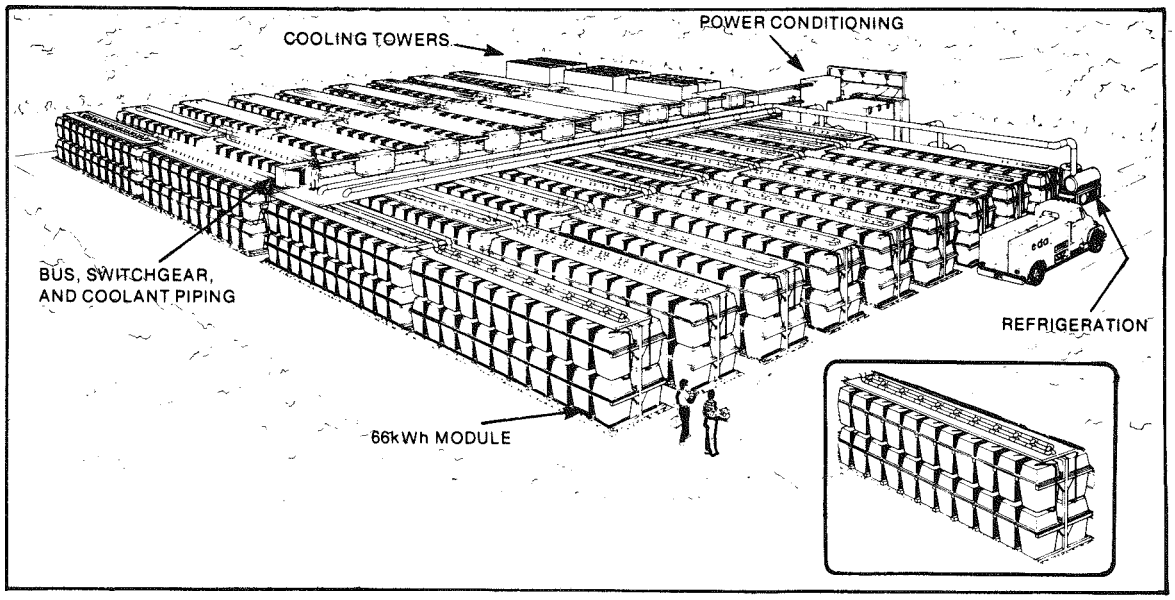

Figure 1. Mark 4 100MWh, 20MW zinc-chlorine peak-shaving battery plant. The plant comprises 1584 battery modules on thirty-six 44-module racks, one of which is shown inset.

For costing purposes, a semi-mature market was assumed, i.e. a production rate of 100 modules per day corresponding to approximately sixteen 100MWh battery plants per year. A conceptual manufacturing plan was prepared, for which the material, labor, and capital equipment required for each step in module assembly were estimated. The important components for a cost standpoint were: porous graphite for chlorine electrodes; electrolyte and gas pumps; heat exchangers; and the case components. The costing was forced so that the resultant costs would approximate to the cost targets. This exercise is useful as it established cost targets for the components and provides guidance for the development program. For the yearly production of 25,000 modules the projected sales were $41 million dollars, corresponding to a selling price of approximately $26/kWh. Balance of plant costs, i.e. for refrigeration, power-conditioning, and installation, were shown to lie at approximately $91/kW. These installed costs are compatible with a bus-bar electricity cost of 50-60 mills/kWh provided spinning-reserve, system-regulation, and transmission credits of $75/kW are assumed.

The overall energy efficiency of the 100MWh battery plant has been projected to be 70%. The electrochemical energy efficiency of the module is expected to lie just above 79%. The difference between these numbers is attributable to the electric energy inputs required to operate the system. In decreasing order of importance, these are: refrigeration, power conditioning, and the module electrolyte and gas pumps.

Successful commercialization of peak-shaving battery plants will hinge ultimately on meeting stringent safety and environmental-impact criteria. For the zinc-chlorine system, these criteria revolve mainly around the question of accidental release and dispersion of toxic amounts of chlorine, the only potential hazard. Chlorine storage in the battery module during charge is based on the formation of solid chlorine hydrate, which decomposes only slowly above 9.6°C. Each battery module contains a maximum of 100 lb of chlorine as hydrate. Credible accident scenarios have been developed and analyzed at EDA in terms of causes, human hazards, atmospheric dispersion, and possible clean-up operations. Even after a worst-case accident and under worst-case meteorological conditions, hazardous levels of chlorine, 50ppm or greater, extend a maximum of 50 feet from the site of the chlorine release. Experimental verification of these analyses is currently underway at the Factory Mutual Research Corporation under a joint contract awarded by DoE and EPRI. From these and similar studies, EDA has concluded that with proper design the zinc-chlorine peak-shaving battery plant will pose negligible health or environment hazards at a substation location in a residential area.

THE MARK 4 MODULE PROTOTYPE was designed, fabricated, assembled, and tested during Phase I. The principal design goals were to deliver 45kWh at an electrochemical energy efficiency of 63%. An exploded view of this module is shown in Figure 2(a). There are three compartments in the module. The uppermost compartment, i.e. above the separator plate, is termed the stack compartment. Located in this compartment are six ten-cell batteries, entitled submodules. There are three tiers with two batteries per tier. The electrolyte pump sits in the sump compartment, shown on the lower right. This pump is magnetically coupled to a motor attached to the outside of the module case. In the store compartment, located on the lower left, chlorine hydrate is formed during charge, stored, and decomposed during discharge. The hardware necessary for these functions comprises two heat exchangers, HX-1 and HX-2, a filter, and a gas pump, which is also magnetically coupled to a motor outside the case. A photograph of the fully-assembled module is shown in Figure 2(b).

In March 1978, the module was tested through ten consecutive charge-discharge cycles, as required by contract. The design target of 45kWh was exceeded in two cycles, while the average delivered energy was 43kWh. However, the electrochemical energy efficiency at ∿50% was below the design target of 63%. The major contributor to this shortfall was the coulombic efficiency which averaged 59%, a full 14% below the design level of 73%. The principal causes of the unexpectedly low coulombic efficiency were:

- Stack Pressure: Excessive heat transfer from the sump to the store caused hydrate decomposition during change. The additional chlorine thus generated taxed the capability of the gas pump to maintain the desired pressure level in the stack compartment. The net effect was a calculated 5-7% loss in coulombic efficiency.

- Zinc Growths: Substantial coulombic-efficiency penalties were incurred in the submodule because of the growth of zinc dendrites around or below the intercell bus bar. Upon elimination of the problem, the coulombic and electrochemical energy efficiencies have been shown to lie at 67% and 79%, respectively.

EDA plans to refurbish the 45kWh module during Phase II. The electrolyte sump compartment will be located directly above the store compartment to minimize heat transfer. Extensive modification of the submodules is also planned in order to minimize intercell dendriting and contact losses.

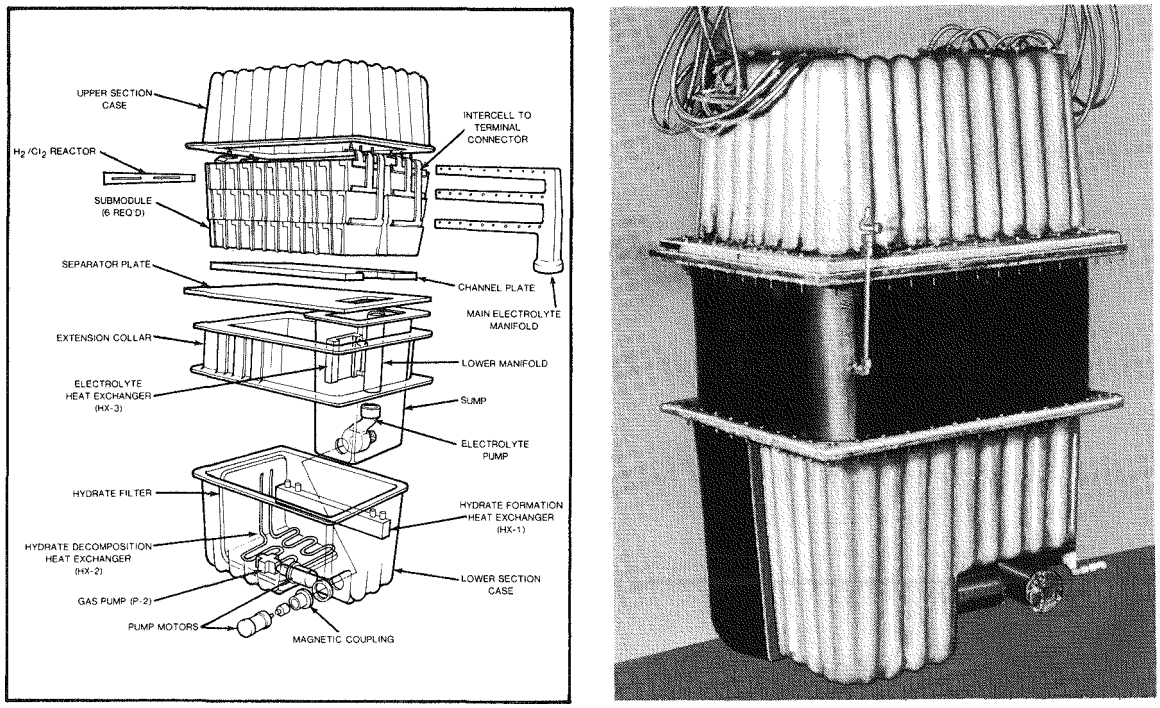

(a) (b)

Figure 2. The Mark 4 module prototype: (a) exploded view showing the major components; and (b) photograph of the assembled module showing the six sets of terminals -- one set per submodule -- and the pump motors attached to the outside of the case.

RESEARCH AND DEVELOPMENT PROGRAMS during Phase I concentrated on the battery stack, which not only determines module efficiency but also dominates the materials and assembly costs. The present cell design is based on the use of electrodes which are 10cm in height and 6cm in width. In the 45kWh module, there are approximately 30 zinc-electrode substrates and 60 chlorine-electrode substrates per kilowatt-hour. During Phase I, the technical feasibility of increasing the width and height was investigated in order to significantly reduce the number of electrode pieces required per kilowatt-hour. The objective of this size increase is to lower fabrication and assembly costs. Modeling studies (followed by experimental verification of the model) suggest that doubling of the present cell width is practical, but that increases significantly greater than a factor of two would provoke formation of undesirable zinc growths on the chlorine-bus side of the electrode. A parallel investigation into the effect of cell height on efficiency suggests that a doubling of the cell height may also be accomplished in future designs without penalty.

In mid-1977, there was a breakthrough in the activation of porous-graphite chlorine electrodes. Up to that time, activation of porous graphite was accomplished by boiling electrodes in concentrated nitric acid. Treatments of 10-13 days were required in order to ensure that the voltaic efficiency of cells containing these electrodes would be acceptable, i.e. at or above 85%. An electrolytic treatment in dilute chloride solutions for a few hours was found to yield electrodes which were more active and stronger. Most importantly, in-situ activation of the porous-graphite chlorine electrode was now possible. Successful scale-up to the 0.75kWh cell level was accomplished during Phase I. A ten-cell submodule was successfully activated by the electrolytic technique early in Phase II of RP226-3.

Four additional major accomplishments of the Phase I development programs are:

- Hydrogen Evolution: Previous to Phase I, hydrogen formation on the zinc electrode had been an intermittent problem at EDA. Indeed, testing of the 20kWh battery of RP226-2 was significantly delayed by excessive hydrogen generation during charge and discharge. During Phase I, it was conclusively established that degradation products, resulting from the activation of the porous-graphite chlorine electrode, would provoke a significant amount of hydrogen generation. Thorough washing of the cell to eliminate these impurities was necessary to reduce the hydrogen-evolution rate to an acceptable level. This phenomenon is presently considered to have been responsible for the problems encountered with the 20kWh system.

- Low-Cost Porous Graphites: Union Carbide PG-60 is presently the porous graphite of choice for use as the chlorine-electrode material. The cost of PG-60 is $5.67/lb corresponding to approximately $20/kWh. At EDA's request, Airco Speer produced a modified grade of their commercial 37G material. The selling price of this grade, S-1029, will be similar to that of 37G, i.e. ∿$2/lb. EDA characterized the electrochemical properties of S-1029 during Phase I and found the material to be near optimal from a performance standpoint. At $2/lb, S-1029 will cost $5-7/kWh which is below the target set for porous graphite in the cost analysis for 100MWh battery plants.

- Low-Cost Plastics: Based on an extensive screening program conducted during RP226-1 and RP226-2, EDA qualified PVC formulations from two suppliers for use in chlorinated zinc chloride. The availability of these formulations will reduce plastic costs by approximately an order of magnitude. The screening program also uncovered a polyester formulation which has been qualified for use as a construction material for the module case.

- Battery Life: The average life of a battery module must exceed 10 years in commercial service. This life criterion corresponds to a requirement that the module undergo between 2,000 and 2,500 full charge-discharge cycles, i.e. five cycles per week for 40-50 weeks per year for 10 years. A 1.7kWh cell system, built and automated as part of RP226-2, has been under test since February 1976. Five-hundred cycles were accumulated on this system through the end of Phase I. There has been no measurable change in either electro-chemical energy efficiency or delivered energy through this period.

DEMONSTRATION OF ADVANCED BATTERY SYSTEMS IN UTILITY SERVICE is the objective of programs currently sponsored by EPRI and the U.S. Department of Energy (DoE). As part of one of these programs, the BEST Facility is presently under construction at Hillsborough, New Jersey. This facility, to be built and operated by Public Service Electricity and Gas of New Jersey (PSE&G) will be ready for use by early 1981. During Phase I, EDA submitted a proposal to DoE to place a zinc-chlorine hydrate battery system in this facility. In September 1978, DoE and Gulf + Western Industries, Inc. (G+W) signed a contract which will lead to the design, fabrication, and assembly of a 4.8MWh zinc-chlorine hydrate battery system. Testing of this battery system in the BEST Facility will occur in the first half of 1981. The total value of the contract, which will be formally started in January 1979, is $11,500,000. Of this total, G+W will provide approximately $1,700,000.

Figure 3 shows the 4.8MWh zinc-chlorine hydrate battery system in Bay #2 of the BEST Facility. The battery system consists of two racks -- each with 44 modules -- and a refrigeration subsystem located outside the bay. Shown also are two chlorine scrubbers, which will be operated only in the unlikely event of module rupture and release of gaseous chlorine. The 4.8MWh zinc-chlorine hydrate battery system will be turned over to PSE&G personnel in mid-1981. A successful demonstration of zinc-chlorine hydrate battery technology at the BEST Facility is expected to lead to the commissioning of a 100MWh demonstration plant in the 1982-5 time frame.

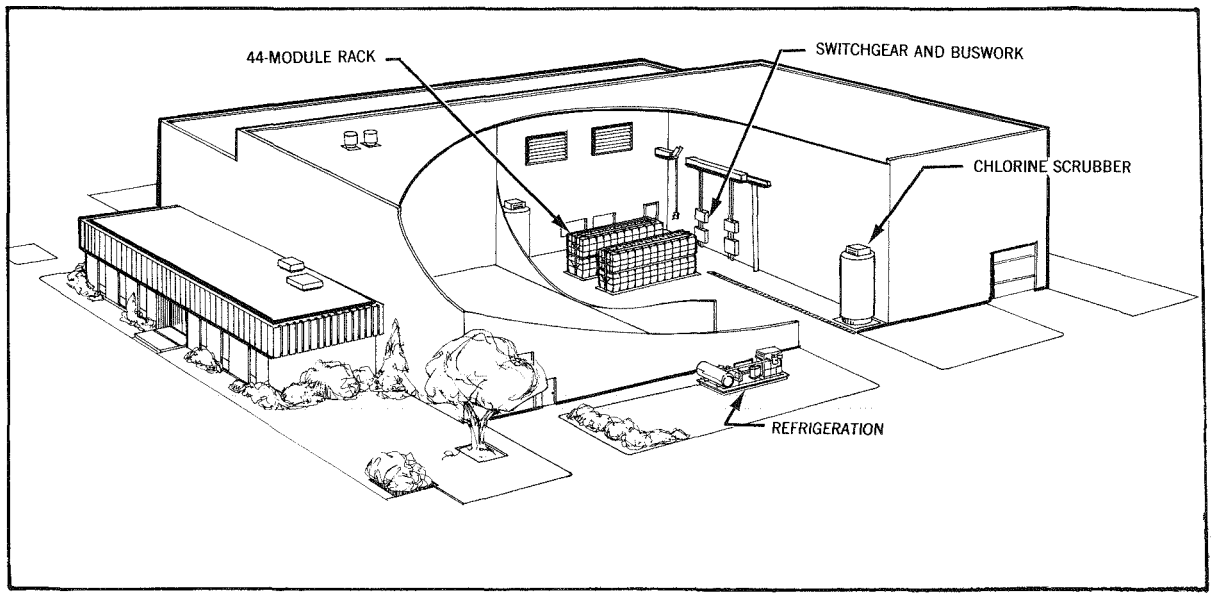

Figure 3. The 4.8MWh zinc-chlorine hydrate battery system in Bay #2 of the Battery Energy Storage Test (BEST) Facility in mid-1981. The system consists of two 44-module battery racks and a refrigeration subsystem.

PART I

INTRODUCTION

Section 1

INTRODUCTION TO PHASE I PROGRAMS OF RP226-3

Since mid-1974, Energy Development Associates (EDA) and the Electric Power Research Institute (EPRI) have jointly funded a research development and engineering program at EDA to develop the zinc-chlorine battery for utility peak-shaving. This is the third in a series of reports describing the progress and problems of this program. Earlier reports have described work performed on RP226-1 and RP226-2 (1-1, 1-2). This report presents the work performed in the first fifteen months -- Phase I -- of a thirty-nine month three-phase program, designated RP226-3. In this introduction, the major accomplishments of RP226-1 and RP226-2 are briefly reviewed, and the work performed in Phase I of RP226-3 is introduced against this background.

RP226-1

In mid-1974, the Electric Power Research Institute (EPRI) and Energy Development Associates (EDA) co-funded a program designated RP226-1 to explore the potential of the zinc-chlorine hydrate battery for utility peak-shaving. EDA designed and built a 1kWh battery system, while EPRI provided the funding for battery testing. The twin objectives of this program were the attainment of an electrochemical efficiency of 70% and the demonstration of stable performance over one-hundred consecutive charge-discharge cycles. Among the more important aspects of the design and operation of this system were the use of ruthenia-catalyzed porous-titanium chlorine electrodes and chlorine desorption from the electrolyte during charge. This latter feature was of considerable importance in minimizing the corrosion of electrodepositing zinc by chlorine dissolved in the electrolyte. Under test, the 1kWh system displayed an electrochemical efficiency of 74.6% ± 1.0%. The performance of the system was stable over the one-hundred cycles required by contract. This work, concluded in December, 1975, has been described in detail in an earlier report (1-1). An independent evaluation of the work by Stanford Research Institute, funded by EPRI under RP370, concluded that the testing was objective and that the reported results were accurate.

In October, 1975, EPRI funded a seven-month study, designated RP226-1-2, directed toward the preparation of a design and a detailed cost analysis of 100MWh zinc-chlorine peak-shaving battery plants. This peak-shaving plant design, designated Mark 2, was based on a preliminary Mark 1 design, used for discussion with EPRI and electric-utility representatives. A description of the Mark 2 design is provided in Part II - Section 4 and elsewhere (1-3), while much greater detail is provided in an earlier report (1-2). This study concluded that the Mark 2 design could meet the cost, performance, and siting criteria developed by EPRI for peak-shaving battery plants. However, chlorine desorption from the electrolyte, as accomplished during operation of the 1kWh system, was revealed by analysis to be impractical because of cost considerations. Further, serious questions were raised as to the operability of the battery system and the significant energy penalty for desorber operation if this technique were employed.

RP226-2

In calendar 1976, EDA conducted a follow-on program designated RP226-2. This program was jointly funded by EPRI and EDA for a total cost of $1,100,000. There were four major objectives: firstly, the automation of the 1kWh system to demonstrate that it could operate in the unattended mode; secondly, the construction and test of two battery systems, sized at approximately 2kWh, in order to permit the making of an informed choice between ruthenia-catalyzed porous-titanium and porous-graphite as a chlorine electrode material; thirdly, the design, assembly, and testing of a 20kWh, 20V battery system, based on the results of the testing of the two ∿2kWh systems; and finally, preparation of an update, in late 1976, of the Mark 2 design and cost analysis, based on the technology improvements in the previous twelve months.

The automation of the 1kWh system ran into immediate difficulties. Because of the abandonment of the chlorine-desorption technique, based on the results of the design and cost study, the electrochemical energy efficiency of the system decreased to ∿60%. A cell-development program was initiated to find a new set of operating conditions in order to recover battery capacity and electrochemical energy efficiency. The system was redesigned and then automated. With the redesign and a new cycling routine, the delivered energy was increased to 1.4kWh. Simultaneously, the electrochemical energy efficiency was raised to approximately 67%. Two additional systems -- a 1.7kWh, 2V system with porous-graphite chlorine electrodes and a 2kWh, 4V system with ruthenia-catalyzed porous-titanium chlorine electrodes -- were also designed, built, and tested to facilitate selection of the chlorine-electrode substrate

material for the 20kWh system. In August, 1976, porous graphite was chosen for the following four reasons: a) the probability of meeting the desired cost target of $5-10/kWh for the chlorine electrodes in a 100MWh battery system was much higher for porous graphite; b) the voltaic-efficiency advantage offered by ruthenia-catalyzed porous-titanium electrodes was significantly reduced during 1976 by the development of improved activation techniques for porous-graphite electrodes; c) operational experience with the 1.4kWh and 1.7kWh systems indicated that a system with ruthenia-catalyzed porous-titanium chlorine electrodes would be more difficult to control effectively because of the sensitivity of cell performance to changes in electrolyte pH; and d) a battery with porous-graphite chlorine electrodes would be intrinsically safer in malfunction, because of the higher hydrogen overpotential of graphite.

A 20kWh, 20V battery system was designed, assembled, and tested in the last third of 1976. The battery stack and the chlorine-hydrate former/store performed to specification in December, 1976. However, excessive hydrogen evolution in the stack during discharge, attributable to electrolyte contamination, delayed coupling of stack and store to form a complete battery system. Following elimination of the contamination problem, the battery ran smoothly as a system in February, 1977. At this point, further delays were caused by a dendrite problem which reduced battery capacity. Finally, ten sequential cycles were taken during May, 1977. The average delivered energy was 15kWh while the average electrochemical efficiency was 60%. An eleventh cycle yielded a delivered energy of 18kWh with the same electrochemical energy efficiency.

A new design of the ultimate 100MWh utility peak-shaving plant, designated Mark 3, was prepared in late 1976. The battery stack modules, each 6MWh, were larger than the 1MWh battery stack modules in the Mark 2 design. However, the single underground chlorine-hydrate store of the Mark 2 design was replaced by twenty-four above-grade stores in the Mark 3 design. The Mark 3 design is described briefly in Part II - Section 4 and elsewhere (1-3). A cost analysis for this design indicated that it would meet the cost criterion for acceptance by the electric-utility industry. All of the work performed on RP226-2 has been described in detail in an earlier report (1-2).

RP226-3

In January, 1977, EDA and EPRI agreed to jointly fund a thirty-nine month program, designated RP226-3. This program, involving total expenditures of $7,600,000, was in three phases: Phase I extending from January 1977 through March 1978; Phase II from

April 1978 through March 1979; and Phase III from April 1979 through March 1980. The major objective of this program was to provide a background of research, development, and engineering activities for an additional program, to be negotiated in 1977/78, which would lead to the design, fabrication, installation, and testing of a zinc-chlorine battery system in the Battery Energy Storage Test (BEST) Facility in the early 1980's.

In the first three months of 1977, three separate analyses helped fashion a major change in the EDA view of the optimum design for 100MWh battery plants. Firstly, the preparation of a design of a 6MWh zinc-chlorine battery system for the BEST Facility, based on the Mark 3 design, cast serious doubt that the 6MWh battery stack could be built even with sophisticated assembly-line techniques. This doubt was reinforced when a detailed design of a 125kWh battery stack, i.e. a segment of the battery module, was prepared and analyzed from the standpoint of fabrication problems. Based on both of these design efforts, it is concluded that the manufacture of 6MWh Mark 3 battery modules would be difficult and costly because of module size and the high packing density of cells. Secondly, an analysis of data for single cells, the 1.7kWh system, and the 20kWh system indicated that, at ambient pressure, electrochemical energy efficiencies in excess of 75% were not achievable in systems with porous-graphite chlorine electrodes. Consequently, overall power plant efficiencies would lie below 65% because of the energy consumed in rectification, inversion, and refrigeration, and by other system auxiliaries. Thirdly and most importantly, exposure of the Mark 3 design to electric-utility representatives led to criticism centered mainly on the safety and environmental aspects of these plants. The possibility that a single line rupture could lead to the release of twenty-five tons of gaseous chlorine, albeit slowly, led a number of representatives of the Florida utilities to declare that the negotiation of permits for siting the Mark 3 plants in residential areas might be difficult.

An elegant solution to these problems of manufacturability, efficiency, and safety was found by switching to a battery-plant design based on a much smaller battery module, sized at approximately 50kWh. In contrast to the Mark 2 and 3 designs, the Mark 4 battery module would contain the necessary equipment for hydrate formation, storage, and decomposition. Thus, this module would be fully integrated, with no interchange of chlorine or electrolyte between modules. Previous experience with a similar type and size of module in the EDA vehicle-battery program indicated strongly that this design was manufacturable. Further, because of the relatively small module size and the integration, in the same package, of battery stack and chlorine-hydrate

store, the battery stack, and consequently the electrolyte, could be held at an absolute pressure substantially below ambient. This in turn would significantly lower the solubility of chlorine in the electrolyte and thus, reduce the corrosion of zinc by dissolved chlorine. The net effect is to offer the prospect of a substantial improvement in coulombic efficiency, and thereby in electrochemical energy efficiency. In addition, as the vacuum in the stack compartment is generated by operation of the gas pump, required for hydrate formation during charge, there is little or no additional efficiency penalty associated with this mode of operation. Another major advantage of the Mark 4 design would be the dispersal of chlorine hydrate in a multiplicity of separate containers across the 100MWh plant. A single line or module rupture in the Mark 4 design would result in the slow release of up to 100 lbs of chlorine, contrasting very favorably with a value of 50,000 lbs for a similar accident scenario in the Mark 3 design.

The five major tasks and associated sub-tasks in the Phase I work statement are shown in Table 1-1. This report describes all of the work performed during Phase I of RP226-3. Because of its scope, the report is broken for ease of presentation into four parts: Part II -- 100MWh Zinc-Chlorine Peak-Shaving Battery Plants; Part III -- 45kWh-Module Design, Assembly, and Initial Testing; Part IV -- Cell and Battery Testing; Part V -- Development Programs. There are four appendices with each appendix being a pre-print or reprint of papers authored by EDA personnel or subcontractors.

Part II of this report is a comprehensive statement on 100MWh zinc-chlorine battery plants, located at utility substations in residential areas. Sections 5, 6, and 8 report work performed on plant design and costs (Sub-task 3.1). The equipment, processing, and labor required to manufacture the battery modules is presented in Section 7 (Sub-tasks 5.1 and 5.2). This treatment, which clearly establishes that module manufacture is essentially an assembly operation, is used as a basis for the cost analysis presented in Section 8. Sections 9, 10, and 11 deal with the safety, environmental, and legal aspects of the siting of 100MWh plants in residential areas (Sub-task 4.3). However, the quality and quantity of work performed and reported in these sections significantly exceeded the scope originally envisioned for Sub-task 4.3 in the work statement.

The design, assembly, and initial testing of the 45kWh battery module (Sub-task 2.1) is presented in Part III, i.e. Sections 13 through 21, of this report. This work was based on an earlier vehicle-battery program, jointly funded by EDA and the U.S. Department of Energy. Extensive modification of the vehicle module design was

Table 1-1

TASKS AND SUB-TASKS FOR PHASE I OF RP226-3

TASK NO. 1 -- 45kWh BATTERY DEVELOPMENT PROGRAM

1.1 Propose and Design 45kWh Battery System
1.2 Layout and Detail Stack, Store, and Auxiliaries

TASK NO. 2 -- 45kWh BATTERY FABRICATION AND TESTING

2.1 Secure Materials and Components; Build and Test Battery
2.2 Build and Test a Duplicate 45kWh Battery System

TASK NO. 3 -- 100MWh BATTERY DEVELOPMENT PROGRAM

3.1 Update Design and Costing of 100MWh Plant
3.2 Battery Component and Processes Development
3.3 Development of Improved Graphite Electrodes
3.4 Specification of Optimum Electrolyte

TASK NO. 4 -- ANALYSIS, TEST, AND EVALUATION PROGRAM

4.1 Materials Evaluation and Test
4.2 Cell and Battery Evaluation and Test
4.3 Siting Analysis

TASK NO. 5 -- PLANNING FOR MANUFACTURE

5.1 Preliminary Process and Quality Documentation
5.2 Incoming Materials Specification
5.3 Identification of Facilities Requirements for Phase II and III
5.4 Preliminary Pilot-Production Planning for Phase III

required, reflecting the greater emphasis on electrochemical energy efficiency in the peak-shaving application. These design modifications centered mainly around the use of water, rather than battery electrolyte, in the chlorine-hydrate store. Although some system problems were encountered, which reduced the electrochemical energy efficiency, 10 consecutive charge-discharge cycles were taken during the month of March 1978.

The results of cell and battery testing, other than for the 45kWh battery module, are presented in Part IV of this report (Sub-task 4.2). Further testing of the 20kWh system, built and tested initially as part of RP226-2, is reported in Section 23. Cycle-testing of the 1.4kWh and 1.7kWh systems continued during Phase I and the results are presented in Sections 25 and 26. The 1.7kWh system, built with porous-graphite chlorine electrodes had accumulated 500 charge-discharge cycles through early April, 1978. Cycle-testing of the 1.4kWh system, constructed with ruthenia-catalyzed porour-titanium chlorine electrodes, was terminated after cycle number 323 because of the failure of the hard-wired logic control system. Section 6 presents the testing results from single cells built during 1975, while Section 28 discusses a future program for the accelerated testing of porous-graphite chlorine electrodes, considered the life-limiting components in the battery stack. Instead of building a duplicate battery module, as called for in Sub-task 2.2, a test system for 8.3kWh submodules was designed and constructed so as to allow testing of the submodule under those conditions anticipated in battery-module operation. This work is reported in Section 24 of Part IV.

Part V of this report presents the results of research and development programs performed during Phase I. Sections 30 and 37 report on the specification of an electrolyte to maximize battery capacity and efficiency (Sub-task 3.4). Section 31 discusses the current-density distribution across the face of the zinc and chlorine electrodes during charge and discharge. The consequent variation in zinc-deposit thickness, and its implications for capacity-density limitation by dendrite formation on the zinc electrode adjacent to the chlorine-electrode bus, are presented in detail. An experimental study of the effect of the height of the electrode and the electrolyte static head is reported in Section 32. The results of a successful materials evaluation and test program (Sub-task 4.1) are presented in Section 33. Principal among the accomplishments of this program was the electrochemical qualification of two PVC formulations for use in the battery environment. A major breakthrough in the activation of porous-graphite chlorine electrodes is reported in Section 34 (Sub-task 3.3). A new electrolytic-activation technique was developed

which permits in-situ electrode activation, i.e. in an assembled submodule. Further, the method results in electrodes which are more active than electrodes activated by earlier techniques involving boiling in concentrated nitric acid for 7 to 10 days. Section 35 presents the results of a program aimed at the selection and qualification of porous graphites, lower in cost than PG-60 (Union Carbide) currently used by EDA (Sub-task 3.3). This program resulted in the identification of a low-cost graphite offering voltaic efficiencies similar to those observed with PG-60. Section 36 reports on a theoretical study of possible techniques to remove foreign gases, principally carbon dioxide, from the gas space in a battery module (Sub-task 3.2). This carbon dioxide which forms mainly during battery charge, is a product of the degradation of the porous-graphite chlorine electrodes.

There are four Appendices: Appendix A, which reports work performed by Professor Jacob Jorné at Wayne State University under contract to EDA, deals with overpotential measurements at electrodes in a zinc-chlorine cell; Appendices B and C, which report work performed under the direction of Professor W. Leidenfrost at Purdue University, discuss improved condensing methods for refrigeration equipment in 100MWh zinc-chlorine battery plants; and finally, Appendix D, which reviews the Mark 2, 3, and 4 battery-plant designs and the reasons underlying the selection of the Mark 4 design, was presented at the 13th IECEC in August, 1978 (1-3).

This section, the next section (Section 2) which explains how zinc-chlorine systems store and deliver electric energy, and Section 3 -- a glossary -- constitute Part I of this report.

REFERENCES

1-1 Evaluation of a 1kWh Zinc Chloride Battery System. Palo Alto, Calif.: Electric Power Research Institute, September 1976, EM-249.

1-2 Development of High-Efficiency, Cost-Effective Zinc-Chlorine Batteries for Utility Peak-Shaving, 1976. Palo Alto, Calif.: Electric Power Research Institute, March 1978, EM-711.

1-3 C. J. Warde, P. C. Symons, C. C. Whittlesey, and H. A. Catherino. "100MWh Zinc-Chlorine Peak-Shaving Battery Plants". In Proceedings of Thirteenth Intersociety Energy Conversion Engineering Conference, Vol I, 1978, p. 755-763. Appendix D in this report.

Section 2

HOW ZINC-CHLORINE HYDRATE SYSTEMS STORE AND DELIVER ELECTRIC ENERGY

A schematic of the zinc-chlorine hydrate system in the fully discharged state is presented in Figure 2-1. It consists of a cell and a separate container termed a store, which is filled with water. As shown, the cell consists of a zinc electrode, a chlorine electrode, and an electrolyte, which is 2.0M aqueous zinc chloride. The zinc-electrode substrate is fabricated of graphite, while the chlorine-electrode substrate may be fabricated from porous graphite or ruthenia-catalyzed porous titanium. In this mode, the cell voltage is 0.0V, as both electrodes are inert, i.e. they do not contain active materials.

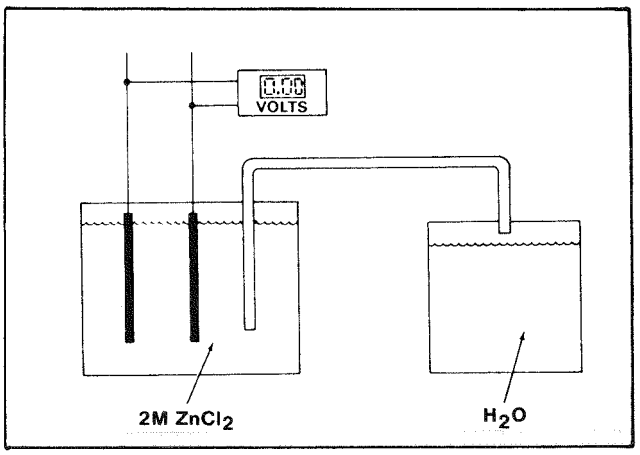

Figure 2-1. Schematic of a zinc-chlorine hydrate system in a fully-discharged state.

In charge, the zinc-chloride electrolyte is electrolyzed. Zinc is plated on one of the graphite substrates while gaseous chlorine is evolved on the other, as shown schematically in Figure 2-2. The chlorine passes from the gas space above the electrolyte into the store where it reacts with water cooled to less than 10°C. Chlorine hydrate, a pale yellow solid, is formed according to the reaction:

$$Cl_2\ (aq) + xH_2O \rightarrow Cl_2 \cdot xH_2O(s) \quad \ldots\ldots\ldots\ldots\ldots\ldots \quad (2\text{-}1)$$

where the value of x, which is dependent on the experimental conditions, can be as low as 5.7. This reaction is exothermic. The heat of formation of chlorine hydrate is approximately -18kCal/mole. Accordingly, the store must be chilled continuously during charge. A notable feature is that, in marked contrast to other battery systems, the charging voltage remains constant during charge.

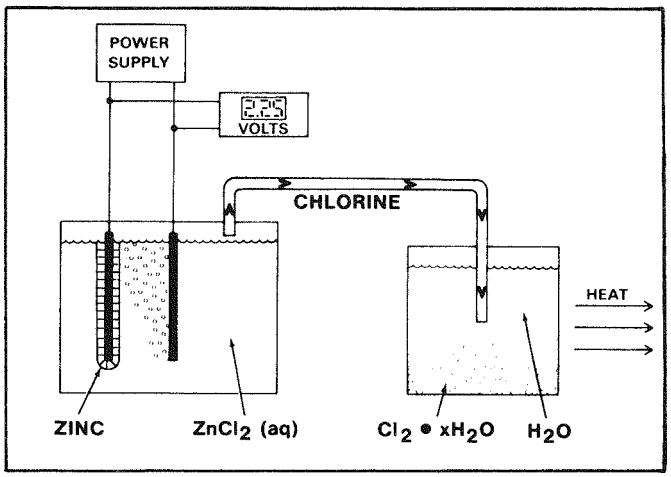

Figure 2-2. Schematic of zinc-chlorine system in the charge mode.

At full charge, the zinc chloride concentraton in the cell has decreased to 0.5M and the store is full of chlorine hydrate, as shown in Figure 2-3. Under standard conditions, the open-circuit voltage is 2.12V, calculable from the standard free energy of the reaction:

$$ZnCl_2\ (aq) \rightleftarrows Zn\ (s) + Cl_2\ (aq) \quad \ldots\ldots\ldots\ldots \quad (2\text{-}2)$$

This reaction is highly reversible. At the zinc electrode, the exchange current density is high (at $\sim$1A/cm^2) and therefore electrode polarizations at practical current densities, i.e. 25-50mA/cm^2, are low. In contrast, the polarization of the chlorine electrode is highly dependent on the level of electrode activation.

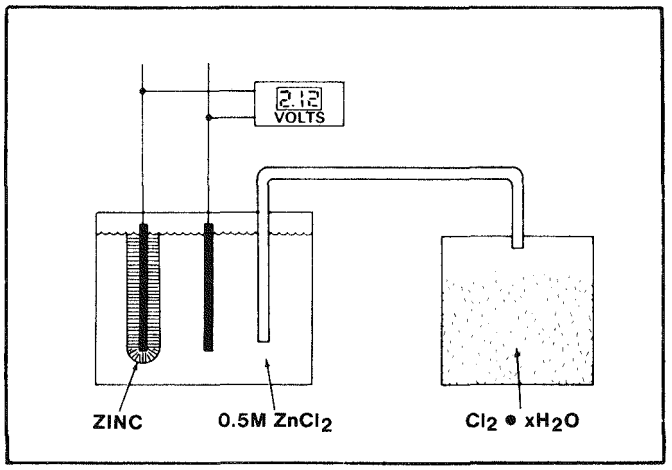

Figure 2-3. Schematic of a fully-charged zinc-chlorine system on open circuit.

To initiate discharge, the chlorine hydrate-water mixture in the store is heated by heat exchange with the warmer (20°C - 50°C) cell electrolyte. Chlorine passes from the store into the electrolyte adjacent to the porous-graphite chlorine electrode, as shown in Figure 2-4. Electrochemical reaction of zinc and chlorine occurs, releasing electrical energy. Heat is generated in the cell because of thermodynamic, electrochemical, and chemical inefficiencies in the cell reaction. Enough of this heat is transferred to the store to cause the desired amount of chlorine evolution by decomposition of chlorine hydrate. Zinc chloride is formed by the electrodissolution of zinc at the anode and chlorine reduction at the cathode. The battery is considered to be fully discharged when all of the zinc is dissolved. The battery thus returns to the fully discharged state, in which the zinc chloride concentration is 2.0M, as shown in Figure 2-1.

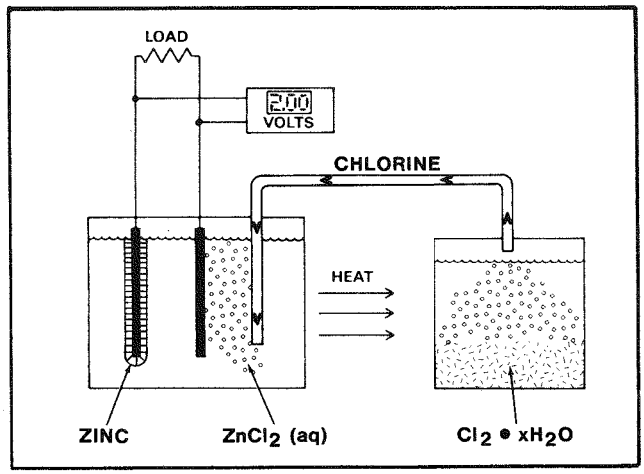

Figure 2-4. Schematic of a zinc-chlorine system in discharge.

The simplified sequence in Figure 2-1 through 2-4 illustrates how the zinc-chlorine hydrate battery system stores and delivers electric energy. In a practical system, however, means must be provided to achieve the desired flows of chlorine, electrolyte, water, and heat, as shown in Figure 2-5. Pump P1 delivers electrolyte to pockets

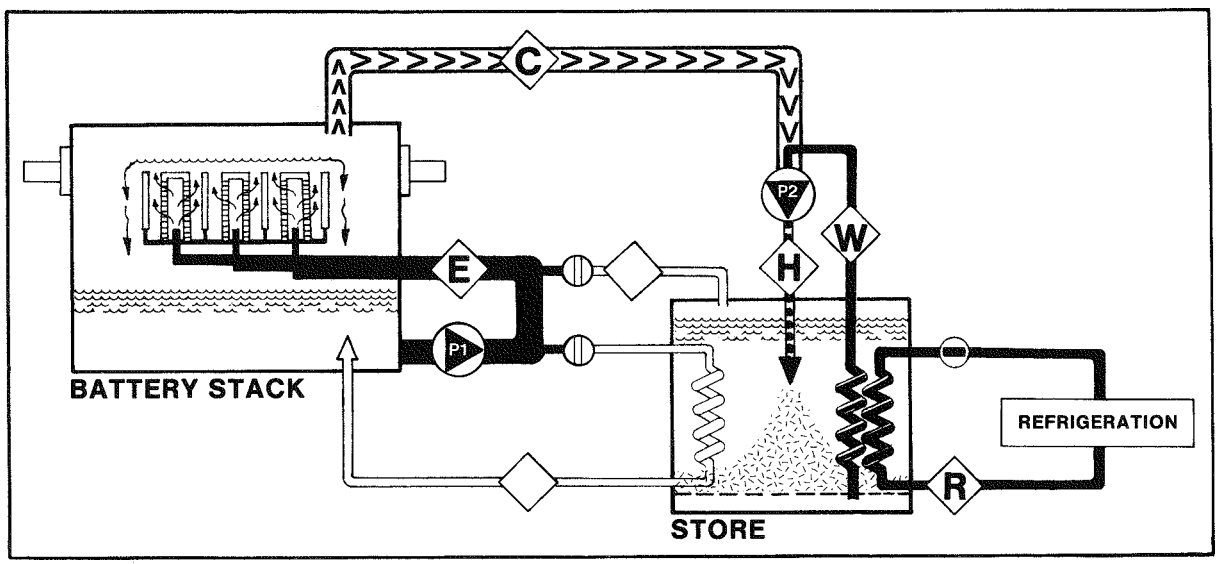

Figure 2-5. Schematic of a Zinc-Chlorine System in Charge

between pairs of porous-graphite chlorine electrodes. The electrolyte passes through the porous-chlorine electrodes into the chamber between the zinc and chlorine electrodes, flows up between the electrodes, and eventually spills through high-resistance cascades back into the sump. Chlorine gas is pumped by P2 through line C. Before entering the pump, the chlorine is mixed with chilled water, which passes through line W and comes from the bottom of the store. The chlorine and chilled water are mixed in the gas pump, chlorine hydrate forms, and the chlorine hydrate-water mixture is deposited in the store through line H. The water in line W is chilled by passage through a heat exchanger. Glycol cooled by means of a refrigeration system is passed through line R into this heat exchanger. It should be noted that the gas pump, P2, may be operated to significantly reduce the pressure above the battery stack and electrolyte sump. This mode of operation serves to lower the concentration of chlorine dissolved in the electrolyte, which in turn reduces the corrosion of zinc, particularly during charge, thereby increasing the electrochemical energy efficiency.

Figure 2-6 shows this system in discharge. The valve in line D is opened, permitting a stream of warm electrolyte to pass through a heat exchanger in the store. Chlorine is formed by decomposition of chlorine hydrate. On development of the required pressure in the store, the valve in line G is opened and chlorine passes into line E on the high pressure side of the electrolyte pump, P1. The chlorine dissolves in the electrolyte, which is then fed to the porous-graphite chlorine electrodes. The

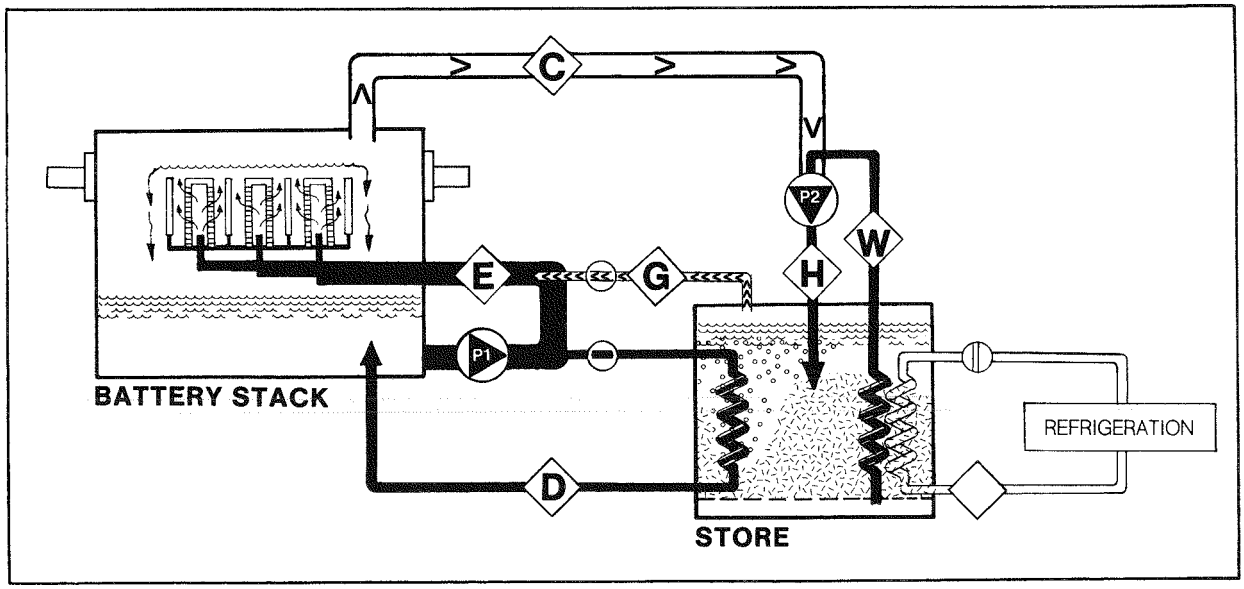

Figure 2-6. Schematic of a Zinc-Chlorine Battery in Discharge

battery stack can now be discharged. Electrodissolution of zinc occurs at the zinc electrode, reduction of the dissolved chlorine occurs at the chlorine electrode, power is available at the battery terminals, and zinc chloride is formed in the electrolyte according to the equation:

$$Zn\ (s) + Cl_2\ (aq) \longrightarrow ZnCl_2\ (aq) \quad \ldots\ldots\ldots\ldots\ (2\text{-}3)$$

In general, the refrigeration system is not required during discharge. The gas pump, P2, recirculates chlorine from the battery-stack gas space. Water continues to flow in line W, thereby reducing temperature differentials in the store.

In addition to the pumps and heat exchangers, shown in Figures 2-5 and 2-6, practical battery systems will include: (a) ultraviolet lights for recombination of hydrogen (formed at the zinc electrode) with chlorine; (b) a non-return valve on line G; (c) a heat exchanger in the electrolyte sump which may be employed for cooling purposes during discharge if the temperature increases above a pre-determined level; (d) temperature and pressure sensors to activate valves, e.g. in lines D and G; and (e) a filter to permit separation of the chlorine hydrate and excess water (for line W) in the store. These additional features are described in greater detail in Parts III and IV, which discuss the design, assembly, and testing of zinc-chlorine battery systems.

Section 3

GLOSSARY FOR ZINC-CHLORINE HYDRATE BATTERY SYSTEMS

Every new technology inevitably develops its own terminology. Zinc-chlorine hydrate battery development at EDA is no exception. To assist the reader, a glossary of terms commonly used at EDA is presented below. It should be noted that the glossary is neither comprehensive nor does it provide an absolute definition of every term.

activation - method of lowering the polarization for chlorine evolution and/or reduction at the chlorine electrode. For porous graphite, two techniques -- treatment in concentrated HNO_3 for 7-13 days or an electrolytic process -- are commonly employed.

baseline current - the dc current flowing in a unit cell at an applied voltage below the decomposition potential of zinc chloride.

battery plant - zinc-chlorine battery plant includes the entire collection of battery strings at a site, bus-work and switchgear, power-conditioning equipment, refrigeration equipment including cooling towers, and control facilities.

battery stack - a combination of cells electrically connected in series and/or parallel.

capacity density - the calculated number of milliampere-hours per square centimeter of zinc electrodeposited during charge, i.e. the product of the average current density and the charge time.

cell imbalance - the performance differences between single cells, unit cells, or submodules. This imbalance is observable in the variation of (a) the cell voltages, as the area of the zinc deposit remaining on the electrode determines the cell voltage; (b) the usable coulombic efficiencies of cells in a submodule.

charge - that phase of battery operation during which zinc is electrodeposited on one electrode and chlorine gas is generated at the other electrode.

charge coulombic efficiency - actual weight of zinc deposited during charge divided by the theoretical weight calculable from Faraday's law.

charge voltaic efficiency - the open-circuit voltage divided by the energy-average charge voltage.

chemical corrosion - any chemical process resulting in the dissolution of electrodeposited zinc. The two main corrosive reactions in the system are the chemical reaction between zinc and dissolved chlorine and the chemical reaction between zinc and hydrogen (hydronium) ion.

chlorine electrode - a solid electric conductor providing a surface for the electron-transfer reactions in charge and discharge between chlorine gas and chloride ions. Both porous graphite and ruthenia-catalyzed porous-titanium have been employed as the chlorine electrode material used in the zinc-chlorine battery. The chlorine electrode is the positive electrode.

cleanout - that phase of battery operation during which any residual zinc remaining after the completion of the discharge is stripped from the electrodes.

coefficient of performance (COP) - cooling effect of refrigerator in Btu divided by the energy input to the refrigerator motor in Btu.

comb-type bipolar battery stack - a busing arrangement in which the chlorine electrodes of one unit cell and the zinc electrodes of another unit cell are fitted into opposite faces of a common graphite bus to form a comblike structure. This design provides a space-efficient way of electrically connecting unit cells in series to form a submodule.

cooldown - that phase of battery operation preceding charge during which the store temperature is brought into the range required for hydrate formation.

coulombic efficiency - the number of ampere-hours delivered by a cell or battery during discharge divided by the number of ampere-hours supplied to the cell during discharge.

current density (apparent) - the quantity of current in amperes per square centimeter of the geometric electrode area.

cycle - one complete sequence of battery operation from standby to cleanout during which the battery is charged and subsequently discharged. Generally, a full cycle involves a five-to seven-hour charge and an approximately five-hour discharge.

delivered energy - the energy delivered during battery discharge in kWh, to the cut-off levels of current density and voltage.

dendrites - tree- or fern-like growths of electrodeposited zinc which may appear on the zinc plate during charge. Capacity density and charge coulombic efficiency may be decreased if they grow sufficiently to contact the chlorine electrode. In addition, nodular or columnar growths (often incorrectly identified as dendrites) may form with similar effects. See also *edge dendrites*.

discharge - that phase of battery operation during which the electrodeposited zinc and dissolved chlorine gas are electrochemically converted back to their respective ionic states, and thereby generating electrical energy at the battery terminals.

discharge coulombic efficiency - the total coulombic efficiency divided by the charge coulombic efficiency.

discharge voltaic efficiency - the energy-average discharge voltage divided by the open-circuit voltage.

edge dendrites - needle-like growths which appear at the edge of the zinc plate during charge. These growths, caused by inadequate electrode masking or misalignment of the zinc and chlorine electrodes, may lead to limitation of the capacity density and reduction of the charge coulombic efficiency.

electrochemical efficiencies - coulombic, voltaic, and energy efficiencies in which energy losses due to auxiliary equipment are not considered.

electrochemical energy efficiency - product of the usable coulombic efficiency and the energy-average voltaic efficiency, i.e. the quotient of the watt-hours delivered during discharge to the cut-off levels of current density and voltage and the charge watt-hours.

electrolyte - a chemical compound which upon dissolution in an appropriate solvent forms ions and thereby renders the solution electrically conducting. In the zinc-chlorine battery the solvent is water, and the electrolyte consists of zinc chloride. Supporting electrolytes, such as potassium chloride and sodium chloride, may also be present to improve electrolyte conductivity.

electrolytic activation - method of activating porous-graphite chlorine electrodes by anodizing the electrode in dilute aqueous chloride.

failure modes - the mechanisms by which a battery component or auxiliary unit fails to perform its required function.

flat-plate chlorine electrode - a chlorine electrode which is produced by cutting a plate of the desired thickness from a block of porous graphite. In contrast to the machined chlorine electrode, an internal cavity is created by the physical separation of the two flat electrodes in a plastic frame.

frame - an assembly, fabricated of plastic, which is used to hold two flat-plate chlorine electrodes. Electrolyte delivered to the chamber, thus formed by electrodes and frame, will flow through the porous chlorine electrode into the inter-electrode gap.

full-power coulombic efficiency - the number of ampere-hours delivered by a cell or battery during discharge, at full-rated current to the point where the cut-off voltage is reached, divided by the total number of ampere-hours supplied to the cell during charge.

hydrate store - a cold-water reservoir in which chlorine gas and water are mixed to form solid chlorine hydrate during charge. The store provides a compact and safe means of storing chlorine gas. Chlorine is rendered available for use during discharge by the passing of heated electrolyte through a heat exchanger in the hydrate store.

hydrogen/chlorine reactor - a chamber containing ultraviolet lights which acts to recombine hydrogen, formed at the zinc electrodes, with chlorine. The reactor thus effectively prevents the build-up of hazardous levels of hydrogen. The hydrogen-chloride gas is returned to the battery electrolyte.

impurities - any organic and/or inorganic substances present in the electrolyte which are not part of the electrolyte formulation.

inerts - any gas present in the battery system other than chlorine, e.g. air, CO_2, H_2. The presence of inerts in the system decreases (a) the partial pressure of chlorine resulting in the requirement of lower temperatures for chlorine hydrate formation, and (b) the solubility of chlorine in the electrolyte, leading to reduced cell voltage during discharge.

inter-cell bus bar - the common graphite bus in the comb-type bipolar cell design. The inter-cell bus bar provides a means of electrically connecting unit cells in series.

inter-cell leakage - the presence of electrolyte paths between unit cells in a submodule due to an incomplete seal between the submodule container and the inter-cell bus bar. Inter-cell leakage may be undesirable as it can (a) result in the establishment of inter-cell leakage current, thereby reducing battery coulombic efficiency, or (b) lead to the formation of inter-cell shorting due to zinc growths.

leakage current - dc current flowing between adjacent cells due to inter-cell leakage. This leads to the self-discharge of zinc and chlorine electrodes attached to the other side of the inter-cell bus bar.

leveling agent - an inorganic additive in the electrolyte, which effects a measurable increase in the battery capacity density by promoting the formation of flat, uniform zinc electrodeposits and a consequent reduction in the growth and number of dendrites or other zinc growths.

machined chlorine electrode - a porous-graphite electrode into which is cut an internal cavity by machining. Two of these electrodes are cemented together with an adhesive to form a chlorine-electrode pair. Electrolyte delivered to the intra-electrode chamber thus formed flows out through the porous electrode.

masking - the practice of covering certain edges of the electrodes with a chemically inert material for the purpose of defining the active area of a cell. Masking is utilized to minimize the probability of the formation of dendrites or other growths at the edge of the zinc plate.

module (Mark 4) - an assembly consisting of a battery stack (sized to deliver ∿50kWh); an electrolyte sump; and a store for the formation, storage, and decomposition of chlorine hydrate.

module (Mark 2) - a similar assembly to the Mark 4 module but without an integrated hydrate store and hence, incapable of independent battery performance. The rated capacity of the Mark 2 module is one megawatt-hour.

module (Mark 3) - a larger version of the Mark 2 module with a rated capacity of six megawatt-hours.

monopolar comb - a busing arrangement in which electrodes of only one polarity are press-fit into one face of a graphite bus. The joining of two monopolar combs of opposite polarities provides a convenient way of electrically connecting single cells in parallel to form a unit cell.

overcharge - the charging of a battery beyond its rated capacity.

overdischarge - a mode in which the battery is operated in discharge with no zinc metal on the zinc electrodes. This process results in chlorine evolution on the zinc electrode. In marked contrast to other battery systems, the Zn/Cl_2 battery does not suffer performance-wise in subsequent charge-discharge cycles because of overdischarge.

overall energy efficiency - the net ac energy output from the battery system divided by the total ac energy input to the system for a complete cycle. The total ac energy input includes energy supplied to auxiliaries and ac-dc conversion equipment.

parasitic current - an electric current flowing in the common electrolyte surrounding a collection of electrochemical cells electrically connected in series. This current is due to either the electrolyte paths in the inlet manifolds or the electrolyte return loops from the cells back to the sump.

polarization - the voltage difference between the actual cell voltage and the theoretical reversible cell voltage when current flows through the cell.

power conditioning - that battery plant subsystem which accomplishes the conversion of ac electric power to dc electric power during the charging of the battery, and the conversion of the dc power output of the battery during discharge to ac power.

pumping efficiency - the product of the pump and electric motor efficiencies. The motor efficiency consists of the power supplied to the pump shaft divided by the electric power supplied to the motor. The pump efficiency consists of the power delivered by the pump divided by the power supplied to the pump shaft.

rack - actual physical collection of modules. The rack includes the piping and wiring networks supplying the modules. A structure comprised of a string of modules, and the piping and wiring networks supplying those modules.

reverse charge - a process which involves coupling a power supply to a cell or battery in order to accomplish chlorine evolution on zinc electrodes and chlorine reduction at chlorine electrodes. The electrode processes are identical to those occurring in overdischarge. This procedure may be employed: a) to remove the last traces of zinc from the zinc-electrode substrate before recharge; and b) to clean the zinc-electrode graphite substrate if exfoliation of the zinc deposit is observed (generally with unworked substrates).

reverse plating - zinc plating on the chlorine electrode. In general, it would only occur on a discharge cycle if the chlorine electrode receives an inadequate supply of chlorine to sustain the applied current density.

single cell - an electrochemical combination of a single positive electrode (referred to as the chlorine electrode) and a single negative electrode (referred to as the zinc electrode).

standby - that phase of automated battery operation during which the battery is in an idle state. The standby phase is always entered after the detection of a system failure.

string - A series-connected set of modules, sufficient in number to obtain the desired battery-plant voltage.

submodule - a combination of unit cells electrically connected in series, housed in a common container, and fed by a common electrolyte manifold. In the Mark 4 design, ten unit cells form a submodule. Six submodules comprise the battery stack in a module.

sump - an electrolyte reservoir, located below the battery stack.

super string - a combination of two or more battery strings electrically connected in parallel. In the Mark 3 design, six battery strings are paralleled to form a 36MWh super-string.

total coulombic efficiency - the total number of ampere-hours delivered by a cell or battery during discharge to zero volts and zero current, divided by the total number of ampere-hours supplied to the cell during charge.

turnaround - that phase of battery operation following charge and during which the electrolyte is chlorinated in preparation for discharge.

unit cell - a combination of a number of single cells electrically connected in parallel. There are ten unit cells in a Mark 4 submodule.

usable coulombic efficiency - the number of ampere-hours delivered by a cell or battery during discharge, at minimum-rated current until the cut-off voltage is reached, divided by the total number of ampere-hours supplied to the cell during charge.

vent hole - a small (∿0.060") hole in the upper surface of a chlorine-electrode pair. This hole permits the release of chlorine from the pocket between the chlorine electrodes.

voltaic efficiency - the energy-average discharge voltage divided by the energy-average charge voltage. Product of charge and discharge voltaic efficiencies. Quotient of electrochemical energy efficiency and usable coulombic efficiency.

zinc electrode - a solid electric conductor providing a surface for the electron-transfer reactions in charge and discharge between metallic zinc and zinc ions. The zinc electrode substrate is fabricated of relatively dense graphite. The zinc electrode is the negative electrode.

PART II

100MWh ZINC-CHLORINE
PEAK-SHAVING BATTERY PLANTS

Section 4

INTRODUCTION TO PART II

BACKGROUND

In order to serve the needs of the electric-utility industry, zinc-chlorine peak-shaving battery plants will be located in the subtransmission or distribution network. The battery plants will be sized, generally in the 5-500MWh range, to meet the peaking needs of a specific industrial, commercial, or residential market. A 100MWh battery plant, which would serve the peaking requirements of a town of 60,000 people, is considered to be a typical size.

The design of battery plants based on the zinc-chlorine couple poses some unique problems in that a multiplicity of battery-stack and store sizes are possible. Chlorine, evolved during battery charging is stored as chlorine hydrate, external to the cell. Thus, it is possible to have a single chlorine-hydrate store for a 100MWh battery plant. During discharge of the battery, chlorine-saturated electrolyte must be delivered, by pumping, to every cell. A stack module -- defined as an integral hydraulic unit with its own electrolyte pump -- can be as small as a single cell. As the stack must be factory-assembled, a practical upper limit on its size is determined by the size of the largest truckable unit (i.e., a package approximately 40 feet in length, 8 feet in width, and 10 feet in height).

In order for a 100MWh battery plant to be acceptable to the electric utility industry, the following criteria must be met:

- Installed Cost: $25/kWh + $75/kW (mid-1977 $)
- Overall Efficiency: 70% +
- Footprint: 8kWh/ft^2
- Maximum Height: 20 ft
- Minimum Siting Restrictions

- Useful Life: 10 Years +
- Unattended Operation

The usual cost and efficiency trade-off exists so that less than 70% efficiency is acceptable, provided the installed cost drops accordingly. This efficiency value does include the penalties associated with rectification and inversion.

The footprint criterion will allow a 100MWh plant to be located on a half-acre site, with the battery components of the plant occupying approximately a quarter-acre. Observation of a maximum height criterion of twenty feet will minimize problems associated with siting of the plant. The environmental intrusion of the plant under normal and abnormal circumstances must be minimal to allow unrestricted siting. To minimize O&M costs, the plant must operate unattended. Thus, the stored energy will be dispatched from a central-station location. The 100MWh plant should be capable of being discharged for 5 hours at 20MW, and charged over a period of 5 to 7 hours. Charging and discharging of the battery totally in shorter time periods should also be possible. However, the practicality of accomplishing this will be predetermined by the rating of the power-conditioning equipment.

REVIEW OF PROPOSED DESIGNS

EDA has completed three distinct designs for 100MWh zinc-chlorine battery plants, as shown in Table 4-1.

Table 4-1

ZINC-CHLORINE PEAK-SHAVING BATTERY DESIGNS

Battery Design	EPRI Contract No.	Inception Date
Mark 2	RP226-1	Nov. 1975
Mark 3	RP226-2	Nov. 1976
Mark 4	RP226-3	Mar. 1977

Exposure of the Mark 2 design to electric-utility, EPRI and ERDA representatives, and to a detailed and critical review within EDA led to the evolution of the Mark 3 design. Similar analysis of the Mark 3 design and a realization of its limitations led to conception of the Mark 4 design.

100MWh Mark 2 Design

An artist's rendition of the Mark 2 peak-shaving plant at a utility substation is shown in Figure 4-1. The plant consists of eleven 10MWh battery strings, each string consisting of ten 1MWh modules connected in series. An additional string is provided to maintain rated capacity despite the need for complete string discharge before recharge. The illustration shows each string arranged in two layers to facilitate terminal-bus connection. A radiator for control of the electrolyte temperature in the battery module is located above the center of each string. In the left background, the power-conditioning equipment and the associated bus-work may be seen. The building in the right background contains refrigeration equipment, other auxiliaries, and control equipment. Adjacent to this building are the cooling towers for the refrigeration equipment.

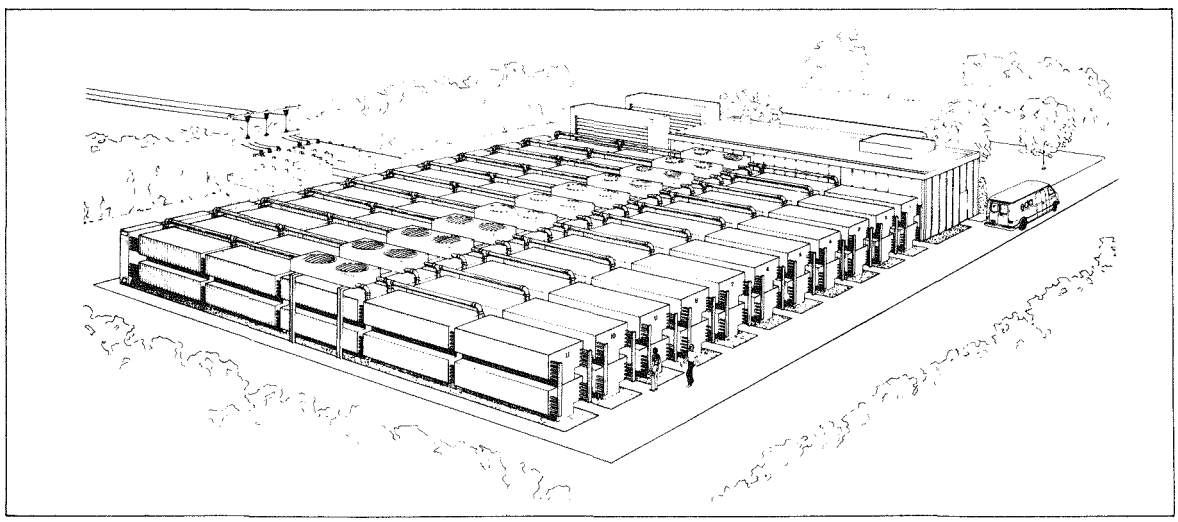

Figure 4-1. Mark 2 Design of a 100MWh Zinc-Chlorine Peak-Shaving Battery Plant

Not shown in Figure 4-1 is a single chlorine-hydrate store which consists of a tank with equipment for hydrate formation and decomposition. This cylindrical tank is located below grade, with approximate height and diameter dimensions of 40 and 35 feet, respectively. Also located below grade are the electrolyte sumps and circu-

lating pumps for each string. The pumps circulate electrolyte for module cooling during charge and for hydrate decomposition during discharge.

Feedback from electric-utility, EPRI, and ERDA representatives, Bechtel personnel, and internal EDA studies indicated that the Mark 2 design could be criticized on the following grounds:

- As the store in this design is underground, it is likely that the design will be limited to certain types of terrain.
- As warm electrolyte must be circulated from each module to heat exchangers in the store in order to provide for decomposition of the chlorine hydrate during discharge, piping will be a major cost for this design.
- Excavation for and construction of the underground store and pump room will be site labor-intensive. It will therefore be a significant expense, particularly if utility labor is employed.
- Uniform distribution of electrolyte with a single pump to each and every chlorine-electrode pair in the five tiers of unit cells poses considerable problems from the standpoints of hydraulic-energy conservation and engineering.
- The transport of chlorine gas to a single store during charge and back to every module during discharge will involve the use of large-diameter piping requiring costly valving technology.

100MWh Mark 3 Design

Minimization of site labor was the major goal of the Mark 3 design. Thus, all components of the battery plant including the hydrate stores and refrigeration equipment were to be truckable without special regulation to the substation location. Each plant component, therefore, had to fit within a volume: 40 feet x 8 feet x 10 feet.

An artist's rendition of the Mark 3 peak-shaving battery plant is shown in Figure 4-2. The plant consists of three superstrings, each delivering 36MWh. Each superstring is comprised of six 6MWh battery modules, each of which is transported to the site separately. Associated with each superstring are eight cylindrical hydrate stores, with associated hydrate formation equipment. It should be noted that the eight stores are coupled, i.e., have a common gas space, with each other and with the six modules comprising the superstring. In the left background, the bus-work may

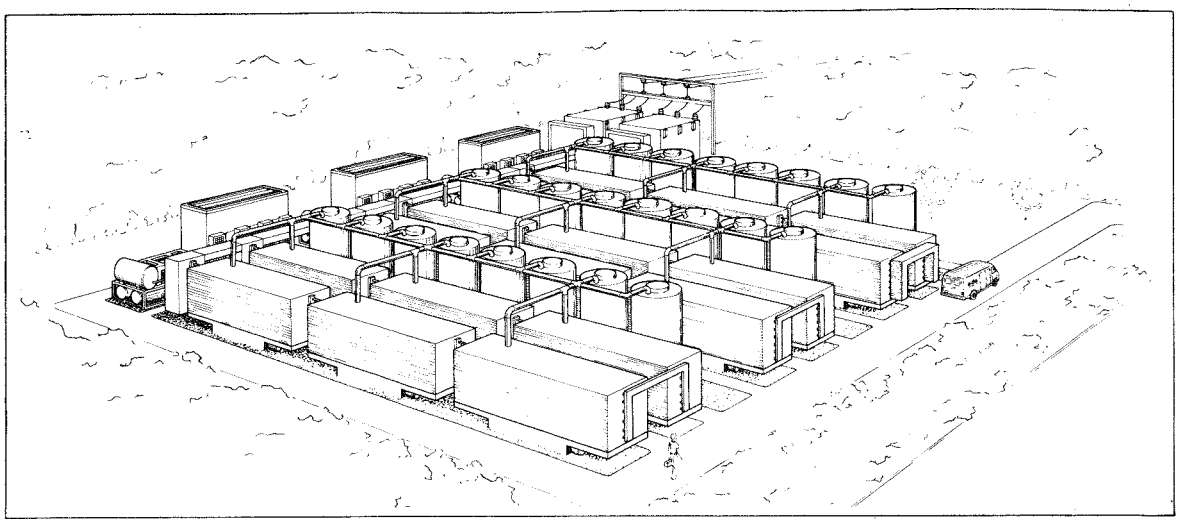

Figure 4-2. Mark 3 Design of a 103MWh Zinc-Chlorine Peak-Shaving Battery Plant

be seen leading to the power-conditioning equipment. Also in the left background may be seen three sets of refrigeration equipment on individual skids, each skid having been transported separately to the substation location.

Although each 6MWh battery module is a separate hydraulic unit with a single sump, there are six electrically-separable submodules in each module. Each of the submodules is fed by its own sump pump. The submodule consists of two levels, each with four parallel runs of seventy-two 1.76kWh cells. One consequence of the electrical isolation of the submodules within each module is that there are six strings within a given superstring, if the submodules on any given level of the six modules comprising the superstring are connected together. In this way, it is possible to have six or less of these strings operating independently within the superstring at any point in time. This is useful from a load-following standpoint. The rated capacity of the battery plant is 103MWh, i.e., seventeen 6MWh strings. One extra 6MWh string is provided because of the need for complete discharge of each string before recharge. A list of definitions is presented in Table 4-2 for clarification purposes.

Criticism of the Mark 3 design by electric-utility representatives centered mainly on the safety and environmental aspects of these plants. The presence of 75 tons of chlorine (25 tons per superstring), even as non-explosive, non-flammable, and slowly-decomposing chlorine hydrate, in a fully-charged battery plant led represen-

Table 4-2

SELECTED DEFINITIONS FOR THE MARK 3 BATTERY DESIGN

Component	Delivered Energy	Average Discharge Voltage
Superstring	36MWh	864V
String	6MWh	864V
Module	6MWh	144V
Submodule	1MWh	144V
Unit Cell	1.76kWh	2V

tatives of a number of Southeast utilities to declare that the granting of permits for siting the Mark 3 plants in residential areas might be problematical. In this design, a single line rupture could release the total chlorine (25 tons) supplied to a superstring since the gas-supply lines to each set of six strings, which form a superstring are interconnected. Representatives of a major Midwest utility which has experience with chlorine, both at its generating plants and on its railroad lines, were more favorable, but pointed out that the responsibility was on EDA to prove the absence of hazard. Another major criticism was leveled at the Mark 3 design as a result of analysis performed at EDA. It was concluded that the stack module would be very difficult to manufacture efficiently and cheaply because of its size and the high density packing of cells.

100MWh Mark 4 Design

Realization of overall plant efficiencies of 65% or greater is dependent on the achievement of electrochemical energy efficiencies in excess of 75%. The major contributor to electrochemical inefficiencies is the coulombic inefficiency during charging of the battery. It may be shown that coulombic efficiencies on charge must lie in excess of 90% if a 75%+ electrochemical energy efficiency is to be achieved, particularly in view of the expected imbalances between cells within a module and between modules in a string. The only technique known to EDA at this time, which will allow achievement of coulombic efficiencies in this range, involves desorption of chlorine from the electrolyte by generation of a partial vacuum over the stack during charge. This reduces the chlorine concentration in the electro-

lyte and thus the loss of zinc by chemical reaction with dissolved chlorine. It should be noted that the only reported electrochemical energy efficiency in excess of 70% for a zinc-chlorine system was reported for a 1kWh cell (fabricated and tested under EPRI Contract RP226-1) in which the stack was essentially operated under vacuum during charge. The electrochemical efficiency was 74.6%, with an overall coulombic efficiency of 80-86%.

Application of this concept to the battery stack in the Mark 2 and Mark 3 designs is considered to be impractical because of the additional structure and materials required to allow the stacks to be placed under the 5 psig vacuum required. Drastic reduction of the battery-stack size was considered for this Mark 4 design, in order to use this desorption phenomenon, with the consequent improvement in electrochemical energy efficiency. Simultaneously, a drastic reduction in the size of the hydrate stores was considered to be desirable in order to improve the acceptance of the 100MWh battery plants from a siting acceptance standpoint. Greater dispersal of the chlorine hydrate in multiple stores would greatly reduce the probability of release of a significant quantity of chlorine to the environment or to nearby residences. With these considerations of drastic size reduction of stack and store in mind, it became obvious that an integrated battery module, i.e. consisting of stack, store, heat exchangers, and hydrate formation equipment, was desirable.

An artist's rendition of a 100MWh battery plant based on this concept is shown in Figure 4-3. The battery portion of the plant consists of 36 racks -- each rack

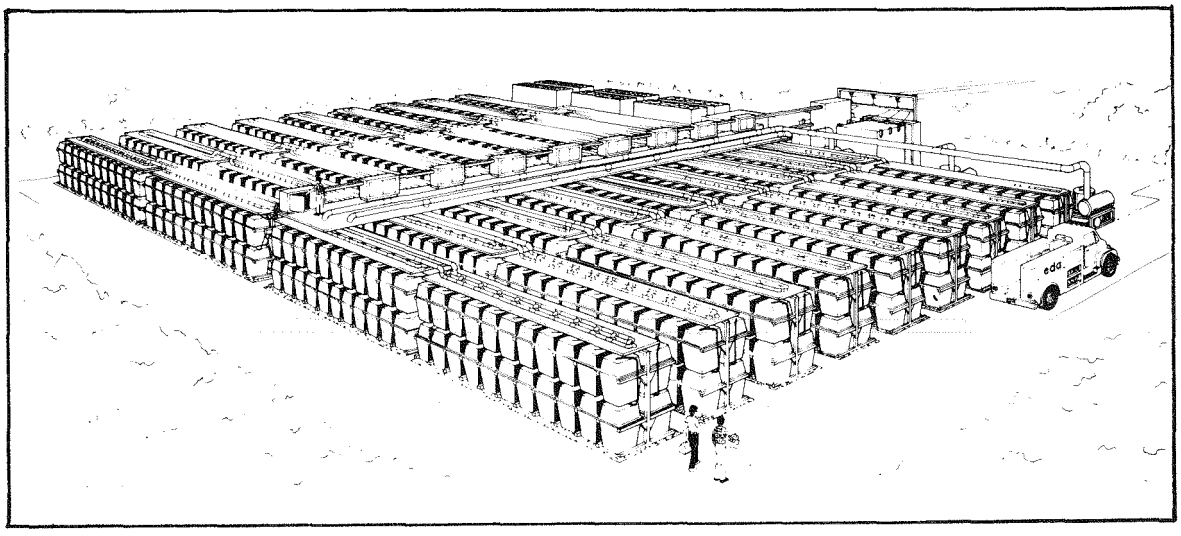

Figure 4-3. Mark 4 Design of a 100MWh Zinc-Chlorine Peak-Shaving Battery Plant

comprising forty-four 66kWh modules. The refrigeration equipment consisting of compressors, condensers, coolant pumps, and cooling towers -- all mounted on skids is located in the background, as is the power-conditioning equipment. The bus-work and coolant piping are shown running centrally through the plant, from right to left.

Coolant is distributed to each and every module by means of a distribution system built into the rack structure on which the individual modules are mounted. This coolant provides for cooling of the battery electrolyte during charge and discharge, and more importantly for chilling of the store during battery charge. For each pair of racks, there are two electrical strings, side by side. Thus, there are thirty-six 2.9MWh dc strings in the battery plant, each with its individual disconnect. This feature provides a load-following capability in increments of 580kW (660 amperes at 880 volts/string). A list of sizes and voltages of all electrochemical units is provided in Table 4-3 for this design.

Table 4-3

SELECTED DEFINITIONS FOR THE MARK 4 DESIGN

Component	Delivered Energy	Average Discharge Voltage
String	2.9MWh	880.0V
Rack	2.9MWh	---
Module	66.0kWh	20.0V
Submodule	11.0kWh	20.0V
Unit Cell	1.1kWh	2.00V

DISCUSSION OF DESIGNS

Each of the three battery designs described in the previous subsections represent extremes in design philosophy -- Mark 2 with its single underground store and large 1MWh stack modules, Mark 3 with its very large 6MWh stack modules and multiple stores above ground, and Mark 4 with its integrated and much smaller 66kWh modules. Table 4-4 summarizes selected design features of the Mark 2, 3, and 4 battery plants. The independently-operable 2.9MWh strings of the Mark 4 design provide better load-following capabilities than do the respective 10MWh and 6MWh strings of Mark 2 and 3

designs. The lower module voltage (20V) of the Mark 4 design minimizes potential parasitic current losses relative to the Mark 2 and 3 module voltages of 100V and 144V, respectively.

Table 4-4

COMPARISON OF SELECTED DESIGN FEATURES

MARK 2 DESIGN FEATURES

- Underground Store
- Eleven 10 MWh Strings
- Footprint: 9 kWh/ft²
- Access Aisles: 3 ft Wide

DEFINITIONS

String	10 MWh	1000V
Module	1 MWh	100V
Submodule	100 kWh	100V

MARK 3 DESIGN FEATURES

- Truckable Stores Above Ground
- Three 36 MWh Superstrings
- Eighteen 6 MWh Strings
- Footprint: 8 kWh/ft²
- Access Aisles: 4 ft Wide

DEFINITIONS

Superstring	36MWh	864V
String	6 MWh	864V
Module	6 MWh	144V
Submodule	1 MWh	144V

MARK 4 DESIGN FEATURES

- Stores Contained in Each Module
- Truckable Racks with 44 Small Modules
- Thirty-six 2.9 MWh Strings
- Footprint: 7.5 kWh/ft²
- Access Aisles: 4.75 ft Wide

DEFINITIONS

String	2.9 MWh	880V
Module	66 kWh	20V
Submodule	11 kWh	20V

The use of the integrated module concept in the Mark 4 design significantly influences the number of major components required for a 100MWh battery plant. Table 4-5 lists the numbers of components in each design.

Table 4-5

NUMBERS OF MAJOR COMPONENTS IN MARK 2, MARK 3, AND MARK 4 DESIGNS OF ZINC-CHLORINE PEAK-SHAVING BATTERY PLANTS

Component	Design Mark 2	Mark 3	Mark 4
Modules	110	18	1,584
Strings	11	18	36
Stores	1	24	1,584
Pumps	125	132	3,168
Refrigerators/Chillers	1	3	3

It should be noted that in general there are few if any economies of scale in electrochemical systems. Once the electrode size is fixed, as it has been to a first approximation for the comb-type bipolar concept based on current-distribution and experimental studies, the electrode cost per square foot for a 100MWh plant will be independent of the module size. As chlorine desorption from the electrolyte can best be accomplished in smaller modules, there is a cost penalty associated with battery-stack scale-up because of the inverse relationship of cost and coulombic efficiency. The Mark 4 design is thereby optimal from a battery-stack standpoint because of its use of chlorine desorption during charge.

Table 4-6 compares the electrochemical design points for the three designs. The voltaic performance goals for all three designs have already been met or exceeded at the single-cell level. EDA recognizes, however, the challenge in reproducibly extending this performance to batteries.

Table 4-6

COMPARISON OF ELECTROCHEMICAL DESIGN POINTS FOR MARK 2, MARK 3, AND MARK 4 DESIGNS

Parameters	Mode	Design Mark 2	Mark 3	Mark 4
Current Density (mA/cm^2)	Charge	33	45	33
	Discharge	30	40	40
Cell Voltage (V)	Charge	2.25	2.25	2.18
	Discharge	2.00	2.00	2.00
Time (h)	Charge	5	5	7
	Discharge	5	5	5
Usable Coulombic Efficiency		90%	90%	87%
Electrochemical Energy Efficiency		80%	80%	79%

The real challenge, however, is in meeting the 90% usable coulombic efficiency goal in the Mark 2 and Mark 3 designs. The 87% goal for the Mark 4 design is more readily achievable, due to the chlorine desorption capability.

Since the Mark 4 design evolved as a result of iterations performed on the Mark 2 and Mark 3 designs, it displays numerous other advantages over the earlier designs. These advantages lie mainly in the areas of performance, scale-up, and siting. They can be summarized as follows:

- Chlorine desorption on charge promotes higher coulombic efficiencies. This feature has already been discussed above.
- Lower voltage per hydraulic unit (module) minimizes parasitic current losses and promotes higher coulombic efficiencies. This feature has also been discussed above.
- Final scale-up from a stack/store standpoint has already been achieved for the Mark 4 design while final scale-up for Mark 2 and Mark 3 designs would be the 100MWh demonstration plant and a 6MWh battery system, respectively.
- The widely-dispersed multiple hydrate stores of the Mark 4 design minimize the probability of accidental release of hazardous levels of airborne chlorine. The respective maximum quantities of chlorine which could be released from the Mark 2, 3, and 4 battery plants due to a single line or battery case rupture are 150,000 lb, 50,000 lb, and 100 lb.
- The Mark 4 design eliminates exposed chlorine transfer lines from store-to-stack and vice-versa.
- The Mark 4 battery operates at a partial vacuum in both charge and discharge which facilitates the use of pressure sensitive safety interlocks to safely self-discharge a battery string subsequent to internally or externally caused failure modes.

BATTERY-SYSTEM ISSUES

Subsequent sections of Part II review the primary technical, cost, safety, and legal issues affecting the commercialization of the "FC+5" battery. "FC+5" denotes a projected state-of-the-art Mark 4 zinc-chlorine battery five years after first commercialization.

Section 5 discusses the electrochemical design points and engineering specifications. Section 6 describes the design of the 100MWh plant and the battery module which forms the basic electrochemical and hydraulic unit of the design. The conceived manufacturing plan for production of 100 modules per day, upon which the projected cost of the "FC+5" battery is based, is presented in Section 7. Section 8 is the design cost analysis, while Sections 9, 10, and 11 discuss potential safety and environmental hazards, plant safety features, and legal aspects associated with the siting of Mark 4 battery plants in residential areas, respectively. Section 12

concerns the projected progression to commercialization and summarizes the major issues. The results of these studies have identified areas of strength and weakness, thereby providing direction for further development efforts.

Section 5

SPECIFICATIONS FOR 100MWh BATTERY PLANT

INTRODUCTION

The design of utility peak-shaving battery plants must meet established criteria in the areas of performance, cost, life, and environmental impact. The primary design criteria for peak-shaving battery plants are presented in Section 4.

This section deals primarily with the performance criterion of 70% efficiency for the battery plant and methods to achieve this goal in the Mark 4 battery. The 70% plant efficiency translates to an electrochemical energy efficiency of ∿80% due to inefficiencies in power conversion and power requirements for operating auxiliary equipment. A set of electrochemical design points are established upon this basis and the engineering specifications are developed from these design points. The specifications are presented for the battery module, which is the basic integral electrochemical and hydraulic unit in the Mark 4 design. The projected specifications are for the state-of-the-art zinc-chlorine battery five years beyond first commercialization. This 66kWh battery module is referred to as the "FC+5" module. Forty-four modules are series-connected to form a 2.9MWh battery string and 36 parallel strings form the 100MWh battery plant. The battery module and plant designs are described in Section 6.

ELECTROCHEMICAL DESIGN POINTS

The electrochemical design points for the FC+5 Mark 4 battery module are listed in Table 5-1. The charge current density of 33mA/cm^2 corresponds to a charge current of 544 amperes for seven hours duration. The corresponding discharge current is 659 amperes (40mA/cm^2) for five hours duration. The corresponding charge and discharge capacities reflect a net round-trip usable coulombic efficiency of 86.6%.

Table 5-1

FC+5 VERSION OF ZINC-CHLORINE
PEAK-SHAVING BATTERY
MODULE

DESIGN POINTS

I.	Time (hours)	
	Charge	7
	Discharge	5
II.	Apparent Current Density (mA/cm^2)	
	Charge	33
	Discharge	40
III.	Voltage (Volts/cell)	
	Charge	2.18
	Discharge	2.00
	Voltaic Efficiency (%)	91.7
IV.	Coulombic Efficiency (%)	
	Charge	92.0
	Discharge	96.0
	Gross Round Trip	88.3
	Unusable Capacity	1.7
	Net Round Trip	86.6
V.	Usable Electrochemical Energy Efficiency (%)	79.4
VI.	Delivered Energy (kWh)	66.0

The projected charge and discharge voltages of 2.18 volts/cell (21.8 volts/battery module) and 2.00 volts/cell (20.0 volts/battery module), represent a projected voltaic efficiency of 91.7%. The resulting electrochemical energy efficiency is therefore projected to be 79.4%. The 1.7% unusable capacity reflects good cell balance in the FC+5 battery module. The battery module is projected to deliver 66kWh of usable dc energy per complete battery cycle.

A complete peak-shaving battery cycle is illustrated in Figure 5-1. It is defined as a charge of seven hours duration at a current density of $33mA/cm^2$, followed by

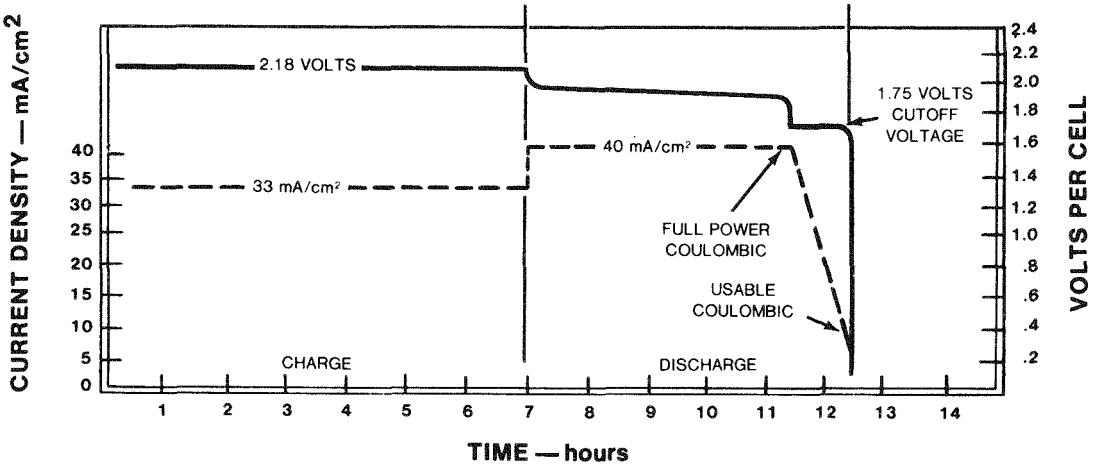

Figure 5-1. Complete cycle regime for zinc-chlorine peak-shaving battery. Note the constant current discharge to 1.75 volts/cell followed by constant voltage discharge to a current density of 5mA/cm^2. The usable capacity and energy have been delivered from the battery at this point in the discharge.

discharge at 40mA/cm^2. The 40mA/cm^2 current density is maintained on discharge until the discharge voltage drops to 1.75 volts/cell, at which time the remainder of the usable energy is removed at constant voltage until the current density drops to 5mA/cm^2. The delivered dc energy per battery module at this point in the discharge is projected to be 66kWh and is defined as the usable delivered dc energy.

At this point in the cycle, a projected 1.7% of the capacity charged still remains in the battery as unusable zinc. This zinc is removed chemically and electrochemically by continuing to slowly circulate chlorinated electrolyte through the battery while it is externally short-circuited. This clean-up operation levels the battery stack for the next cycle. Most likely it will be performed and controlled at the battery string level. Since this process is an internal battery string function, which impacts neither the current nor voltage inputs nor outputs either to or from the plant, it does not appear in the cycle regine illustrated in Figure 5-1.

MASS FLOWS AND SYSTEM OPERATION

Figure 5-2 is a positional and operational schematic of the FC+5 battery module. It illustrates the relative positioning of the major components. The basic operation of the FC+5 battery module will be controlled by a pressure sensor located in the stack compartment of the module. A back-up pressure sensor, located in

the store compartment, will override a failed primary sensor and control the self-discharge of the battery in this failure mode. The only exception to pressure control is temperature control of the coolant supply, via valve V2, which overrides the pressure control, via valve V3, in one mode of operation during discharge. An average 5 psi pressure differential is maintained between the store and the stack during charge and discharge using a gas pump (P2) to transfer gas from the stack to the store via line (5). Pressure relief of the store is accomplished via line (7) which injects gas into the main electrolyte line (1) and recirculates

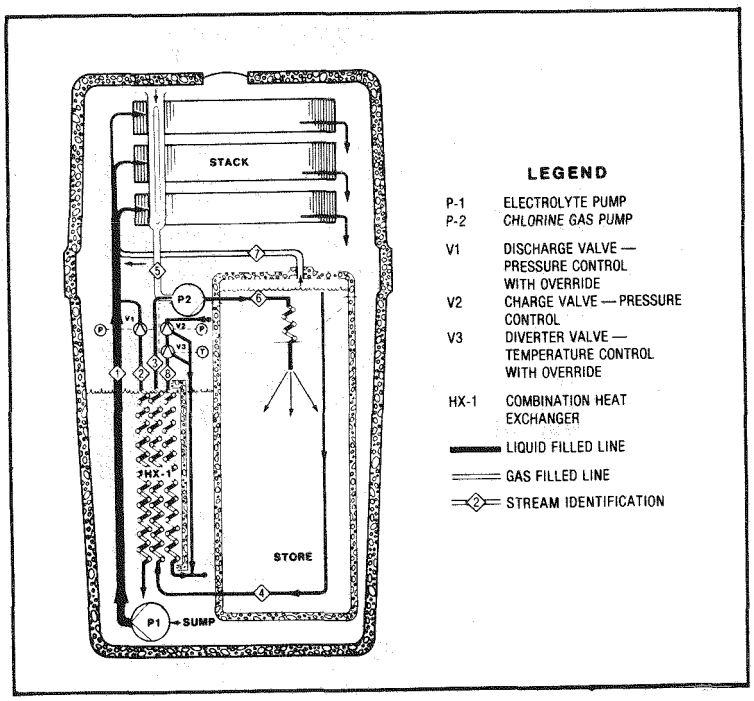

Figure 5-2. Positional and operational schematic of the FC+5 battery module. Note the self-contained operational design.

the gas back through the stack. Absolute pressure control is accomplished during charge by controlling the rate of chlorine hydrate formation and during discharge by controlling the rate of chlorine hydrate decomposition. The hydrate formation rate on charge is controlled by the rate of heat removal from the store fluid, which is controlled by the flow of coolant through the hydrate formation side of heat exchanger HX1 (line 8). The hydrate decomposition rate on discharge is controlled by the rate of heat transfer to the hydrate which is controlled by the flow of 50°C

sump electrolyte through the hydrate decomposition side of heat exchanger HX1 [line (2)]. Store fluid is circulated through HX1, via lines (3) and (4), during charge and discharge to reject and accept heat respectively.

During the charge mode, the main electrolyte pump (P1) feeds electrolyte to the chlorine electrodes in the stack via line (1). Electrolyte overflows from the cells of the stack, collects in separate return lines, and returns by gravity to the sump. The chlorine gas generated during charge is pumped from the stack, via line (5), by the gas pump (P2) where it is mixed with chilled store fluid from line (3) to form chlorine hydrate. The store fluid is chilled in HX1 just prior to being mixed with the chlorine gas. The store is held at approximately ambient pressure during charge by controlling the rate of hydrate formation as previously described. The gas pump (P2) establishes an average 5 psi pressure differential between the store and the stack by transferring gas from stack to store. Pressure relief of the store is accomplished via line (7), as previously described. The -5 psig established on the stack accomplishes dechlorination of the electrolyte during charge.

During discharge mode the electrolyte pump (P1) feeds chlorinated electrolyte to the chlorine electrodes in the stack via line (1). Again electrolyte overflows the stack and returns by gravity to the sump through separate return lines. Chlorination of the electrolyte is accomplished by injecting gaseous chlorine at 3 psig via line (7), into the main electrolyte line (1). Chlorine gas is formed in the store by decomposition of chlorine hydrate. Transfer of heat from the 50°C electrolyte, flowing in line (2), to the 11°C store fluid, flowing in line (3), accomplished in the decomposition side of HX1, provides the heat required for hydrate decomposition. Absolute pressure control of the stack at -2 psig is accomplished by controlling this rate of heat transfer to the store fluid and thus the rate of hydrate decomposition. The gas pump (P2) is again utilized to establish the average 5 psi pressure differential between the stack and the store. Temperature control of the sump is accomplished during discharge by controlling coolant flow to HX1 via line (8).

ENERGY BALANCES

The electrochemical energy balance for the battery stack is summarized in Table 5-2. The various electrochemical energy losses are calculated from the voltaic and coulombic efficiencies of Table 5-1. A total of 15.5kWh of energy is lost per cycle due

to inefficiencies occurring in the battery stack on charge and discharge. The coulombic losses are greater on charge due to the higher concentration of dissolved chlorine in the electrolyte, while the voltaic losses are greater on discharge due basically to increased chlorine electrode polarization. The ratio of usable delivered dc energy to the dc energy input yields the projected electrochemical energy efficiency of 79.4%.

Table 5-2

ELECTROCHEMICAL ENERGY BALANCE SUMMARY
FOR BATTERY MODULE

	Capacity (Ah)	Energy (kWh)
CHARGE MODE		
A. Input to battery	38,073	83.00
B. Electrochemical losses		
1. Coulombic	3,046	6.64
2. Voltaic		2.10
STORED DURING FULL CHARGE STANDBY MODE	35,027	74.26
DISCHARGE MODE		
A. Electrochemical losses		
1. Coulombic	1,401	
2. Voltaic		3.96
B. Usable delivered from battery	32,979	65.96
UNUSABLE AT END OF DISCHARGE	647	1.54

The energy balance for the battery module system is presented in Figure 5-3. Rectification and inversion efficiencies are each assumed to be 98%. Justification for these conversion efficiencies is derived from the demonstrated charge and discharge voltaic performance (flat voltage-time profiles) of zinc-chlorine batteries which

permits utilization of standard, high efficiency power conversion equipment (5-1). The energy requirement projected for auxiliaries during charge is 6.07kWh while the requirement on discharge is 1.25kWh.

The greater auxiliary energy requirement on charge is primarily due to the refrigeration requirement to form and store chlorine hydrate (3.05kWh). The total energy required for auxiliaries during one complete charge-discharge cycle is 7.33kWh. The net usable delivered ac energy output is projected to average 63.38kWh per battery module. This corresponds to an overall ac to ac energy efficiency of 69.8%.

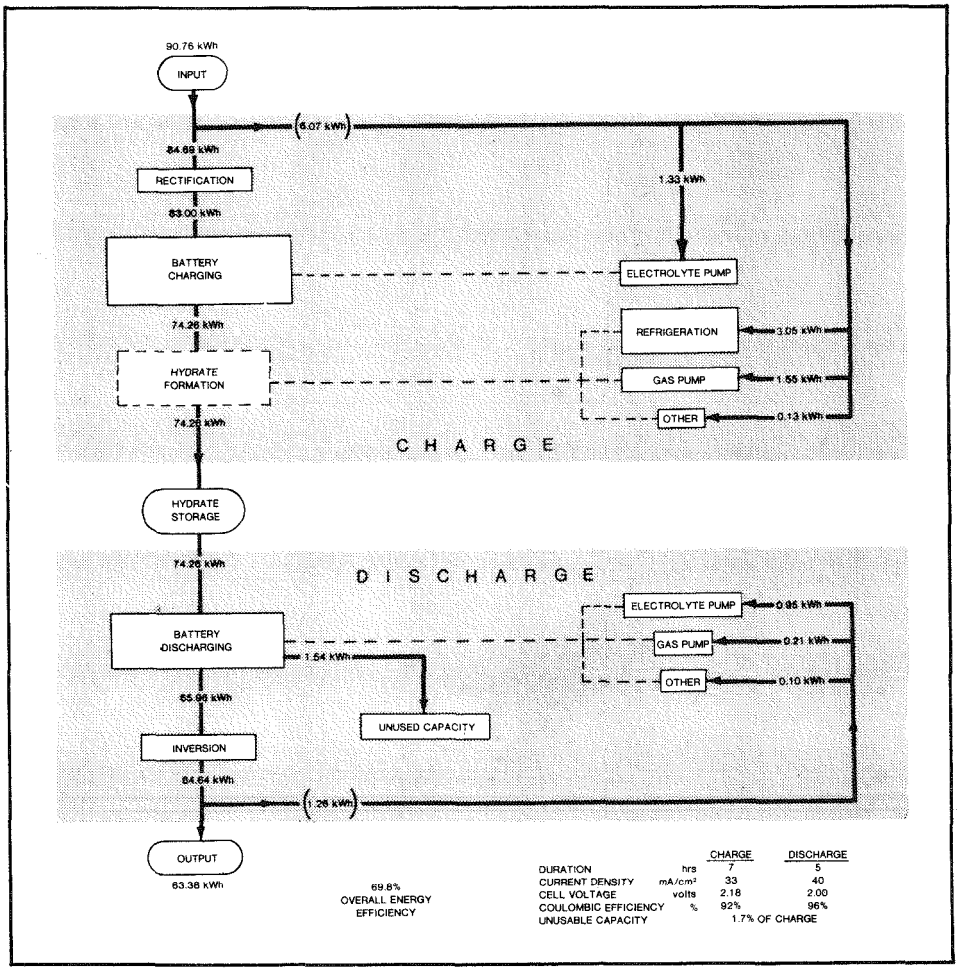

Figure 5-3. Energy Flow Diagram - FC+5 Version Battery Module

Table 5-3a is a heat balance summary for the FC+5 battery module. It summarizes the various heat gains and losses in the stack and store during the seven-hour

Table 5-3a

HEAT BALANCE SUMMARY FOR 7 HOUR CHARGE

		kWh
I.	Stack	
	A. kWh	
	Charged	83.00
	Stored	74.26
	B. Heat gains	
	Electrochemical inefficiency	8.74
	Pump heats	
	electrolyte pump (100%)	1.33
	gas pump (70%)	1.09
	Total heat gain	11.16
	C. Heat losses	
	$\Delta H-\Delta G$ (13.7kCal/mole)	10.36
	Battery to store	
	partition	1.06
	H_2O vapor transfer	1.18
	Battery to environment	0.40
	Total heat losses	13.00
	D. Net heat loss	1.84
II.	Store	
	A. Heat gains	
	Formation of hydrate (652 moles x 18.6kCal/mole)	14.07
	Pump heat (gas pump) (30%)	0.47
	Battery to store	
	partition	1.06
	H_2O vapor transfer	1.18
	Total heat gain	16.78
	B. Work to remove heat at C.O.P. of 5.5	3.05

charge. The projected net heat loss in the stack compartment of only 1.84kWh suggests the temperature will remain relatively constant without additional heating or cooling. Assuming a C.O.P. (coefficient of performance) of 5.5 for the refrigeration equipment, the work required to remove heat from the store to form and store the chlorine hydrate during the charge mode will be 3.05kWh. The C.O.P. of 5.5 is justifiable based on the Mark 4 peak-shaving plant design, which utilizes three refrigeration units of approximately 100,000 Btu/minute capacity.

Table 5-3b summarizes the projected heat gains and losses in the stack and the store during the five-hour discharge. The projected net heat gain in the stack of 3.99kWh will require some cooling during discharge to maintain temperature control. This small amount of cooling, when supplied by the same refrigeration units used to form the chlorine hydrate during charge, will require an additional 0.73kWh of energy if temperature control is deemed necessary. The heat requirement for decomposing chlorine hydrate during the discharge is projected to be 12.76kWh. This heat will be transferred from the stack electrolyte to the chlorine hydrate by means of the heat exchanger.

PROJECTED CHEMICAL WEIGHTS AND VOLUMES

Table 5-4 summarizes the chemical weights and volumes in the stack and sump areas of the FC+5 battery module. The initial electrolyte volume is 218.5 liters of 34% (by weight) aqueous zinc chloride. During the seven-hour charge, 46.2kg of gaseous chlorine will be transferred to the store compartment and stored as 140.1kg of chlorine hydrate. Simultaneously 42.7kg of metallic zinc will be deposited and stored in the stack. The electrolyte at the end of the seven-hour charge will be approximately five percent by weight aqueous zinc chloride and will occupy a volume of 195 liters. Approximately 100 liters of electrolyte will be contained in the stack and plumbing and the remainder will be contained in the sump compartment.

Table 5-5 summarizes the chemical weights and volumes in the store compartment of the battery module. Prior to charge, the store contains 281.5 liters of chlorine saturated water and all gas spaces are occupied by gaseous chlorine at ambient pressure or less, depending on the temperature. Similarly in the stack compartment, the electrolyte is saturated with chlorine and the gas spaces are occupied by gaseous chlorine at ambient pressure or less. The free chlorine in the system totals approximately 1kg. During charge the 46.2kg of chlorine combines with 93.9kg of water to form 140.1kgs of chlorine hydrate ($Cl_2 \cdot 8H_2O$). This quantity of hydrate occupies

Table 5-3b

HEAT BALANCE SUMMARY FOR 5 HOUR DISCHARGE

I.	Stack	
	A. kWh	
	Stored	74.26kWh
	Unused	1.54kWh
	Removed on discharge	72.72kWh
	Delivered on discharge	65.96kWh
	B. Heat gains	
	Electrochemical inefficiency	6.76kWh
	Pump heats	
	electrolyte pump (100%)	0.95kWh
	gas pump (70%)	0.15kWh
	$\Delta H-\Delta G$ (13.7kCal/mole)	10.17kWh
	Total heat gain	18.03kWh
	C. Heat losses	
	Battery to store	
	heat exchanger	12.76kWh
	partition	0.76kWh
	H_2O transfer	0.23kWh
	Battery to environment	0.29kWh
	Total heat loss	14.04kWh
	D. Net heat gain	3.99kWh
II.	Store	
	A. Heat required to decompose hydrate (640 moles x 18.6 kCal/mole)	13.81kWh
	B. Heat gains	
	Pump heat (gas pump) (30%)	0.06kWh
	Battery to store	
	partition	0.76kWh
	H_2O transfer	0.23kWh
	Total heat gain	1.05kWh
	C. Additional heat supplied to hydrate store through heat exchanger	12.76kWh

Table 5-4

FC+5 VERSION OF PEAK-SHAVING BATTERY
STACK WEIGHTS AND VOLUMES

Cl_2 Generated	46.2kg
Zn Stored	42.7kg
$ZnCl_2$ Decomposed	88.9kg
Total $ZnCl_2$*	99.0kg
Total H_2O	192.7kg
Total Electrolyte	291.7kg
Total Electrolyte Volume	218.5ℓ
Stack and Manifold	100.0ℓ
Sump Volume	118.5ℓ

*34% to 5% $ZnCl_2$ by weight

Table 5-5

FC+5 VERSION OF PEAK-SHAVING BATTERY
STORE WEIGHTS AND VOLUMES

Cl_2 Stored	46.2kg
8 H_2O	93.9kg
Cl_2 Hydrate	140.1kg
Hydrate Volume (ρ = 1.23)	113.9ℓ
Excess Liquid (37.8% solids)	187.6ℓ
Fluid (without Cl_2)	
volume	281.5ℓ
weight	281.5kg
10% Gas Space	28.0ℓ
Fluid (with Cl_2)	
volume	301.5ℓ
weight	334.5kg
TOTAL VOLUME	309.5ℓ

113.9 liters of volume, intermixed with 187.6 liters of water, to occupy a total volume of 301.5 liters. The mixture is 37.8% (by volume) solids and weighs 334.5kgs. A compartment volume of 309.5 liters is provided to accommodate the volume expansion in the store during charge.

The 1264 lbs of electrolyte and store fluid may be added to the projected stack weight of 210 lbs, and an assumed weight for the auxiliaries and the case of 226 lbs to give a total projected module weight of 1700 lbs. A similar estimate of projected volume requirements results in a total projected module volume of 23 ft^3 resulting in a projected packaged battery module density of 73.9 lb/ft^3.

DISCUSSION

The specifications described above assume some significant but reasonable technological developments in several areas. In the area of electrochemical performance the voltaic performance goal has already been demonstrated at the single-cell level. EDA recognizes, however, the challenge in reproducibly extending this performance to batteries. Another challenge comes with coupling the 91.7% voltaic efficiency with an 86.6% usable coulombic efficiency to provide the 79.4% usable energy efficiency. It is anticipated that developments in the areas of stack design and electrolyte composition, in conjunction with the chlorine desorption feature, will provide this performance.

Another topic associated with electrochemical performance is charge capacity. The seven-hour charge at $33mA/cm^2$ corresponds to a charge capacity of $231mAh/cm^2$. Charge capacities of this magnitude have been demonstrated on 1977 submodules and modules with a minimum of zinc dendrite formation. This of course must again be coupled with the high electrochemical efficiencies.

Another area requiring technological developments is system auxiliaries. The multipurpose heat exchanger proposed for chilling and heating store fluid, as well as controlling electrolyte temperature, is a new concept. Once this concept is proven to be technically practical and cost-effective it must be developed into an operable piece of hardware integral with the overall system. Continued efforts in hydrate store development are also necessary to achieve the storage density of 13.8% chlorine by weight or 37.8% solids by volume.

The development of high-efficiency special-purpose gas and electrolyte pumps, exhibiting a high degree of reliability, is also indicated. It should be noted that the

energy requirements for these pumps are not very significant and that lower efficiencies than those specified will not significantly affect the overall plant efficiency. If, for example, the electrolyte pump efficiency were 50%, rather than 60%, the overall plant efficiency would drop from 69.8% to 69.4%. The effect is quite negligible and a thorough cost analysis would have to be performed to determine if any significant cost advantage is realized in going to a more efficient but more expensive pump design.

The other major auxiliary power consumer is the refrigeration unit required for hydrate formation and temperature control. The C.O.P. of 5.5 is a conservative value especially since the batteries will most often be charged during evening hours when the ambient temperature is low.

Several other subsystems also require development. One such subsystem is a passive H_2/Cl_2 reactor. Present technology uses a light source of the appropriate wavelength and intensity to initiate and sustain efficient recombination of H_2 with Cl_2. For safety and reliability purposes a passive (inert catalyst) reactor needs to be developed to replace the light reactor subsystem which can fail due to bulb failure or power failure.

Another subsystem, which will apparently be needed, is an HCl recovery system. The gaseous HCl formed in the reactor is transferred to the store compartment with chlorine gas where it lowers the pH of the store fluid. Simultaneously the pH of the electrolyte increases due to loss of hydrogen ion. The HCl recovery system would strip the HCl from the gas exiting the reactor and return it to the sump electrolyte, thereby maintaining pH control in both store and sump fluids.

One final subsystem required for continuous unattended operation will be referred to as the inerts rejection subsystem. A product of graphite electrode degradation is carbon dioxide gas. As this gas or ambient air leaking into the battery accumulates, system control and battery performance will degrade. Therefore the partial pressures of these gases need to be controlled at low levels. A preliminary investigation of this topic is presented in Part V, Section 36 of this report.

Considerable thought has been directed at additional features which need to be incorporated into a 100MWh peak-shaving battery plant to meet the design criteria which have been established in areas other than performance and basic operation. These features are presented and discussed in subsequent sections.

REFERENCE

5-1 Private Communication with C.J. Amato, OMI-Udylite, Oxy-Metal Industries Corporation, Detroit, Michigan, August 16, 1976.

Section 6

DESIGN OF A 100MWh BATTERY PLANT

INTRODUCTION

The design presented here envisions a 100MWh zinc-chlorine peak-shaving battery plant intended for public utility use on the distribution or subtransmission network. For this duty the battery may be located in any urban industrial, commercial, or residential area. In order to be acceptable for this service the design must provide a means of achieving all specifications set forth in the preceding section. Meeting these criteria requires an efficient operating battery which can be produced and installed inexpensively.

MARK 4 BATTERY CONCEPT

The design currently conceived to best meet all these specifications has been evolving at EDA for several years. The Mark 4 concept is a direct descendant of earlier Mark 2 and Mark 3 designs (6-1). Whereas the earlier studies proposed large high-density stack packages with separate remote large-volume hydrate stores, the Mark 4 is based on a large number of much smaller stack-store combination modules.

This concept evolved from comprehensive analysis of the completed designs and cost studies prepared under EPRI contracts for the earlier Mark 2 and 3 proposals. Criticisms of these designs included such areas as the transport of chlorine from stack to store, the cost of specialized site construction, provisions for field-erected systems, and the acceptance of large volume chlorine storage.

In addition to these concept limitations, two other factors greatly influenced the direction of the Mark 4 design. One came from laboratory experience with the 8 and 20kWh test batteries. Charge coulombic efficiencies in excess of 90% are necessary in order to have a battery that will meet the established performance specifications. The only practical technique now known to EDA that can allow charge coulombic efficiencies of this magnitude involves desorption of chlorine from the electrolyte by reduction of pressure in the stack region. This reduces the chlorine concentration in the electrolyte and thus the loss of zinc metal by chemical reaction with dissolved chlorine. Subjecting the large stack structures of Mark 2 or Mark 3 to even a small vacuum would be costly and impractical. A reduction of the battery case size was needed in the new design.

The other factor pointing to the small module concept was the conservation of development time and money. To reach the commercial stage for large battery stack assemblies or very large hydrate store systems would require a step-by-step process of testing larger and larger laboratory models, each presenting a new set of challenges in construction and operation. EDA's mobile-battery program had already settled on a unitized zinc-chlorine battery package for installation on board automotive vehicles. Accepting this size (50-60kWh) and type would cease the reiteration process for peak-shaving application and allow immediate concentration on development of the final configuration. Such a program would also offer the possibility of sharing a good deal of development with the mobile programs.

A small battery case containing both stack and store would allow operation at reduced pressure, keep all chlorine gas sealed inside, and permit complete factory testing. At the same time, such a concept disperses the chlorine hydrate stored on site into may small non-interconnected containers. In the remote event of a severe mishap, the likelihood of a significant chlorine release to the atmosphere is greatly diminished. Restriction of site excavation is also removed by this approach. The Mark 4 design described here is based on this concept - the use of a large number of rather small fully-integrated battery modules racked together to form large-capacity peak-shaving plants. Except for the supply of chilled coolant from an external source, each module is a self-contained, completely sealed operating battery. It is not intended that such a module be field serviced. If a module malfunctioned it would be replaced, and returned to the factory for repair.

GENERAL DESCRIPTION OF 100MWh BATTERY PLANT

An artist's view of a 100MWh peak-shaving battery plant based on this Mark 4 module concept is shown in Figure 6-1. The main portion of the plant, the battery proper, consists of 36 racks each containing 44 individual modules. Each module is designed to deliver 66kWh dc. The chiller equipment, consisting of skid-mounted refrigeration

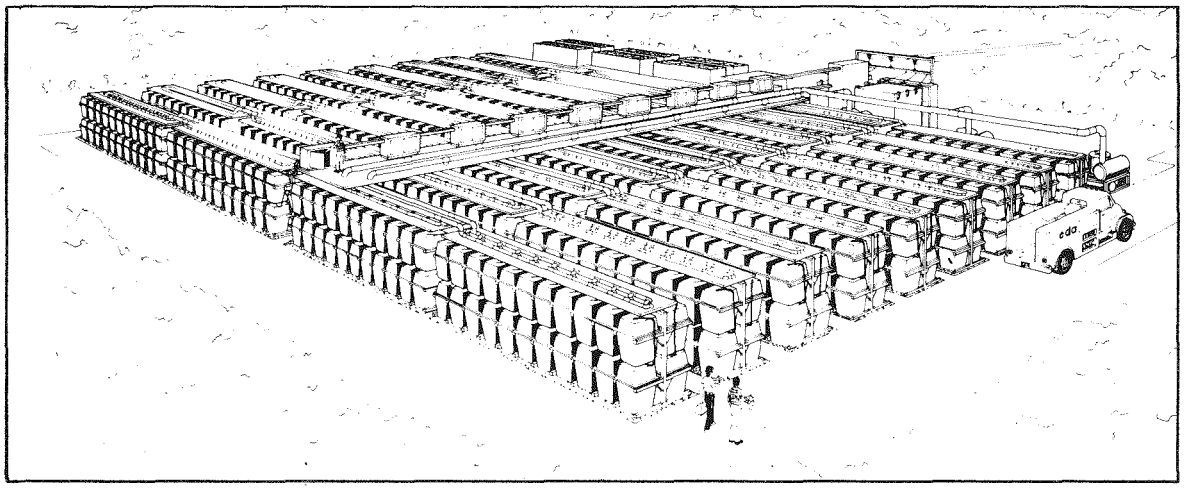

Figure 6-1. General view of 100MWh peak-shaving zinc-chlorine battery substation. Note overhead bus and chillant distribution systems. Thirty-six racks make 36 strings, each with a capacity of 2.9MWh.

equipment, circulating pumps, and the associated cooling towers is located in the background. Also, in the rear center is shown the power conditioning equipment for converting between transmission system ac current and battery dc current. Running overhead down the center of the plant is the bus system and the piping to distribute chilled coolant. Along the bus is shown the switchgear cabinets where the individual battery strings are connected to the plant. Each electrical string is composed of forty-four 20-volt modules wired in series. Since each module is a 66kWh package, each string has a capacity of 2.90MWh dc. These strings will charge at 959 volts and discharge at 880 volts on the average. Figure 6-2 illustrates two of the typical rack assemblies. It shows the arrangement of series connections by flex buses between modules and the method of distributing coolant and other hook-ups to each. It should be noted that each pair of racks contains two complete strings. When all 36 strings are connected, the plant will have a capacity of 104.5MWh dc. After appropriate derating for auxiliary ac power consumption and power inversion losses, the plant will have a rated output capacity of 100.4 ac.

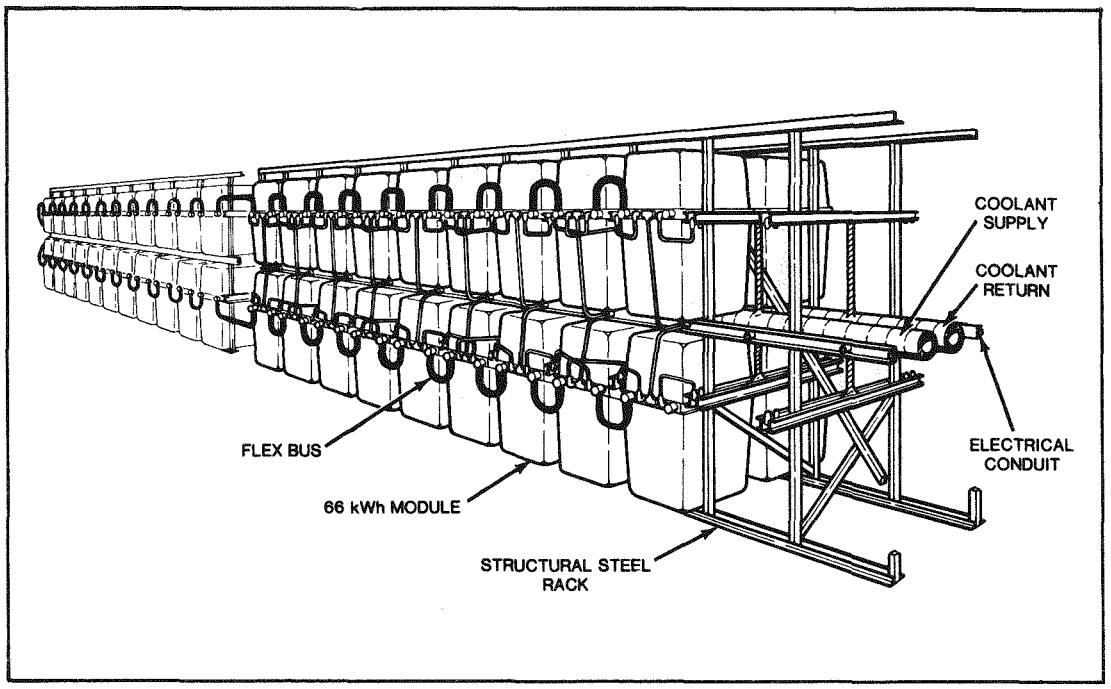

Figure 6-2. Detail of Mark 4 battery rack assembly. Two racks are depicted with flex buses shown connecting individual modules in series down the top row and back along the bottom row of opposite side. Eight modules are omitted to expose the rack structure.

One possible arrangement for a battery site is shown in plan and elevation in Figure 6-3. It will be noted from the dimensions given in this drawing that the desired 20-foot height limitation is easily met. Also it can be determined that the 104.5MWh battery plant occupies 13,000 square feet of land giving a footprint of 7.53kWh/ft^2 based on the dc plant output. This approaches the target of 8.00kWh dc/ft^2 originally established as a design criterion. The initial thrust of this design effort was on producibility and cost rather than maximizing density. It is probable that future work can seek other tradeoffs to develop a footprint at or above the target. Working against this improvement, however, is a desire to increase the service aisle width from 4 feet 9 inches to 7 feet. This may be necessary to facilitate removal of individual modules. Unfortunately, access space enlargement has a very detrimental effect on land usage figures. The site plan depicted in figure 6-3 has a footprint of 7.22kWh/ft^2 when based on the ac output capacity of the plant. None of these calculations include surrounding land, roadways, or space for power conditioning facilities. Nevertheless, even with a generous allowance for these, the site required for this substation is less than a half-acre.

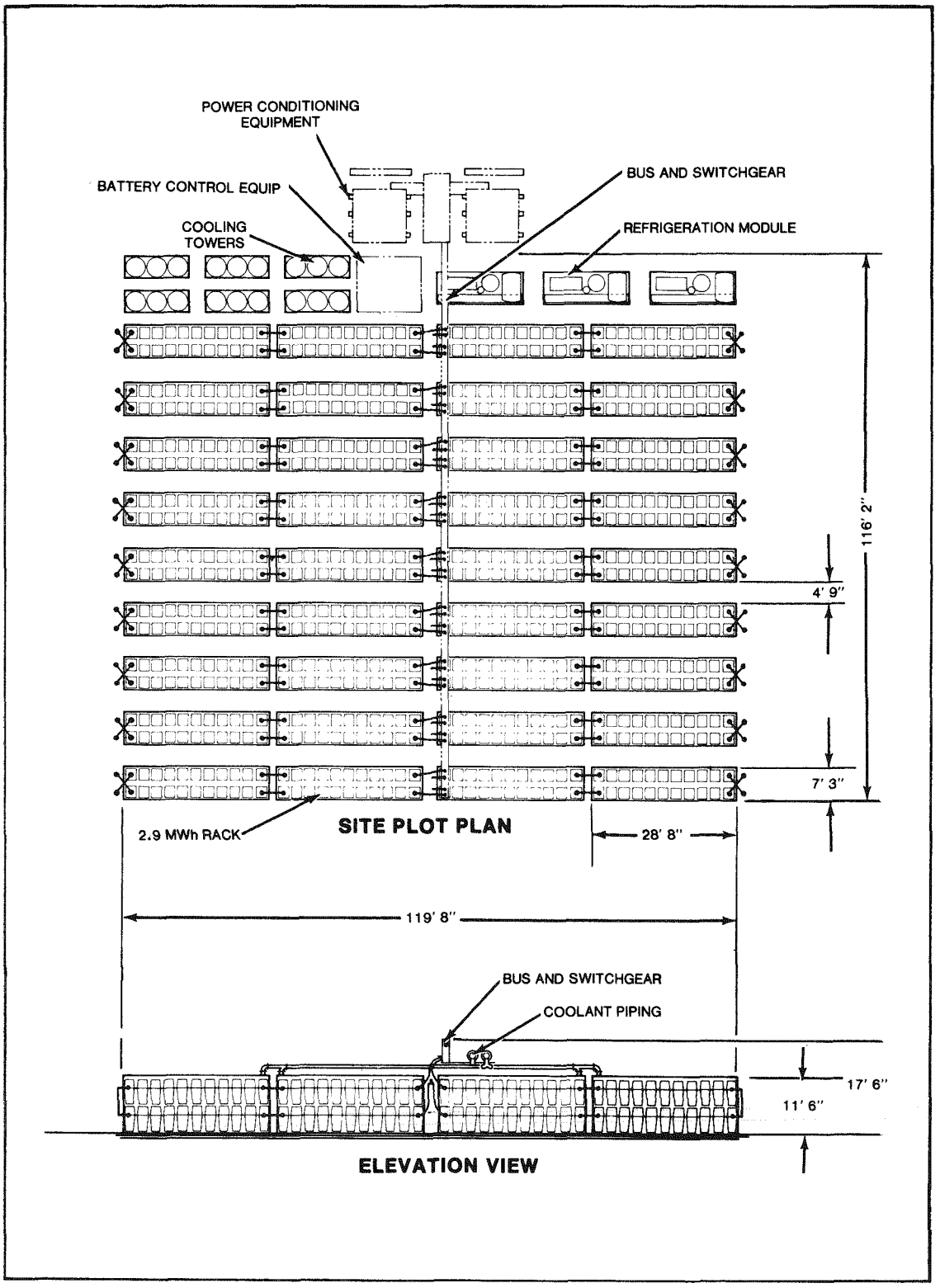

Figure 6-3. Plan and elevation layout of one arrangement for a 100MWh Mark 4 battery plant.

BATTERY MODULE

The plant just described contains 1,584 separate operating battery modules. Quite obviously the design features that make for efficiency, reliability, and economies in these individual units are of the utmost importance. The bulk of the engineering effort to date has been concentrated in this area.

The proposed general arrangement of a battery module is illustrated in Figure 6-4. Note that it is divided into two sections separated by a shelf-like member called a chassis structure. The cover for each section seals to the edges of this divider. The upper section houses the battery stack while the lower section contains the sump and store compartments as well as most auxiliary equipment.

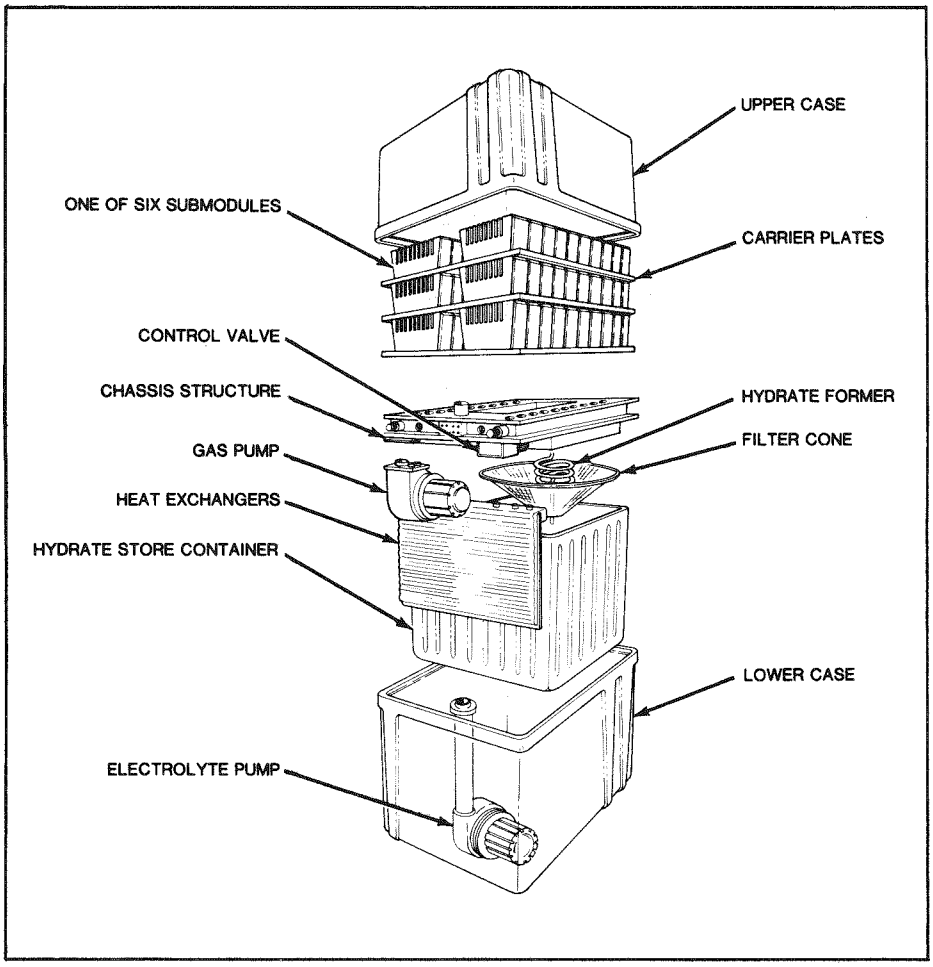

Figure 6-4. Exploded view drawing of proposed Mark 4 battery module. Note that all components are mounted directly to chassis structure before case parts are sealed in position.

Battery Stack

The battery stack, being the energy storage unit, is the fundamental part of the package. Here the anodes and cathodes are paired in the comb-type bipolar arrangement depicted in Figure 6-5. Also detailed in this figure is the functional concept of the flow-through type chlorine electrode used in the zinc-chlorine cell. Two flat plates of porous graphite with a chamber between make up one chlorine electrode. A single flat plate of graphite is used for the zinc electrode.

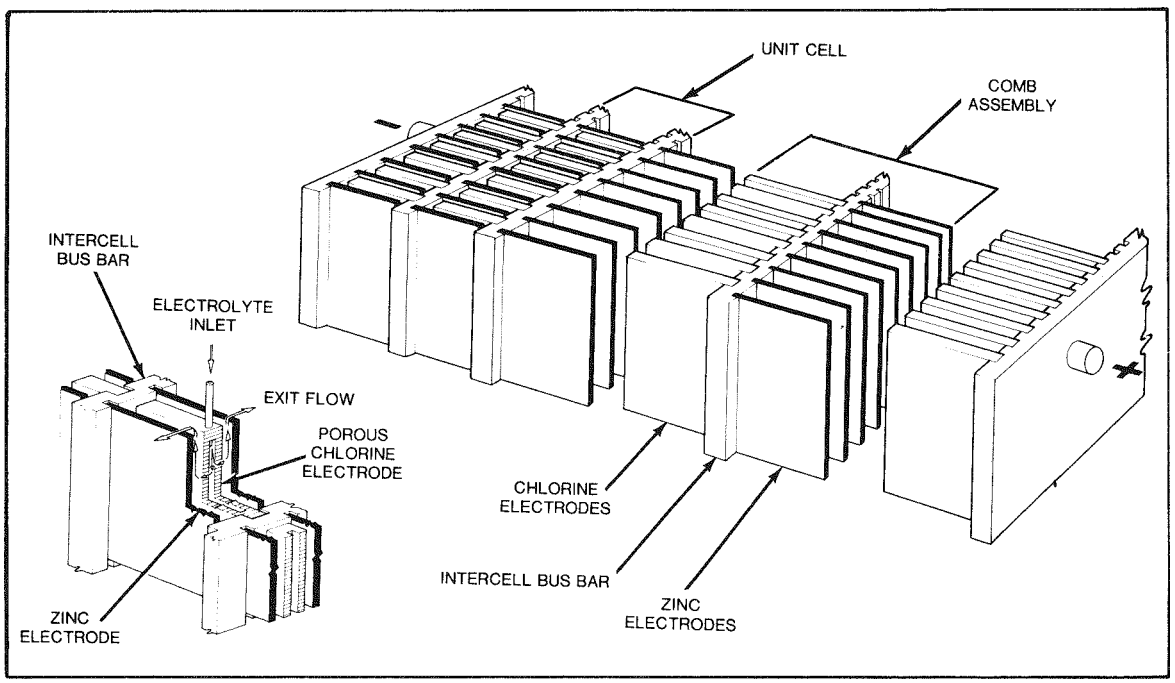

Figure 6-5. Comb-type bipolar arrangement of basic electrodes in zinc-chlorine battery.

The basic unit cell is composed of chlorine electrode faces paired with an equivalent number of zinc electrode faces. Such a unit cell discharges at a nominal 2 volts and has a 1.1kWh dc rating. These unit cells are assembled together, ten in series, via the bipolar array to form a submodule of the stack. This submodule is the fundamental operating element - an electrically and hydraulically separate unit. Six submodules are arranged two abreast in three tiers to compose the complete battery stack in one module.

Electrodes

It can be determined from the above that there are large numbers of electrode plates in each module. Considerable thought is being given to the manufacturing requirements of this potentially costly item. These electrodes are rectangular flat-graphite plates. Currently the chlorine plates are detailed for cutting from saw-sized blocks of 37G grade porous graphite (Airco Speer Co.). The "as cut" surface is suitable and a generous tolerance of ±0.005 inches is allowed for ease of manufacturing. The zinc electrode will be produced by the same methods with the same open tolerances from fine-grained CS grade graphite (Union Carbide). Sharp edges on the top and bottom of these electrodes will be rounded. No other secondary operations are required. The total graphite content for all the electrode plates in one module is 2135 cubic inches (1-1/4 cubic feet).

To complete a chlorine electrode, two flat porous-graphite plates are mounted in a frame assembly. This frame is illustrated in Figure 6-6. It is designed as four snap-together precision-molded pieces serving several important functions. First, it holds the two electrode plates apart and seals the edges so as to form a hydraulic chamber between them. Electrolyte is supplied to this chamber through a flow-regulating passage molded into the frame. The sealer strip completes the enclosure of this supply passage that leads from a socket at the bottom to an inlet nozzle near the top. Vents molded in each upper corner of the frame prevent any trapped gases from accumulating inside the cavity. In addition to these hydraulic functions, the frame also isolates the electrodes electrically and provides the required positioning and structural support to the graphite. An important detail of the sealer strip section is the flexible lip that insures consistent and accurate masking of the mating zinc electrode face even with appropriate production assembly tolerances. The snap-on cap, identical top and bottom, is ribbed to provide stiffness and yet minimize any restriction to upward exit flow of electrolyte. The frame assembles so that one vertical edge of the two graphite plates is exposed for later electrical contact with the intercell bus bar.

The zinc mask is a separate plastic extrusion serving much the same function as the sealer strip portion of the frame. This item mounts to the vertical edge of each zinc electrode after the combs have been intermeshed during submodule assembly. It serves to position the zinc electrode midway between adjoining chlorine electrodes. This mask also has flexible edges to act as accurately positioned screens for the adjacent electrode faces. The frames and masks of one unit-cell contain eleven cubic inches of injection molded plastic. For a complete 66kWh module these parts require 660 cubic inches of material.

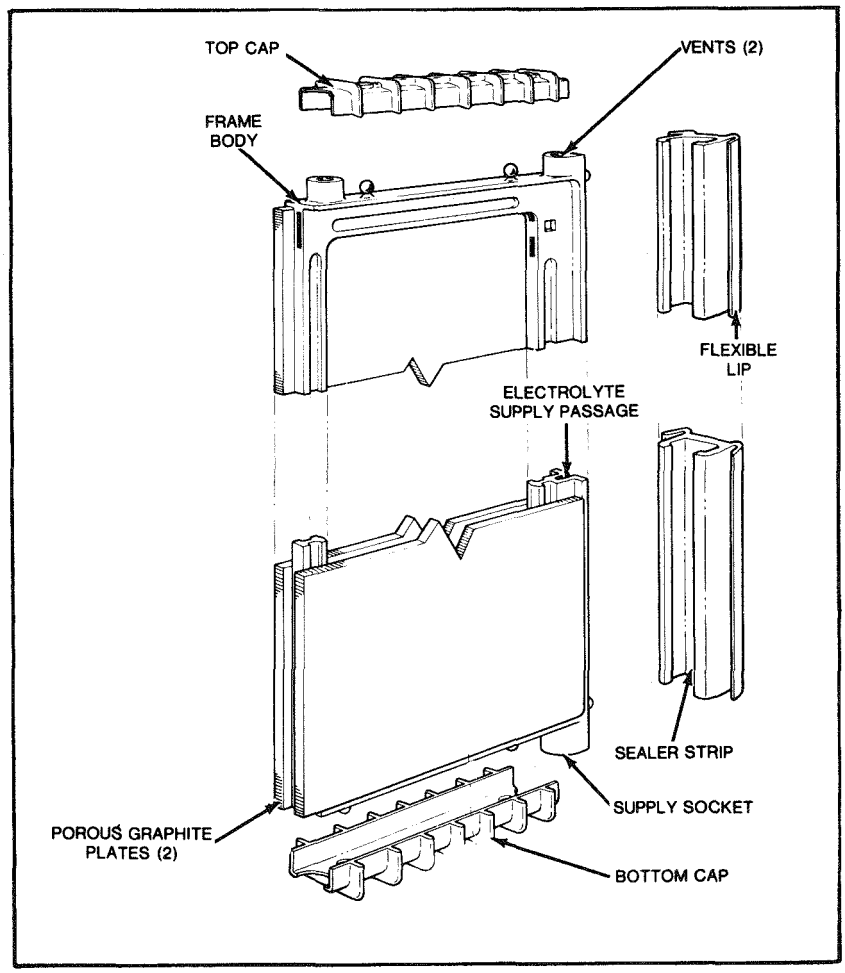

Figure 6-6. Exploded view drawing of chlorine electrode frame assembly. Note that flat graphite plates are held in place by snap-together plastic parts.

Following preparation of the electrodes, the next step in stack build-up is to construct the comb assembly. An intercell bus bar made from AGSX graphite (Union Carbide) is employed here to serve two fundamental functions. Slots gang-sawed into each face of the bar receive chlorine electrodes on one side and zinc electrodes on the other, thus providing a common electrical connection for all electrodes of one type in a cell and a series connection to the opposite type in an adjoining cell. Also the intercell bus, acting as a partition across the electrolyte tray, hydraulically separates one unit cell from the other.

Submodule

The electrolyte tray mentioned above organizes ten unit cells into a basic submodule of the stack. Nine identical comb assemblies, intermeshed one with another, and a unique half-comb at each end, assemble into one 20 volt, 11kWh submodule. In this design, the surrounding tray is assembled from sections which are made of two nesting injection-molded parts. There are 60 inner and 60 outer sections in each battery module. Therefore, a single 100MWh plant requires ninety-five thousand parts of each type. Obviously this quantity can justify quality precision parts from sophisticated tooling.

As each tray section is assembled, passages are formed for the management of electrolyte flow to and from the unit cell and to provide accurate location, support, and sealing for each separate comb assembly. Ten such units designed to snap together with an adhesive sealer, plus two special end sections, form the complete electrolyte tray for each submodule.

The assembly of this submodule is planned sequentially, beginning with an end section and half-comb of chlorine electrodes. Next will be added a typical tray section and then a typical comb assembly - sliding the zinc electrode set into the previously placed chlorine set. Then another tray section will be added and so on.

As each section of tray is brought into place, a series of upstanding nozzles molded in a recessed portion of the tray bottom are engaged into the feeder passage sockets of the chlorine electrode frames. By this means, electrolyte is uniformly distributed from the manifold chamber of the tray into each chlorine electrode pack. The exit flow from each unit cell is collected in a weir basin and drained by gravity through a series of separate channels under the tray bottom. By these means a long, high resistance path is maintained to minimize parasitic current flow from one cell to another or to the electrolyte sump. The completed submodule has a manifold inlet port and an outlet port in the bottom for each of the ten unit cells contained inside.

Chassis Assembly

As illustrated in Figure 6-7, the lower portion of the case not only provides an electrolyte sump but also encloses the other operating equipment. The major items are: electrolyte pump, gas pump, chilling heat exchanger, hydrogen/chlorine reactor, the chlorine-hydrate store container, and the hydrate former and filter. Also

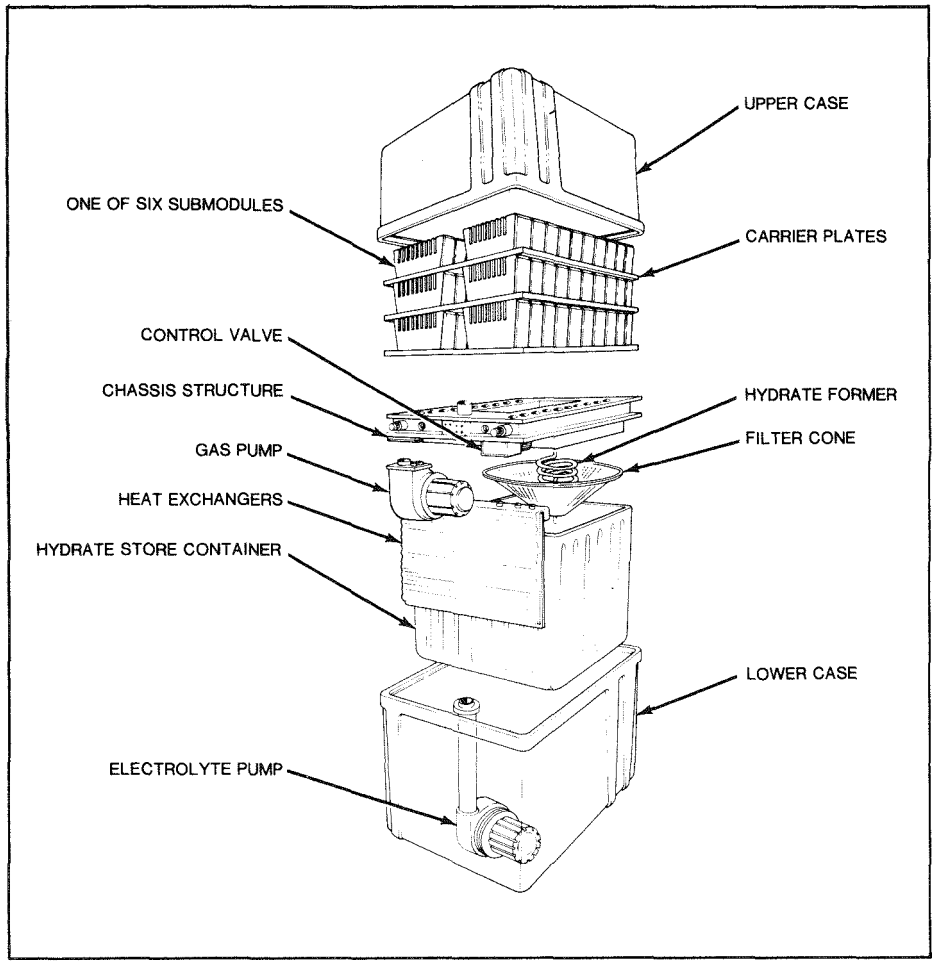

Figure 6-7. Exploded view drawing of Mark 4 battery module. Note that all connections to interior of case pass only through edge of chassis structure.

the control valves to operate the various subsystems are contained inside the case. To facilitate an assembly line approach to module buildup, the dividing shelf is developed into a chassis frame structure. This three layer assembly is constructed of several molded plastic parts bonded together to form a network of fluid distribution passages and several related mounting pads. It also provides a framework to which each of the major components of the system can be bench-assembled. As each of these components is mounted in place, the internal conduits of the chassis automatically provide the liquid and gas interconnection required between each element. Thus, most of the "piping" and most of the supporting structure for the battery module is provided by this chassis. In keeping with the assembly line concept, the chassis is designed to provide all the external connections required to

the module. The terminal posts are brought out through sealing glands molded in the front edge. Here also is placed the electrical connections for the pump power and module control data harnesses.

Close by on the same face are the connections for external coolant circulation so all will be accessible when the module is later installed in the rack. More importantly, however, by grouping all these outlets that breech the gas-tight casing in the edge frame of the chassis, they can be accomplished during final assembly and thoroughly tested before being enclosed by the case.

Pumps

Two pumps are required to operate this system. One is the main electrolyte circulation pump. The other is the hydrate-forming mechanism which draws chlorine gas from the stack area, intimately mixes it with chilled store liquid, and injects the resulting hydrate into the store vessel. The cost and dependability of these pumps must be considered extremely important in meeting the targeted specifications for this system. Also, because the power used for pumping reduces the net power output of the battery, efficiency must be stressed.

The design presented here incorporates a highly specialized fully-submersible pump-motor combination with canned rotors for each assembly. Achieving these efficiencies will require a pump carefully designed for this one specific job and engineered with absolute minimum losses in bearings and seals as well as very low hysteresis losses. Submersion eliminates openings in the battery case and the resulting sealing problems. It also provides constant cooling and, being consistent with the chassis mounting concept, greatly facilitates assembly of the module. A design that can be volume-manufactured with great precision at a reasonable cost will have to be developed to operate unattended for thousands of hours. Effort will be needed to develop such a single-purpose specialized package. However, at present, no particular technical problem is foreseen that would prevent successful achievement. A more complete discussion of zinc-chlorine battery-pump testing and evaluation is presented in Section 17 of Part III.

Final Assembly

After the bottom section of the module assembly is complete and checked, the stack is installed on the upper side of the chassis structure. The pair of submodules for each layer are mounted to a carrier plate. As each submodule is placed in position,

a set of tubular sleeves connect each unit cell manifold to an electrolyte feed chamber in the plate. When each carrier is mounted in the stack assembly, this feed chamber is connected by a similar but larger sleeve to the pump discharge ducts. Each carrier plate also contains channels to collect and route the returning electrolyte through chassis openings to the sump.

After the stack has been assembled, the electrical bus connections at the ends of each submodule are made. Titanium-clad copper buses lead from each external terminal post to pick up the flex connectors at the end of all submodules. A portable spot welder will make these connections. The flex connectors for each submodule are finger-like extensions of the titanium plate previously secured by welding to the graphite end-comb bus bars. At this point, with assembly complete except for enclosure, the module will likely be installed in a special test fixture and given a complete final checkout of all electrical, mechanical and hydraulic functions. After acceptance, it will be thoroughly cleaned and prepared for sealing.

The upper and lower case parts that enclose the battery module are designed for fabrication from a suitable fiber-reinforced plastic. A glass-reinforced polyester case, manufactured by a technique such as the matched-die process, is assumed for the purpose of costing in Section 8. The structual-foam manufacturing process, which is rapidly becoming a well-established widely-used technique for molding large rigid plastic parts, is a viable alternative for the case parts. Suppliers are presently developing fiber reinforcing techniques for this process, as well.

After inspection, each case section will be brought into place enclosing the upper and lower portions of the entire battery assembly. Each half will be pressure sealed to the edge section of the chassis structure. Leak testing to insure a proper seal will complete the assembly procedure. Overall dimensions of the finished module are 28-inches wide, 40-inches long, and 60-inches high.

RACK ASSEMBLY

The final stages of manufacture are those associated with assembling a number of completed modules into an appropriate package for peak-shaving applications. One of the objectives of this design was to maximize the work done under the controlled conditions of the factory and to minimize the labor required at the site. Another was to produce as efficient a shipping package as practical. Distribution from factory by over-the-road trucking is considered essential. Therefore, the reason-

able limitations of size and weight imposed by this handling method comprise a significant design criterion. Furthermore, it is necessary to achieve as dense a battery installation as practical in order to meet the target of 8kWh per square foot of occupied property.

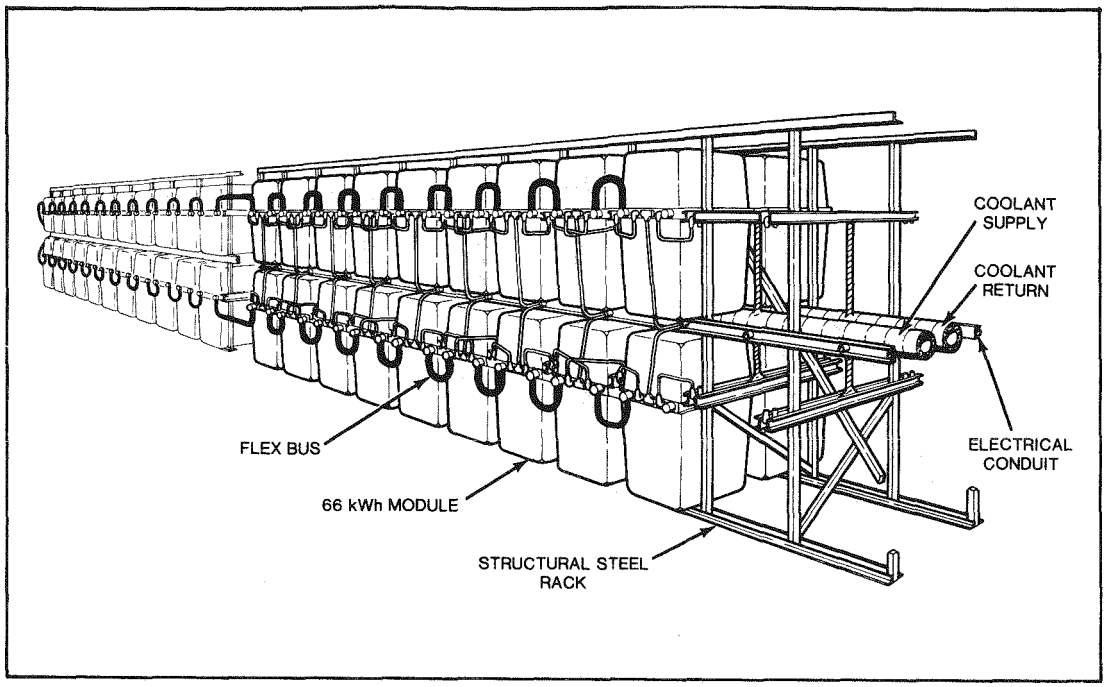

Figure 6-8. Detail of rack assembly showing central coolant and electrical distribution to each of the 66kWh modules. The drawing shows a second rack assembly in the background connected with flex buses.

The current design meets these criteria by factory-mounting 44 completed but dry modules onto one structural steel rack. The rack supports an array of modules two high and eleven long on each side as illustrated in Figure 6-8. Down the center of the rack is installed a piping system to distribute chilled coolant from a central source to each module. Short removable connecting pipes are used between the distribution points on the rack supports and the heat exchanger outlets of each module. This scheme allows each module to be removed independently, even in an operating system. Of course, the coolant distributor terminates in fittings provided for later connection to a central refrigeration source.

In the manufacturing plant all the individual electrical connections will be completed. Flex buses for dc power will be installed between each module. A pump-

power feed and module control harness pre-wired into the rack assembly will be plugged into each module and the whole assembly performance tested before leaving the factory.

The racking concept insures the use of well-trained highly-supervised labor and specialized factory equipment for total assembly and inspection of a very major portion of the battery plant. The use of factory test stands can insure that a complete and fully qualified 2.9MWh string is delivered to the customer. No labor affecting the operation of the battery need be performed in the field. The completed rack, ready for shipment, measures 87 inches wide, 28 feet 8 inches long and 11 feet 6 inches high. A dry shipping weight/rack, based on the projected dry module weight of 436 lbs/module and a projected total rack weight of 7,416 lbs, is estimated to be 26,600 lbs. This dry weight and the dimensions for length and width are quite suitable for highway trailer loading. The height of the load, however, may require some special routing. Upon delivery to the customer's utility site, the rack will be leveled on prepared footings, filled, and connected to the station bus and distribution networks.

BALANCE OF PLANT

There is, of course, more to a utility substation battery plant than the 36 factory-built racks just described. There is a system for providing chilled coolant to the hydrate formers. There is the dc power bus system. There is the power conversion or conditioning system that connects to the transmission network. There is the control system that operates and monitors the battery operation. In addition there will be related site preparation, structures, enclosures, and electrolyte handling facilities. Taken all together these are considered here as the "balance of the plant". For the most part this design intends these to be standard industrial components. Each will be supplied by competent specialists in the trade. Each will be engineered specifically for this purpose to take full advantage of all conditions and to meet the desired standards of quality, reliability, and efficiency.

Chilled Coolant System

The system which distributes chilled coolant to each battery module for hydrate formation will consist of four parts. These are a basic-1250 ton unitized refrigeration plant, a glycol-type coolant pumping station, a set of evaporative cooling towers for both refrigerant condensing and for direct glycol cooling, and a prefab-

ricated piping network to serve as a glycol distribution network. The first three items will be skid-mounted packages delivered to the site as pretested operational units. They may be described as follows:

- Refrigeration Skid - This package will contain a 1500-HP, 3600-rpm, 4160-volt motor driven rotary-screw R-22 compressor, an expander for chilling the glycol-type coolant, and a liquid-cooled shell and tube condenser with receiver. The package will be complete with full pressure lube system, automatic controls for loading between 10% and 100% of rated capacity, safety and relief equipment, and all necessary accessories and piping.

- Cooling Tower Skid - This package will consist of five 300-ton induced draft evaporative cooling towers. Each will be supplied complete with sumps, pumps, fans, approved wet deck, distribution basin, louvers, drift eliminators and all control, safety, and monitoring equipment.

- Coolant Pumping Station Skid - This package will contain three 4000-gpm 100-HP motor-driven coolant pumps. Each will be supplied from a single receiver tank and piped into a discharge manifold with valving to circulate a glycol/water-type coolant. The package will be complete with all necessary starters, operating and safety controls, and related accessories.

Also supplied by the refrigeration contractor will be an engineered piping system to circulate the chilled glycol-coolant throughout the array of battery module racks. This will be supplied as a complete set of prefabricated and pretested assemblies including pipes, fittings, valves, and connectors.

The design shows this piping system located overhead as is the bus system. This affords complete unrestricted access at ground level to all modules in every rack. In this case the prefabricated-insulated-glycol-distribution network will be erected at the site after the racks and refrigeration equipment are in place.

An alternative to be considered for some sites is the standard industry practice of installing the coolant distribution network underground. The added site preparation costs, in some cases, would be offset by the reduction of certain insulation expenses. Certain circumstances (terrain) might make this the preferred installation method, as well as provide free access for servicing of all modules.

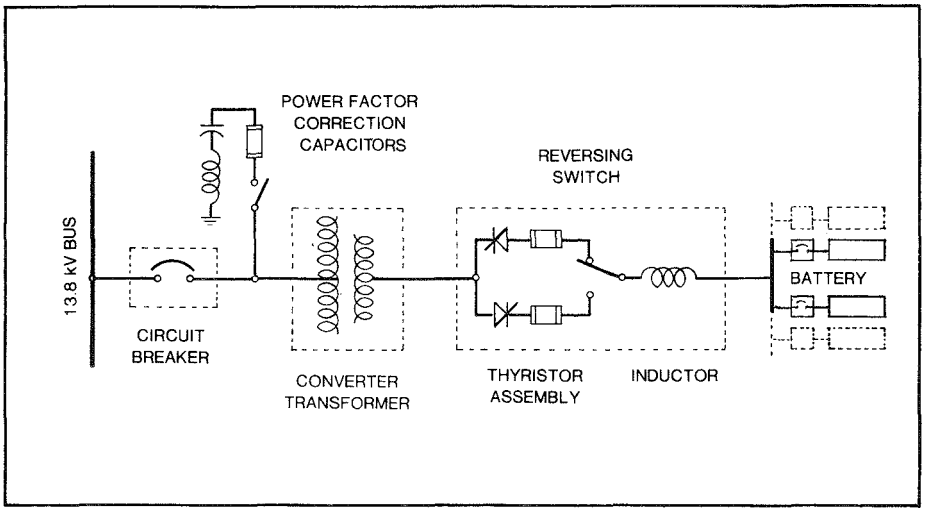

Figure 6-9. Single line diagram of power converter for use with a 100MWh zinc-chlorine peak-shaving battery plant.

Power Conditioning Equipment

The design and capacity of the power converter planned for this substation battery is based on existing technology and is very similar to the thyristor-controlled rectifier equipment currently supplying dc power to the chlor-alkali and metal refining industries. There is presently installed several hundred megawatts of this equipment with single units as large as 40 megawatts, operating successfully at rated capacity day in and day out 24 hours a day. Figure 6-9 schematically illustrates the converter designed for use with the zinc-chlorine battery in an electric utility peak-shaving substation. The major elements are described as follows:

- AC Circuit Breaker - A conventional air circuit breaker is used to disconnect the substation from the bus in the event of a fault. The circuit breaker is rated according to the 13.8KV bus short circuit capacity.

- Converter Transformer - The transformer is of a conventional rectifier-type design. It is oil immersed, forced-oil/forced-air cooled.

- Thyristor Assemblies - The thyristor assemblies are arranged to achieve a 3-phase bridge circuit configuration. The thyristor devices used are of flat package type. The geometry of each parallel thyristor group is such as to achieve current sharing (with ±10% of the design value) among the paralleled thyristors.

- Reversing Switch - The switch is used to reverse polarities when switching the mode of operation from charge to discharge. The reversing switch is motor-operated and is electrically interlocked with the AC breaker and thyristor circuits to insure that the switching is performed under no-load conditions.

- DC Inductor - The DC inductor is supplied to allow commutation (switching) of the thyristors when the system is operating in the discharge mode. It also limits the fault current into the converter in the event of a converter fault. In the charge mode, the inductor provides for current smoothing if so required by the battery system.

- Power Factor Correction Capacitors - The capacitors are supplied to insure high power factor performance. The series inductors are provided to prevent harmonic resonance within the system.

The power rating of a converter package is determined by the maximum charge voltage and the maximum discharge current that must be accommodated. As a consequence of the flat time-voltage profiles for the zinc-chlorine battery on both charge and discharge, the rating of this conversion equipment can be kept low. With a discharge voltage only 10% lower than the charge voltage for the battery, the converter rating need be only 10% greater than the power output rating of the battery system.

The uncorrected power factor is proportional to the ratio of the discharge voltage to the charge voltage; therefore, if this ratio is high, as in the case of the zinc-chlorine system, the needed capacity of power factor correction capacitors is minimized. Furthermore, should it be required that the power factor remain relatively constant throughout the discharge cycle, the flatness of the zinc-chlorine battery discharge profile would minimize the need for automatic switching devices in the power factor correction circuit.

The power conditioning equipment will be designed to the highest industrial or utility standards and will meet the latest applicable standards of ANSI, IEEE, and NEMA. The basic specifications for the system are outlined in the following paragraphs:

- DC Rating - 23MW, 24KA, 960V dc

- AC Rating - 23MW 13.8KV (±2-1/2%) 3 phase 60 Hertz.

- Reserve Rating - The converter is rated to supply 100% full power continuously with at least one thyristor per phase out of service.

- Efficiency - 98% at full power rating -- each way.

- Power Factor - Corrected to achieve value required by utility customer.

- Control - Accuracy to ±1% of rating, stability to ±0.5% of rating.

- Instrumentation and Monitoring - Recording or indicating instruments for all voltages, currents, power, and ampere-hours. In addition, monitor signals will be provided for overcurrents; overtemperatures; oil, air, and coolant calculation pressures; or thyristor fuse failure.

- Temperature Ratings - Ambient 40°C maximum, 30°C daily average. Transformer 65°C hot spot rise, 55°C average. Converter internal ambient 40°C maximum. Thyristor junction temperature 100°C.

- Cooling - The transformer is cooled by forced circulation of the immersion oil through a forced air-to-oil heat exchanger.

  Thyristor cooling is by means of continuously de-ionized water (to ensure minimum corrosion due to electrolytic action between parts at different potentials) recirculated through a water-to-water heat exchanger.

  Enclosure cooling for buswork, fuses, etc., is by means of forced air circulation through air-to-water heat exchanger.

- Physical Dimensions - The equipment, packaged on three skids for delivery to the site, will occupy a space 18-feet by 38-feet by 12-feet high and will have a total weight of approximately 150,000 pounds.

DISCUSSION

The ensuing paragraphs present the more significant advantages and disadvantages of this concept and compares them to other proposals that have been previously considered. Certain elements of the design that are thought to present some difficulties are discussed. An attempt is made to suggest the direction that might be taken to overcome these difficulties.

Mark 4 Advantages

Earlier work on zinc-chlorine battery plants envisioned strings of relatively few, very large stack modules connected to a few separate large-capacity stores. This is

in contrast to the present concept of a great many small modules with both stack and store integrated into a single package. Some significant construction and siting advantages are revealed by comparing these divergent concepts. Firstly, the small package is duplicated many, many times. This, and its modest size, make it very amenable to the classic assembly-line method of manufacture. This not only applies to construction but to quality control and proof testing. Also, since a number of these small modules are packaged together in a shippable end-use rack, a complete 2.9MWh portion of the plant is fully provable at the factory. None of this is possible with earlier concepts. Testing of the earlier alternates was possible only after field erection was complete.

Herein is suggested another advantage of the Mark 4 over previous designs. Coolant liquid, a standard glycol-mix, is the only medium circulating about the plant site. This can be accomplished using ordinary materials and standard trade practices. In prior concepts both liquid electrolyte and gaseous chlorine needed to be piped between each stack module and a remote store container. Such piping would be successful only by employing very specialized skills and techniques. Also, of course, such an exposed piping system would be more vulnerable to damage or to leakage. In Mark 4 all electrolyte and chlorine are safely sealed within the integrated module.

This is another advantage of the Mark 4 design. The module case is only a 35 cubic foot container, whereas the module case in earlier designs approached 450 cubic feet. Such large assemblies would need multiple exterior attachments for such items as gas and liquid piping, pump installations, and power terminals. All this implies a difficult sealing procedure important for retaining the battery material, and for the exclusion of air. The self-contained Mark 4, on the other hand, is designed to be hermetically-sealed at the factory. No service of the module is intended, therefore only the liquid drain plug, the electric power and control terminals, and small fittings to circulate coolant fluid breach the case. These can be factory-sealed and inspected before delivery.

As has been stressed in earlier sections of this report, the only way currently known to achieve the very high coulombic efficiencies and thus the desired operating efficiencies in this battery is to charge the stack while under a small vacuum. This reduces the chlorine dissolved in electrolyte and reduces chemical corrosion losses of zinc metal. This requirement was not fully appreciated when previous concepts were proposed. Those large stack structures were designed to operate only at

atmospheric pressures. To make them structurally capable of supporting even a very modest vacuum would be very inefficient and costly. The much smaller surfaces of the Mark 4 module can be more effectively engineered to withstand the stresses of operating at reduced pressure. By combining the insulating and structural qualities of a rigid foam core, a cost-effective, lightweight case can advantageously be developed.

The EDA zinc-chlorine battery contains very little chlorine gas and no liquid chlorine at all. In a fully-discharged battery, 98% of the required chlorine is held in a zinc chloride salt solution. In a fully charged battery, 88% of the chlorine is held as solid hydrate crystal in chilled water, with 10% remaining combined in salts. During discharge, the hydrate is warmed and releases gaseous chlorine for transfer from the store to the battery cells to combine electrochemically with zinc to produce electric power during discharge. This is performed under controlled conditions within the sealed battery case.

If by some remote chance a catastrophic event would allow the stored hydrate to be expelled from its insulated container or to absorb a great deal of heat quickly from an outside source, it could result in chlorine gas entering the surrounding atmosphere. In this very unlikely event it would be better to have the hydrate dispersed in many separate containers rather than one or two very large ones. It is an advantage that only 30 gallons of hydrate are sealed in each Mark 4 module compared to some 2000 gallons or more collected in the large stores of earlier proposals.

Mark 4 Disadvantages

Of course, the advantages discussed above for this concept have not come freely. They have been paid for with the price of certain counterbalancing disadvantages. Generally these are the corollaries of the advantages sought in earlier proposals.

Unit package size is the most obvious contrast between this and earlier studies. While it is generally true that electrochemical systems do not benefit from scale-up, this is not true for some of the mechanical auxiliary systems. A single 100MWh zinc-chlorine peak-shaving battery plant, for instance, holds 92,000 gallons of electrolyte and 127,000 gallons of hydrate. Other things being equal it is more efficient and less expensive to store these quantities in a relatively few large tanks than in hundreds of small tanks.

Similarly, a typical 100MWh peak-shaving plant requires the circulation of about 154,000 gallons of electrolyte each minute. It is generally recognized that this can be accomplished with least cost and most efficiency using a few of the largest practical size pumps possible. EDA employed 110 separate 1400gpm pumps in early proposals. This Mark 4 design employs 1,584 separate pumps each at 95gpm to do this same job. Certainly, the cost of power and possibly the cost of pumps will be higher with this multiple concept. As explained elsewhere in this report, the small submersible pumps proposed for this application efficiently handling acidic zinc chloride salt solutions sealed inside a battery for 2000 cycles must be very highly-developed, special-purpose units. Because of the number of such pumps required, the manufacturing cost will be one of several important design criteria. Considering this aspect, 1,584 small mass-produced pumps might have a capital cost competitive with 110 large custom-built pumps.

Much the same philosophy must be applied to heat exchangers, control units, and hydrate-forming devices. All are small specialized components used in great numbers in the Mark 4 proposal. In earlier designs fewer were used -- each a large, efficient unit. It must be determined whether the economics of mass production can successfully compete with the economies of scale in these large hydraulic mechanisms and storage facilities.

Another disadvantage of the Mark 4 suggested from the preceding considerations is the matter of reliability. Previous designs required 110 motors, pumps, or control elements and from 3 to 24 hydrate forming devices to work together at once for a complete plant. The Mark 4 design requires 1,584 motors, pumps and controls, as well as 1,584 hydrate formers all to work together at once for a total plant. Needless to say, the failure of a few components will affect a much smaller portion of the plant but the incidence of failure will be greater. As yet, there is no experience with multiple groupings of zinc-chlorine batteries. Not enough is known about what effect the malfunction of one component or one module in such an array would have on the overall performance. More work will be needed to determine reliability predictions. It is certain, however, that extremely reliable components are needed.

An additional disadvantage of the Mark 4 design is the accumulation of inert gases in the battery modules. Earlier versions with remote stores collected and piped chlorine gas to the few hydrate formers. These large accumulated quantities of gas were passed through an electrolytic chlorine/inerts gas processor to remove carbon dioxide and air that are found mixed with the chlorine. Whether introduced by

leakage or generated by electrochemical reaction, these foreign gases tend to degrade the system's performance if allowed to accumulate. The type of gas processor envisioned for these central systems is possibly unsuited for scaledown to the smaller, unvented units. The Mark 4 module concept may require a different approach to handling these inert gases. Concepts in this area are being developed and some are discussed in Part V, Section 36 of this report.

Table 6-1 summarizes the advantages and disadvantages that are discussed in these paragraphs. The cost savings and the cost penalties of the straight economic factors appear offsetting. Much weight needs to be given to the safety and the performance advantages. In the long run, of course, these too will translate into important economic points. Assuming that the problem of handling foreign gases is satisfactorily solved, the major limitation on the small module concept is reliability. A substantial amount of engineering will be required to bring this to a satisfactory level from both the operational and manufacturing standpoints. On balance, the Mark 4 is the most satisfactory design yet proposed to approach all the criteria known at present.

Table 6-1

ADVANTAGES AND DISADVANTAGES OF MARK 4 CONCEPT

Advantages

- Practical method of chlorine desorption
- Widely-dispersed chlorine storage
- Hermetically-sealed case
- Only coolant piping on site
- Maximum use of assembly line techniques

Disadvantages

- Many small auxiliaries affect reliability
- Economies of scale replaced by economies of mass production - possible cost penalty
- Requires new approach to inert-gas handling

REFERENCE

6-1 Development of High-Efficiency, Cost-Effective, Zinc-Chlorine Batteries for Utility Peak-Shaving, 1976. Palo Alto, Calif.: Electric Power Research Institute, March 1978, EPRI EM-711.

Section 7

MANUFACTURE OF COMPONENTS FOR 100MWh BATTERY PLANT

INTRODUCTION

What follows is a conceptual manufacturing plan conceived for the purpose of estimating the factory cost of the first commercial-plus-five zinc-chlorine battery. Although the processing appears to be specific, a complete set of product design drawings for each detail part that specifies the material, dimensions, tolerances, and quantities is not available to develop an actual plan. The conceptual manufacturing plan is based on the engineering specification and design concept as presented in Sections 5 and 6, and a production rate of 568 battery rack assemblies (25,000 battery modules) per year.

Since insufficient information is available for performing meaningful economic analyses of alternatives, major components such as pumps, case, heat exchangers, hydrate container, chassis structure, hydrogen/chlorine reactor, filter, store coil, electrical connectors, valves and other plastic parts were arbitrarily determined to be purchased items. The above items are similar to existing manufactured products and, by extrapolation, reasonable cost estimates were obtained.

In respect to the battery design, it must be emphasized that many trade-offs are to be made between the present engineering design and the ultimate production design; and, as cost and design studies become more detailed, the discrepancies between the present design and the production design become more evident. Many evolutionary changes are expected in the transition from the present technology to a semi-mature technology.

MANUFACTURING PROCESS

The manufacturing process, which is primarily an assembly operation, is divided into the following areas:

- Graphite processing area
- Module assembly area
- Rack assembly area

Graphite Processing Area

The graphite processing area is a highly automated operation that machines large quantities of graphite components, and assembles these components and purchased items into the submodule assembly. The following production rates of components and subassemblies are required to produce 600 submodules per three-shift day;

- Comb assemblies -- 6600/day
- Zinc bus bars -- 600/day
- Chlorine bus bars -- 600/day
- Intercell bus bars -- 6000/day
- Chlorine electrode assemblies -- 120,000/day
- Chlorine electrode plates -- 240,000/day
- Zinc electrode plates -- 126,000/day

In brief, graphite electrodes and bus bars are machined in the graphite process area, utilizing state-of-the-art equipment such as band saws, belt sanders, slicing machines, slotting machines, and drill presses. These components and other purchased items are assembled with other purchased items with yet-to-be-specified conveyor and automated assembly machines. Submodule process/route sheet, Table 7-1, and submodule assembly flow sheet, Table 7-2, provide a more detailed description of the submodule manufacturing process. The submodule assembly flow sheet describes the sequence, operation, material flow, and estimated man-hours for each operation. The submodule process route/sheet, which is keyed to the assembly flow sheet with the number of each operation, provides a more detailed description of each operation and the equipment used.

Table 7-1

SUBMODULE ASSEMBLY ROUTE/PROCESS SHEET

Operation Number	
1	Graphite blocks to be used for preparing graphite buses are received, inspected and inventoried.
2	These graphite blocks are transported from inventory and fed into band saws that size them into blocks having the length and width dimensions of the bus.
3	The sized block is conveyed to another set of band saws that slice the sized blocks into bus bar blanks.
4	The blanks are passed between a set of ganged saws producing slots in the buses.
5	The buses are cleaned and inspected for conformance with specification.
6	A portion of the prepared buses are sorted for construction into end-buses. Holes are bored into the buses.
7	These buses are backed by titanium sheet and welded to the bus through the holes.
8	Graphite blocks to be used for preparing the zinc electrode plates are received, inspected, and inventoried.
9	The graphite blocks are transported from inventory and fed into band saws that shape them into smaller sized blocks having the length and width dimensions of the plate.
10	The sized blocks are transported and loaded into slicing machines that size the blocks into plates of specified thickness.
11	The sliced plates are cleaned and inspected. They are then conveyed to the comb assembly, operation 17.
12	Porous graphite blocks to be used for preparing the chlorine electrode plates are received, inspected, and inventoried.
13	The graphite blocks are transported from inventory and fed into band saws that shape them into smaller sized blocks having the length and width dimensions of the plate.
14	The sized blocks of porous graphite are transported and loaded into machines that slice the blocks into plates of specified thickness.
15	The sliced plates are cleaned and inspected.
16	The plates are assembled into plastic frames producing chlorine electrode assemblies. These are conveyed to operation 17 -- comb assembly.
17	The buses and end buses from operation 7 merge with the electrodes from operations 11 and 16 in the comb assembly machines. The electrodes are pressed into the slots in the buses.
18	The finished combs are transported to the submodule assembler. This device alternately positions combs and tray sections together to build up a submodule. As parts are completed, a carrier plate is set into position and the tube connections pressed in place. The assembly is inverted so as to be ready for the next operation.
19	This submodule assembly is transported to a test stand where it is filled with activating solution and activated.
20	The submodules are tested upon completion of the activation in order to assess conformance with specifications. This operation completes the submodule assembly.

Table 7-2

SUBMODULE ASSEMBLY FLOW SHEET

(Labor given in manhours per module)

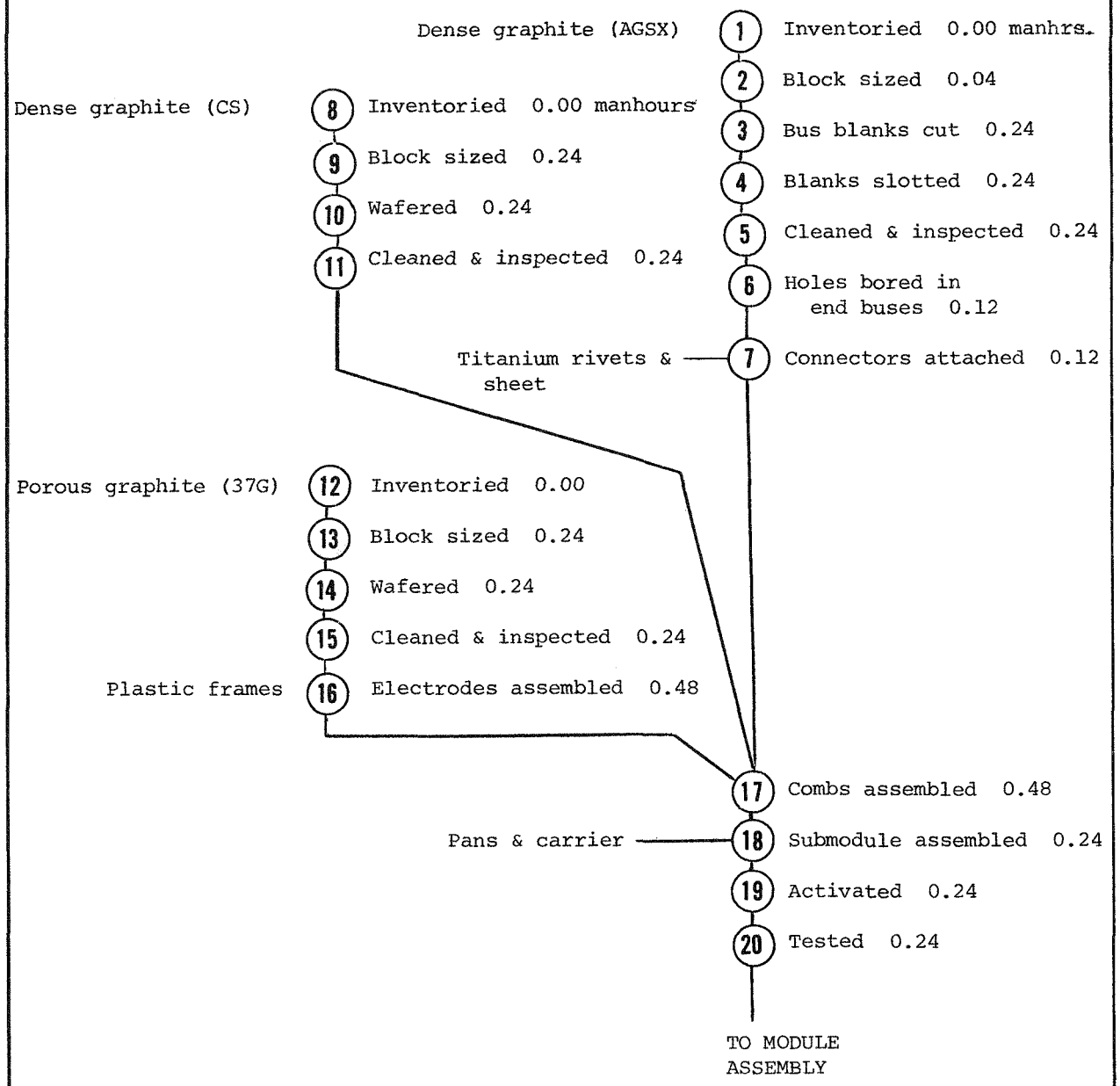

Module Assembly Area

The module assembly area is an assembly line operation that utilizes hand labor and simple tools to assemble the battery module at a rate of 100 modules per day on a

two-shift operation. Figure 7-1 visualizes the module assembly. The module assembly route/process sheet and flow sheet, Tables 7-3 and 7-4, are included to provide a description of the module assembly manufacturing process.

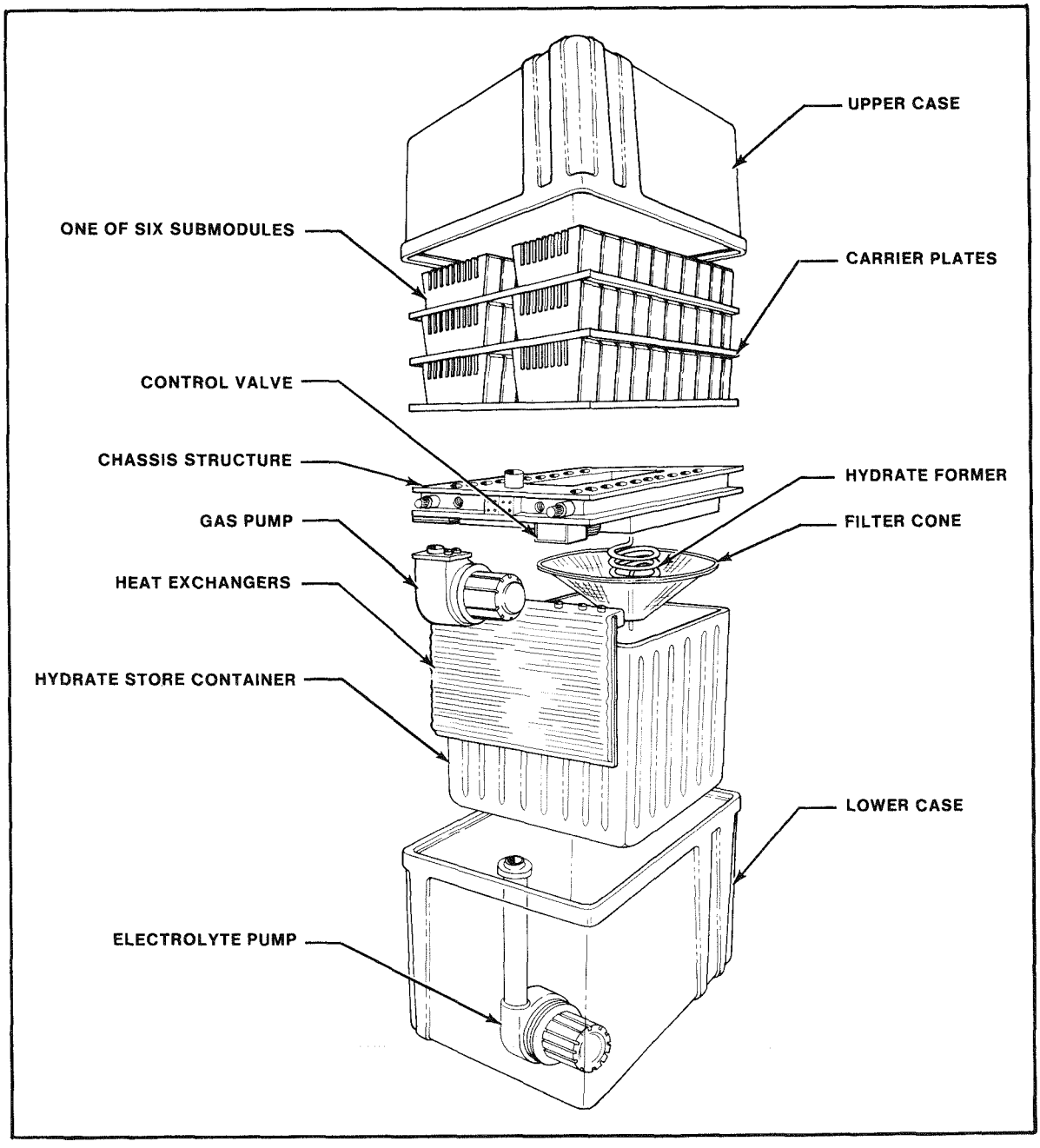

Figure 7-1. Exploded drawing of proposed Mark 4 battery module. Note stack supported in upper section by chassis while sump, store, and auxiliaries are mounted to underside.

Table 7-3

MODULE ASSEMBLY ROUTE/PROCESS SHEET

Operation Number	
21	The chassis structure is received partially assembled. The manifold assembly parts are cleaned and prepared for subsequent operations. The reactor assembly is installed in the receptacle provided. The control valve is installed on the side of the manifold plate. The probe connections are threaded through and sealed into the orifices provided. The external current terminals are installed at this time.
22	The chassis structure assembly is placed on a conveyor, top surface down. The filter assembly is then attached.
23	Through the center of the filter assembly, the store coil is passed and inserted into the chassis structure.
24	The store tube is placed over the store coil (hydrate former) and filter assembly. It is then sealed to the chassis structure.
25	The electrolyte pump, coupling and motor combination is installed with a standpipe that serves to route the outgoing flow through the chassis structure. The electrical lines from the pump motor are threaded through the designated opening in the integrated manifold.
26	The gas pump, coupling, and motor combination are installed together with connecting tubes. These tubes are inserted and sealed into the chassis structure.
27	The heat exchanger is installed and connected into the designated openings in the chassis structure.
28	The lower case is installed and sealed in place. The assembly is now turned over for the next operation.
29	Six submodules, as prepared in step 7, are installed on the top surface of the chassis structure.
30	The electrical connectors are installed so as to interconnect each submodule and the electrode terminal taps on the chassis structure.
31	The case cover is placed over this assembly and bonded in place.
32	The module is filled with helium and leak-checked.
33	A 1% sample of the production batteries is filled with $ZnCl_2$ and cycled as a performance check.

Table 7-4

MODULE ASSEMBLY FLOW SHEET

(Labor given in manhours per module)

Chassis structure	21	Assembled 0.32 manhours
Valve		
Probes		
Reactor		
Filter	22	Installed 0.04
Store coil	23	Mounted 0.04
Store container	24	Bonded in place 0.08
Electrolyte pump	25	Mounted 0.16
Gas pump	26	Mounted 0.16
Heat exchanger	27	Installed 0.16
Lower case	28	Bonded in place 0.16
SUBMODULES ASSEMBLIES	29	Installed on manifold plate 0.32
Electrical connectors	30	Attached 0.32
Case cover	31	Bonded in place 0.16
Helium	32	Leak test 0.16
$ZnCl_2$ electrolyte	33	Sample modules cycled 0.00

Rack Assembly Area

The battery rack assembly area is a fixed position operation that installs 44 battery modules into a steel rack with the appropriate controls, buses, and plumbing at a rate of 2.27 racks per day. Battery-rack route/process sheet and flow sheet are included as Table 7-5 and 7-6.

Table 7-5

BATTERY RACK ASSEMBLY ROUTE/PROCESS SHEET

Operation Number	
34	The steel rack components are assembled. The modules are mounted and secured in place.
35	The rack and modules are wired. This is done with a wiring harness for delivering power to the auxiliaries subsystems and carrying the sensor information. The rack control package is installed. The modules are bused together.
36	The coolant lines are installed and interconnected to each module.
37	The modules are filled with electrolyte and tested. The electrolyte is then removed from the battery.
38	The rack is prepared for shipment.

Table 7-6

BATTERY RACK CONSTRUCTION FLOW SHEET

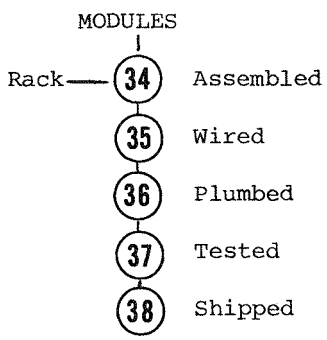

Direct Labor per rack = 160 manhours

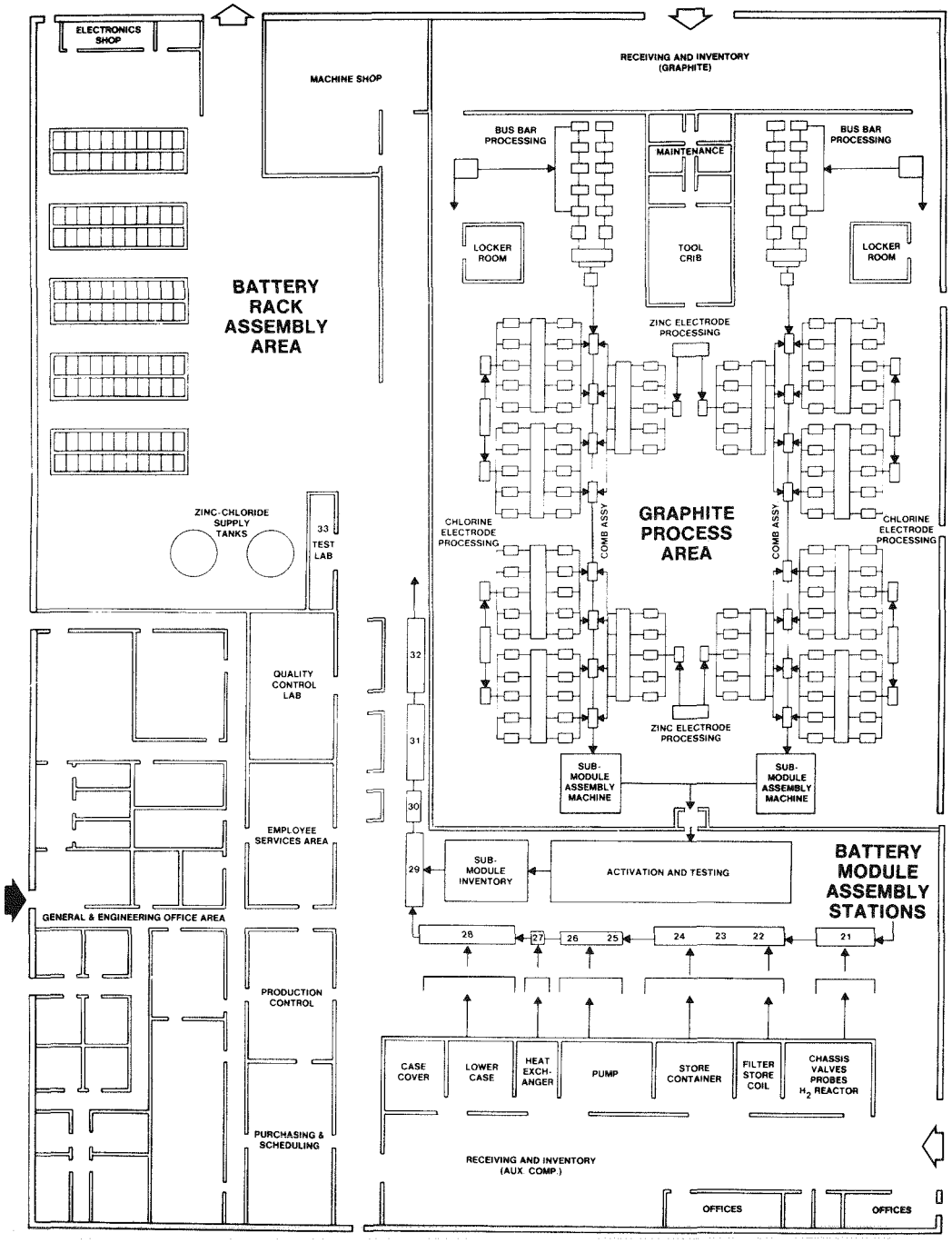

Figure 7-2. Battery Plant Layout

MANUFACTURING PLANT

A schematic layout for a zinc chlorine battery manufacturing plant, sized to produce 100 battery modules per day, is shown in Figure 7-2. The plant will occupy 125,000ft^2, have a labor force of 207 employees (84 staff and 123 direct), and will be divided

into three major work areas that will be equipped with 174 production machines, a submodule activation station, and a module test station. The basis on which this layout is derived is presented below.

Table 7-7 summarizes the type of process equipment required in terms of quantity and estimated cost, and references the operation or operations where the equipment is utilized. The following is an analysis of the previous processing scaled to a 100 module/day capacity. The justification for the equipment is summarized in Table 7-7, together with the projected labor requirements.

Table 7-7

PROCESS EQUIPMENT, MANPOWER AND PLANT CAPACITY REQUIREMENTS

Capacity Note - Operations 1-20 produce 600 submodules per day on a three-shift per day basis. This is consistent with a 100 module per day (6338kWh/day) production level.

Operation Number	Graphite Processing	
1	The incoming inspection and inventorying of the AGSX dense graphite blocks is an indirect item. The indirect labor requirements and general plant requirements have been estimated. This listing is presented in another tabulation.	
	Process equipment cost	No major equipment
	Estimated direct labor	No direct labor
2	The block is sized by passing it through a series of belt sanders. This operation removes both the surface skin of the graphite and brings these blocks to within the length and width dimensional tolerances. This is a fast operation capable of removing thin layers of graphite at 40 feet per minute. This same equipment, also, removes the skin from the blocks in operations 9 and 13. The blocks are loaded and handled automatically.	
	Process equipment cost 2 compound belt sanders at 50K$/ea	100,000
	Estimated direct labor	4 man-hours
3	The blocks are cut into slabs on automatically fed bandsaws. The daily production is 6,600 blanks. Each requires a 10-inch cut at a feed rate of 3 inches/min plus a 0.5-minute reset per blank. This requires 421 hours of cutting. On a twenty-four hour basis, 20 bandsaws in continuous operation are required.	
	Process equipment cost 20 bandsaws at 15K$/ea	300,000
	Estimated direct labor	24 man-hours

Table 7-7
(continued)

Operation Number	Graphite Processing
4	The blanks produced in the preceding operation pass between an upper and lower set of gauged saws producing slots. Allowing a fifty second cycle time for each of the 6,600 blanks produced per day, 4 machines are required for operation on a 24-hour basis. Process equipment cost 4 slotting machines at 20K$/ea — 80,000 Estimated direct labor — 24 man-hours
5	The bus bars are cleared and inspected. This is automatic operation in which the blanks are cleared of dust and inspected for cracks and broken edges. Process equipment cost Bus cleaner and comparator 2 machines at 15K$/ea — 30,000 Estimated direct labor — 24 man-hours
6 & 7	For every eleven (11) buses, two are prepared as end buses. This operation involves drilling six holes per end bus, attaching a titanium sheet to one side and then fastening the sheet to the bus through the holes. Twelve-hundred end-buses are required every 24 hours corresponding to a production rate of 50 pieces per hour. Process equipment cost 2 driller-fasteners at 25K$/ea — 50,000 Estimated direct labor — 24 man-hours
8	Same as operation 1 except that the graphite blocks are CS material. Process equipment cost — No major equipment Estimated direct labor — No direct labor
9	The skin is removed from the block using the same equipment described under operation 2. The resulting blocks are then sized so as to produce a block having the length and width dimensions of the electrode plate. This sizing is done by bandsaws having a 4.5 minute cycle time. Two cuts are required in order to produce three sized blocks. In order to make 1,067 cuts over a 24 hour period, 4 bandsaws are required. Process equipment cost 4 bandsaws at 15K$/ea — 60,000 Estimated direct labor — 24 man-hours
10	The blocks are automatically loaded into slicing machines. These machines are required to produce 126,000 plates per day. Taking a 13.5-second cycle time per plate, 20 machines are required.

Table 7-7
(continued)

Operation Number	Graphite Processing	
10 (cont'd)	Process equipment cost 20 slicing machines at 36K$/ea	720,000
	Estimated direct labor	24 man-hours
11	Same as operation 5 except that the cleaning and inspection is of electrode plates made of CS material. Also, the operation must process 96 plates per minute over a twenty-four hour period.	
	Process equipment cost Plate cleaner and comparator 4 machines at 10K$/ea	40,000
	Estimated direct labor	24 man-hours
12	Same as operation 1 except that the graphite blocks are porous 37G material.	
	Process equipment cost	No major equipment
	Estimated direct labor	No direct labor
13	The skin is removed from the block using the same equipment described under operation 2. The block is then sized as described in operation 9, except that approximately twice the number of plates are required.	
	Process equipment cost 8 bandsaws at 15K$/ea	120,000
	Estimated direct labor	24 man-hours
14	Same as operation 10 except that the machines are required to produce 240,000 plates over a 24 hour period. Forty machines are required.	
	Process equipment cost 40 slicing machines at 36K$/ea	1,440,000
	Estimated direct labor	24 man-hours
15	Same as operation 5 except that the cleaning and inspection is of plates made of 37G material. Also, the operation must process 167 plates per minute over a 24 hour period.	
	Process equipment cost Plate cleaner and comparator 8 machines at 10K$/ea	80,000
	Estimated direct labor	24 man-hours
16	The porous plates are assembled into chlorine electrodes by bonding them into an injection-molded plastic frame. This machine is automatically loaded and has a cycle time of 35 seconds. Forty machines are required for production over a 24-hour period.	

Table 7-7
(continued)

Operation Number		
	Graphite Processing	
16 (cont'd)	Process equipment cost 40 chlorine electrode assembly machines at 47.5K$/ea	1,900,000
	Estimated direct labor	48 man-hours
17	The combs are assembled in this operation. The buses, zinc electrodes and chlorine electrodes are conveyed and loaded into the assembly machines. The comb assembly operation presses these assemblies into the slots on one side of the bus counterbalanced by the pressing of the dense electrodes into the groove on the other side of the bus. This operation also schedules the end bus assembly which requires that electrodes be inserted on only one face. The comb assembly has a cycle time of 3.8 minutes so that sixteen machines are required.	
	Process equipment cost 16 comb assemblers at 45K$/ea	720,000
	Estimated direct labor	48 man-hours
18	The submodule assembly operation requires an assembly machine that locates the comb assemblies and end-comb assemblies, interlaces the submodule pan sections and then locates the submodule carrier over the pan. Upon completing this assembly, the submodule is turned over so that the shelf rests on a conveyor taking it to the next sequential operation. The cycle time for this operation is three minutes per submodule. This operation is staffed by one worker per shift.	
	Process equipment cost 2 assembly machines at 100K$/ea	200,000
	Estimated direct labor	24 man-hours
19 & 20	The submodules are transported to the activation and test work station. Twenty-five test positions are required having a sixty-minute cycle time. The associated equipment includes a hood, rectifiers and a data acquisition system. The automated operation and the visual inspection of twenty-five submodules per hour per shift are made.	
	Process equipment cost 25 test stations complete	250,000
	Estimated direct labor	48 man-hours
	Module Assembly	

Note: Operations 21-38 are based on two shifts per day.

Table 7-7
(continued)

Operation Number	Module Assembly
21	The module assembly begins by the inspection and check of the chassis structure. All parts are checked for obstructions. A valve, three probes, and the reactor are installed. This operation is performed by 2 workers per shift. Process equipment cost — No major equipment Estimated direct labor Assembly — 32 man-hours
22 - 24	On an assembly line, the assembly from operation 8 is modified by three successive operations at a single station. The filter, the store coil, and the store tub are installed. These are fast hand operations performed by one worker per shift. These are routine hand operations. Process equipment cost — No major equipment Estimated direct labor — 16 man-hours
	At this point, the chassis structure lies flat on the assembly line with the tub attached. The electrolyte pump is connected with a section of plastic manifold-piping. The sealed electrical wires are threaded through the chassis structure. The operation is performed by one man per shift. Process equipment cost — No major equipment Estimated direct labor — 16 man-hours
26	Similarly, the gas pump is installed. Process equipment cost — No major equipment Estimated direct labor — 16 man-hours
27	The heat exchanger is installed rapidly by hand. One man is required for the entire production. Process equipment cost — No major equipment Estimated direct labor — 16 man-hours
28	The lower case is placed over the assembly and bonded in place. One man per shift operates the bonding equipment that seals the lower case to the integrated manifold assembly. Process equipment cost Lower case sealing equipment — 10,000 Estimated direct labor — 16 man-hours
29	In this operation, the submodule assemblies arrive together with the lower case assemblies. The lower case is inverted and the submodules located and secured. The finished assembly is then conveyed to the next station. An estimated 2 men per shift is required. Process equipment cost — No major equipment Estimated direct labor — 32 man-hours

Table 7-7
(continued)

Operation Number		
	Module Assembly	
30	The electrical connectors (i.e., the internal module buses) are installed and connected. This assembly is estimated to require 2 people per shift.	
	Process equipment cost	No major equipment
	Estimated direct labor	32 man-hours
31	The case cover is bonded in place. This is performed by one man per shift.	
	Process equipment cost	
	Case cover sealing equipment	10,000
	Estimated direct labor	16 man-hours
32	The modules are helium leak-tested to check the sealing. One man performs this task per shift.	
	Process equipment cost	
	Helium leak-test equipment	30,000
	Estimated direct labor	16 man-hours
33	The module production is sampled and a test cycle is run to determine adherence to operating specifications. This is a quality assurance check which does not involve direct labor.	
	Process equipment cost	
	Rectifier, controller, data acquisition system	60,000
	Estimated direct labor	No direct labor
	Battery Rack Assembly	
Note:	Since a rack contains 44 modules, the production rate of completed battery racks is 2.27 per day, on the average. The estimated labor rates will be given in terms of the labor requirement per rack and the labor requirement per 100 modules (one day's productions).	
34 - 38	These assembly operations deviate from the assembly line concept. Each rack is assembled in a bay area by a crew of workers. Only small tools are required for the direct processing. The transport of parts is considered indirect for accounting purposes. The operations are staggered but in some cases take place simultaneously. This includes rack assembly, module installation, wiring, plumbing, testing and shipping. The construction of a rack takes place over about a two day period.	
	Process equipment cost	No major equipment
	Estimated direct labor	162 man-hours/rack
		68 man-hours/100 modules

Plant Layout

As previously stated, the manufacturing plant is described as divided into three areas, graphite processing, module assembly, and battery rack assembly. The graphite process area is subdivided into two process lines with eight comb assembly machines and one submodule assembly machine being central to each subdivided process line. Each of the two lines is supported by a bus bar processing line, four chlorine electrode processing lines, and two zinc electrode processing lines. The bus bar processing line consists of ten bandsaws, two slotting saws, one bus cleaner and comparator machine, and one drill-fastener machine. Each of the four chlorine electrode process lines consist of one bandsaw, five slicing machines, one plate cleaner and comparator, and five chlorine-electrode assembly machines. The zinc-electrode process line consists of one bandsaw, five slicing machines, and one plate cleaner and comparator. One belt sander processes graphite blocks for the bus bar, chlorine electrode, and zinc electrode process lines. The graphite process area will require 17 operators on each of the three shifts.

The module assembly area consists of ten work stations that assemble the module by successive addition of components to the chassis structure. This assembly area will require 13 operators on each of two shifts. Except for the case sealing equipment utilized at stations 28 and 31, the battery module is assembled by hand labor and small tools.

The rack assembly requires five work bays and 23 assemblers on each of two shifts to produce 227 racks per day.

DISCUSSION

As stated in the introduction, the prerequisite for a manufacturing plan is a complete set of production design drawings and a production rate. The detail and accuracy of the manufacturing plan is then limited by the completeness and accuracy of the design drawings. Presently, much remains to be done. However, there is value in attempting to detail the processing. It provides a basis for measuring progress. The original intention, however, for embarking on this analysis was to provide a basis for rationalizing a manufacturing cost. The principle is well known. Since there are a large number of discrete steps involved, the estimated cost of the aggregate parts provides a reasonable basis for projecting the overall cost. It is the overall cost estimate which is the item of concern in the cost analysis which follows.

Section 8

COST ANALYSIS FOR 100MWh BATTERY PLANT

INTRODUCTION

The costing projects the selling price of the zinc-chlorine battery when produced in high volume and supported by a semi-mature technology. Further, this cost study attempts to be more comprehensive than previous costings. In so doing, estimates were made for a number of accounts having a minor effect on the overall costing. The value in doing this is that it focuses thought and discussion on the implications of those estimates. Of immediate value is the identification of areas requiring further research and development in order to achieve the semi-mature technology assumed.

In the preceding sections, the engineering specification and a design concept were presented. In the purposes of this report, the presumption was made that they describe the ultimate battery. It must, however, be emphasized that many trade-offs remain to be made between the engineering and the production designs. Also, as these cost and design studies become more detailed, the discrepancies between these designs become more evident. It follows that many evolutionary changes are to be expected as the gap narrows between present technology and a semi-mature technology.

For the purposes of cost analysis, a manufacturing plan was simulated. This allowed the various cost estimates to be assigned to specific and well-defined cost areas. The sequence which follows lists the cost of materials, equipment, plant, direct and indirect labor, and plant overhead, in addition to the manufacturing selling price. Although the simulated manufacturing plan was conceived solely for the purpose of cost estimation, it was presented in the preceding section of this report under the title, "Manufacture of Components for 100MWh Battery Plant". It must not be inferred that the battery can or cannot be actually manufactured in the manner specified.

There is insufficient information to pass judgment on this issue.

MATERIALS AND LABOR

The materials cost project those costs existing at the production level of 100 modules per day or 25,000 modules per year. The dollar figures are referenced to mid-1977. Presented below are discussions of the major cost items: graphite, pumps, heat exchangers, plastics, refrigeration systems, and power conditioning systems.

Graphite

Graphite is a major cost item in the zinc-chlorine battery system. The ultimate cost of graphite in the battery is determined by a series of factors, the two most significant being:

- stack design; specifically, the need for tight tolerances
- development of efficient graphite shaping methods

The optimal graphite selection is intimately connected with the design of the graphite stack. Essentially, any practical design must make electrical contact between the graphite parts and provide a means for passing liquid through the porous faces of the chlorine electrode. In the former case, the electrical contact is made by joining the graphite parts together by some mechanical means. This may be done by gluing, wedging, or pressing an electrode into a machined slot. At the present stage of development, gluing graphite together to make electrical contact has been demonstrated as feasible. The wedge method was used in the 20kWh EPRI battery design. The press or interference-fit joint has been most extensively tested. From a design standpoint, the tolerances on the parts become tighter as one goes from gluing to press-fitting. This requirement for tight tolerances increases the cost of the component parts. The other design consideration is the need to provide a means for directing liquid through the faces of the porous electrode. Essentially, the liquid is introduced into a chamber whose walls are made of porous graphite. The chamber can be formed either by machining the graphite to form the chamber or using flat plates of graphite and forming the chamber by plastic end caps. Substantial experience in operating electrode systems has been accumulated with the all-graphite chlorine-electrode package. It is readily apparent that the hollowing-out operation - known as "hogging out" - is wasteful of graphite and, as a result, is substantially more expensive than using flat plates. The added expense applies not only to the waste of material but, also, to an extra milling operation. The flat plate concept was also used in the 20kWh EPRI battery design. The philosophy there was

one of allowing a very loose tolerance on the graphite of about ±5 mils. The plastic component, as a result, was designed so as to be the high precision component capable of compensating for the lesser tolerance on the graphite. The rationale for this approach is that precision parts can be made of plastic by injection molding and at a low cost. It is evident that plastics are moldable, which is an efficient forming operation, whereas graphite must be cut, which is the most inefficient forming operation known.

This leads to the question of design tolerances, in general. In respect to the electrodes, there exists a transitional tolerance limit, about ±2 mils, above which is easily achieved in a single roughing operation. An example of this is a saw cut. In order to achieve a lower tolerance, one or more finishing operations is necessary. A supplementary grinding operation is an example of this. This accounts for increased labor costs. However, precision operations require surface references from which to measure. That is, in order to produce parallel surfaces to within a very tight tolerance, it is necessary to first produce a reference surface. This means that a certain amount of material must be removed in order to produce the first reference surface at the desired flatness. Consequently, there is an increased material cost. As a general reference, given below is a table showing how tolerances affect machining costs. It was published by the Airco Speer Carbon Products Department in their Manual of Carbon and Graphite (8-1).

Table 8-1

HOW TOLERANCES AFFECT GRAPHITE MACHINING COSTS

Cost of part held to ±0.001in represents 100%

TOLERANCE ±in	RELATIVE COST %
0.015	25
0.010	30
0.005	40
0.003	60
0.001	100
0.0005	250
0.00025	425

This same consideration applies to the method of joining the graphite electrodes to the buses. The design utilizing the press-fit concept requires tight tolerances. The reason for this is that numerous electrodes must be inserted into slots on each graphite bus surface over a distance of several inches and having a supporting thickness of ∿1/4 in. It is, of course, evident that the top surface of the bus will be the nominal bus length plus the sum of the interferences, whereas the center line of the bus remains at nominal length. Therefore, the bus must become bowed. The bus, under these conditions, is stressed but remains stable so long as the net stress is below the yield point of the graphite. It should be clear that care must be exercised in controlling the amount of interference between the slots and the inserted electrodes. As one might expect, the cost of machining numerous slots having tight tolerances on the walls is not insignificant. The quoted price of preparing such a bus is about fifty-two dollars of which six dollars is the material cost. Later in this section, a discussion of graphite machining will be presented. For the sake of balance, these tight tolerances make a fully-automated assembly of the buses a relatively simple matter. Quotes are in hand for the design and construction of the equipment. One proposed approach for minimizing the need for tight tolerances is to use electrodes made of a softer graphite. In this way, the graphite of the plate will be formed by the cutting action of the edges of the mating slot in the bus and the softer graphite will also yield to take up stress. The wedge concept for joining the electrodes to the bus also operates in this manner. That is, a highly compliable wedge is pressed into the gap existing between the oversized slot and the electrode. Finally, the glued joint requires a minimal concern for tight tolerance specification.

In respect to the graphite as received in the shape of a block, it must undergo a shaping operation. It is evident that the efficient shaping operations cannot be used - forming, casting, or molding. This leaves the most inefficient method, cutting. The reason for this is that cutting entails a kerf loss, i.e. the material cut away. This loss corresponds to the thickness of the tool doing the cutting. A good rule that applies to the thickness of a circular saw or cut-off wheel is that in order to keep the tool from wandering from its intended path, the thickness of the tool should be 1/40 of the depth of the cut. Attempts to experimentally reduce this factor only served to emphasize its validity. Consequently, the minimum saw thickness to achieve a 2.5-inch depth is 0.0625 inches. This type of cut easily maintained a ±2.5-mil tolerance on the cut surface. However, if an electrode to be cut is 40-mils thick and has a kerf loss of 62.5 mils, more graphite is wasted than is utilized in the form of machined electrodes. Further, should higher tolerances

than ±2 mil be required, the sawed plate must be made thicker, say 80 mils, in order to be subsequently machined to the desired tolerance and, at the same time, achieve a 40-mil nominal thickness. By including losses associated in sizing the block so as to achieve the outside plate dimension, the yield of electrodes made to high tolerances is about 20% of the graphite block. Since graphite is such a costly contribution to the battery, increasing the yield well over 50% can be accomplished by:

1) using a single cut to produce the plate
2) finding a more efficient (thinner) cutting tool

The implication of 1) suggests that a lower tolerance plate be accepted. Consequently, the stack design must be able to accommodate this. Such designs are already being tested in the laboratory. The second method has been the subject of some study within EDA. Rather sophisticated cutting devices have been developed in other industries for cutting thin plates with a minimum kerf loss. Presently, more information is required as to the limits of the efficiency of these machines. Indications are, however, that the kerf loss can be reduced to 30 mils or less and the resulting plate produced with a tolerance of ±1 mil. The finish on the plate appears more than adequate on a single pass of the cutting tool. One such method is being used to produce finished electrodes for EDA. The method appears promising.

For the sake of completeness, the preparation of slotted buses with high precision slot widths has been described earlier. The efficient use of materials is not a problem here. As mentioned earlier, the difficulty lies in the labor cost in carefully meeting the tolerance requirements on the slot widths. Automated methods for reducing the cost of preparing these bus bars is a matter of current study.

For the purposes of projecting the FC+5 costs of the graphite materials, the projected stack design described earlier will be assumed. The manner of assembly and the design rationale have been discussed. Essentially, three different graphite materials are specified. The first is a porous material used for preparing the chlorine electrodes. The other two are dense graphites, one softer (less hard) than the other. The softer graphite is used for the zinc electrode whereas the harder material is used for the bus. In respect to the relative costs of the graphites, the porous material is far more expensive.

The current price of available porous graphite is $2.31 per pound. Specifically, the material referenced is an Airco Speer product identified as 37G having a density

of 1.35 grams per cubic centimeter. The direct material cost per plate is computed by converting the volume of a plate (11.26cm^3) to a weight per plate. The cost per plate is obtained by multiplying the cost per pound of the graphite by the weight per plate and dividing by an efficiency factor. This efficiency is determinable as the product of the efficiencies of two operations. The first is a block sizing which divides the block as received into small blocks whose height and width correspond to the plate dimensions. The efficiency of this sizing operation depends on the size of the block received. Since the number of graphite blocks purchased is sufficiently large, the block can be ordered to a pre-specified dimension. A reasonable efficiency for this sizing is 0.90. The large inefficiency comes from the kerf loss associated with slicing the sized blocks. For every electrode thickness of 0.050 inches, a kerf of 0.030 inches is required. This is a conservative estimate easily achievable by existing slicing techniques used in other industries. Work is in progress in order to determine its lower limit. This slicing efficiency is 0.625 giving a total efficiency of 0.563 for producing the electrode plates. The direct material cost per plate is, therefore, 11.3 cents.

A similar calculation can be performed for the dense graphite to be used as the zinc electrode. Here, a Union Carbide product identified as CS graphite is the material being considered for use. The cost of this material is 90 cents per pound in the form of blocks. Since this electrode is 0.040 inches in thickness, the overall efficiency is reduced. Given the graphite density of 1.76 grams per cubic centimeter, and an overall cutting efficiency of 0.514, the cost per plate is 5.0 cents.

The direct material cost per bus bar is computed from the following considerations. The graphite used is a Union Carbide product known as AGSX selling for 84 cents per pound. The cutting is expected to be done by a bandsaw producing a kerf loss of 0.0625" per bus bar. Allowing a 10% loss for sizing, the efficiency of cutting is calculated as 0.720. Taking the denstiy of AGSX as 1.74 grams per cubic centimeter, the direct material cost per blank is 88.2 cents. The cost of the graphite components per module is determined from the materials list, i.e. there are six submodules per module with each submodule containing eleven bus bars, 210 zinc electrodes, and 400 porous electrode plates.

Pumps

The pumps required for each module will be of a submersible type and made of materials fully compatible with the system environment. The concept is well known although the

actual design requires some development. Discussions with pump manufacturers indicate that a sealed pump-coupling-motor combination could be manufactured in the quantities desired for under $100. The two pumps, although slightly different in terms of the pumping mechanism, are virtually identical for costing purposes. The cost figure selected represents an extrapolation of the costs of smaller pumps that are commercially available. It is highly probable that the eventual pump cost will be less than that projected in the costing.

Heat Exchangers

The heat exchanger is conceived as a standard production item made from titanium sheet stampings. Discussions with titanium fabricators have indicated that the proposed design is amenable to low cost production provided that the volume of production is high enough to distribute the cost of the extensive tooling and equipment required. The projected cost of the heat exchanger was determined in consultation with a representative of Titanium Manufacturing, Inc. The estimated price of $96.07 is considered reasonable at the production volumes specified (Section 7).

Plastics

Throughout the construction of the battery, plastics of various kinds are used in different places and for different purposes. No fluoro-plastic materials will be used. Three generic plastics are being considered. They are reinforced polyesters, high density polyethylene and polyvinyl chloride. Materials programs currently in progress are in the process of specifying the total compound to be used for each plastic -- see Part V, Section 33. These materials will be formed or molded into the shapes required with insignificant material losses.

The case and store container are significant cost items constructed from plastic materials. Glass-reinforced polyester is the material of choice having an average wall thickness of 0.25 inches. The method of production will be or resemble a matched-die process. The capital investment required is warranted by virtue of the large production volume. The cost estimate for this component is based on calculating the material content so as to arrive at the material cost and allowing a fabrication cost equal to the direct material cost. This cost estimate may be somewhat conservative and could be reduced after further analysis.

Refrigeration System

A cost estimate was made for a complete refrigeration system on skids for outdoor

installation. This estimate includes complete field installation including field labor and presumes that all utilities are within five feet of the skid placement. Also included in the cost is installation, test, checkout, start up, and instruction. The estimate was $459,000 for a 100MWh load-leveling station and was presented by Ray Johnson & Associates, Inc.

Power Conditioning and Switchgear

The power conditioning system costs are a noteworthy consideration for the zinc-chlorine system. By virtue of the characteristically flat charge and discharge profiles and that the difference between these voltages is approximately 10% at all times, a significant economy can be achieved. Voltage variations in all battery systems must be regulated for delivery into an ac distribution system. In addition to the voltage transformation, an impedance correction must also be made in order that the converter losses will not be excessive. The impedance correction involves the addition of reactive components with high current capability. Should the requirement for battery voltage regulation exist, the impedance correction must be variable. Doing this is expensive. In that perspective, the costs associated with a complete converter system which includes a transformer, rectifier, inductors, reversing switch, harmonic filter, all ac and dc switchgear with housing, and field labor for installation, was estimated at $906,000 for the 100MWh zinc-chloride battery system as a consequence of its favorable charge-discharge profile. The estimate was given by Udylite Corporation.

Tables 8-2, 8-3, and 8-4 group the battery components and assemblies in terms of their direct material and labor content. Table 8-5 identifies the costs associated with installation. The major material contributions were discussed above. The direct labor costs depend on the direct labor content, which in turn is based on the manner in which the battery is processed. For the purpose of projecting these labor costs, a process plan was conceived. This plan has been presented in the preceding section. That processing is offered in justification of the labor cost data given.

INVESTMENT, INDIRECT AND OVERHEAD COSTS

Having created a process plan, another imaginative exercise followed, the objective of which is to visualize a production facility with a 25,000 module per day capacity. This simulated manufacturing plan is presented in the previous section. The reason for creating such a plan was to provide a basis for estimating the total investment, the indirect and overhead costs.

Table 8-2

MATERIALS AND LABOR COST PER MODULE

Category	Direct Materials	Direct Labor
STACK SUBASSEMBLY		
Zinc electrodes	$ 63.00	$ 5.40
Chlorine electrodes	271.20	5.40
Electrode masking	9.62	.00
Bus bars	58.21	7.50
Comb and end comb assembly	.00	7.20
Submodule pans	10.61	.00
Submodule carrier	14.04	.00
Submodule assembly	.00	5.40
MODULE ASSEMBLY		
Chassis structure	23.27	2.40
Hydrogen reactor	9.60	.00
Store filter assembly	2.00	.00
Store coil	8.56	.00
Case components and store container	117.22	.00
Electrolyte pump	99.70	.00
Gas pump	99.70	.00
Heat exchanger	96.07	.00
Electrical connectors	35.95	.00
Valve	3.00	.00
Battery assembly	.00	13.20
Misc. (fittings, probes, adaptors, small hardware)	15.00	.00
PRIME COST TOTALS	$936.75	$46.50

Table 8-3

MATERIALS AND LABOR COST PER RACK

Component	Materials	Direct Labor
Modules (44)	$41,217	$2,046
Rack structure	3,300	0
Bus materials	11	0
Rack control package	200	0
Plumbing for coolant	300	0
Wiring harness	500	0
Assembly	0	1,200
TOTALS	$45,528	$3,246
PRIME FACTORY COST	$48,774	

Table 8-4

BATTERY PLANT MATERIALS AND LABOR COST
(000 omitted)

Component	Materials	Field Labor
Refrigeration system	$ 459	$0
Power conditioning equipment, bus work, switchgear	906	0
Plumbing for coolant	3	0
Outdoor shelter ($16/ft^2 estimated)	230	0
Control package	30	0
System assembly	0	10
TOTALS	$1,628	$10

Table 8-5

BATTERY RACK INSTALLATION

	Cost (000 omitted)
Shipping 500 miles x 36 racks	$ 36
Unloading and Installation Field labor	15
Electrolyte Materials	114
TOTAL	$165

Table 8-6 summarizes the process equipment and their associated costs. For the sake of convenience, a distinction was made between the process equipment and the physical plant. The latter is understood to include the remaining investment in the plant equipment. Another way of viewing this is that it includes all equipment that affects the processing indirectly. Table 8-7 was compiled as a basis for estimating the remainder of the physical plant investment. The cost figures are estimates based on the experience of the persons queried. No attempt was made to

write a specification for this equipment. The cost figures, therefore, constitute what is believed to be a reasonable allowance for a large number of small items. Consequently, the total should be a good estimate of the aggregate whole. Further, this figure makes a small contribution to the total investment given in Table 8-8.

The total investment includes an estimate of the total working capital. Ordinarily, a rule of thumb is 30% of the Net Sales Billed. For convenience, the prime costs were used. It would not be possible at this stage to justify this working capital estimate without having simulated the business in operation. In that case, the financial statement of the business could be projected which would give a basis for justifying the rule of thumb. The figure stated is considered a reasonable allowance for the working capital of the business.

Table 8-6

PROCESS EQUIPMENT COST

Operation Number	Number Required	Item	Cost (000 omitted)
2, 9, 13	2	Compound belt sander @ 50k$/ea	$ 100
3, 9, 13	32	Bandsaws @ 15k$/ea	480
4	4	Slotting machines @ 20k$/ea	80
5	2	Bus cleaner and compactor @ 15k$/ea	30
11	4	Plate cleaner and comparator @ 10k$/ea	40
15	8	Plate cleaner and comparator @ 10k$/ea	80
10, 14	60	Slicing machines @ 36k$/ea	2,160
6, 7	2	Driller-fastener @ 25k$/ea	50
16	40	Chlorine electrode assembler @ 47.5k$/ea	1,900
17	16	Comb assemblers @ 45k$/ea	720
18	2	Assembly machines @ 100k$/ea	200
19, 20	25	Submodule activation and test @ 10k$/ea	250
28, 31	2	Case sealing equipment @ 10k$/ea	20
32	1	Helium leak test equipment @ 30k$/ea	30
33	1	Rectifier, controller and data acquisition system @ 55k$/ea	55
		Subtotal	6,195
		10% Installation	620
		30% Contingency	1,860
		COST	$8,675

Table 8-7

PHYSICAL PLANT
(Excludes process equipment)

Item	Cost (000 omitted)
Building, parking lot, heating and air conditioning	rented
Plumbing and drains	$ 40
Shipping and receiving docks	50
Air make-up system	50
Compressed air system	30
Deionized water system	10
Lunchrooms, showers, change rooms	10
First aid and nurse's room	10
General storage	10
Security and supervisory services	20
Computer system	100
Waste treatment system	120
Dust collection and bagging	80
Storage tanks	20
Fume hoods and scrubber system	150
Refrigeration equipment	100
Electrical shop	60
Machine shop	100
Quality Control laboratory	80
Standards laboratory	60
Custodial storage and equipment	20
Shipping and packaging	10
Hi-lo transports: 4 @ 10,000 each	40
Electrical power conditioning equipment	40
Welding equipment	30
Workbenches, cabinets, etc.	30
Office furniture and partitions	40
Emergency standby power system	40
Engineering laboratory	100
Design and drafting equipment	20
Transports and conveyors	500
PHYSICAL PLANT INVESTMENT	$ 1,970

Table 8-8

SUMMARY OF INVESTMENT COST

Item	Cost (000 omitted)
Process equipment	$ 8,675
Physical plant	1,970
Working capital (0.30 x prime factory costs)	8,313
INVESTMENT	$ 18,958

Table 8-9

LABOR REQUIREMENTS

INDIRECT

Functional Area	Staff
Finance	7
Personnel	4
Manufacturing	
Production Scheduling and Purchasing	8
Production Control	8
Quality Control	15
Manufacturing Engineering	15
Process Engineering	5
Engineering	
Design Engineering	10
Evaluation and Test Engineering	10
Marketing (Customer Service)	2
TOTAL - INDIRECT	84

DIRECT

Area	Personnel
Submodule Assembly	51
Module Assembly	26
Rack Assembly	46
TOTAL - DIRECT	123

By virtue of having estimated the investment, the ROI can be calculated and the depreciation, a significant overhead account, can be estimated. To simplify the estimate, a ten-year straight-line depreciation schedule will be assumed for all equipment. The major account in the overhead is the indirect labor. Table 8-9 projects the indirect labor by functional area. Also listed, for reference, is the direct labor. From this, the factory overhead was estimated and listed with the assumptions made in Table 8-10. The building is assumed to be rented at $\$3.75/ft^2$/ year and has 125,000 ft^2 of space. The minor overhead accounts were estimated. Table 8-11 calculates the overhead rate at 177% which is reasonable.

Table 8-10

OVERHEAD COST DISTRIBUTION

		Cost (000 omitted)
Indirect Labor		
84 people x \$12/hr (avg) x 40 hr/wk x 52 wk/yr =		\$ 2,096
Depreciation (straight line over 10 years)		
Process equipment	8,675	
Physical plant	1,970	
	10,645 ÷ 10 =	1,065
Rent for Building (including taxes and insurance)		
125,000 ft^2 x \$3.75/ft^2/yr =		469
Indirect Materials		200
Utilities		100
Repairs and Maintenance		200
Miscellaneous		100
	TOTAL	\$ 4,230

Table 8-11

OVERHEAD RATE

	Cost (000 omitted)
Direct Labor Cost (983mh/day x 250days/yr x $7.50/mh)	$ 1,843
Fringes @ 30% of Direct Labor	$ 552
Established Overhead Cost	$ 4,230
Overhead Rate $= (\frac{\text{Overhead costs x 100}}{\text{DL + Fringes}})$	176.6%

MANUFACTURING COST AND SELLING PRICE

Having accomplished this, the estimated selling price for the battery can be computed assuming a yearly production of 25,000 modules (Table 8-12). This corresponds to 15.8 100MWh peak-shaving plants per year. A note must be made regarding the balance of plant cost. A priori, the pricing based on a $/kWh plus $/kW suggests that a distinction was made between the energy and power dependent cost components. This, strictly speaking, was not the case. The distinction made was for the purpose of dividing the battery according to the operational life expectancy of the components. Upon attempting to draw the lines of demarcation between equipment groupings, those having a 10-year life expectancy appeared to be energy dependent, whereas those having a 30-year life expectancy appeared to be power dependent. The distinction, therefore, was one of convenience.

In summary, the projected selling price of the 100MWh zinc-chlorine peak-shaving plant is $25 per kWh plus $89 per kW with a $2 per kWh allowance for installation when:

a) produced at a rate of 15 plants per year,
b) the plants are 100MWh in size, and
c) a semi-mature technology exists.

Deviations from these conditions would affect the selling price accordingly.

DISCUSSION

Introduction

The cost analysis for the zinc-chlorine battery presented above serves the immediate purpose of projecting and justifying a selling price for the battery. The

Table 8-12

MANUFACTURING COST

Yearly Production - 25,000 Modules
(568.2 Battery Racks)
(15.78 Battery Plants)

	Cost (000 omitted)
Direct Materials	
$45,528/rack x 568.2 racks/yr	$ 25,869
Direct Labor and Fringes	2,395
Overhead	4,230
FACTORY COST	$ 32,494
General Service and Administration (9%)	$ 2,924
Investment 18,958	
ROI (30% of Investment)	5,687
PROJECTED BATTERY RACK SALES	$ 41,105
SELLING PRICE PER KILOWATT HOUR	$25.94

BATTERY RACK INSTALLTION

Materials, Field Labor and Services (see Table 8-4)	$ 165
PRICE PER KILOWATT HOUR	$ 1.64

BALANCE OF PLANT COST
(Per 20MW/100MWh Plant)

Purchased Auxiliary Components	$ 1,628
Field Labor Expense @ $25/hr	10
BALANCE OF PLANT TOTAL	$ 1,785
SELLING PRICE PER KILOWATT	$89.27

organization of the presentation, however, had a greater purpose in its design. It should be evident to the reader that only one plan or model was presented for achieving the cost goals for the battery. Obviously, many alternate plans are conceivable. By selecting one, breaking it into its component parts and reviewing its consequences, the analysis provides a sound basis for decision making.

Substantially, a model has been conceived together with criteria and values for measuring it against others. Also, considerations that are essential to the successful achievement of the commercialized battery become evident. This is another way of saying that in respect to the battery development program, yesterday's minor details are today's major concerns. It is to the advantage of the developmental effort to identify and define its predictable problems in order that solutions might be anticipated.

In that perspective, an engineering specification was detailed that included the energy and mass flows together with schematics illustrating the operational aspects. Also, a system design, consistent with the engineering specification, was drawn to illustrate the battery as well as attempt to identify possible problem areas. A completely detailed design is not available. However, more than enough is available for envisioning the physical battery structure. The costing was considered from its broadest perspective. That is, the costing is intimately related to the design considered, the materials used, the processing, the production volume, the investment, and the technology available. An attempt was made to reconcile all of these factors and calculate a selling price.

Components and Equipment Development

In the projected cost estimates for the heat exchangers and pumps, the component costs projected by qualified vendors are considered reasonable in terms of materials, labor, and vendor contribution margin. However, development of specific designs remain to be done followed by appropriate capital expenditures by the vendors in order to increase their productivity. The production volume of 25,000 modules per year can support the amortized investment cost in the vendor's selling price. The plastics considered are in the final stages of qualification. Those materials must then be molded or fabricated for specific battery applications. Appropriate tooling and equipment design must take place. For example, complex molded pieces must be produced and the cell casing must be prepared using minimum amount of material yet having sufficient mechanical strength. As is evident from the process description,

assembly and transportation equipment of some complexity must be specified and designed. This is not inherently difficult but would be costly by virtue of the number of machines required. This latter point already has raised some comment. In certain situations, large numbers of identical pieces of machinery were specified. This equipment is currently available for the prices quoted.

However, the investment in the aggregate of identical machines would, very likely, pay for a specialized piece of equipment that would do the entire job for a substantially smaller investment. Although this is probably the case, such a machine does not yet exist. The probability of designing and building such a machine is good. For the purpose of the costing, the available equipment was used.

Graphite to Graphite Joining

An area of the processing that has received much discussion is the joining of the graphite plates to the graphite buses, specifically, the zinc-electrode plates and the bus. These discussions have ranged widely with opinions expressed pro and con on each issue. What follows is a brief discussion of some of the aspects of this problem and some alternate solutions. It is the author's hope that the positions on the issues are properly represented.

The press-fit contact between the electrode and the bus has been demonstrated as being effective. The development which follows is to be viewed as a traditional dialog inherent in reconciling an engineering design with a production design. The press-fit contact was adequate from a performance standpoint but the requirement that exists for high tolerances -- presently used in the engineering models -- is very wasteful in terms of graphite which in turn effects the cost of the battery. As presently visualized, a looser tolerance -- consistent with efficient use of graphite -- will be used. In order to make the press-fit, the graphites will be selected so that the bus material is harder than the plate material. They will, effectively, self-machine themselves upon insertion. This approach is plausible. The graphites selected for use have not been tested as yet to determine whether they operate as projected. The problem that may arise is that the electrodes will act as wedges in the grooves of the bus. It is possible that the resulting stress will exceed the break point resulting in scrap losses. The probability of this happening and, at the same time, the projected scrap rate has not been determined. Various other options still exist. A softer graphite can be developed. Alternatively, sorting procedures can be resorted to in order to select graphite parts. This would require an additional capital investment. It is, also, possible to bond

the graphite into the slots by a gluing or plastic welding operation. Again, extensive fixturing would be required. Lastly, a design modification could be made wherein tabs are secured to the electrode edges and the electrodes are subsequently connected together into combs. This opens the door to substantial changes in stack design philosophy and would also require further development of already existing bonding technology.

It is evident that many options are available for developing a production prototype. It is not a problem of not knowing how to join graphite but, rather, how to do it in the best possible way.

Influence of Porous Graphite Cost on Selling Price

Graphite is the most expensive single component in the zinc-chlorine battery. Porous graphite -- one of the graphite types used -- contributes in largest part to the cost of the graphite. As a result, an equation was derived to mathematically describe the selling price as a function of the cost of porous graphite. This equation is written as follows:

$$S = 2.012\ G + 21.28$$

where S is the selling price in $/kWh and G is the cost of porous graphite in $/lb. Doing this permits plotting and/or tabulating the function. Table 8-13 lists a series of selected points. The bracketed quantities refer to the actual costs of specific materials. The figure 2.32 refers to the cost per pound of the Airco Speer 37G material on which the costing given earlier was based. The $5.67 figure is the present cost per pound of Union Carbide's PG-60 graphite in block form. As used here, the selling price calculation implies that the PG-60 has the same physical properties as 37G -- conductivity, resistance to liquid flow, and density. The table shows the sensitivity of the selling price to the cost of a 37G-like graphitic material. The table shows that variations in the cost of porous graphite do not by themselves make the battery uneconomical.

COSTING BY THE ADL METHOD

The following discussion addresses itself to the costing method prepared by James H. B. George of Arthur D. Little, Inc. The section is patterned to correspond to the format presented in the Electric Power Research Institute Interim Report EPRI 787-1, November 1976.

Table 8-13

SELLING PRICE AS A FUNCTION OF GRAPHITE COST

Porous Graphite $/lb	Rack Selling Price $/kWh
0	21.28
1	23.29
2	25.30
(2.32)	(25.95)
3	27.31
4	29.33
5	31.34
(5.67)	(32.69)
6	33.35

Production Rate

The ADL costing specifies a production volume of 25 battery plants per year. The analysis given in the preceding text was performed as a 25,000 module per year basis which corresponds to a production volume of 15.78 plants per year. It will be assumed that all costs can be extrapolated as a linear function. This is, actually, not a good method since some economies of scale serve to reduce prices. Regardless, the cost estimates will be presented according to this method.

Operating Schedule

The assembly facility operates on a 2-shift basis for 250 days per year -- an exception being the graphite cutting work stations which will operate on a 3-shift basis. The size of the investment for achieving production would not warrant allowing the equipment to remain idle during the third shift. Reserve equipment will be included so as to maintain production capacity and allow for equipment maintenance.

Production Yield

Although recommended by the ADL method, EDA cannot knowingly apply a 95% product yield when the graphite production yield is known to be as low as 56% and graphite is the single most expensive component in the system. A realistic efficiency number will be used in the costing in place of the 95% figure.

Labor Rate

The direct labor rate is taken as $7.50 per hour.

Overhead Rate

For purposes of this estimate, 150% will be taken on direct labor and 10% on purchased materials as the overhead cost.

Rent

Rent will be taken at $3.75 per square foot.

Equipment Depreciation Schedule

The total investment will be amortized over a 10-year period on a straight-line basis.

Working Capital Requirements

The working capital will be estimated as 30% of the factory cost.

ROI and Taxes

The before taxes ROI will be taken as 30% of the capital investment. The tax rate is assumed to be 50% of the earnings.

The selling price presented in Table 8-14 specifically excludes the power conditioning equipment -- rectifer, inverter, associated switchgear, and installation.

Comparison of Costing Methods

In principle, the costing approaches used -- EDA and ADL -- are identical. The differences lie in the depth to which the costing proceeds. For example, in the ADL method, the overhead rate was assumed. The EDA method attempted to estimate the accounts comprising that overhead and then calculate it. Since the assumptions made in the ADL report were reasonable estimates to begin with, the EDA study serves to support and justify their reasonableness. Insofar as the accuracy of the estimates are concerned, it could be difficult to say that such a difference is significant. The EDA method, however, is directed toward a longer range purpose. By projecting the individual accounts, a basis for manufacturing simulation and analysis is created.

Table 8-14

100MWh BATTERY SELLING PRICE

Item		$/kWh
Labor		
Direct labor	1.17	
Field labor	.25	1.42
Materials and Purchased Components		24.75
Overhead		
10% of Materials	1.75	
150% of direct labor	1.76	2.93
Equipment Depreciation		.67
Rent		
125,000 ft^2 x \$3.75/ft^2/yr		.30
After Tax ROI		
15% of Total Investment		1.80
Taxes		
(= After Tax ROI)		1.80
Selling Price ($/kWh)		33.67

CRITIQUE ON COSTING

Preconceived Cost Objectives

The cost projections made were based on certain preconceived cost objectives. These objectives were set at \$25 per kilowatt-hour plus \$75 per kilowatt. The costing approach directed itself at achieving these objectives by the most expeditious means. The lowest-cost components conceivable at the time were used. Although this was convenient and fast, a better but more time-consuming approach exists; specifically, by starting with a current prototype design, and item by item, reducing the cost of individual components until the cost bogey is achieved. The reason why this is a more valuable approach is that it identifies specific areas of cost reduction, specifies the size of the cost improvement, and projects specific improvements. In this way a list of cost reduction areas can be prepared

together with a figure of merit -- in terms of dollars -- specifying the relative significance of the projects to reduce cost. This would provide an ideal management tool for establishing priorities on the various zinc-chlorine development programs.

Battery Design

The battery design, upon which the costing was made, is not fully detailed. Consequently, a parts list does not exist. The costing attempted to project costs for the major identifiable components and include a miscellaneous category to cover the minor and unidentified items. This cost category may be in error by the significant amount; however, its impact on the selling price is minor by virtue of its small size.

Simulated Manufacturing Plan

The simulated manufacturing plan presented in Section 7 was conceived for the purpose of justifying the allowance used. From this plan, costs were developed for direct labor, investment, indirect labor, and overhead. It is noteworthy that this plan was intended as a general study and could differ significantly from the eventual plan to be used in manufacture.

Start-Up Costs

The low labor costs require a production system that is highly automated. Starting production under these circumstances entails substantial start-up costs. These costs have not been included in the costing for the reason that a semi-mature technology (first commercial plus five years) was assumed.

REFERENCE

8-1 "Manual of Graphite", Airco Speer Carbon-Graphite, p. 7.

Section 9

SAFETY AND ENVIRONMENTAL HAZARDS ANALYSIS FOR 100MWh BATTERY PLANTS

INTRODUCTION

As peak-shaving battery plants are intended for public utility siting on the distribution or sub-transmission network in residential areas, as well as in other areas, the design criteria include the requirement of minimum siting restrictions. The only potential hazard associated with the siting of zinc-chlorine battery plants in residential areas is the possibility for accidental release of toxic amounts of chlorine gas. This section briefly reviews the environmental and physiological effects of chlorine and analyzes the potential hazards associated with accidental chlorine release.

Most of the chlorine in the battery exists in the form of either aqueous zinc chloride, a very stable salt solution, and chlorine-hydrate, also a very stable clathrate compound at low temperatures (9.6°C). Besides these two forms, a small quantity of chlorine is present in the gaseous form in the gas space of the battery and dissolved in the electrolyte and store fluid. This will be referred to as "free chlorine", as it is in a relatively free state.

Under normal conditions the battery is sealed and operated under partial vacuum, thus eliminating the possibility of chlorine leakage into the atmosphere. However, the possibility of abnormal operation or accident cannot be ruled out and the release of chlorine and subsequent spread in the atmosphere must be analyzed in the event of such mishaps.

In the event of either of the two mishaps, the rate and mode of free chlorine (defined above) escape into the atmosphere depends on the type of damage to the battery. A small battery case fracture results in an inflow of air into the battery because

of its vacuum operation. This inflow causes internal battery pressure to reach ambient pressure. Only then will chlorine begin leaking into the atmosphere by molecular diffusion, a very slow process. In the open atmosphere the presence of this chlorine can hardly be noticed. In case of a major accident causing breakup of the battery into pieces, all the free chlorine will be released instantaneously. Because of the small volume of this gas, there would be neither cloud formation nor high concentrations of chlorine in the air except in close proximity to battery. The entire episode lasts such a short time and its effect on the environment would be so minimal that any further consideration of this gas from the safety aspect is considered unnecessary. Henceforth in this report the chlorine being considered is either in the form of zinc chloride or chlorine hydrate.

The percentage of total chlorine present as zinc chloride or hydrate depends on the state of charge of the battery. A completely discharged battery contains all the chlorine as zinc chloride. An electrochemical reaction is needed to release chlorine from this solution. Hence chlorine in this form or a completely discharged battery containing chlorine only in this form does not constitute a safety or environmental problem.

As charging of the battery commences, zinc chloride is decomposed to form metallic zinc and gaseous chlorine. Zinc becomes plated on the zinc electrode substrate and evolved chlorine mixes with cold water in the hydrate former to form hydrate which is stored in the storage compartment of the battery. At the beginning of the charge, the store contains only water. As charging progresses, more and more hydrate mixes with this water and all the water needed for hydrate formation is obtained from the store so that concentration of hydrate in the mixture increases faster than the rate of charging. The hydrate flakes have a higher specific gravity ($\rho \simeq 1.23$) than water, but due to constant circulation of water in the store, the hydrate flakes stay afloat forming a slurry. As the concentration of hydrate in the mixture increases, the slurry thickens while the turbulence in the store gradually decreases. This leads to a slow but steady separation and settlement of hydrate at the locations where turbulence is least, such as the corners of the store. This transition occurs at about 30% into the charge. Beyond this stage during charge, a part of the hydrate is in the form of a cake and the remainder as a slurry. The percentage of the latter gradually decreases to near zero at full charge when all the hydrate is formed into a single block.

The quantity of suspended hydrate in water slurry increases to a maximum of 30% of the full charge and then decreases. The volume of hydrate block will be from zero

up to 30% into the charge cycle and from then on gradually increases to a maximum of 10.6 cu ft at full charge, containing 46.2kg of chlorine.

Upon completion of the charge (7 hours), during the next several hours, there will be no change in the form of chlorine stored. This period is followed by a discharge cycle which lasts for ∿5 hours. During this period, hydrate is gradually decomposed to release chlorine to form zinc chloride. As the decomposition proceeds, the volume of hydrate block decreases. Following the discharge the battery will again be idle for several hours before the next charge cycle begins.

ACCIDENT SCENARIOS

Chlorine in hydrate is the only form which would be released to the ambient in case of an accident or malfunction of the battery controls. From the above discussion it appears that there are only two critical stages in each complete cycle where the hydrate spill from the battery may be the maximum for each mode, namely the slurry and the hydrate block. The critical stage with each is when volume is the largest. The slurry occurs at 30% into the charge cycle and the hydrate block occurs at full charge. Analyses of these two cases will define the upper limits of chlorine release from an accident involving this battery.

For either accident to occur, the damage to the battery has to be of a major nature. Hydrate is stored in a separate container within the battery case. For all the slurry to spill, both battery and store cases have to be pierced at the bottom. Damage at any other level results in only partial spillage of the slurry. When fully charged, the hydrate block is rigidly formed in the store. To remove it from this space, complete destruction of both the walls on at least one side of the battery and a severe impact to dislodge it from the store are required. Both of the above accidents, either spilling the slurry or dislodging the hydrate block from the store are very unlikely to occur. A more likely accident would involve the decomposition of hydrate within the damaged battery case and chlorine, as it is released, escaping into the atmosphere. Hence it seems to be appropriate to calculate the chlorine release rates and its dispersion in the atmosphere for all three cases, namely the spilling of slurry and hydrate block and decomposition of hydrate in the store.

In all the three cases discussed above, chlorine is released by the decomposition of hydrate which is an endothermic reaction. Under atmospheric pressure this reaction occurs at about 9.6°C and the heat of decomposition is 18.6kCal/mole. Hence the

decomposition rate depends on the rate of heat transfer to hydrate.

For convenience let us designate the spillage of slurry and block and the decomposition of hydrate in the store as Scenarios I, II, and III respectively. In the former two cases, hydrate is exposed to the air and the ground and hence the heat transfer rates to the hydrate in these cases depend on the ambient conditions. The battery case itself is provided with very good thermal insulation, primarily to minimize the standby losses (which are caused by chlorine release from hydrate). During charge and discharge, the rest of the battery parts (sump and stack) could be as warm as 50°C and there is continuous heat transfer from these parts to the store. This heat transfer will be significantly larger than any that is possible from the ambient air (at about 37.8°C) through the double walls and the battery insulation and hence it should constitute the worst case for this accident (Scenario III). Table 9-1 gives a comparison of the three scenarios.

Table 9-1

COMPARISON OF THE ACCIDENT SCENARIOS

	Scenario I	Scenario II	Scenario III
Location of hydrate	on the ground	on the ground	in the store
Maximum Cl_2 content	13.86kg	46.2kg	46.2kg
Texture of hydrate	slurry	cake	slurry or cake
Source of heat transfer	ground and air	ground and air	electrolyte and other battery parts
Probable time of day	around 1:00 a.m.	6:00 a.m. to 2:00 p.m.	11:00 p.m. to 7:00 p.m. next day

HEAT TRANSFER MODELS AND CHLORINE-RELEASE RATES

Scenario I

As explained earlier, this accident scenario represents the worst possible conditions, when the battery is charged to 30% of the full charge and the maximum quantity of hydrate is in the form of a slurry. Major damage to the battery at this stage could result in the escape of all this slurry. As this slurry is drained onto the

ground, most of the water is filtered through the solids leaving a heap of hydrate on the ground. The size, shape, and extent of the spread of this heap on the ground depends on the constitution of slurry, how fast it is drained, and surface properties of the ground. For the present analysis it is assumed that it will form the segment of a sphere with a contact angle of 45° at the edges. Figure 9-1 is a sketch of the slurry on the ground. The density of hydrate in this heap is assumed to be $0.8gm/cm^3$ with the voids occupied by water and gas. At 30% of the full charge, the weight of hydrate formed will be 42.03kg and hence the volume of the heap will be 52.53 liters. For the geometry assumed, the ground contact area is $6.087ft^2$ and the surface area is $7.127ft^2$. The following are the assumptions, and initial boundary conditions used in the calculation of heat transfer to the spilled hydrate.

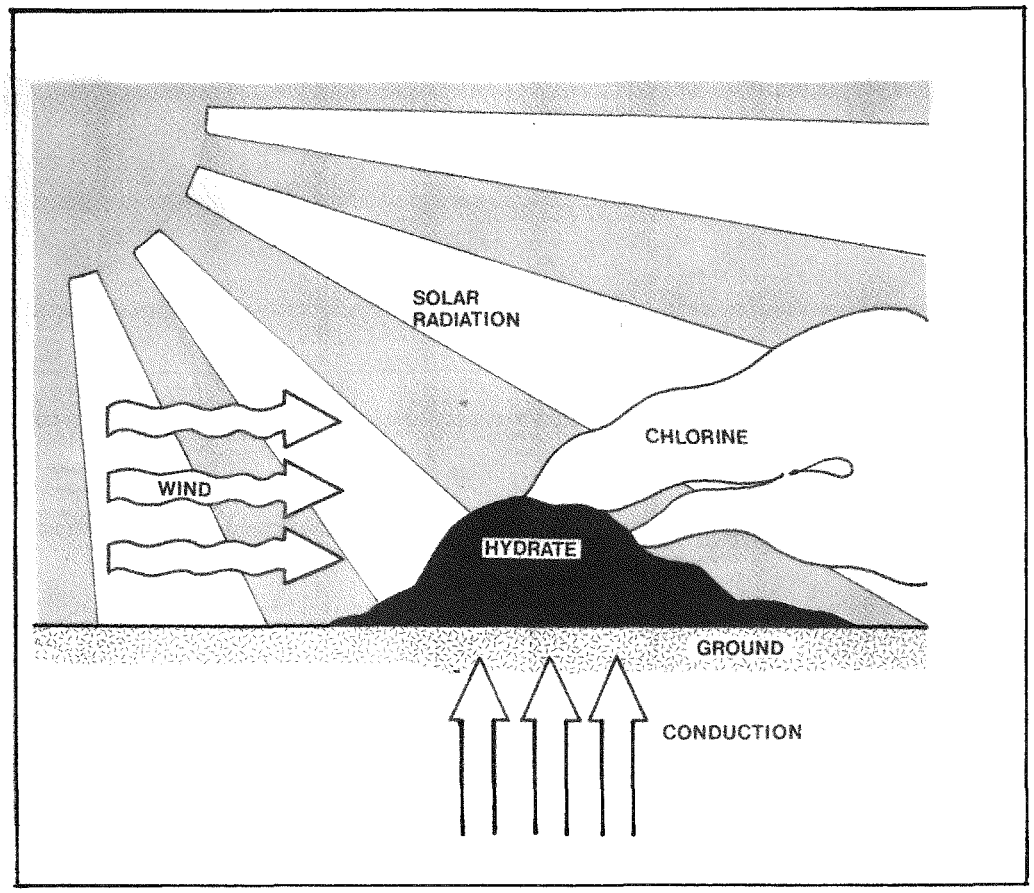

Figure 9-1. Diagram showing heat transfer into a hydrate slurry spilled onto the ground. Note: For the accident described in the text, no solar radiation occurs.

- There is no heat transfer contribution from solar radiation since this accident (and also the worst meteorological conditions) occurs at night.
- The ground is at a uniform initial temperature of T_a (37.8°C).
- The atmospheric temperature is also T_a (37.8°C).
- There is no lateral conduction in the ground.
- Decomposition of hydrate occurs at T_h (9.6°C).
- Wind speed = 2m/sec (explained later in this section).

The total rate of heat transfer (Q_T) to the hydrate is given in general form by equation 9-1.

$$Q_T = Q_R A_R + Q_{cv} A_{cv} + Q_{cd} A_{cd} \qquad (9\text{-}1)$$

where

Q_T = total rate of heat transfer to the hydrate

Q_R = rate of heat transfer due to radiation per unit area of hydrate exposed to the radiation source

A_R = area of hydrate exposed to the radiation source

Q_{cv} = convective heat flux to the surface

A_{cv} = convective heat transfer surface area

Q_{cd} = conductive heat flux to the hydrate from the ground

A_{cd} = area of contact between hydrate and ground

Calculation of $Q_R A_R$.

Q_R = 0 since this occurs at night. (9-2)

and hence

$Q_R A_R = 0$

Calculation of $Q_{cv} A_{cv}$. The convective heat transfer coefficient between the air and the hydrate block is a function of the boundary layer characteristics, properties of the air and the transpiration effect of chlorine released. There is turbulence present in the air, but under the stability conditions assumed it will be very low and hence a parallel flow of air is assumed. This tends to give a slightly

lower heat transfer coefficient. Because of the complex nature of the problem, the transpiration cooling effect of the chlorine released is ignored and this will likely more than offset the error introduced above. Even though the surface is a segment of a sphere, the boundary layer effects may be closer to that of a flat plate than a complete sphere. Nusselt number, N_u, for a flat plate in the laminar range is given by equation 9-3 (9-1).

$$N_u = \frac{hD}{K} = 0.664\ P_r^{1/3}\ E_r^{1/2} \qquad (9\text{-}3)$$

where

P_r = Prandtl number for air

R_e = Reynolds number for the flow

h = convective heat transfer coefficient

K = thermal conductivity of air at the boundary layer on the surface

D = diameter of the spill.

Substituting the values for the properties of air, dimensions of the spill and wind velocity in equation 9-3 and solving for 'h' we obtain:

$$h = 1.049 \text{Btu/hr}\cdot\text{ft}^2$$

so the heat flux

$$Q_{cv} = h(T_a - T_h)$$

and

$$Q_{cv} \cdot A_{cv} = h(T_a - T_h)\ \frac{\pi D^2}{4}$$

$$= 379 \text{Btu/hr}\cdot\text{ft}^2 \qquad (9\text{-}4)$$

Calculation of $Q_{cd}A_{cd}$. For the conditions assumed, heat transfer to the hydrate at the interface by conduction is given by equation 9-5 (9-2).

$$Q_{cd}A_{cd} = \frac{K\ A_{cd}(T_a - T_h)}{\sqrt{\pi\ \alpha\ \tau}} \qquad (9\text{-}5)$$

where

K = thermal conductivity of the floor

T_a = initial ground temperature

T_h = contact surface temperature

α = thermal diffusivity of the ground

τ = time from the instant of hydrate spill

$A_{cd} = 6.082\ ft^2$

For a peak-shaving plant with the batteries stationary, safety can be improved significantly by proper material selection for construction.

Any ground surface material with low thermal conductivity, heat capacity, and density can markedly reduce the conductive heat transfer to the hydrate. For the present analysis the ground is assumed to have been covered with scrap cork or a material with similar properties. Substituting these properties and the assumed temperatures in equation 9-5, we obtain the conductive heat transfer to hydrate at one minute after the spill as:

$$Q_{cd}A_{cd} = 218.7\text{Btu/hr} \qquad (9\text{-}6)$$

Substituting equations 9-2, 9-4, and 9-6 in equation 9-1, the total heat transfer to hydrate at one minute after the spill is given as:

$$Q_T = 0 + 379 + 218.7$$

$$= 597.7\text{Btu/hr}$$

If h_{fg} is the latent heat of decomposition of hydrate, then the chlorine release rate V is given by:

$$V = \frac{Q_T}{h_{fg}} \qquad (9\text{-}7)$$

Scenario II

The hydrate cake, as it forms, will be a prism with a rectangular base. The dimensions of the base (parallel to the ground) are 2.5ft x 2ft. The height of the

prismatic block depends on the state of charge and reaches 2.16ft at full charge. A fully-charged battery module contains 46.2kg of chlorine contained in a $10.6ft^3$ block of chlorine hydrate. The block is porous and the voids are filled with water. In case of severe damage to the battery, this block could be dislodged from its position and dropped onto the ground. As explained in Scenario I, the ground is covered with scrap cork. The block is likely to land on its base (2.5ft x 2ft) as it drops from the store.

The decomposition rate of this block depends on the rate of heat transfer to it. Depending on the ambient temperature, heat transfer occurs by conduction from the floor, by convection from the air and by radiation from the sun. After completing the charge, on a typical day, the battery will be on standby from 6:00 a.m. till about 2:00 p.m. Spillage of this block is possible at any time during this period. Hence the heat transfer and chlorine release rates are calculated with and without radiation to represent the daytime and nighttime conditions respectively.

Figure 9-2 is a sketch of the hydrate block spilled from the battery store and resting with its base on the floor.

The following are the assumptions, boundary conditions, and initial conditions for the calculation of heat transfer to the hydrate block.

- Intensity of solar radiation is $300Btu/hr \cdot ft^2$ and the absorptivity of the surface is 0.5.
- The ground is at a uniform initial temperature of T_a (37.8°C).
- The atmospheric temperature is also T_a (37.8°C).
- Lateral conduction in the ground is assumed to be zero.
- Decomposition of hydrate occurs at T_h (9.6°C).
- Wind speed is assumed to be 2m/sec.

The total rate of heat transfer Q_T to the hydrate is again given by equation 9-1.

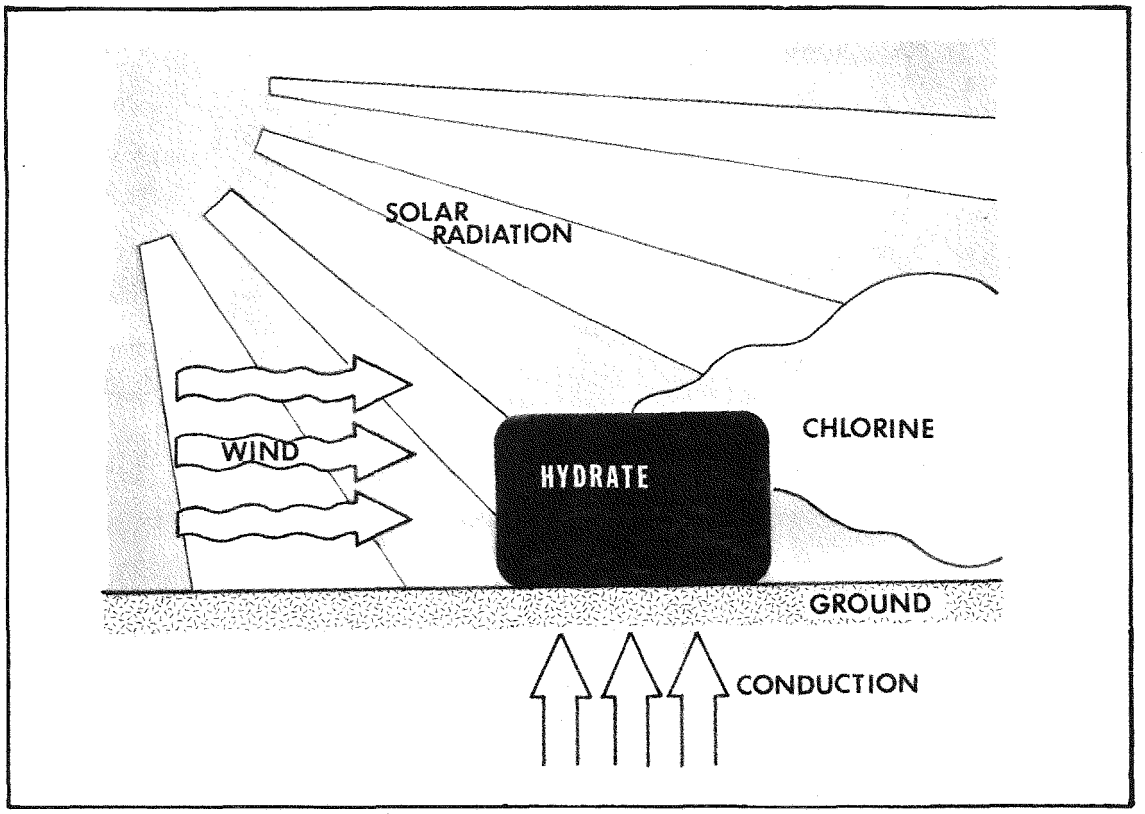

Figure 9-2. Diagram Showing Heat Transfer into a Hydrate Block on the Ground

Calculation of $Q_R A_R$. Assuming that solar radiation is normal to the surface:

$$Q_R = 300 \times .5 = 150 \text{Btu/hr} \cdot \text{ft}^2$$

$$Q_R A_R = 150 \times 2.5 \times 2 = 750 \text{Btu/hr} \cdot \text{ft}^2$$

Calculation of $Q_{CV} A_{CV}$. The convective heat transfer coefficient between the air and the hydrate block is a function of the boundary layer characteristics, properties of air, and transpiration effect of chlorine released. There is turbulence present in the air, but under the stability conditions assumed it will be very low and hence a parallel flow of air is assumed as in Scenario I. This tends to give a slightly lower heat transfer coefficient. Because of the complex nature of the problem, the transpiration cooling effect of the chlorine released is again ignored which likely more than offsets the above introduced error. Nusselt number 'Nu' for the top and two side surfaces parallel to the wind direction is given by equation 9-9.

$$Nu = .664 \, Pr^{1/3} Re^{1/2} \qquad (9\text{-}9)$$

where

Pr = Prandtl number for the fluid (air)

and

Re = Reynolds number for the flow

Evaluating the properties of air at film temperature and substituting in equation 6-9

$$Nu = \frac{hD}{K} = 184.5$$

or

$$h = 1.107 \text{Btu/hr} \cdot \text{ft}^2 \text{°F} \qquad (9\text{-}10)$$

and

D = length of the hydrate block (2.5ft)

For the leeward and windward sides of the block, the heat transfer coefficient is assumed to be the same as on the other sides and hence the total heat transfer by convection is

$$Q_{cv}A_{cv} = 1.107 \times (100\text{-}49.3) \{2.5(2 \times 2.16 + 2) + 2 \times 2 \times 2.16\}$$

$$= 1372 \text{Btu/hr} \qquad (9\text{-}11)$$

Calculation of $Q_{cd}A_{cd}$. Q_{cd} for the hydrate block is identical to that of slurry. But the contact area A_{cd} between the block and ground will be smaller than the base area of the block. When two rigid rough surfaces are brought into contact, actual contact area will only be a small fraction of the area of the contact surfaces. Conductive heat transfer occurs only through this contact area. For the present case, we can assume that 25% of the base area is the effective conduction area for the transfer of heat between the ground and hydrate block.

$$A_{cd} = 2.5 \times 2 \times 0.25 = 1.25 \text{ft}^2$$

Substituting the appropriate values in equation 9-5, the conductive heat transfer to the block from the floor at one minute after the spill is:

$$Q_{cd}A_{cd} = 44.91\text{Btu/hr} \tag{9-12}$$

Total heat transfer to the hydrate during daytime

$$Q_T = 750 + 1372 + 44.9$$

$$= 2167\text{Btu/hr} \tag{9-13}$$

Total heat transfer during nighttime

$$Q_T = 1372 + 44.9 = 1417\text{Btu/hr} \tag{9-14}$$

By substituting the heat transfer from equations 9-13 and 9-14 in equation 9-7, the corresponding chlorine release rates can be obtained.

Scenario III

In this case the heat transfer to the store occurs from the sump and stack of the battery whose operating temperatures are higher than that of the store. If the accident occurs at any time other than when the battery is charging or discharging, the heat transfer and chlorine release rates are going to be negligible even under the most adverse atmospheric conditions and hence can be ignored.

The total heat transfer rate Q_T to the hydrate during charge or discharge is

$$Q_T = 516.8\text{Btu/hr} \tag{9-15}$$

(for details see Table 5-3a).

Gas release rate for this case can be obtained by substituting the value for Q_T from equation 9-15 in equation 9-7.

ENVIRONMENTAL AND PHYSIOLOGICAL EFFECTS OF CHLORINE

Chlorine is a phytotoxic agent and is known to cause from minor damage to death to plants depending on the level of exposure and condition of the plant. Different

species of plants have varying degrees of resistance to chlorine exposure and there is no common threshold level causing damage to all plants. Plants under water stress exhibited higher degree of resistance than those under no water stress. In an accident involving 30 tons of chlorine in a rural area, all the native grasses and clover burned and became brittle and other plants suffered severe damage. However, the damage was considered to be local and temporary. In the same accident corrosive damage to the farm equipment was severe where the metal was covered with dew drops. In the presence of water, chlorine forms dilute hydrochloric and hypochlorous acids and becomes very corrosive. Chlorine reacts with most common metals under normal atmospheric conditions due to the presence of atmospheric moisture.

Chlorine is primarily a respiratory irritant and Gay (9-3) summarizes the reaction as minimal burning sensation of mucous membranes on mild exposure and severe irritation of the throat, nose, and eyes sometimes accompanied by paroxysmal (a fit, attack) cough on moderate exposure to chlorine. The symptoms of mild exposure will normally clear in a few minutes without any treatment. Severe exposure may result in productive cough, difficulty in breathing, and often cyanosis. Treatment is needed for all these patients, but most of them will return to work on the following day. If a person is trapped in an area of high chlorine concentration, it results in a medical emergency.

The above classification of degree of exposure by Gay is qualitative. Fieldner (9-4) et al prepared a list of industrial gases and their toxic doses for the Bureau of Mines under the title, "Gas Masks for Gases Met in Fighting Fires". Table 9-2 is an extract for chlorine from this list. Selected values from this table of 3.5ppm for an odor detection level and 50ppm for a health hazard level are used to describe the extent of the dispersion zones as a result of accidental chlorine release from Mark 4 battery plants.

ATMOSPHERIC DISPERSION OF CHLORINE

Accidental release of chlorine, as described in the previous scenarios, results in contamination of the air in the vicinity of the chlorine release source. In order to evaluate the magnitude of the resultant hazard, it is necessary to determine the concentration of chlorine as a function of distance from the release source.

Turbulent dispersion of chlorine (or any other gas) depends primarily on the wind velocity and atmospheric stability conditions at the location. These conditions

Table 9-2

PHYSIOLOGICAL RESPONSE TO VARIOUS
CONCENTRATIONS OF CHLORINE GAS

Effect	Parts of Chlorine Gas per Million Parts of Air, by Volume (ppm)
Least amount required to produce slight symptoms after several hours exposure	1
Least detectable odor	3.5
Maximum amount that can be inhaled for one hour without serious disturbances	4
Noxiousness, impossible to breathe several minutes	5
Least amount required to cause irritation to throat	15.1
Least amount required to cause coughing	30.2
Amount dangerous in 30 minutes to one hour	40-60
Kills most animals in very short time	1000

vary over a wide range with the place and time. Sometimes these conditions aid in rapidly dispersing the pollutants thus keeping the pollution levels very low, and sometimes they are stagnant resulting in local accumulation of pollutants and creating episodes like the ones experienced by London and Los Angeles. It is impossible to predict the meteorological conditions for any given time. Pasquill (9-5) has proposed six stability classes to describe the diffusion characteristics of the lower atmosphere. These are based on wind speed, solar radiation, cloud cover, and time of the day, i.e. day or night. Pasquill's classes range from very unstable (class A) to moderately stable (class F) and are reproduced in Table 9-3.

Table 9-3 establishes the relationship between the wind velocity, insolation and Pasquill's stability class. From the table, it is obvious that Pasquill F, with 2m/sec wind, is the worst condition from diffusion point of view. This occurs only in the night and hence there is no solar radiation. Scenario I is possible only at night, whereas Scenarios II and III are possible during day as well as night. For the accident described by Scenario III, chlorine release rates are independent of weather conditions, since decomposition energy is obtained from within the battery. Hence dispersion calculations for Scenarios I and III with the above listed meteorology, results in the worst possible spread of chlorine from these accidents.

Table 9-3

RELATION OF TURBULENCE TYPES TO WEATHER CONDITIONS

A - Extremely unstable conditions

B - Moderately unstable conditions

C - Slightly unstable conditions

D - Neutral conditions*

E - Slightly stable conditions

F - Moderately stable conditions

Surface wind speed/ m/sec	Daytime insolation			Nighttime Conditions	
	Strong	Moderate	Slight	Thin overcast or ≥ 4/8 cloudiness†	≤ 3/8 cloudiness
<2	A	A	B	--	--
2	A-B	B	C	E	F
4	B	B-C	C	D	E
6	C	C-D	D	D	D
>6	C	D	D	D	D

*Applicable to heavy overcast, day or night.

†The degree of cloudiness is defined as that fraction of the sky above the local apparent horizon which is covered by clouds.

Chlorine concentrations in the air in the vicinity of the accident under these conditions are calculated and isopleths for 50, and 3.5ppm levels are presented in Figures 9-3 and 9-4 for the above two accidents respectively. For Scenario II, the chlorine release rates are highest during daytime under bright sun, but the dispersion characteristics of the atmosphere are more favorable during daytime. Chlorine concentrations in the air from this accident during night under the same conditions as for the other two accidents are calculated, and the results are presented in Figure 9-5. For comparison, dispersion calculations are repeated for daytime conditions under bright sun. From Table 9-3, under strong insolation, as the wind speed increases, its stability also increases. An increased wind speed causes increased advective dilution, but an increased stability decreases the dispersion rate across the wind stream. The former tends to accelerate the process of dilution and the latter tends to decelerate this process. For the present analysis a low wind speed (2m/sec) and the corresponding stability class (Pasquill's class A) under bright sun are selected for the above daytime dispersion calculations. Isopleths at different levels from these calculations are presented in Figures 9-3 through 9-6.

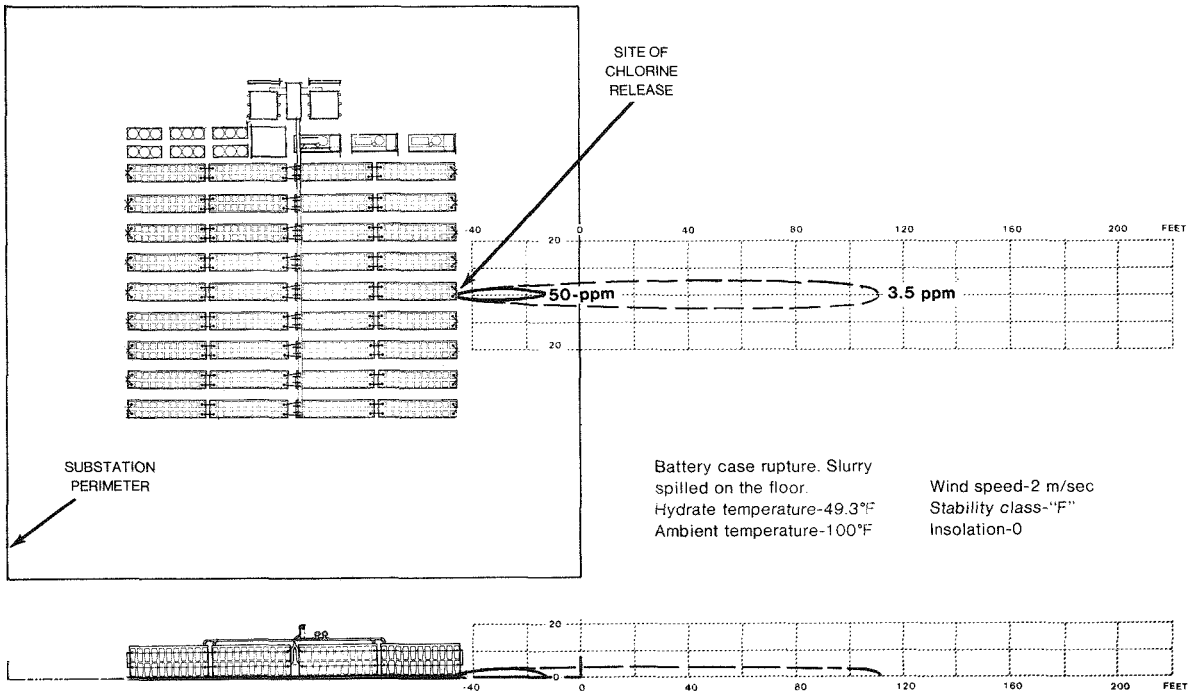

Figure 9-3. Chlorine dispersion from major battery accident under worst possible conditions. Isopleths of 50 and 3.5ppm indicate the hazardous and odor threshold levels respectively.

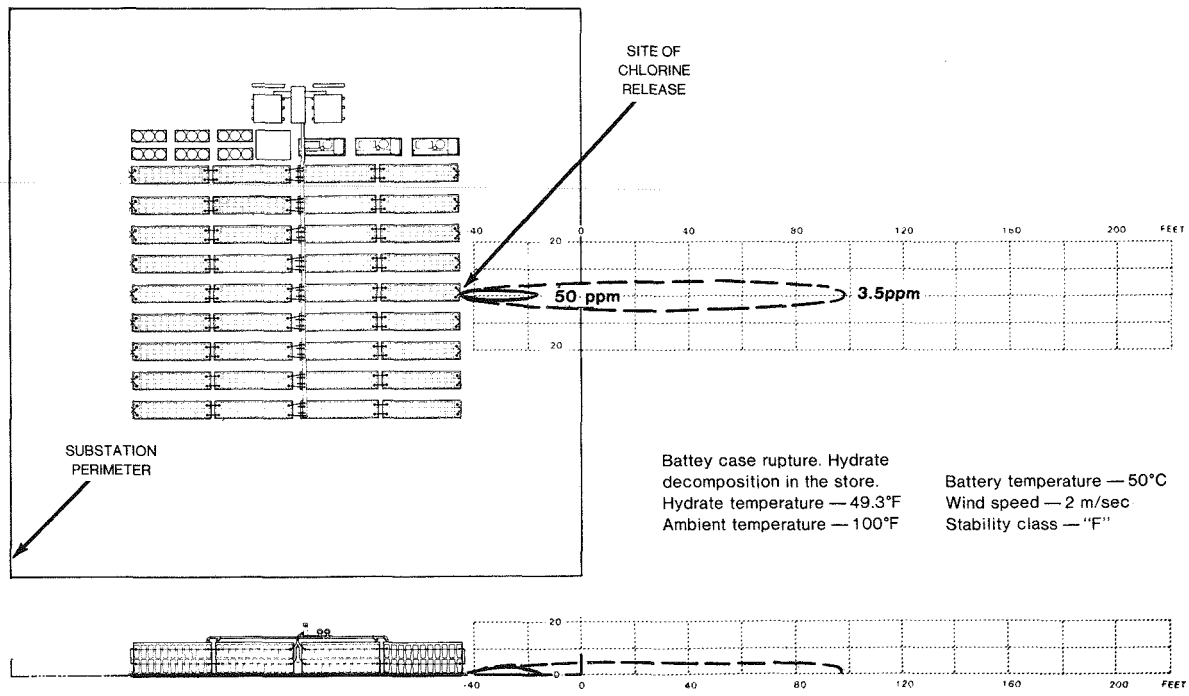

Figure 9-4. Chlorine dispersion from a more probable very major battery accident under the most stagnant atmospheric conditions (Table 9-3). Isopleths of 50 and 3.5ppm indicate the hazardous and odor threshold levels respectively.

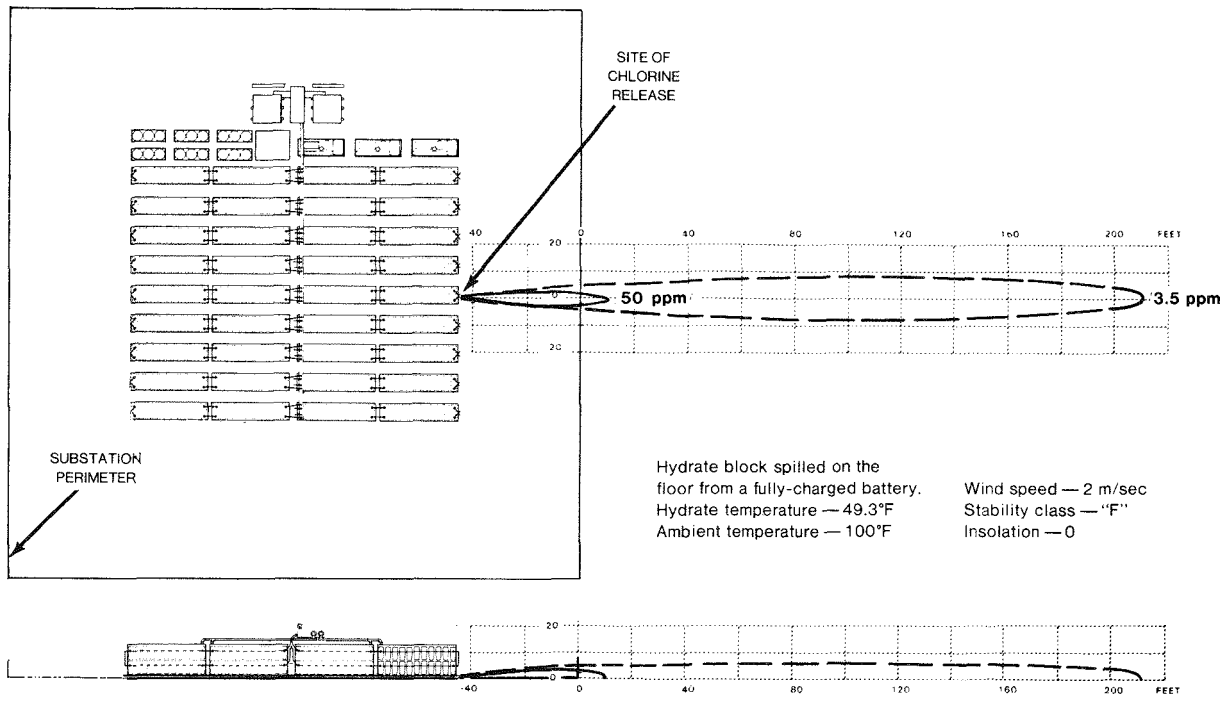

Figure 9-5. Chlorine dispersion from the worst case battery accident with the most stagnant meteorology (Table 9-3). These isopleths indicate the worst spread of chlorine that can ever occur from a zinc-chlorine battery module. Note the vast difference in areas covered by the odor threshold (3.5ppm) isopleth and hazard level (50ppm) isopleth. The spread is long but narrow.

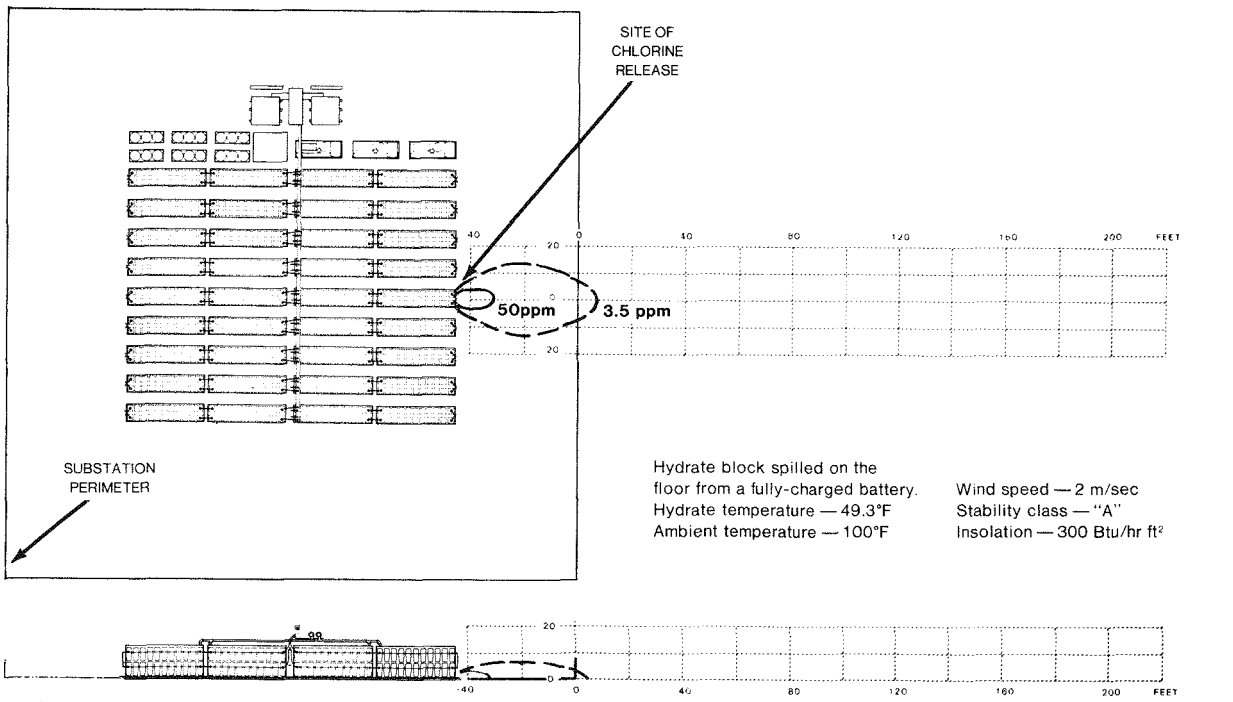

Figure 9-6. Spread of chlorine from a daytime accident releasing chlorine at about the highest possible rates under an assumed meteorology to attain these rates. The isopleths at both the odor threshold (3.5ppm) and hazard level (50ppm) are wider but confined to shorter distances from the accident.

Atmospheric dispersion calculations are based on the plume model -- and modified Sutton's equation (9-6) for such a model is:

$$\chi(x,y,z,H) = \frac{V}{2\pi\sigma_y\sigma_z U} \exp\left[-1/2\left(\frac{y}{\sigma_y}\right)^2\right]\left\{\exp\left[-1/2\left(\frac{z-H}{\sigma_z}\right)^2\right] + \exp\left[-1/2\left(\frac{z+H}{\sigma_z}\right)^2\right]\right\}$$

where

U = wind velocity

χ = concentration of chlorine in the air

x = coordinate of the point in the downwind direction from the leakage source

y = coordinate of the point in the crosswind direction from the leakage source

z = height of the point above ground level

H = height of the plume center line (0 meters)

V = rate of chlorine release from the source

σ_y and σ_z are obtained from Pasquill-Gifford charts for the class of stability assumed.

This model ignores the effects of molecular diffusion and gravitational spread. In the atmosphere, certain levels of turbulence are always present and the mixing of air by this mechanism is a few orders of magnitude larger than that due to molecular diffusion. For this reason the effect of molecular diffusion is not normally included in the solution of such problems. Chlorine is a heavier gas and hence gravity effects play a significant role in spreading chlorine clouds laterally along the ground. However, an analysis on the gravity spread of liquid natural gas by Gemeles et al (9-7) indicates that such effects are negligible for spills of LNG as large as $1250M^3$ occurring in ten minutes. The chlorine release rates from the battery accident are orders of magnitude smaller than these, and hence an analysis for gravity spread of chlorine was deemed inappropriate.

The rates of chlorine release for Scenarios I and II are a function of time. The rates are the highest immediately following the spill and decrease gradually with

time. This is primarily because of the gradual cooling of the ground. For both these cases, isopleths are prepared for the rate of chlorine release at one minute following the accident. The dispersion equation is derived for a steady state release. Use of this equation in the present case with gradually decreasing rate introduces some error. Actual concentrations at any time after one minute following the spill will be smaller than the ones presented in Figures 9-3, 9-5, and 9-6. Similar trends exist for Scenario III also, because of the gradual cooling of the batteries.

The 3.5ppm odor detection level extends far beyond the 50ppm hazardous level in all cases. People have to pass through 3.5ppm level before they can reach higher and uncomfortable levels. The pungent odor of chlorine discourages people from entering the dangerous concentration area.

RESULTS AND DISCUSSION

Isopleths presented in Figures 9-3, 9-4, and 9-5, are the chlorine concentrations in the vicinity of an accident involving a zinc-chlorine peak-shaving battery under a host of adverse conditions occurring concurrently. Even though the probability of occurrence is extremely low, these isopleths represent the worst that could ever result from an accident involving this battery. The following worst case conditions are used to obtain these isopleths.

- For Scenarios I and II, the chlorine release rates are the highest for each mode occurring when the respective volumes of the hydrate are the maximum possible.
- For Scenario III, the accident occurs at the time when the sump and stack are very warm.
- For dispersion, the most adverse meteorological conditions from Pasquill's table are assumed to be present.
- Since these conditions occur at night, the examples are at night.
- Night temperatures are in general lower, but for these scenarios the temperatures are assumed to be 37.8°C.
- The accident is the worst conceivable for each case producing the maximum possible effect from the chlorine-release point of view in each case.
- Chlorine is normally very reactive element. In this case all the chlorine as it is released is assumed to spread without any of it reacting with the materials in its path.

In a peak-shaving station, the batteries are stationary. Any physical accident has to be caused by the movement of objects brought into the yard either for maintenance, repair, or other reasons. It is very unlikely that such operations will be performed during nighttime. Also, the discharge rate of this battery depends on the supply of chlorine to the electrodes. Because of the limited chlorine supply at the electrodes, thermal runaway of this battery under short circuits is eliminated. Under equipment malfunction, the damage to the battery will be very limited and chlorine release rates will be much smaller than those resulting from the assumed accidents.

Equilibrium temperatures of hydrate under atmospheric pressure is 9.6°C. At temperatures lower than this, decomposition rates will be extremely low. Hence the chlorine release rates at ambient temperatures below 9.6°C can be ignored. As the ambient temperature increases above this level, there is a continuous heat transfer to the hydrate. As the temperature increases from 9.6°C to 37.8°C (100°F), the chlorine-release rates increase linearly from zero to a maximum of the calculated level for Scenarios I and II. Hence at 23.9°C (75°F), the concentrations will be about half as much as they are shown in the isopleths.

Representation of Scenario II in the daytime, even under intense insolation and the corresponding meteorological conditions resulted in the spread of chlorine at the selected concentrations to much smaller areas than during the night, even though the chlorine-release rates are larger. This represents the worst conceivable result from this battery during daytime with the several adverse constraints assumed in the calculation.

CONCLUSIONS AND RECOMMENDATIONS

The analysis of the accident scenarios above clearly indicate that odor threshold levels of chlorine concentration reach beyond the perimeter of the substation assuming a site area of one acre. These isopleths are a result of several assumptions to represent the worst possible accident scenarios from the battery plant. A more probable accident will result in concentrations several-fold smaller than the ones presented here. Topography of the area and buildings will modify the dispersion characteristics of the atmosphere significantly. In general, these deviations tend to accelerate the process of dispersion reducing the spread of high concentrations beyond the site. The meteorological conditions also vary over a wide range from place to place. Hence site-specific isopleths have to be prepared to determine the chlorine spread for a given location in case of an accident.

The calculations presented here are based on several assumptions. Experimental work in the area of heat transfer and dispersion of chlorine must be performed to determine the validity of these assumptions. Chlorine-release rates and dispersion characteristics are the two main factors controlling the chlorine concentrations in the vicinity of the accident. Both of them are dependent on the existing meteorological conditions at any time. The relationship is such that a wide variety of dispersion conditions are possible for any given chlorine release rates and vice versa. Hence a computer model interconnecting these two effects over all the possible meteorological conditions has to be developed, to determine the most credible chlorine-release occurrence for any given site. Until these two tasks are completed a definite answer to the question of the safety of these open battery plants cannot be answered conclusively.

REFERENCES

9-1 E.R.G. Eckert Drake Jr. Analysis of Heat and Mass Transfer. New York: McGraw-Hill, p. 319.

9-2 J.P. Holman. Heat Transfer. 2nd ed. New York: McGraw-Hill, p. 80.

9-3 H.H. Gay. "Exposure to Chlorine Gas". J.A.M.A., March 2, 1963, pp. 166-167.

9-4 A.C. Fieldner, S.H. Katz, and S.P. Kinney. "Gas Masks for Gases Met in Fighting Fires". Bureau of Mines Technical Paper #248. Wash. D.C.: Government Printing Office, 1921.

9-5 F. Pasquill. Meteorology, 90, 1961, 33.

9-6 O.G. Sutton and J. Roy Quart. Meteorol. Soc., 73, 1947, 426.

9-7 A.E. Gemeles and E.M. Drake. "Gravity Spreading and Atmospheric Dispersion of LNG Vapor Clouds". Cabot Corp. Research Paper 110-183, presented at Fourth International Symposium on Transport of Hazardous Cargoes by Sea and Inland Waterways, 1975.

Section 10

SAFETY FEATURES OF 100MWh BATTERY PLANTS

INTRODUCTION

As peak-shaving battery plants are intended for public utility siting on the distribution or sub-transmission network in residential areas, as well as in other areas, the design criteria include the requirement of minimum siting restrictions. As discussed in Section 9, the only potential hazard associated with siting zinc-chlorine battery plants in residential areas is the possibility for accidental release of hazardous amounts of chlorine gas. The results of the hazards analysis indicate that even the worst-case accident involving a single battery module does not present a major safety problem. This section discusses safety features inherent in the Mark 4 battery design and supplemental safety features which can be utilized to eliminate the possibility of common mode failures, involving multiple battery modules, as well as reducing the probability of chlorine release resulting from internally and externally caused failure of single battery modules.

INHERENT SAFETY FEATURES

A unique feature of zinc-chlorine batteries is the storage of chlorine as chlorine hydrate. Use of this storage medium offers numerous advantages over other halogen storage methods.

- Since chlorine hydrate is a solid, having a large heat of formation, tank rupture does not lead to massive chlorine gas leakage.
- The system can be operated very close to ambient pressure thus conferring greater safety on the system.
- Chlorine hydrate appears to offer cost advantages since the complex uses water at virtually zero cost.

- The enthalpy of formation of chlorine hydrate is sufficiently large so as to provide significant battery cooling in discharge.

- It is unnecessary to dry the chlorine before hydrate formation which leads to capital cost, operating cost, operational reliability, and safety advantages.

- Storing the halogen external to the electrochemical cell prevents activated stand losses by direct reaction of chlorine with zinc.

The first two advantages are related to safety and permit consideration of the battery for the peak-shaving application.

Review of Basic Design and Operation

Basic operational and design descriptions of the Mark 4 battery are presented in Sections 5 and 6. Only those features relating to safety will be reviewed in this section.

An artist's rendition of the 100MWh Mark 4 plant is shown in Figure 10-1. The battery portion of the plant consists of 1584 battery modules, each containing its own hydrate store compartment, which eliminates exposed chlorine transfer lines.

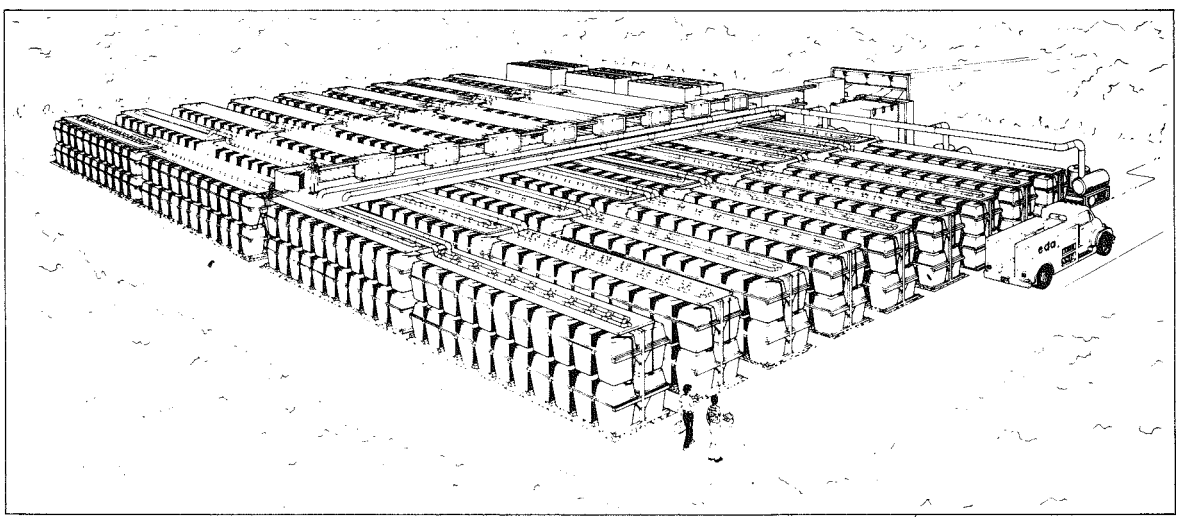

Figure 10-1. General view of 100MWh Mark 4 zinc-chlorine peak-shaving battery plant. Note the absence of chlorine transfer lines and the wide dispersal of stored chlorine over 1584 separate store compartments.

Each 66kWh module has the capacity to store 102 lb of chlorine as chlorine hydrate at full charge. This corresponds to 81 tons of stored chlorine dispersed over slightly more than a quarter-acre.

To meet the needs of the electric utility industry in realizing maximum benefit from its baseload and intermediate generating equipment, the batteries will be charged during periods of low public demand and discharged during periods of high public demand. Figure 10-2 illustrates a simple public demand curve for a daily cycle.

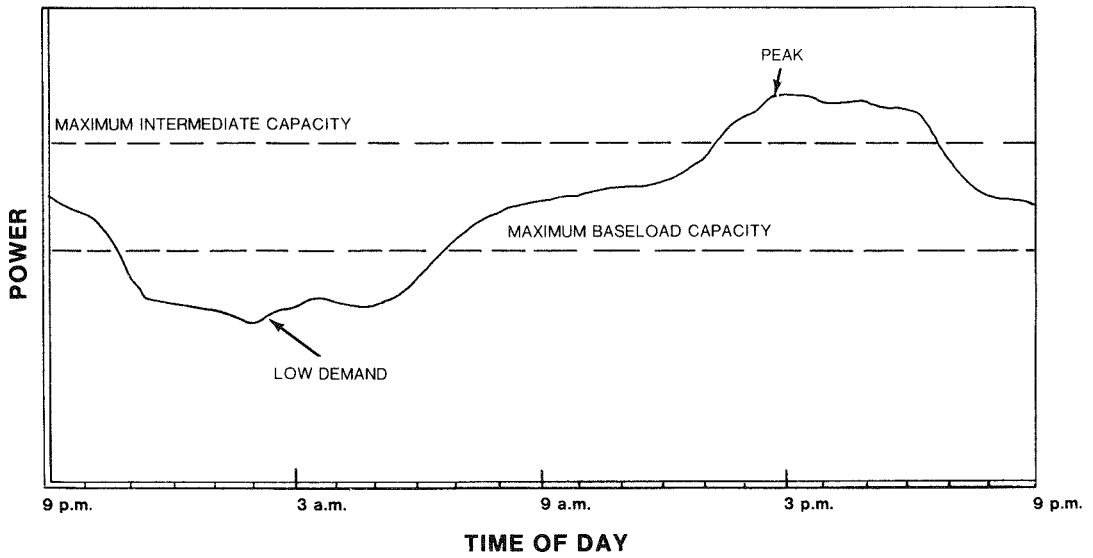

Figure 10-2. Daily Public Demand Curve for Electricity

The Mark 4 battery plant will accept baseload or intermediate generated power during low public demand periods, store it electrochemically during average demand periods, and return it to the utility network to supplement baseload and intermediate generated power during peak demand periods. Each 2.9MWh battery string can operate independently to take full advantage of available power during low demand periods and to incrementally supplement generated power during peak periods. This load-following capability is provided in 580kW increments from each of the 36 battery strings.

Figure 10-3 illustrates the effect of this cycle phenomena on the quantity of chlorine stored as chlorine hydrate in the battery modules. Notice that during

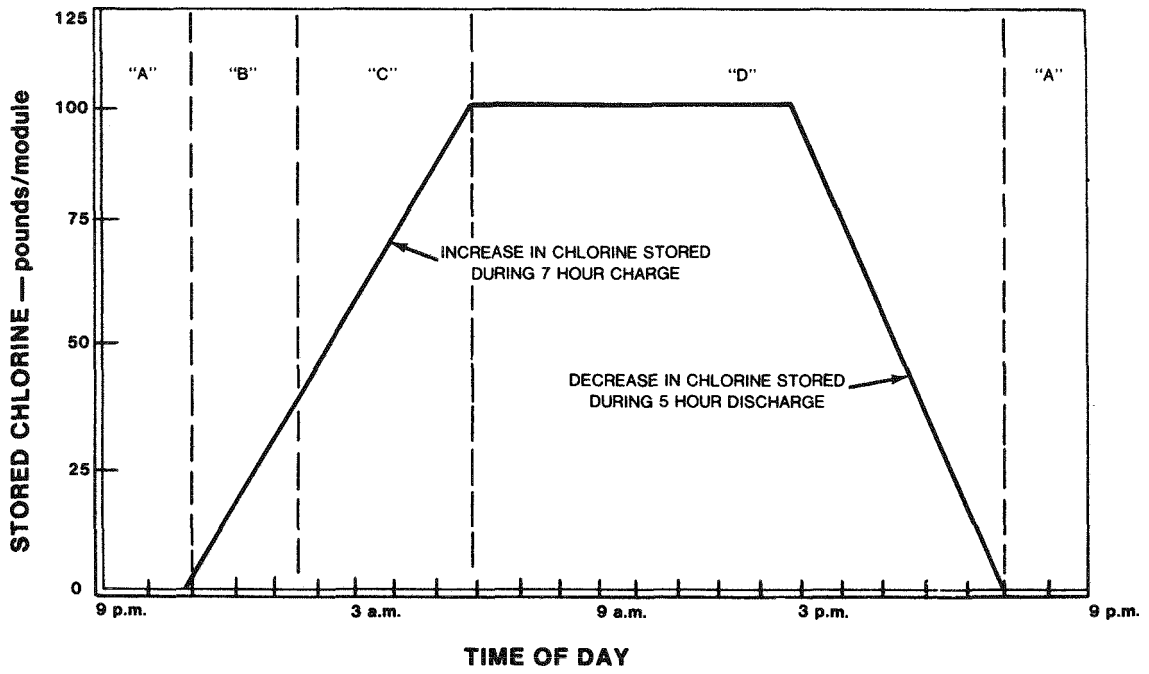

Figure 10-3. Variation in quantity of chlorine stored per battery module during a 24-hour cycle.

four hours of this cycle (zone "A") no chlorine is stored as chlorine hydrate and the battery is completely discharged and innocuous. From 11 p.m. until 6 a.m. the battery is being charged and chlorine is being stored at a constant rate. This period is divided into two zones -- "B" and "C". Zone "B" is where the majority of the stored hydrate is in the form of a slurry while zone "C" is where it begins forming a solid cake and by the end of charge the hydrate is essentially a solid block. This state is maintained until 2 p.m. when the discharge process is initiated. During discharge the hydrate block decomposes at a constant rate and continues to shrink in size. By 7 p.m. the discharge is complete, all the hydrate is decomposed, and the battery is again innocuous. On weekends this innocuous state can be maintained from 7 p.m. on Friday until 11 p.m. on Sunday when the charging process is again initiated during the low demand period.

The above discussed features are those which are inherent in the Mark 4 design and operation. They can be summarized as follows:

- Near ambient pressure and temperature operation due to storage of chlorine as chlorine hydrate.
- Suppressed chlorine gas release rates resulting from accidents, due to storage of chlorine as hydrate.

- Wide dispersal of stored hydrate and a maximum of 102 lb of chlorine released due to single tank rupture.
- No external chlorine transfer lines.
- Complete discharge capability renders the battery innocuous for at least four hours per day and during extended stand periods.

Supplemental Safety Features

In order to confer additional safety on the Mark 4 battery numerous features have been conceived to supplement the inherent features described above. These operational and design features can be summarized as follows:

- Numerous safety interlocks at the module level to monitor possible failure modes and safely control battery operation.
- Three levels of control [(1) module, (2) string, and (3) plant] which interact with one another to provide uninterrupted plant operation while properly decommissioning a malfunctioning battery string.
- Use of a non-combustible coolant, for temperature control and hydrate formation, in order to eliminate the common mode failure of pool fires.
- Chlorine sensors, connected to alarm systems to signal on-site maintenance personnel and a remote load dispatcher of an accidental release of chlorine gas.
- If deemed necessary for residential siting, an enclosure around the battery portion of the plant incorporating chlorine absorbing or scrubbing capabilities.

The safety interlocks currently projected for the FC+5 battery modules are:

- Back-up pressure control for decommissioning of battery modules.
- A failsafe passive H_2/Cl_2 reactor to insure low H_2 partial pressures in the modules.
- Sail sensors to monitor and signal pump failures.
- All internal and external failure modes will decommission the module and associated battery string via a self-discharge process at the ten-hour rate or slower.

During normal operation the battery modules will be controlled with a pressure sensor located in the stack compartment. Should this primary sensor fail, a back-up pressure sensor located in the store compartment will override the primary sensor, from which the decommissioning of the module will be controlled.

In order to provide uninterrupted, catalyzed recombination of evolved hydrogen gas with chlorine gas, a passive H_2/Cl_2 reactor will be developed to replace the fluorescent-light reactor currently in use. The light reactor can fail either due to loss of power or bulb failure. While inoperable the partial pressure of hydrogen would then accumulate to a hazardous level. The passive reactor renders this potential hazard negligible.

Sail sensors or similar devices will be located on the high pressure side of the pumps to monitor pump failures. Pump failures, as well as all other internal failure modes, when sensed will cause decommissioning of the battery module and the associated battery string via a self-discharge process at the ten-hour discharge rate or slower.

Three levels of control, which interact with one another, will accomplish the decommissioning of malfunctioning battery strings, as well as provide uninterrupted operation of the battery plant. For example, if a failure mode is sensed and confirmed in one of the modules, the module control addresses the string control which in turn overrides the individual module controls to decommission that string. This interactive control system will be sophisticated and will likely require a significant development effort.

The potential for pool fires, caused by leakage and subsequent ignition of combustible coolant fluids, could cause multiple battery module failures resulting in significant chlorine release rates. To eliminate this possibility a non-combustible coolant fluid will be utilized for temperature control and hydrate formation. No other mechanisms have as yet been identified which could cause multiple battery module failures leading to sizeable chlorine release rates and volumes.

Should an accident result in the release of chlorine gas from the plant, numerous ground-level chlorine sensors, located around the plant perimeter, would sense the leak and signal alarms, both at the plant and at monitoring stations. The audio alarm at the plant would warn maintenance personnel in the area of a potential hazard. The remote alarm could be a conventional fire alarm sounded at the local fire station or at the central dispatch location. The dispatcher could then notify the proper authorities. Trained firemen could effectively carry out clean-up operations.

Clean-up of accidentally spilled chlorine hydrate could involve interim measures to reduce the rate of heat transfer to the hydrate, as well as permanent disposal measures. Covering the spilled hydrate with foam or canvas cloth will effectively reduce convective and radiative heat transfer to the hydrate thereby reducing the chlorine release rates. A water spray of the chlorine gas envelope will absorb chlorine gas and reduce the concentration of airborne chlorine in the vicinity of the spill. These interim measures can be instituted until the remaining hydrate can be removed from the plant site and transported in an insulated container to an appropriate location for disposal.

Another safety feature under consideration is a building to enclose the battery portion of the plant which incorporates its own clean-up or chlorine scrubbing capabilities. The enclosure would incorporate multiple chlorine scrubbers as part of a recirculating air system which would be activated upon the accidental release of chlorine gas. Properly engineered and constructed to ensure a minor amount of air exchange with the ambient, the enclosure could render the facility rather innocuous regardless of the magnitude of the accidental chlorine spill. A less costly and perhaps more effective alternative is to provide a minor amount of controlled air exchange during scrubber operation to minimize or eliminate the normal uncontrolled diffusive exchange, thereby practically eliminating any release of chlorine to the ambient. This could be accomplished by venting a controlled portion of the return scrubber-exhaust gas to create a slight negative pressure inside the building. Still other alternatives such as individual string enclosures are also possible and should be evaluated for performance and cost effectiveness, as well as serviceability. A building, less scrubbers, is included in the cost analysis presented in Section 8. The incorporation of a scrubber system will not drastically affect the overall cost projection.

DISCUSSION

The Mark 4 design and operation have already received appreciable attention from the safety and environmental viewpoints and will continue to do so. The integral module concept, itself, significantly reduces the possibility of accidental release of toxic amounts of chlorine. The use of chlorine hydrate, instead of liquid chlorine, as the chlorine storage medium further reduces the potential health and environmental hazards in the immediate vicinity of an accidental spill. Table 10-1 compares the pertinent properties of these two storage media. These properties affect the rate at which chlorine gas can be liberated from these media upon spillage.

Table 10-1

COMPARISON OF SELECTED PROPERTIES WHICH ILLUSTRATE THE RELATIVE DIFFICULTY IN FORMING GASEOUS CHLORINE FROM CHLORINE HYDRATE AND LIQUID CHLORINE

	$Cl_2 \cdot 8H_2O$	Liquid Chlorine
Physical form	solid	liquid
Latent heat to form gaseous chlorine (kCal/g•mole)	18.6	4.88
Minimum temperature to form gaseous chlorine (°C)		
Decomposition temperature	9.6	--
Boiling point	--	-34.05

In the form of a solid, hydrate, unlike liquid chlorine, will not flow along the ground and thus exposes much less surface area to ambient heat transfer sources. Hydrate also has a 3.8 times greater latent heat for chlorine gas release than does liquid chlorine. This difference, as well as hydrate's higher gas formation temperature (smaller thermal driving force) significantly reduce the chlorine gas release rates under all ambient conditions. Combination of this safety advantage with additional design and operational safety features, to eliminate common mode failures and minimize the probability of accidental chlorine release, should confer an acceptable level of safety on the zinc-chlorine battery in this application.

More comprehensive studies will be performed to develop a sound position statement in the area of safety. These studies include:

- FMEA's at the module, string, and plant levels.
- Computer modeling studies of chlorine release and dispersion.
- Experimental verification studies of chlorine release and dispersion.

The failure modes and effects analyses (FMEA's) may suggest additional common mode failures and/or the need for alternative safety features which could prove more effective in controlling the chlorine gas release hazard. The experimental studies will provide verification or refinement of present mathematical models which will permit comprehensive computer analyses of the probable accident scenarios. At present it appears that a building around the battery portion of the plant is the most effective method of confining and handling accidentally released chlorine from plants located in residential areas.

Section 11

LEGAL ASPECTS OF BATTERY PLANT SITING IN RESIDENTIAL AREAS

INTRODUCTION

One of the principal applications of the zinc-chlorine battery will be to serve in the sub-transmission network of electric-utility systems. Initially, the battery plants will be built in conjunction with existing and planned distribution substations. These substations are located throughout the region served by the utility, and many are located in residential districts.

Traditionally, residential districts are the most restricted areas in terms of the buildings permitted and uses made of the land. This situation is further complicated by the potential environmental risks associated with the zinc-chlorine system. In essence these are legal questions which must be considered in determining the ultimate suitability of zinc-chlorine batteries for residential siting.

This section introduces the various laws and regulating agencies pertinent to residential siting of zinc-chlorine battery substations. The direct and indirect effects of federal, state, and local laws are reviewed with respect to the public utility industry, environmental agencies, land use, and planning. The guidelines of various state and local commissions, considered representative of a norm, are presented. Also discussed are the factors or considerations which will be used in application of siting laws and suggested means of obtaining certification.

SITING CONSIDERATIONS

As with any decision the advantages must be weighed against the disadvantages. In this case, the need for and benefits of zinc-chlorine battery plants must be evaluated for possible impact on a residential environment. Evaluation criteria are based on construction, operation, and failure of the system.

The impact of constructing zinc-chlorine plants on a residential environment will be minimal. This is primarily due to the manufacture of the modules and assembly of the strings at a separate facility. Furthermore, there is no need for underground excavation or special foundation for the plant.

Normal system operation will have an insignificant effect on local environment. In this mode the impacts basically will consist of low levels of heat and noise from the refrigeration equipment. Traffic from supply trucks will not be a consideration because of the expected longevity and low required maintenance of the system.

The possibility of accidental release of chlorine gas to the surrounding atmosphere is the only significant environmental impact if the system should fail. As stated in the preceding sections, the basic design and operation of the plant, as well as numerous additional safety features, have minimized this possibility. This event is reduced to near impossibility if the plant is enclosed. Nevertheless, this risk can never be totally eliminated.

Any potentially negative aspects of the system must be counterpoised with the need for and benefits of zinc-chlorine battery plants. The immediate need for an alternative method of supplying peak demand electricity is well known. Presently, the electricity generated for peak demand is supplied from diesel engines and combustion turbines. These power plants are fired by distillate oil and natural gas. The supply of these fuels is rapidly decreasing while the demand for electricity is greatly increasing.

Energy storage offers the alternative of supplying peak demand from baseload electricity, which is generated from coal and nuclear fuels. Although several energy-storage technologies are currently being developed, advanced batteries offer distinct advantages over the other concepts. Among these are short lead time for construction, small land area requirements, and modular construction which allows for later additions as the demand for electricity increases (11-1). These batteries will also benefit the utilities by providing electricity during power failures, meeting minute-to-minute demand fluctuations, and providing spinning reserve.

Of the advanced battery group, the zinc-chlorine battery is the furthest developed technically and will be the first to be tested in the Battery Energy Storage Test (BEST) Facility. Its advantages include near-ambient temperature operation, complete-discharge capability, and low material costs (graphite, zinc, chlorine, water, plastics, and polyesters).

PUBLIC UTILITY LAW

Federal

By definition those who supply or generate electricity for public consumption are included in the general term public utility. Since public utilities will be the consumers of energy-storage technologies, the laws which affect them will ultimately affect the energy-storage technologies.

Until August 4, 1977, the Federal Power Commission (11-2) was the agency of control over non-nuclear aspects of the electric utility industry. Its purpose was to assure an abundant supply of electricity throughout the country with the greatest possible economy, and regard for proper utilization and conservation of natural resources. This was to be accomplished through voluntary cooperation of the utilities with regional reliability councils, through jurisdiction over the licensing of hydro-electric power plants on navigable streams, and control of the wholesale rates and the services of electricity transmitted interstate.

However, the generation and intra-state distribution of electricity were not under the control of the commission. On August 4, 1977, President Carter signed the Energy Organization Act (11-3) which established the Department of Energy as a cabinet level agency. The purpose of the act was to integrate the major energy functions into a single department in the executive branch, and ultimately to be responsible for a comprehensive national energy program. Under this act, the Federal Energy Regulatory Commission was created. In essence, this body assumed the responsibilities of the Federal Power Commission. No mention was made in the act of any jurisdiction over any matter which would concern the commercialization of energy-storage technologies.

Although the federal government does not exercise direct control over siting and construction of non-nuclear and non-hydro generating facilities at this time, several bills have been proposed which would allow federal control (11-4, 11-5). Part of the reason that these bills are not law today is probably due to the strong feelings that the utilities have favoring state authority over site certification (11-6).

The policy of the federal government may have an indirect effect on the siting of battery plants. The Energy Supply and Environmental Coordination Act (11-7) gave the Federal Energy Administration the authority to prohibit any power plant from

burning natural gas or petroleum products when coal could be used instead. Other conditions also must be satisfied, but it is clear that generation of electricity by oil and gas combustion is not favored. This policy is advocated by President Carter's national energy program presently before Congress. The program seeks to force a change from the use of oil to coal by increasing taxes on oil and giving tax credits for equipment changeover (11-8).

Energy-storage technologies are founded on the principle of generating electricity from baseload coal- or nuclear-generated electricity. Presently, electricity needed during peak demand is generated by combustion turbines operating on oil and gas. Considering their position on oil and gas consumption, it is not surprising the government views favorably the introduction of energy-storage technologies. The federal government, through the Department of Energy (DoE), is currently funding some of the developmental work of several technologies. The zinc-chlorine battery alone is under a $1.2 million contract with DoE, and another $10 million is expected from DoE for the assembly and initial testing of a 4.8MWh battery. This battery will be used for large-scale testing in the Battery Energy Storage Test (BEST) Facility in 1981. This kind of support would indicate that if federal legislation governing the siting of energy storage facilities is introduced in the future, its purpose will probably be to ease requirements rather than to impose new ones.

State

Control over the utilities is primarily exercised by the states, and is administered by the Public Service (or Utility) Commission. All of the states exercise control over rates and capitalization, but only 25 states have passed laws regulating power facility siting (11-9). Figure 11-1 illustrates which states have state siting regulations.

In some states, such as Michigan (11-10), the Public Service Commission's jurisdiction is limited to rates and issuance of securities. The location of power facilities is considered to be a managerial function of the utilities themselves, and not a concern of the commission beyond its effect on the rates to the consumer. Other states, such as Illinois (11-11), require a "certificate of convenience and necessity" to be issued by their commission as a prerequisite to construction of any new plant. The general requirement to the issuing of such a certificate is that the project will promote the public convenience and is necessary thereto.

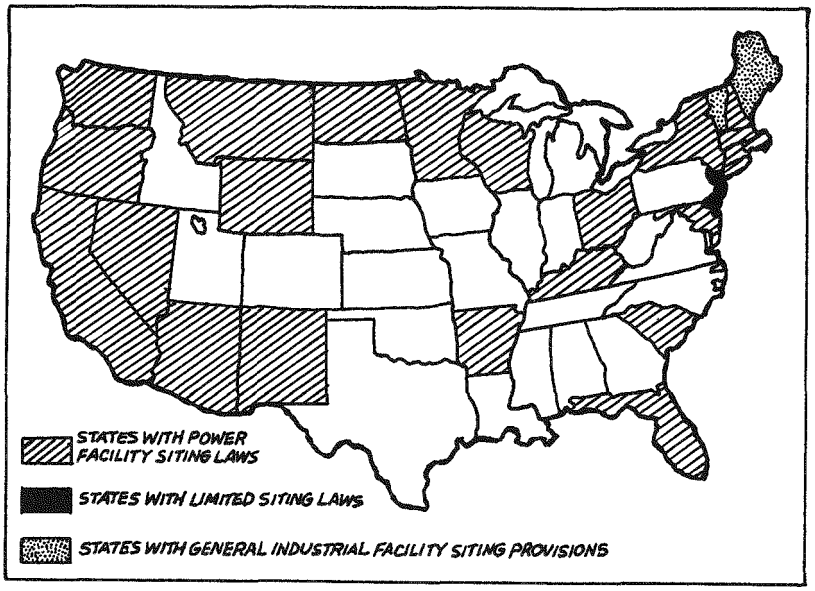

Figure 11-1. Present position of state governments on siting regulations for power facilities. Note only 25 states have laws regulating siting.

Maryland was one of the first states to expand the authority of its Public Service Commission to include the certification of power plant sites (11-12). Their Power Plant Siting Program is comprehensive. It includes plans for monitoring the environmental impacts of existing plants, evaluation of the impact of future plants, socio-economic considerations to maximize the benefit to society, and the acquisition of sites suitable for future construction. Although the plan looks for a one-stop decision, the Maryland localities still can continue to exercise considerable control of siting through zoning and building codes (11-13).

One of the states which has a one-stop decision law is Washington (11-14). Although it relates to thermal power plants, energy storage technologies would be within the meaning of the act. This act provides for an attorney to be appointed to represent environmental concerns, studies of potential sites to be made, and most importantly the provisions in this law preempt any local laws at the plant site.

The usual purpose of these state siting laws is to coordinate the various levels of state and local regulations, and thereby decrease the delay in the licensing process. The provision for a single forum where all interests concerned may be heard, if handled properly, can be a benefit both to the utilities and to the consumer. However, if state governments are not given the authority for a one-stop

decision, confusion may result. The effect of these laws will be profound on zinc-chlorine battery plants. The success of these battery plants depends upon being situated in any residential community where utility substations currently exist. If a state commission found that these battery plants would be suitable for residential siting, this would amount to a design certification that would be applicable to most communities.

ENVIRONMENTAL LAWS

Federal

The major environmental concern with the zinc-chlorine battery is air quality. This area of the law is largely governed by the Clean Air Amendments of 1970 (11-15). This act gave the Environmental Protection Agency the authority to establish national ambient air quality standards (11-16), standards of performance for new stationary sources (11-17), and national emission standards for hazardous air pollutants (11-18). At the present time neither an ambient air quality standard nor a new source standard exist for chlorine gas (11-19). However, the administrator is empowered to establish a standard on any air pollutant which in his judgement has an adverse effect on public health and welfare. The absence of these standards regarding chlorine may be attributed to the fact that chlorine gas is not considered to be a major pollutant.

The EPA also has not issued a hazardous gas pollutant emission standard on chlorine gas. The definition of a hazardous air pollutant in the act is an "air pollutant to which no ambient air quality standard is applicable and which, in the judgement of the administration, may cause or contribute to an increase in mortality or an increase in serious irreversible, or incapacitating reversible, illness" (11-20).

No air pollution standards have been issued by the EPA concerning chlorine gas, even though more than 10 million tons of this gas are produced each year (11-21). This indicates that chlorine gas is capable of being produced and contained with safety, and that the risk of chlorine emissions to the environment is minimal.

Another federal act capable of regulating chlorine gas is the Toxic Substance and Control Act (11-22). This act empowers the EPA to regulate the manufacture; processing; and distribution in commerce, use, and disposal of a chemical substance or mixture which may present an unreasonable risk of injury to health and environment. Although several chlorine related compounds have been suggested for testing, chlorine gas is not among them (11-23).

An act which does regulate chlorine gas is the Occupational Safety and Health Act of 1970 (11-24). This act is intended to protect the health and safety of persons in all places of employment. The current standard regarding chlorine gas is set at 1ppm (approximately $3mg/m^3$) (11-25). However, the National Institute of Occupational Safety and Health has recommended a new standard: "Exposure to chlorine shall be controlled so that no worker is exposed to chlorine at an airborne concentration greater than 0.5 parts of chlorine per million parts of air for any 15 minute sampling period" (11-26). These standards, although useful to employees, do not bear on the environment outside the plant.

The National Academy of Sciences has provided guides for standards concerning public exposure to chlorine gas (11-27). These standards are referred to as the short-term public-exposure limits (STPL's), and the public-emergency limits (PEL's). They are not meant to represent any health hazard to the public, but indicate the possibility of some temporary discomfort at these levels. Table 11-1 summarizes these guidelines.

Table 11-1

GUIDELINES FOR PUBLIC EXPOSURE TO CHLORINE GAS

	STPL's	PEL's
10 minutes	1.0ppm	3ppm
30 minutes	0.5ppm	2ppm
60 minutes	0.5ppm	2ppm

Another national environmental control concerning chlorine is the transportation of the gas. The Department of Transportation (DOT) is the regulatory agency, and it has issued comprehensive and strict regulations covering chlorine gas (11-28). The DOT has designated chlorine as a hazardous material. As such, no person may transport chlorine gas in commerce within the U.S. unless the gas is handled and transported in accordance with the hazardous materials regulations. These regulations (11-29) cover such topics as the type and specification of cylinders, labeling, transport vehicle placarding, securing of package in the vehicle, procedures in the case of vehicle accidents, and the requirement of notice to the DOT when spillage occurs.

State

In one form or another the states have an environmental protection agency and an occupational safety and health administration. Taking Michigan as an example, the Departments of Labor and Health administer the Michigan Occupational Safety and Health Act (11-30). This act incorporates the federal standards by reference, and therefore covers the exposure of workers to chlorine.

Issues regarding air pollution are regulated by the Air Pollution Control Commission in Michigan (11-31). This commission consists of a director or deputy of the Department of Public Health, the Department of Natural Resources, Department of Agriculture, and eight citizens of the state appointed by the Governor. Of these citizens there must be two representatives of industrial management (one a professional engineer), two representatives of local governing bodies, a full-time air pollution control officer, a licensed doctor of medicine, a member of organized labor, and two representatives of the general public. This commission has power over issuing permits needed to begin construction, installation, and operation of any process which may be a source of air contaminant (11-32). A process is defined as any equipment, device, or contrivance for changing any materials whatever or for storage or handling of any materials, and all appurtenances thereto. From this language it appears that this commission will have jurisdiction over zinc-chlorine battery substations.

Once given jurisdiction over licensing or permits, the commission may require an environmental-impact statement (11-33). An EIS is required for any administrative action which may have a potential significant impact on the human environment that could adversely affect the public health and welfare. Many states now require environmental-impact statements, and the conditions for them generally follow those of Michigan. The content of these statements usually include:

- a description of the proposed action
- the need for an objective of the action
- a description of the existing environment
- potential impacts on the environment
- any unavoidable adverse impacts

LAND USE AND PLANNING LAW

State

Many states have planning legislation, but the functions of state planning agencies vary greatly among the states (11-34). The usual function of these planning agencies has been to provide technical assistance to the local governments. However, Vermont has enacted a Land Use and Development Act (11-35) with both regulatory and planning functions. This act established a statewide environmental board and district environmental commissions. The environmental board is empowered to adopt a capability and development plan designed to guide economic development in the state consistent with environmental aims. The commissions are empowered to issue permits as a precondition to construction of any commercial or industrial development, and the issuance is dependent upon satisfying a strict set of environmental criteria.

Local

Land use and planning have been historically exercised by local authorities through zoning, building codes, and site-plan reviews. Zoning is an exercise of the police power which is derived from the state. The states usually delegate this power to counties, regions, cities, and townships (11-36). Zoning power is granted for the purpose of promoting health, safety, morals, or the general welfare of the community (11-37).

These goals are accomplished by the development of a master plan for the development of the community. The plan provides for the division of the community into districts. These districts usually include (11-38):

- one and multiple family residential districts
- trailer court districts
- office service districts
- local business districts
- general business districts
- manufacturing districts
- agricultural districts

Each district has certain restrictions which must be conformed to by the local landowners. These restrictions cover such topics as lot sizes, building types, building sizes, building or land uses, yard regulations, and community facilities (schools,

churches, parks, libraries, and public activities). In this paper only the restrictions in residential districts need be considered. This is because utility substations are generally permitted uses in the other districts.

Although electricity has been a necessity for many years, considerations of aesthetics, land value, and safety make the siting of electric substations in residential neighborhoods a somewhat difficult task. The weapon used by the residents is zoning power governing utilization of the land. In the absence of a controlling statute with the power to overrule zoning, the weight of authority indicates that even publicly-owned electric facilities are subject to zoning control (11-39). However, several court decisions have held that flat prohibitions would be invalid and that municipalities may reasonably regulate an electric substation and transmission line (11-40). Reasonable regulation implies demonstrating that no other sites were available which would involve less disruption of the zoning plan or result in less damage to the neighboring property.

Three options exist which may allow an electric substation to be located in a residential district even if it is presently a prohibited land use. The first is to seek an amendment to rezone the district or permit the use. However, the effect of this option would probably be extensive and not likely to be approved by the local board of appeals. A variance could be applied for, but the criteria for obtaining it are usually rigorous. There normally must be a showing of hardship, extraordinary circumstances applicable only to that property, and the use must not be detrimental to the public welfare, safety, health, and comfort of the inhabitants.

The final and recommended method of obtaining zoning relief is to obtain a special permit for intended use. In this case, the conditions are not nearly as rigorous as with variance. It merely must be shown that the use will not be injurious or tend to have an adverse effect on the adjacent area.

The second method of exercising power over local land use and planning is through a requirement that a building permit be obtained. Prior to the issuance of the permit, a site plan is required and must be approved by the local planning commission (11-41). This document must consider such matters as layout, construction, traffic, noise, parking spaces, landscape, loading areas, vegetation, periodic maintenance, refuse, and the effect upon public health, safety, morals, and general welfare.

Although comprehensive zoning legislation has decreased the use of nuisance law, private individuals may still turn to the court for protection (11-42). According to common law, there are private and public nuisances. A public nuisance impairs the health, safety, and comfort of the community; whereas a private nuisance interferes with the use and enjoyment of another's land. Interference with the land, in the case of private nuisance, includes the occupant's comfort, health, and peace of mind. If a use is found by a court to be a nuisance, compensatory damages may be

SUMMARY

The need for zinc-chlorine batteries and the benefits which will be derived from their use far outweigh the possible environmental effects which may occur. The need exists for the conservation of and substitution for petroleum and natural gas-based fuels. These are the fuels which are used by the diesel engines and combustion turbines to supply electricity during the hours of peak demand. The zinc-chlorine battery presents the alternative of using efficiently produced baseload electricity to meet this demand. Baseload generated electricity is derived from coal and nuclear fuels. This method would also add to the reliability of the utility network. Once charged, these batteries would allow for immediate resumption of service in the event of a power plant failure.

The environmental risk that the zinc-chlorine battery would present to a residential area would be minimal. Although chlorine gas has a characteristic noxious odor, the chance of the gas being released to the environment, even in small quantities, is remote. The modular design of the battery, the building, and the scrubber will ensure that gas leaks are contained within the substation. Furthermore, the zinc-chlorine battery will be thoroughly tested in the Battery Energy Storage Test Facility before introduction into the utility industry.

Under the present laws, the federal government will have little direct effect on the issue of residential siting. However, DoE has recognized the potential benefits of energy storage. The DoE is currently supplying developmental funds in millions of dollars to several energy storage candidates including the zinc-chlorine battery. If energy storage technologies were available to supply 5% of the nation's total electricity requirements, a substantial savings in petroleum and natural gas-based fuels will be realized. This national concern certainly will have an indirect effect upon the integration of zinc-chlorine battery plants into the utility network.

Although state laws are quite varied, it is clear that residential siting will not be obtained without the stamp of approval from some state agency. This state agency may be the public utility commission itself, an energy facility site evaluation council, or the department of health. Approval will be in the form of a license to operate, or through an environmental impact statement review. Of the possible regulatory methods, a one-stop state-certification procedure would present the proper forum for the issue of residential siting to be heard. This procedure would allow all of the interested parties to be represented. The state commission could be comprised of legal, technical, economic, and environmental professionals. An approval from the commission would then amount to a design certification that would be applicable to most residential communities. Consequently, subsequent applications for residential sitings would be reduced to a formality unless local authorities made a showing of unusual circumstances. Without a one-stop state-certification procedure the utilities will be subject to the review procedures in each municipality within the state. Coordination with various state agencies must also be maintained.

In those states without a state-certification procedure, the siting process may be more time consuming but siting approval will not be difficult. First of all, utility substations are frequently located in residential areas. The siting procedure is nothing new to either the municipalities or to the utilities. The substations usually serve the area where they are situated, and an increase in the tax base for the community is realized. In the case of zinc-chlorine battery substations, the land requirements are minimal and electrical service will be made more reliable. Aesthetic considerations may be compensated by landscaping and vegetation. The effect of constructing the system on local environment will be minimal because the battery and supporting equipment will be manufactured elsewhere. Noise, traffic, water requirements, and refuse will be insignificant. Finally, the risk of chlorine gas being released to the environment will be remote.

CONCLUSIONS

In less than ten years, the zinc-chlorine battery will be ready for introduction into the electric-utility industry. Although the distribution of the battery plants into the subtransmission network will initially be a utility decision, the siting of the plants in residential areas will ultimately be a legal decision. This section has discussed the laws relevant to the question, as well as the considerations which will be used in applying these laws. From this material it is felt that the following conclusions may be drawn:

- Zinc-Chlorine battery plants are environmentally suitable for residential siting.
- The present legal framework will also find the zinc-chlorine battery acceptable for residential siting.
- A one-stop state-certification procedure would present the proper forum for the issue of residential siting to be heard.

The zinc-chlorine battery is a new technology which has the potential for benefiting both the utility industry and its customers on a nation-wide scale. Its application will help to realize the national goal of conservation of and substitution for petroleum and natural gas-based fuels. Finally, the design and operation of the battery have illustrated the firm commitment, in the continuing development of this technology, to the preservation of a safe and healthy environment.

REFERENCES

11-1 "Battery Storage". EPRI Journal, Palo Alto, Calif.: Electric Power Research Institute, February 1976, p. 33.

11-2 Federal Power Act, 16 USE 791 et seq.

11-3 Energy Organization Act, 91 STAT 565 et seq.

11-4 Notre Dame Lawyer. "Power Plant Siting - A Road Map of the Problem". Journey, Vol. 48, December 1972, p. 273.

11-5 "Power and the Environment, A Statutory Approach to Electric Facility Siting". Washington Law Review, Vol. 47, 1971, p. 35.

11-6 Ibid, p. 42.

11-7 Energy Supply and Environmental Coordination Act, 15 USCS 791, 1974.

11-8 "Where the Carter Plan Stands". Time Magazine, November 28, 1977, p. 85.

11-9 Evans. "State Environmental and Siting Laws for Power Facilities". Power Engineering, August 1976, p. 51.

11-10 Title 22, Public Utilities, sec. 22.13 (6).

11-11 Chapter 111-2/3, Public Utilities, sec. 56, Illinois Annotated Statutes.

11-12 Zeni. "Maryland Pioneers State Siting Program". Electical World, April 1, 1976, p. 30.

11-13 Berlin, Cicchetti, and Gillen. Perspective on Power, A Study of the Regulation and Pricing of Electric Power. The Ford Foundation, p. 93.

11-14 Thermal Power Plants, Site Locations, Washington Revised Statutes (80.50: .010 - .900).

11-15 Clean Air Amendments of 1970, 42 USCA 1857, Pub. L. No. 91-604, 84 State 1676.

11-16 Ibid, sec. 109.

11-17 Ibid, sec. 111.

11-18 Ibid, sec. 112.

11-19 36 Fed. Reg. 22384 (1971), 40 CRR pt. 50.

11-20 Reference 11-15, section 112(a) (1), 42 USCA 1857 c-7 (a) (1).

11-21 National Academy of Sciences, Committee on Medical and Biological Effects of Environmental Pollutants. Chlorine and Hydrogen Chloride. April 1976.

11-22 Toxic Substance and Control Act, Public Law 94-469, 90 Stat 2003, October 11, 1976.

11-23 Council on Environmental Quality. Federal Register, Vol. 42. Wednesday, October 12, 1977.

11-24 Occupational Safety and Health Act, 29 USE 651, 1970.

11-25 Department of Labor, Occupational Safety and Health Standards. Fed. Reg. 37(202): 22102 - 22356, October 18, 1972.

11-26 U.S. Dept. of HEW. National Institute for Occupational Safety and Health. Criteria for a Recommended Standard...Occupational Safety and Health, May, 1976.

11-27 Committee on Toxicology of the National Academy of Sciences. Guides for Short-Term Exposures of the Public to Air Pollutants. VII Guide for Chlorine, March 1973.

11-28 Department of Transportation 49 USC 1651; Hazard Materials Regulations 49 CFR 170-179, 1971.

11-29 Ibid.

11-30 Michigan Occupational Safety and Health Act, act #154, P.A. 1974.

11-31 Air Pollution Control Act, act 348, P.A. 1965.

11-32 Department of Natural Resources, Air Pollution Control Commission, General rules, MCLA 336.11 - .508.

11-33 Michigan Executive Order, 1974-4, 1975, part 5 (2).

11-34 Hagman. Urban Planning and Land Development Control Law. West Publishing, 1971.

11-35 Vermont State Land Use and Development Act, 10 Vt. Stat. Ann. 6001 et. seq.

11-36 In Michigan, act 184, P.A. 1943; MCLA 125.12, .32, .101, .271.

11-37 Department of Commerce. Standard State Zoning Act. 1926.

11-38 Harrison Township Zoning Ordinance, amended through ordinance 149.1, August 10, 1977, sec. 300.

11-39 Williams, Norman Jr., American Land Planning Law, Volume 3. 1975, p. 630.

11-40 Ibid.

11-41 See reference 11-38.

11-42 See reference 11-34.

Section 12

DISCUSSION OF PART II

BACKGROUND

EDA has completed three distinct designs for 100MWh zinc-chlorine battery plants -- Mark 2, 3, and 4 designs. Of these, the Mark 4 design offers distinct advantages in the areas of performance, scale-up, and siting, as discussed in Section 4. Presently, EDA is actively pursuing the development of the Mark 4 battery to make it a commercially acceptable product at the earliest possible date.

A major milestone in the progression to commercialization is the production of a 4.8MWh battery for testing at the Battery Energy Storage and Test (BEST) Facility in Hillsborough, New Jersey. This 4.8MWh battery consists of two 2.4MWh battery racks of the Mark 4 design as shown in Figure 12-1. The forty-four battery modules on each rack will be bused in series to form a nominal 880-volt, 2.4MWh battery string. Each module is projected to deliver 54.8kWh of usable dc energy. Each rack will have its own microprocessor for module and string control, which will interface with the main computer at the BEST Facility. The racks will be shipped complete with coolant manifolds and external bus connections. Upon arrival they will be properly positioned, filled with electrolyte and store fluids, and connected to the coolant headers and main bus to form independently operable battery strings.

PROGRESSION TO COMMERCIALIZATION

To meet the performance criterion for commercial peak-shaving batteries requires upgrading of module performance. The projected progression in the area of electrochemical performance is summarized in the comparison of established design points for the various versions of the Mark 4 modules given in Table 12-1.

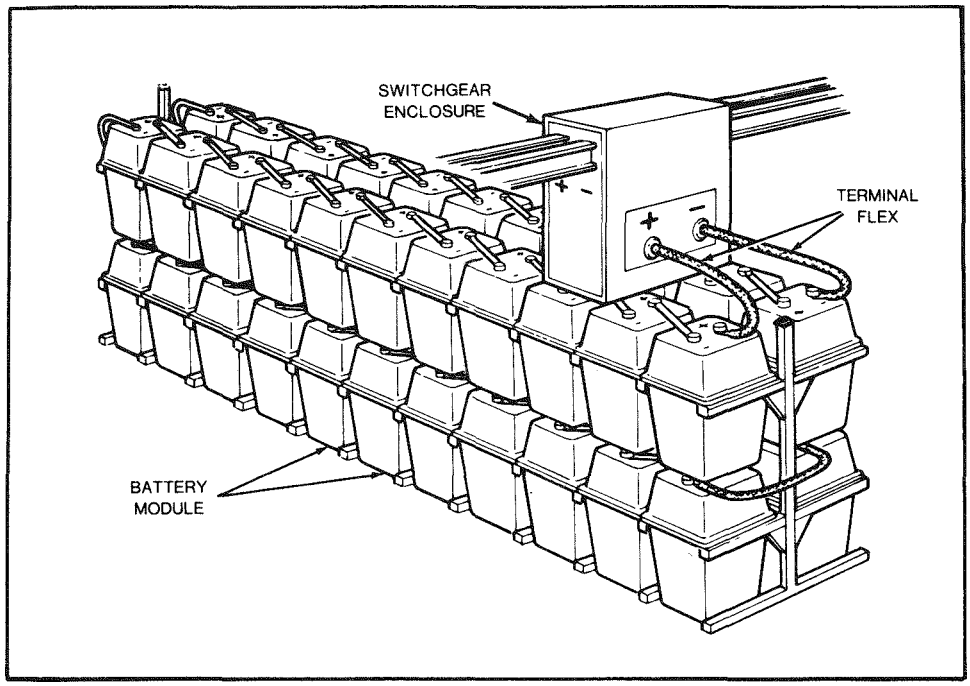

Figure 12-1. Perspective view of 2.4MWh zinc-chlorine BEST battery rack. Note inter-module busing to form a battery string from each rack.

Table 12-1

ELECTROCHEMICAL DESIGN POINTS FOR
MARK 4 BATTERY MODULES

Parameter	Now 1977-78	BEST 1980-81	FC 1984-85	FC+5 1989-90
Charge:				
Current density, mA/cm^2	28	30	30	33
Voltage, V/cell	2.20	2.20	2.18	2.18
Coulombic efficiency, %	85.0	90.0	91.0	92.0
Discharge:				
Current density, mA/cm^2	32	35	36	40
Voltage, V/cell	1.90	1.90	1.96	2.00
Coulombic efficiency, %	91.0	96.0	96.0	96.0
Round Trip Efficiencies:				
Total coulombic, %	77.3	87.4	87.4	88.3
Unusable coulombic, %	4.0	4.0	2.0	1.7
Usable coulombic, %	73.3	83.4	85.4	86.3
Voltaic, %	86.4	86.4	89.9	91.7
Energy, %	63.3	72.0	76.8	79.4
Delivered Energy, kWh	45.0	54.8	57.9	66.0

The projected improvements in electrochemical battery module efficiencies are illustrated graphically in Figure 12-2. The major projected improvement between now and the BEST battery modules is in coulombic efficiency. Only minor improvements in coulombic efficiency are projected between the BEST battery modules and the commercial battery modules. These early improvements in coulombic efficiency are expected as a result of a concentrated development effort during Phase II of the EPRI-EDA contract. Only minor improvements in voltaic performance are projected throughout the progression to commercialization. Between now and the BEST battery module the voltaic efficiency is expected to be held at the same level despite minor increases in the charge and discharge current densities. Minor improvements in voltaic efficiency are projected between the BEST modules and the first commercial (FC) modules as the current densities are held at essentailly the same level. Again, some minor improvements are expected between the FC modules and the FC+5 modules as the charge and discharge current densities are increased slightly. Coincident with these efficiency improvements there are slight improvements in projected charge capacities, going from 196mAh/cm^2 now to 210mA/cm^2 for the BEST and FC modules and up to 231mAh/cm^2 for the FC+5 modules. During this eleven-to-twelve year period the electrochemical energy efficiency is projected to increase steadily from the mid-sixty percent range to almost eighty percent.

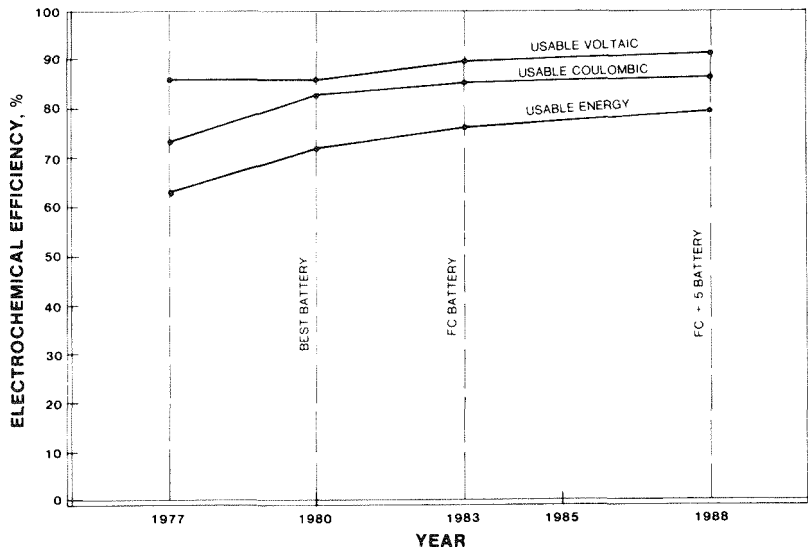

Figure 12-2. Projected improvement trends in electrochemical performance from now through commercialization.

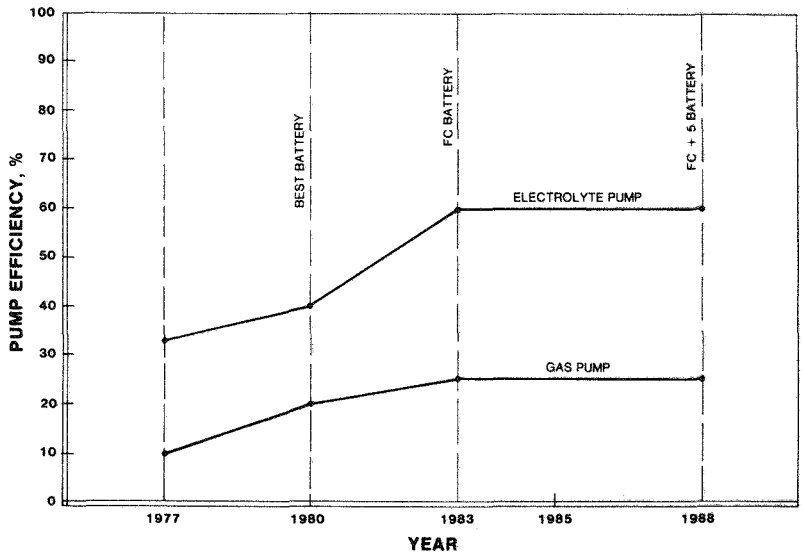

Figure 12-3. Projected improvement trends in pump efficiencies from now through commercialization.

Figure 12-3 illustrates graphically the projected improvements in pump efficiencies during this period. The major improvements in electrolyte pump efficiency are expected between the BEST battery modules and the FC modules. Improvements in gas pump efficiency are expected to be gradual between now and the FC modules. Since the energy requirements for these pumps are negligible their efficiencies will not significantly affect the plant efficiency. This phenomenon is illustrated in Figure 12-4. This is also true of the refrigeration units which will likely operate at a COP in excess of the projected 5.5, but this will have only a minor impact on the net efficiency of the plant. The electrochemical efficiency of the FC+5 battery essentially determines the net efficiency and performance of the plant. Therefore, to meet the performance objectives of ∿70% plant efficiency EDA should continue to concentrate on electrochemical performance.

Figure 12-5 illustrates the bottom line projected improvements in terms of plant efficiency and usable ac energy delivered per battery module. The 98% conversion efficiencies (ad-dc and dc-ac) are assumed for all three versions. Assuming all the projections are met the FC+5 Mark 4 battery will operate at a net energy efficiency of 69.8% and deliver 63.4kWh of usable ac energy per battery module or 100.4MWh ac for the plant. The performance advantages realized in the Mark 4 design over the Mark 2 and 3 designs enhance the probability of attaining these performance objectives.

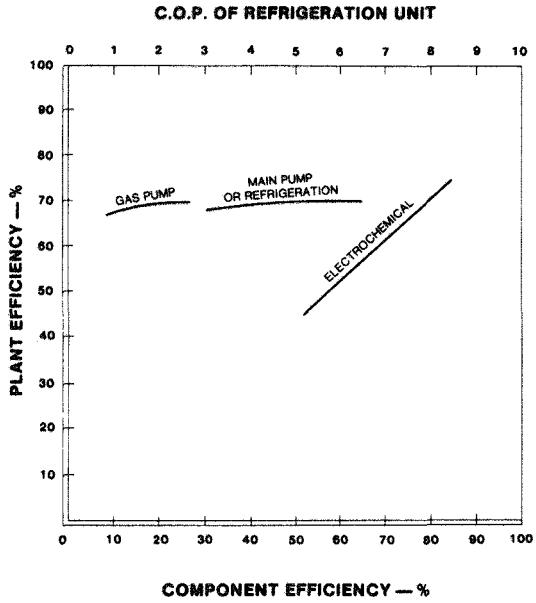

Figure 12-4. Effect of auxiliary component efficiencies on overall plant efficiency. Note the effects of auxiliary component efficiencies are insignificant in comparison to the effect of electrochemical efficiency.

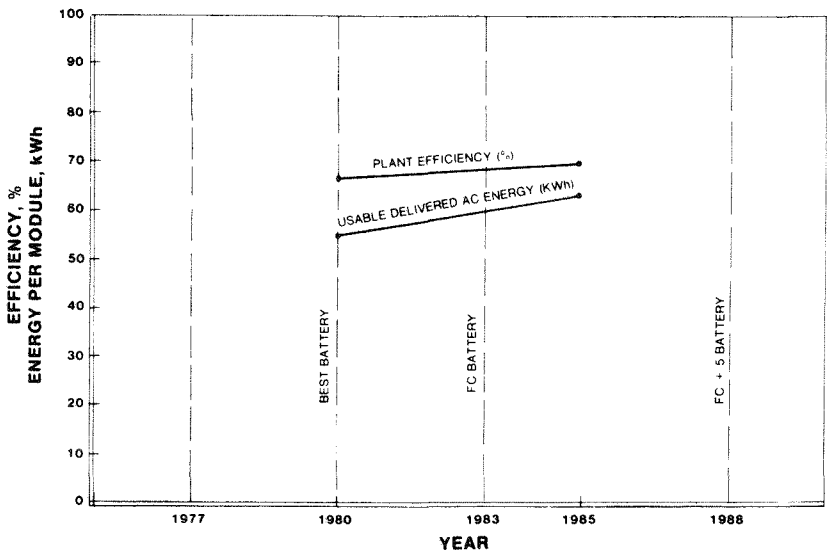

Figure 12-5. Projected improvement trends in plant efficiency and usable delivered ac energy per battery module from BEST through commercialization.

SUMMARY OF BATTERY-SYSTEM ISSUES

The Mark 4 battery must meet established criteria in areas other than performance to become commercially acceptable. These areas include manufacturability and cost, life, reliability, and siting. The design must lend itself to mass-production manufacturing techniques, while using conventional low-cost materials of construction. The target selling price is $25/kWh and $75/kW (1977 $). The $25/kWh objective refers to components having a ten-year life expectancy, while the $75/kW objective refers mainly to components having a thirty-year life expectancy. The design should also lend itself to factory assembly thereby minimizing on-site labor costs. It must be capable of operating reliably and safely with minimal attention and maintenance. The plant size, appearance, safety, and environmental impact must be acceptable for siting at utility substation locations in residential areas. These issues have been addressed in the preceding sections.

Manufacturability and Cost

The issue of manufacturability has not been adequately addressed and cannot be until detailed engineering drawings of the components are available. A simulated manufacturing plan was conceived as part of the cost study. Although this plan may bear little resemblance to the actual plan, it does suggest that the Mark 4 battery is manufacturable using assembly-line techniques.

This plan was used in the costing of the Mark 4 battery to develop costs for direct labor, investment, indirect labor, and overhead. In the absence of detailed drawings the costing projects costs for the major identifiable components and includes a miscellaneous category to handle the minor and unidentifiable items. The projected costs of $26/kWh plus $89/kWh with an installation charge of $2/kWh were obtained in this study by forcing the analysis to approach the preconceived objectives. As such, it identifies cost objectives for individual components. The results further suggest that economies of mass-production, possible with this design, may balance the economies of size, achievable with the previous designs.

Factory Assembly

The Mark 4 design lends itself to factory-completed operational units truckable to the site. Each truckable battery rack contains its own coolant supply and return manifolds, control wiring harness, and 44 pre-bused battery modules. Upon arrival at the site each pair of racks is positioned end-to-end and series-connected to form two strings. Upon connection to the main coolant distribution and return lines,

connection of the control harnesses and after filling the 88 module with electrolyte and store fluids, the two strings are operational with a minimum of on-site labor.

An additional advantage of these factory-completed operational units is the inherent capability for factory checks prior to shipment.

Reliability

The reliability of the Mark 4 design with its 3,168 pumps and 1,584 heat exchangers is a major issue. Pump development efforts should stress reliability, as well as performance. The fully-submersible pumps in common use today demonstrate very good reliability and this feature is expected to be transferrable to battery application. From an overall plant reliability and availability standpoint, if a pump fails in a Mark 4 module, the 2.9MWh string can be switched out, affecting only 2.8% of the plant capacity. Furthermore, servicing of the module can take place after module replacement, which is easily accomplished in this design. Thus, despite the multiplicity of pumps in this design, the reliability and availability of the plant could be equal to or better than for the Mark 2 and 3 design plants.

Residential Siting

With respect to residential siting, the size and appearance of the 100MWh Mark 4 plant will be acceptable. The battery portion of the plant will occupy less than a third-acre of land at a footprint of 7.5kWh/ft^2 with a maximum height of 17.5ft. Should a building be required for safety and environmental purposes it can also be held to approximately the 20 ft height requirement and designed to be aesthetically acceptable.

The major issues with respect to residential siting are safety and environmental intrusion. The Mark 4 design demonstrates significant advantages over the Mark 2 and 3 designs in these areas. It disperses the maximum 81 tons of stored chlorine over 1584 separate stores to give a maximum of 102 lb of stored chlorine per battery module. Also, there are no exposed chlorine transfer lines. The Mark 2 and 3 designs utilize larger, centralized stores with exposed transfer lines. A single line rupture in the Mark 2 and 3 designs could release 75 tons and 25 tons of chlorine respectively. Still the questions of potential safety and environmental hazards exist. They are addressed in Sections 9 and 10 which discuss the results of a preliminary hazards analysis and projected safety features for Mark 4 battery

plants respectively. At the present time it appears that a building around the battery portion of the plant is the most effective method of confining and handling accidently released chlorine from plants located in residential areas. More comprehensive studies in the areas of both safety features and accidental release and spread of chlorine will be performed to properly evaluate the probability of accidental chlorine release and the resultant hazards posed by open battery plants of the Mark 4 design.

Siting procedures are nothing new to either the utilities or local municipalities despite the fact that current statutes regarding siting are extremely diverse nationwide. Local substations serve the communities in which they are located through improved services and an increased tax base. Construction impacts will be minimal due to a minimum of on-site labor. Land use, as well as noise, traffic, water requirements, and refuse will be minimal. Approval for siting Mark 4 battery plants in residential areas should not be difficult if the associated environmental and safety risks can be demonstrated to be minimal in comparison to the benefits derived from them.

PART III

45kWh BATTERY MODULE
DESIGN, ASSEMBLY, AND TESTING

Section 13

INTRODUCTION TO PART III

The design, evaluation, and redesign process for 100MWh peak-shaving zinc-chlorine hydrate battery plants, discussed in Part II of this report, initially focused on designs having individual modules of substantial size. For example, the Mark 2 and Mark 3 designs had a module size of 1MWh and 6MWh, respectively. Further analysis and consultation regarding these large modules revealed some potential problems that appeared difficult to overcome. These problems were: manufacturing difficulties because of the size and density of packing of cells; fluid distribution problems within the stack system; and safety concerns over the large chlorine hydrate stores associated with these battery modules. Battery efficiency analysis also indicated a benefit in operating the battery stack under a reduced pressure during charge. Lowering the stack pressure reduces the dissolved chlorine concentration in the electrolyte, decreases the zinc/chlorine corrosion reaction, and thus increases the charge amp hour efficiency. Reduced pressure operation was considered impractical for the 1MWh or the 6MWh modules.

In March, 1977, the Mark 4 100MWh peak-shaving battery design was developed to answer the basic criticisms of the Mark 2 and 3 designs. This design utilized 58kWh complete batteries as the basic modular unit with some 1760 modules comprising the 100MWh plant. After an EPRI-EDA design review the small complete module concept was accepted and a development program to design, assemble, and test one such module was initiated. This module was to be a 45kWh unit capable of demonstrating 10 cycles at >65% electrochemical energy efficiency.

The development program to design, build and test the 45kWh peak-shaving battery unit is reported in seven sections which together make up the "45kWh Module Design, Assembly, and Initial Testing" report. These sections are:

MODULE DESIGN

In this section, the design points for the 45kWh module, selected to meet the battery performance criteria, are discussed. From these design points a system design including control system was developed and components specified.

COMPONENT DESIGN AND QUALIFICATION

Within a self-contained peak-shaving battery module eight major component areas are identified:

- Submodule
- Electrolyte and Gas Pumps
- Electrolyte Manifold System
- Valving
- Heat Exchangers
- Hydrogen/Chlorine Reactor
- Module Case
- Control System

The first two areas, the development of the submodule and the pumps, are summarized in this section but, because of their significance in determining battery performance, Sections 16 and 17 of this report are devoted to a detailed description of the submodule and pump development activities, respectively.

The electrolyte manifold system serves two major functions in this recirculating electrolyte battery system. The first is to distribute flow uniformly from one pump to 1320 chlorine electrode pairs at a minimum hydraulic head, while the second is to minimize parasitic currents through this common electrolyte system. A description of the manifold system developed to accomplish both these objectives is given.

Of the three valving operations within the battery module, two were accomplished with commercially available solenoid valves, modified to allow the actuator to penetrate the case, while the third was developed at EDA. This latter valve, a

mechanical relief valve designed to hold a constant pressure differential between stack and store, is detailed.

Heat exchangers were developed to cool the store solution for hydrate formation, to decompose hydrate during module discharge, and to maintain temperature in the electrolyte. The hydrate formation heat exchanger was a tube-in-shell design developed for the mobile program while the other two were specific to the peak-shaving battery. All three heat exchangers are described.

The hydrogen/chlorine reactor is used to recirculate the small quantity of hydrogen generated during battery operation back into the system as aqueous hydrogen chloride. An efficient fluorescent light reactor system developed for the mobile battery program was utilized directly for this peak-shaving battery module and is described.

Kynar-lined fiberglass cases were called out in the design of the 45kWh module. The Kynar lining was needed as case protection against the chlorinated electrolyte while the fiberglass structure was necessary to contain the 5-10 psi operating pressure in the system. Case deflection data under pressure is presented in this section. The control system for the 45kWh module was straightforward in concept. On charge, glycol temperature was the control parameter, while on discharge, pressure in the stack gas space was utilized. The effectiveness of this system is discussed.

SUBMODULE ASSEMBLY AND QUALIFICATION

The basic stack design for the 45kWh module called for six 20-volt, 7.5kWh submodules to be electrically connected in parallel. Six individual submodules were, therefore, built and individually qualified to assure performance. These submodules were built using mid-1977 technology. This technology dictated that chlorine electrodes be activated by nitric acid boiling and matched chlorine electrodes be bonded together to form the electrode pairs. Recent technology (mid-1978) dictated electrochemically activated chlorine electrodes held in pairs by a frame structure. Qualification of the individual modules was undertaken by charging to full capacity from ∿25% zinc chloride at a pH of ∿0.1 at 30^{o}C with no leveling agent. The specific electrolyte for peak-shaving battery operation was still being developed and was, therefore, not available for the qualification runs.

PUMP TESTING AND EVALUATION

Both the main electrolyte pump and the gas pump were assembled and fully evaluated. The evaluation included basic fluid/gas handling characteristics, efficiency, negative suction head testing, and the start of a life test program. Mounting techniques were also developed for leak-free sealing of these magentically coupled devices.

CHLORINE HYDRATE FORMATION AND DECOMPOSITION

The method selected for forming chlorine hydrate during the charging operation of the module was known in principle to work but was a relatively untried technique. This technique involved the contacting of cold store solution with chlorine gas within a gas pump to form hydrate. Careful balancing of conditions such as glycol coolant temperature, pump inlet pressure, store liquid flow rate, chlorine gas flow rate, and pump outlet plumbing was necessary in order to form hydrate at the required rate, maintain a vacuum in the stack, and prevent hydrate blockage in the pump inlet or outlet system. A determination of filter area to achieve the desired chlorine storage density was also necessary. The relationship between hydrate decomposition, heat exchanger configuration, and area and the rate of chlorine evolved for module discharge was measured so as to size this heat exchanger for the 45kWh module.

MODULE ASSEMBLY

The actual building of the 45kWh module was treated as a one-of-a-kind operation with the hand fitting at EDA of the individual components that make up the battery. In general, the stack and manifold structure were built in-house while the majority of the other components were built to EDA specifications by outside vendors. Assembly/layout drawings, assembly diagram sheets, and a bill of materials were prepared to cover this assembly operation.

INITIAL TESTING

The culmination of the first phase of the EDA-EPRI contract for module development was a ten cycle performance verification test. Performance parameters such as battery capacity, charge and discharge voltaic performance, coulombic efficiency, general battery control characteristics, and repeatability of performance were determined and discussed.

Section 14

MODULE DESIGN

INTRODUCTION

The design of the battery module was based on a self-contained and integrated module unit; i.e., with its own store, hydrate former, stack, heat exchangers, and other components necessary for module operation. The basic design criteria for this battery module included:

- Delivered Energy -- 45kWh
- Energy Efficiency -- 65% (excluding auxiliaries)
- No-Load module voltage -- 21.2 volts
- Type of submodule -- comb-type bipolar
- Number of submodules -- six, electrically in parallel
- Type of hydrate store -- water
- Type of package -- self-contained

DESIGN POINTS AND PROJECTED PERFORMANCE

The electrochemical design points for the module are summarized in Table 14-1. A charge current density of 28mA/cm^2 corresponds to a charging current of 462 amperes for the 45kWh module. The design charge capacity of 200mAh/cm^2 represents a 7-hour charge. The corresponding discharge current is approximately 528 amperes or 32mA/cm^2 with the discharge lasting approximately 5 hours. The projected charge and discharge coulombic efficiencies are 87.0% and 91%, respectively, and represent an overall coulombic efficiency of 77.3%. The unusable capacity at the end of the discharge is projected to be 4% of the total ampere-hour charge capacity of the battery. This unusable capacity is an estimate of the battery capacity that cannot be discharged at a usable voltage. The projected charge and discharge voltages are 22.0 and 19.0 volts at the charge and discharge current densities of 28 and 32 mA/cm^2, respectively. These voltages represent a voltaic efficiency of 86.4%. A combination of 73.3% usable coulombic efficiency and 86.4% voltaic efficiency results in an overall electrochemical energy efficiency of 63.3%. To achieve these

Table 14-1

ELECTROCHEMICAL DESIGN POINTS FOR 45kWh MODULE

	Parameter	Design Points
I	Time (hours)	
	Charge	7
	Discharge	∿5
II	Apparent Current Density (mA/cm^2)	
	Charge	28
	Discharge	32
III	Voltage	
	Charge	22.0
	Discharge	19.0
IV	Voltaic Efficiency (%)	86.4
V	Coulombic Efficiency (%)	
	Charge	85.0
	Discharge	91.0
	Total Round Trip	77.3
	Unusable Capacity	4.0
	Net Round Trip	73.3
VI	Net Energy Efficiency (%)	63.3
VII	Delivered Energy (kWh)	45

electrochemical goals the remainder of the battery system was specified as follows:

- 30% $ZnCl_2$ by weight at beginning of charge
- 5% $ZnCl_2$ by weight at end of charge
- 11% by weight of chlorine stored as chlorine hydrate in a water store (for ease of hydrate formation dilute zinc chloride, S.G. 1.03, was used rather than pure water)
- 30% by volume of solid hydrate in store
- On charge stack gas space pressure to be approximately -5 psig
- On discharge stack gas space pressure to be approximately 0 psig
- Differential pressure between stack and store to be approximately 10 psi during charge and 5 psi during discharge

SYSTEM DESCRIPTION

Figure 14-1 shows the operational schematic for the 45kWh battery module. This schematic characterizes the various flow streams within the module during charge and discharge operations.

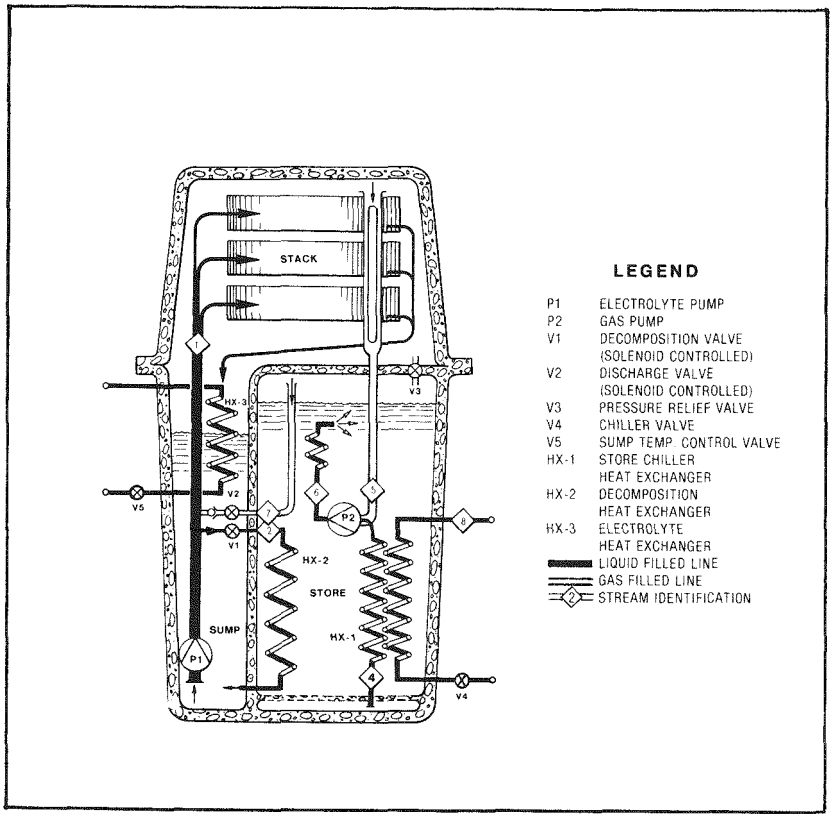

Figure 14-1. Schematic of 45kWh Battery Module Showing Electrolyte Flow

During charge, the main electrolyte pump (Pl), immersed near the bottom of the sump, pumps electrolyte from the sump to the stack at the rate of 85 gpm via line 1, the main electrolyte manifold. The electrolyte is distributed from this main manifold into three two-way submodule manifolds and then to the sixty individual cell manifolds. From each cell manifold the electrolyte is further distributed into twenty-two chlorine electrode pockets. After the electrolyte flows through the porous

electrodes and overflows the cell, it flows through a resistance channel (to limit parasitic current losses) and returns back to the sump by gravity.

During charge as zinc is plated on the graphite zinc substrate, chlorine gas is evolved on the porous graphite counter electrode at the rate of approximately 28 NPT liters/min. This chlorine is transported from stack to store by a positive displacement gas pump. The gas pump is operated such that a negative pressure is created in the stack gas space. This negative pressure lowers the partial pressure of the chlorine gas over the electrolyte and thus the solubility of chlorine in the electrolyte is lowered.

Since the coulombic inefficiency of the battery is primarily determined by the chemical corrosion of zinc by chlorine, the stack vacuum plays a major role in determining the coulombic efficiency of the battery. A photochemical reactor to react any hydrogen with chlorine using a fluorescent light as the light source is installed on the gas line to the gas pump. The hydrogen chloride formed by this reactor is transferred to the store. At the gas pump inlet, chlorine gas is mixed with chilled water from the store and chlorine hydrate is formed. The water to form the hydrate is taken from the bottom of the filter and is chilled by the hydrate heat exchanger (HX1) just prior to being mixed with chlorine gas as shown in line 6. The formed hydrate is pumped into the store. Store pressure is maintained by relief valve, V3, so designed that a pressure difference of 10 psig is established and maintained between the stack and the store gas space. Since -5 psig is created in the stack compartment by operating the gas pump, the store pressure will be settled automatically by the mechanical valve at +5 psig.

During discharge, all flow streams flow in the same direction as on charge. The main electrolyte pump (P1) feeds chlorinated electrolyte to the chlorine electrodes in the stack via the feeding manifolds. Again, the electrolyte overflows the cells and returns to the sump. Chlorination of electrolyte is accomplished by injecting chlorine gas at the inlet of the main electrolyte pump, as shown in line 3, while the solenoid valve, V1, is open. The chlorine gas is generated by decomposing the stored chlorine hydrate. The decomposition of hydrate is accomplished by opening valve V2 and by allowing the warm electrolyte (30-50^{o}C) in the sump to flow through the decomposition heat exchanger (HX2) in the store. The demand for chlorine is served by measuring stack pressure, thus battery control on discharge is affected by switching valve V2 according to stack pressure. The gas pump is operated at lower speed on discharge since it is only used to provide gas recirculation. On

both charge and discharge conditions, control of the electrolyte temperature (in sump) is accomplished by using electrolyte heat exchanger, HX3. An external coolant (glycol or water) is used as the heat transfer media (line 9).

ENERGY BALANCE

Figure 14-2 shows the energy diagram of the 45kWh battery module. The total energy input to the module is 71.07kWh, excluding the energy requirements for the auxiliaries, over the 7-hour charge duration. It is estimated that 10.38kWh is required

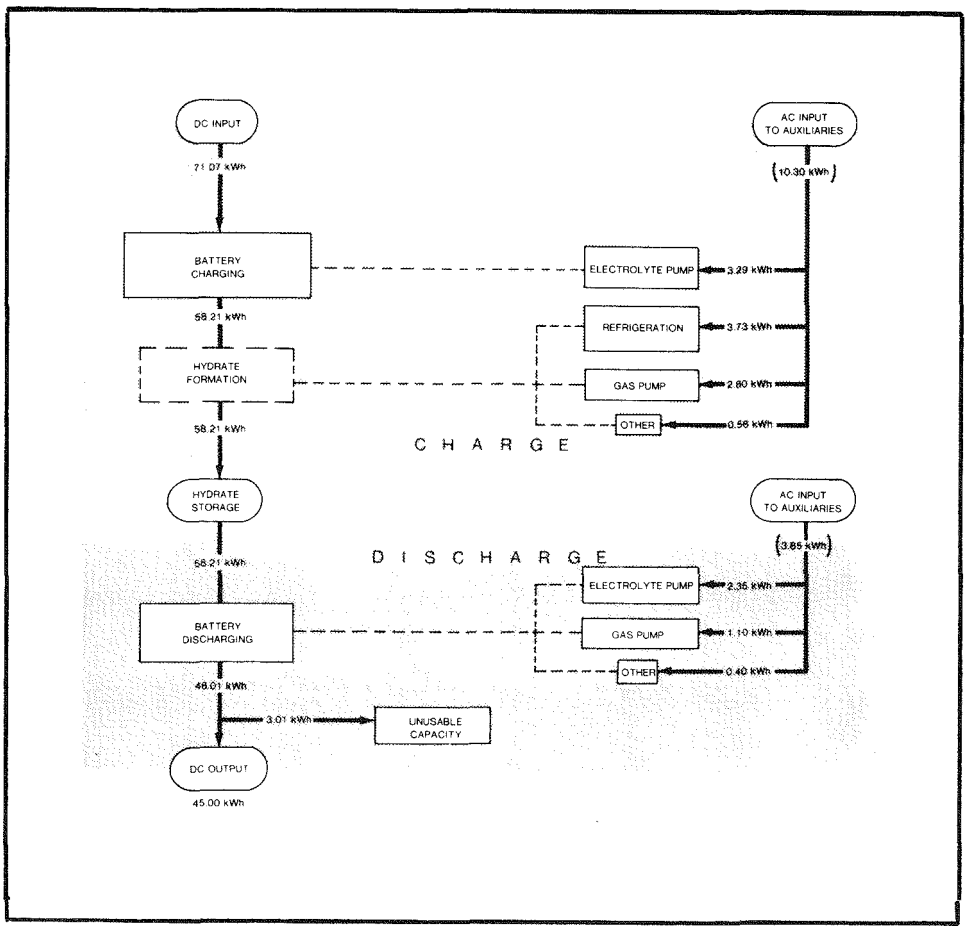

Figure 14-2. Energy Flow Diagram of the 45kWh Load Leveling Module

for the auxiliaries. The storage energy is projected to be 58.21kWh at the end of charge. The charge inefficiencies due to voltaic and coulombic inefficiencies are approximately 2.20kWh and 10.66kWh, respectively. On discharge, the inefficiency due to voltaic and coulombic inefficiencies are 5.5kWh and 4.7kWh, respectively.

Thus, the total output energy is 48.01kWh. A 3.01kWh inefficiency is considered reasonable for the unusable energy, in this first generation full-size load leveling module. This results in a net usable energy of 45kWh. A summary of the overall electrochemical energy balance is tabulated in Table 14-2.

Table 14-2

ELECTROCHEMICAL ENERGY BALANCE SUMMARY

	Capacity (Ah)	Energy (kWh)
I. Charge		
A. Input to Battery	32,304	71.07
B. Losses		
(1) Coulombic	4,846	10.66
(2) Voltaic		2.20
II. Stored in Battery	27,458	58.21
III. Discharge		
A. Losses		
(1) Coulombic	2,471	4.70
(2) Voltaic		5.50
B. Unusable	1,292	3.00
C. Usable Delivered from Battery	23,695	45.01

HEAT AND MASS BALANCE

Tables 14-3 and 14-4 summarize the projected heat gain and losses in the stack and store compartments during 7-hour charge and 5-hour discharge. The three heat exchangers used in the battery module are sized according to these heat flows.

Table 14-3 summarized the heat balance for the 7-hour charge. The net heat gain in the stack compartment is 5.35kWh. The total heat gain in the store compartment is 15.20kWh. This translates into 3.04kWh of actual inefficiency if the refrigeration equipment had the same coefficient of performance as that projected for a 100MWh peak-shaving installation, that is, a c.o.p. of 5. The c.o.p. of the refrigerator does not affect the size of the hydrate formation heat exchanger since a total of 15.2kWh over 7 hours or 31.13kCal/min still has to be removed from the store.

Table 14-3

HEAT BALANCE FOR 7 HOUR CHARGE

I. Stack Compartment		
A. Energy Input		71.07 kWh
Energy Stored		58.21 kWh
B. Heat gain - Electrochemical Inefficiency		12.86 kWh
Pump Heat (75% of Estimated Power)		2.47 kWh
	Total	15.33 kWh
C. Heat Losses		
ΔH-ΔG (average of 13.7 KCal/mole between 30% and 5% $ZnCl_2$)		8.15 kWh
Battery to store (through sump wall)		1.23 kWh
Battery to environment (est)		0.2 kWh
Water vapor (carryover to store)		0.4 kWh
	Total	9.98 kWh
D. Net heat gain on charge		5.35 kWh
II. Store Compartment		
A. Heat gain - Hydrate formation @ 18.7 KCal/mole x 511.6 mole		11.12 kWh
Pump heat (80% of power)		2.24 kWh
Battery to store		1.23 kWh
Environment to store (est)		0.21 kWh
Water vapor (carryover from stack)		0.4 kWh
	Total	15.20 kWh
B. Work to remove heat at c.o.p. of 5*		3.04 kWh

Table 14-4

HEAT BALANCE FOR 5 HOUR DISCHARGE

I. Stack Compartment		
A. Energy Summary		
Stored		58.21 kWh
Unused		3.00 kWh
Removed on Discharge		55.21 kWh
Discharged		45.01 kWh
B. Heat gains		
Electrochemical inefficiency		10.20 kWh
Pump heat (75% of power)		1.76 kWh
ΔH-ΔG (13.7 KCal/g-mole, 441 g/mole)		7.03 kWh
	Total	18.99 kWh
C. Heat losses		
To hydrate through heat exchanger		8.15 kWh
To hydrate through sump wall		1.23 kWh
To environment (est)		0.2 kWh
	Total	9.58 kWh
D. Net Heat gain		9.2 kWh
II. Store Compartment		
A. Heat to decompose hydrate		9.59 kWh
B. Heat gains		
From pump (80% power)		0.88 kWh
From Battery		1.23 kWh
From environment		0.21 kWh
Heat from Heat Exchanger		8.15 kWh

Table 14-4 summarizes the heat gains and losses for the 5-hour discharge in the stack and store compartments. The net heat gain in the stack compartment is 9.2kWh. An electrolyte heat exchanger is, therefore, required with a capability of removing the heat at the rate of 26kCal/min. The hydrate decomposition heat exchanger must have a minimum heat transfer rate of 23.4kCal/min to provide sufficient chlorine to sustain a 5-hour discharge.

Table 14-5 summarizes the projected weight and volume of the stack and the store. The stack compartment is designed to allow the zinc chloride concentration to swing from 30% at the beginning of charge to 5% at the end of charge. The total charge capacity of the battery is 27,458 Amp-hour which is equivalent to 81.42kg of $ZnCl_2$. Thus, the total volume of 30% zinc chloride required in the stack compartment (including the sump) is 210 liters. Since the stack requires approximately 100 liters to fill up all the six submodules and the manifold system, a sump with a volume of 110 liters is needed. The volume of water required in the store is 268.1 liters, based upon the storage of 38.14kg of Cl_2 (or 115.6kg of $Cl_2 8H_2O$) and 12.5% chlorine in the store by weight. At the end of charge, the stack compartment contains 192 liters of 5% $ZnCl_2$ solution and 33.5kg of Zn plated on the negative electrode. In the store, 115.6kg of chlorine hydrate is stored along with 191kg of water. The volume of this hydrate-water mixture is 285 liters. An extra 14 liters of space is allowed in the store as a gas space giving a total store volume of 300 liters (10.56 cu ft).

Table 14-5

SUMMARY OF MASS BALANCE OF 45kWh MODULE

	Stack		Store	
Initial Condition Total Wt = 541.71	30% $ZnCl_2$ 210 liters Sp.Gr. = 1.2928 81.43kg of $ZnCl_2$ 190kg of H_2O		268.1 liters of H_2O 268.1kg of H_2O 1.82kg of extra Cl_2	
	Total	271.43kg	Total	270.28kg
End of Charge Total Wt = 541.71	33.50kg Zn 11.61kg $ZnCl_2$ 190kg H_2O		38.14kg Cl_2 (5% extra) 115.6kg of $Cl_2 \cdot 8H_2O$ of Sp.Gr. = 1.23 33% by volume of solid 191kg of H_2O Final volume of 285 liters Final weight 306.6kg	
	Total	235.11kg	Total	306.6kg

Section 15

MODULE COMPONENT DESIGN AND QUALIFICATION

INTRODUCTION

In order to operate the battery module as a complete self-contained package, each component associated with the battery system requires qualification and characterization. In this section, the development work for the major battery components is presented. These components are:

- Stack
- Electrolyte and Gas Pumps
- Electrolyte Manifold
- Valving
- Heat Exchangers
- H_2/Cl_2 Reactor
- Module Case
- Control System

STACK

Figure 15-1 shows the assembled stack. It consists of six 20V, 7.5kWh submodules stacked into three tiers. Each submodule has its individual set of terminals for external (to the module case) paralleling of the six submodules into a 20V x 45kWh battery module. Each submodule, as shown in Figure 15-2, consists of 10 bipolar comb-type unit cells in series with an area of 2750 cm^2 per unit cell. The submodule has a no-load voltage of 21.2 volts. The submodules have a dry weight of 16.3kg and measure 10.5" wide x 29.5" long x 5.5" high. Each of the submodules was pre-tested and qualified before installation. Details of the assembly and qualification of submodules are described in subsection 15-3.

ELECTROLYTE AND GAS PUMPS

Two pumps are used in this module system; namely, the main electrolyte pump and the gas pump. The former provides the electrolyte circulation to each of the cells

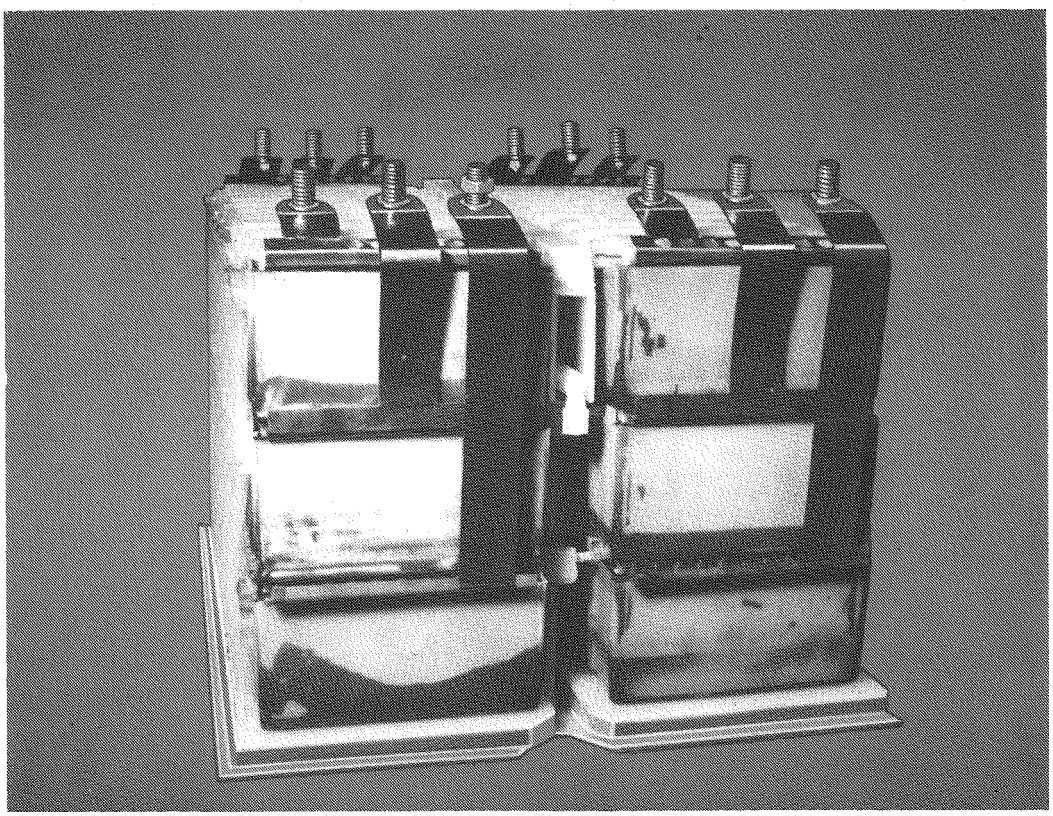

Figure 15-1. Stack Assembly for the 45kWh Peak-Shaving Module

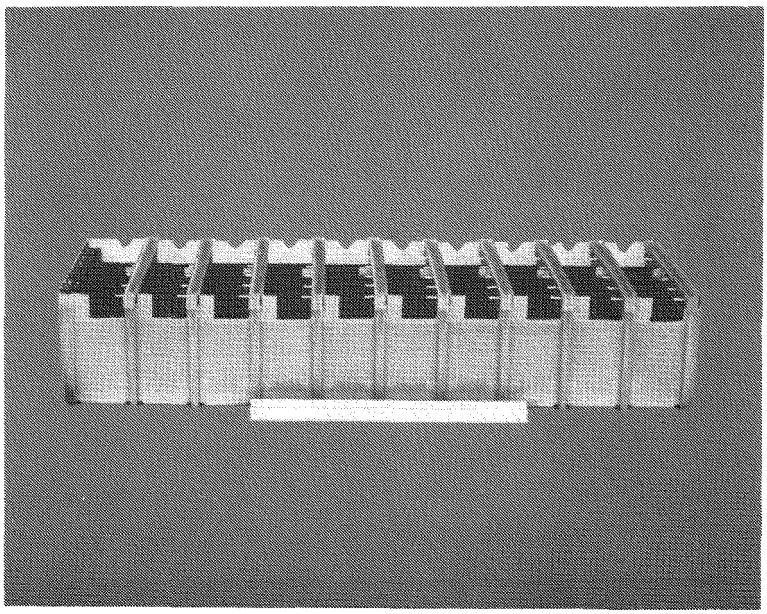

Figure 15-2. 7.5kWh Submodule

in the stack on charge and discharge. The latter is used to transport the evolved chlorine gas from the stack compartment to the store and to mix this chlorine with chilled water to form chlorine hydrate. The gas pump also ensures gas circulation through the H_2/Cl_2 reactor system to maintain low hydrogen concentration within the battery. Both the gas and electrolyte pumps are magnetically coupled to the motor to ensure leak-free operation.

The electrolyte pump was designed to supply electrolyte at a flow rate of 2cc/min-cm^2. With a total electrode area of 164,820 cm^2, an overall flow rate of 330 liter/in, or 87 gpm, was required.

The following specifications were drawn up for the electrolyte pump:

- Flow rate at 87 gpm of zinc chloride solution at 4 psig ΔP
- Inlet condition of -4 psig (-5 psig above liquid level plus 1 psi of liquid head)
- Motor to be magnetically coupled to the pump
- Normal operating speed 1500 rpm for maximum bearing life

A centrifugal pump with 5" closed impeller suspended between two bearings was designed and developed. The pump-only efficiency was approximately 42% at 1600 rpm, 10 ft of water head ($\sim$4 psig) at the flow rate of 85 gpm. Details of electrolyte pump design and development are discussed separately in Part III, Section 17.

For the gas pump the following conditions were specified:

- Inlet pressure of -5 psig
- Chlorine gas flow rate of ∿40 STP liters/min
- Liquid flow rate of 11 liters/min
- Motor to be magnetically coupled to the pump
- Maximum speed 1950 rpm

A modified ECO G-10 positive displacement gear pump was chosen for this pumping application. This pump was magnetically coupled using rare earth magnets and driven by a Bosch 48 volt dc motor. The pump was calculated to have a hydraulic efficiency of approximately 30%* based upon the theoretical power required for pumping the liquid and compressing the gaseous phase of the two phase flow.

ELECTROLYTE MANIFOLD

The electrolyte manifold was designed not only to meet the requirement of uniform flow distribution but also to provide adequate ohmic resistance between cells to minimize the parasitic current losses in this common electrolyte system.

Figure 15-3 shows the main electrolyte manifold which feeds into 60 unit cells. In

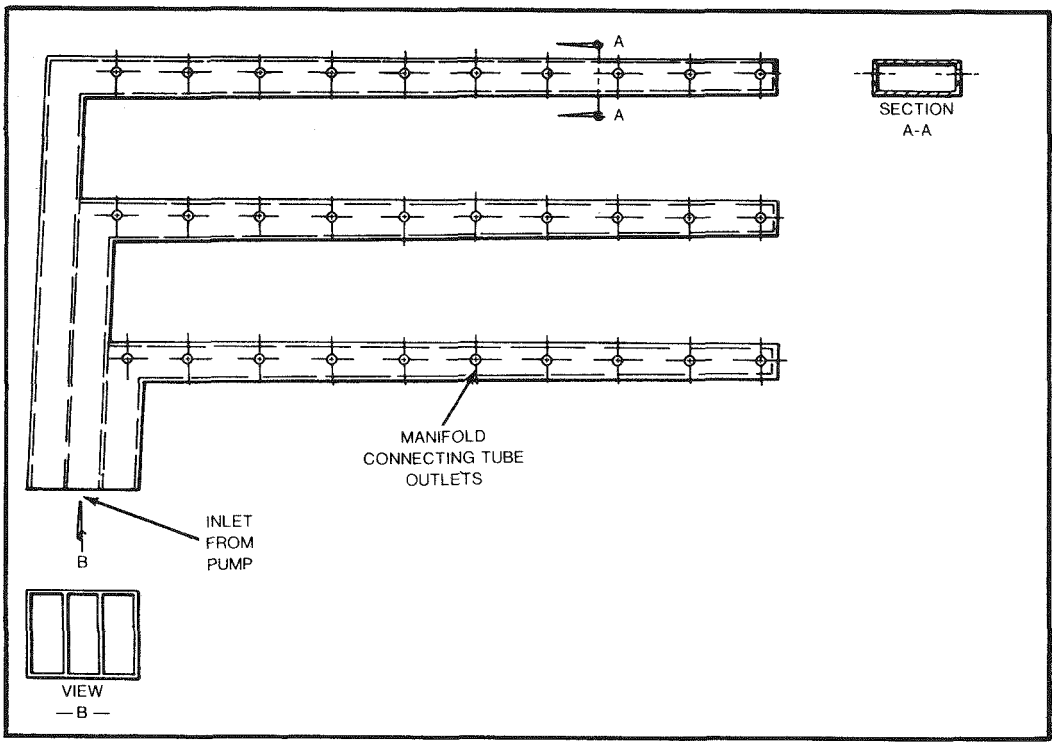

Figure 15-3. Main Electrolyte Manifold

*Theoretically, the pump requires 70 watts of energy. Actual energy input to gas pump is 316 watts. At 75% motor efficiency actual energy used to pump hydrate is 237 watts. Thus, pump efficiency is 30%.

each unit cell, there are 22 Teflon feeding tubes for 22 pairs of chlorine electrodes. The small diameter Teflon tube is located near the chlorine bus and extends down into the chlorine electrodes. These feeding tubes are used as sized orifices and provide a constant pressure drop and constitute the major single pressure drop for the entire manifold system. The total pressure drop of the feeding manifold was 3.5 psig of which 1.25 psig was attributable to the small feeding tubes. For return flow to the sump, electrolyte overflows from one side of each unit cell into a collecting cup and then returns to the sump via a resistance path (electrolyte channel plate). The electrolyte channel plate, as shown in Figure 15-4, is designed so that each channel can discharge 5.5 liters/min, the amount of electrolyte from each unit cell, at an available pressure drop of 5.5" of electrode head for

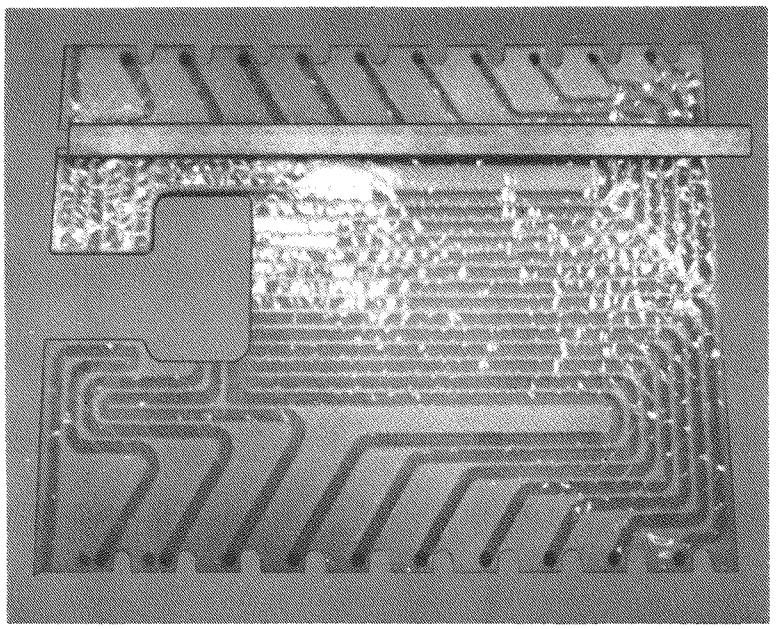

Figure 15-4. Electrolyte Channel Plate

the lowest level of submodules and 11" and 16.5" of electrolyte head for the middle and upper submodules, respectively. Testing showed a channel with 0.785 x 0.625 cross-section and 40" length gives approximately 200 ohms of resistance with electrolyte composition of 2M $ZnCl_2$ and 1M KCl and met the flow requirements.

A computer network analysis of the parasitic current losses through this manifolding system was made. Figure 15-5 shows the parasitic losses in a submodule, when charged at 77 amps at a charge voltage of 22.8 volts. The calculation is based

upon the inlet and outlet resistances of 213 ohms and 375 ohms, respectively. The electrolyte resistivity was taken to be 3 ohm cm. A maximum of 0.21 amps of current deviation for the middle cell at a 77 amps submodule charging current was calculated. This is considered a very low value.

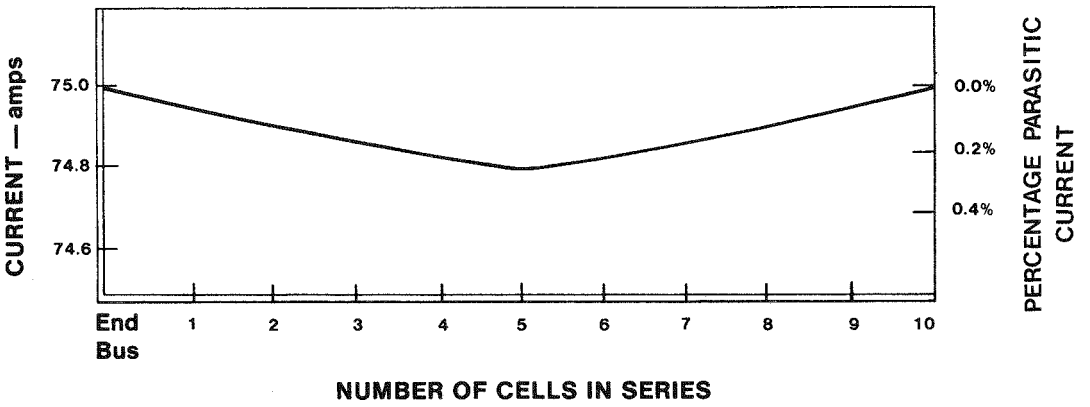

Figure 15-5. Parasitic Current Distribution Across a Submodule with Ten Cells Connected in Series at a Charge Current of 75 Amps

VALVING

Three types of valves were used in the 45kWh module: normally closed solenoid valves, check valves, and a mechanical pressure relief valve.

The solenoid valves used for this battery module were Valcor 110V ac normally closed valves. These valves were so modified that they could be sealed to the battery case wall with the main Teflon body located inside the battery. Thus, all the flow connections could be made internally. The electrical actuator remained accessible on the outside of the case. Figure 15-6 shows the two check valves used in the 45kWh battery system. These valves were modified 3/8" Hayward ball check valves. The modifications included the utilization of a gravity rather than a spring actuated check and fabrication from Kynar rather than PVC.

A mechanical relief valve designed to open at a differential pressure of 10 psi between the stack and the store was developed. As shown in Figure 15-7, this valve consists of a ceramic rod 0.375 inches in diameter and 4.075 inches in length

sliding within a ported graphite sleeve. A weight of 1.1 pounds on this rod defined the 10 psi pressure differential required to fully open the valve. The rate of gas flow as a function of pressure is shown in Figure 15-8.

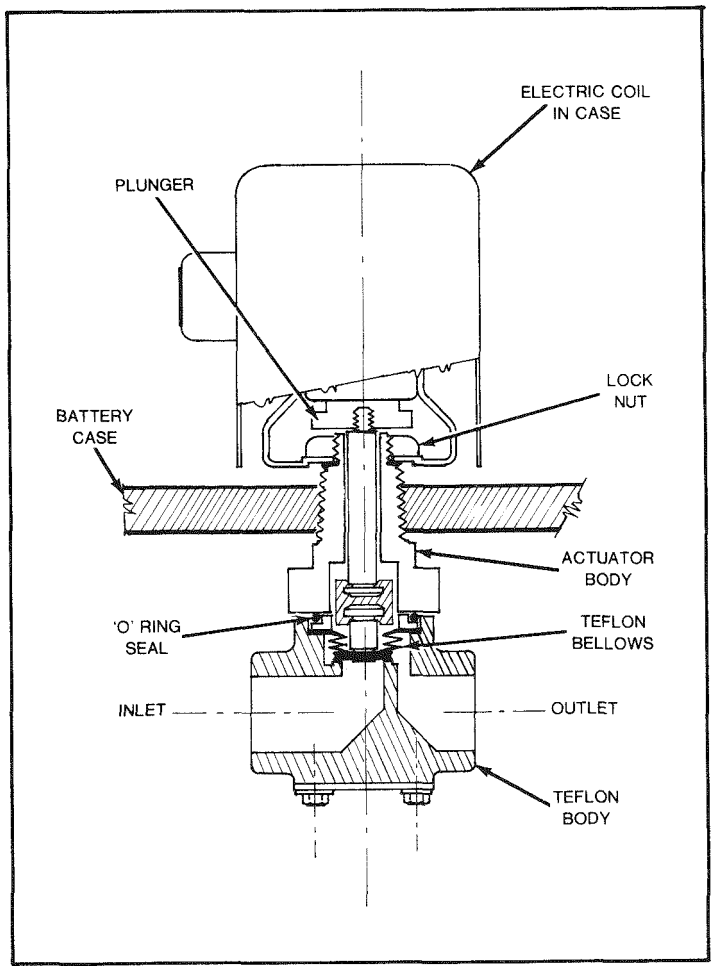

Figure 15-6. Modified "Valcor" 110V ac Normally Closed Solenoid Valve

HEAT EXCHANGERS

Three heat exchangers are required in the battery system, a hydrate formation heat exchanger, a hydrate decomposition heat exchanger, and a main electrolyte heat exchanger. The design of each of these heat exchangers is discussed below:

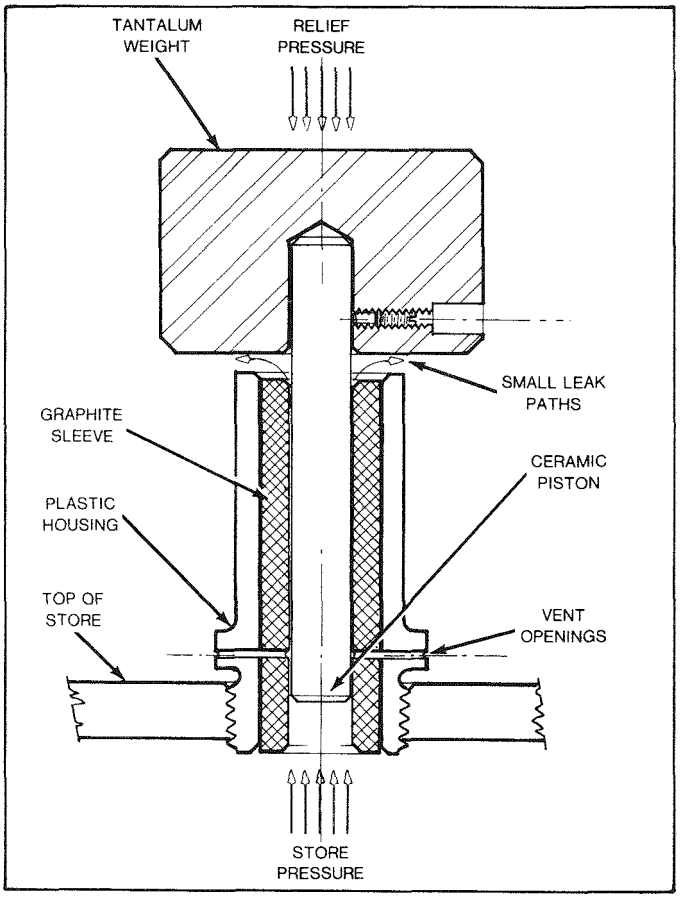

Figure 15-7. Mechanical Pressure Relief Valve. Maintains a predetermined differential pressure between the stack and the store.

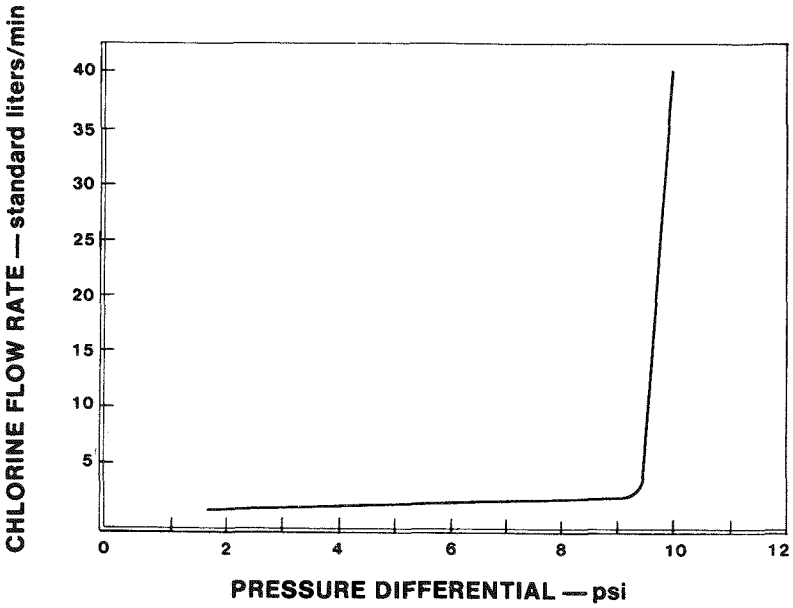

Figure 15-8. Relationship Between Gas Flow Rate and Pressure Differential for the Mechanical Relief Valve

Hydrate Formation Heat Exchanger

This heat exchanger operates only under the charge mode. It removes the heat generated by hydrate formation, heat transferred from the environment into the hydrate store and other heats due to the inefficiencies of the mechanical devices. A summary of the total heat load to the hydrate heat exchanger is tabulated in Table 15-1. A total of 29.62kCal/min of heat has to be removed from the store on

Table 15-1

ESTIMATED HEAT LOAD OF HYDRATE CHILLER

Heat due to hydrate formation at 1.22 g-mole/min, and 18.7kCal/g-mole	22.81kCal/min
Heat due to gas pump inefficiency pump efficiency @ 80% of power	5.08kCal/min
Heat transferred from sump wall	0.6 kCal/min
Heat from surrounding (1" insulation)	0.33kCal/min
Heat due to water vapor carryover	0.80kCal/min
Total Heat Load	29.62kCal/min

charge. Besides the 22.8kCal/min of heat generated from the hydrate formation, an estimated 5.08kCal/min of heat is introduced to the store due to the inefficiency of the gas pump. Heat transferred from the sump to the store and from the environment to the store are estimated to be 0.6 and 0.33kCal/min, respectively. Water vapor at 30^{o}C carried over by the chlorine gas during charge adds approximately 0.8kCal/min to the store.

Utilizing a store solution recirculation rate of 10 liters/minute through the heat exchanger, the temperature of the recirculating solution must be cooled to $\sim$3^{o}C below the store temperature to remove the 29.62kCal/min heat load and maintain store temperature.

A tube-shell type heat exchanger was chosen for the application. As shown in Figure 15-9, the tube bank consists of 150 thin wall titanium tubes, with in-line arrangement.

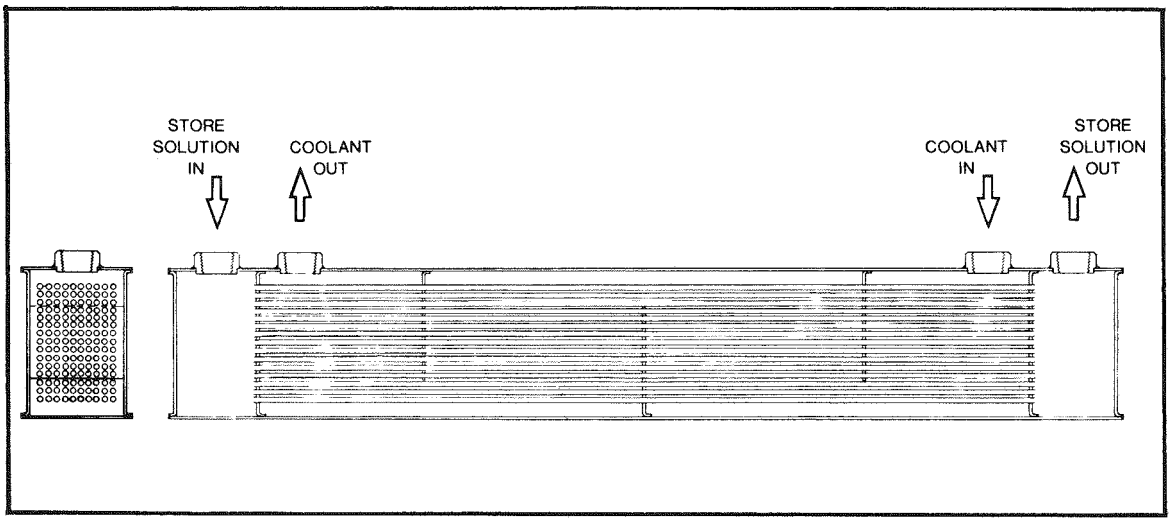

Figure 15-9. Tube-Shell Type Hydrate Formation Heat Exchanger

An overall heat transfer coefficient of 240 Btu/F°ft^{2}hr was calculated for this heat exchanger based upon the coolant flow of the shell side at the rate of 10 gpm with a mean temperature gradient of 2.6°C between the shell side and the tube side.

Decomposition Heat Exchanger

This heat exchanger only operates on discharge and provides the 30.5kCal/min of heat required for hydrate decomposition. A single-pass heat exchanger coil fabricated from thin-wall titanium tube was selected for this application.

Main Electrolyte Heat Exchanger

From energy balance calculations, the maximum heat gain to the electrolyte is on discharge and is of the order of 2kW or 7400 Btu/hr. A simple immersed coil with coolant flowing inside the coil was selected for this heat exchange operation.

HYDROGEN/CHLORINE REACTOR

Hydrogen gas is generated at the zinc electrode surfaces during battery operation. Although the rate of the H_2 evolution is very low, the concentration of H_2 gas accumulated over a number of cycles becomes significant in a closed system. Thus, a technique for removing hydrogen from the system is required. A photochemical technique for reacting hydrogen and chlorine was selected as the most practical hydrogen removal system. Figure 15-10 illustrates the reactor chamber used in the load leveling module. The reactor operates in conjunction with the gas pump which draws the gases from the stack compartment through the reactor chamber. In this chamber the gases are exposed to two fluorescent lights which reduce the hydrogen concentration to a very low level in the gas stream. These lights are inexpensive, readily available, and have an expected life of 6000 hours. The total power consumed by the reactor is approximately 20 watts (including transformer losses), and may be supplied from either an ac or dc source. The hydrochloric acid formed in the reactor is carried into the store compartment by the gas pump.

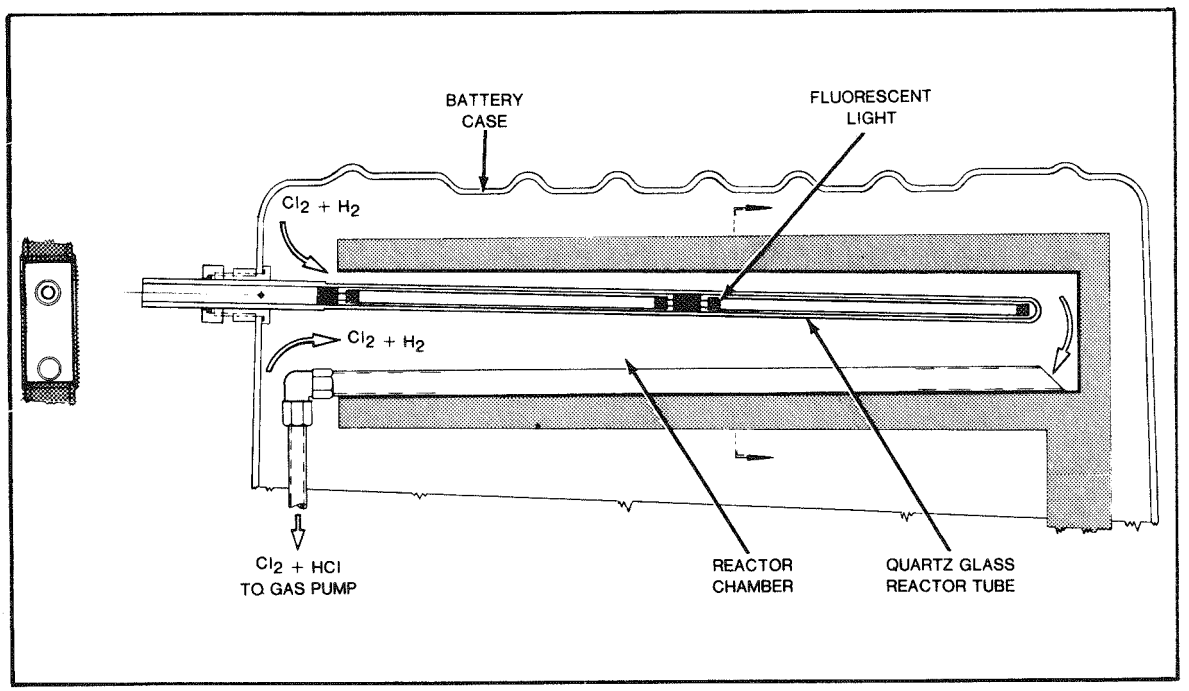

Figure 15-10. Photochemical Reaction Chamber for Recombining Hydrogen with Cl_2 Gas

MODULE CASES

The four-part module case is illustrated in Figure 15-11. The function of each of these components is described below:

- The upper case contains 6 submodules. Twelve terminal holes plus one hole for reactor light are available for external connections.
- The support plate serves as shelf for the submodules and also separates the stack compartment from the gas space of the store compartment.
- The lower and extension case contains both the hydrate store and a separate sump compartment. The sump compartment is bolted onto the support plate and has the same gas space of stack compartment. The sump has a total volume of 5.3 cu. ft. and the store compartment has a volume capacity of 13 cu. ft. It is calculated that net volume for sump and store is 4.2 cu. ft. and 11 cu. ft., respectively, after taking into account the volume of the installed components such as pumps, filters, manifolds, heat exchangers, etc.

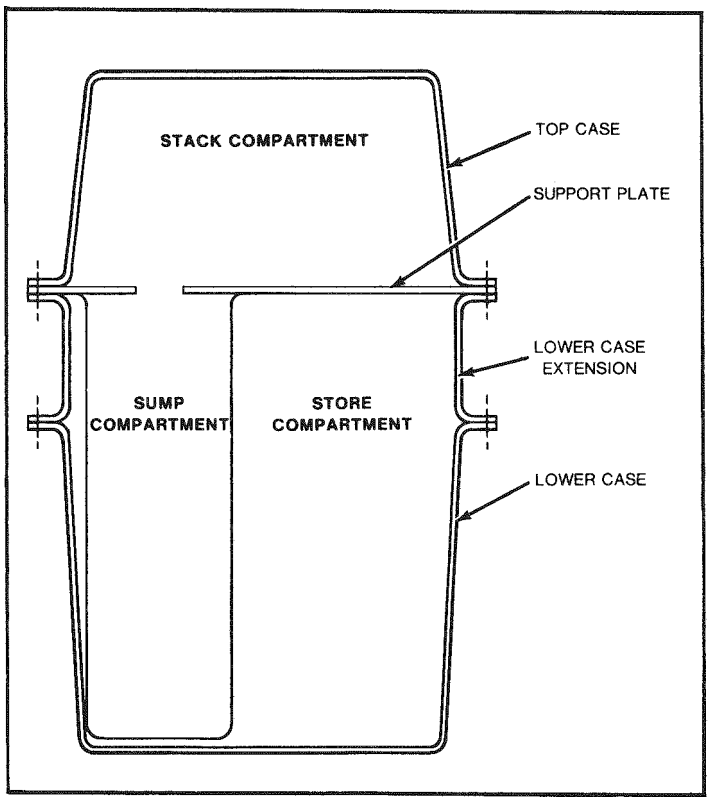

Figure 15-11. Four Part Module Case for the 45kWh Peak-Shaving Module

All the case sections had vacuum-formed Kynar liners to ensure stability to the battery environment. A fiberglas cloth with polyester binder case wall was built up on top of this liner. The walls were ribbed to reinforce this free-standing structure such that with a 3/8" wall thickness a working pressure of 10 psig could be contained.

Figure 15-12 shows the test results for case deflection under pressure. These results showed that the case was satisfactory for its intended operational pressures.

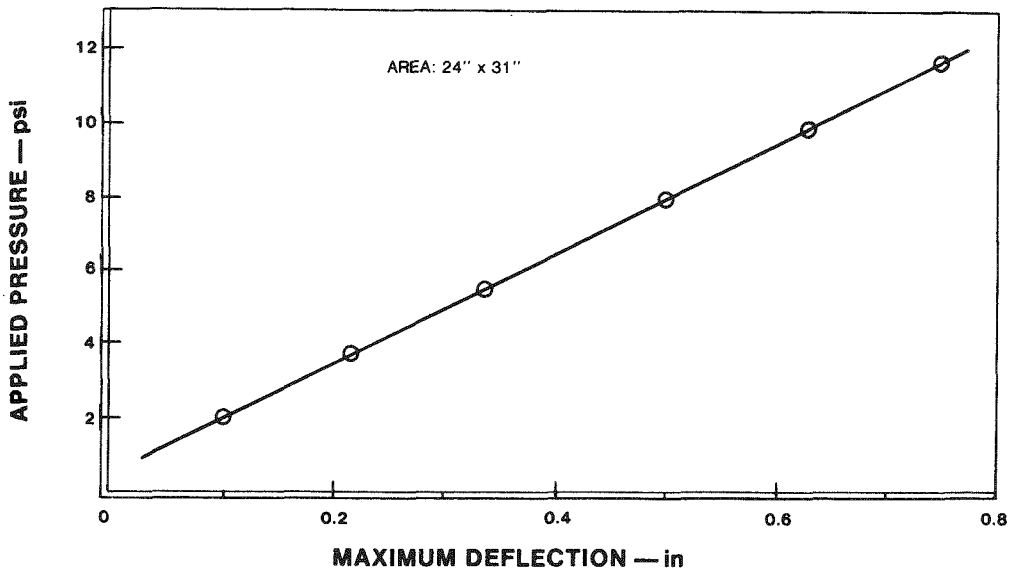

Figure 15-12. Deflection of the Lower Case of the 45kWh Peak-Shaving Module.

CONTROL SYSTEM

Control during charge was maintained by controlling the glycol/water coolant at a temperature of 5.2 $\pm$ 0.2^{o}C and the glycol flow rate of 32 liters/minute through the hydrate formation heat exchanger. The gas pump was operated at a constant speed of $\sim$2000 rpm throughout the charge. During discharge, stack pressure was chosen to control battery operation. When the stack pressure fell below the control point, an automatic pressure controller opened a solenoid valve which allowed warm stack electrolyte to flow through a decomposition heat exchanger in the store. The chlorine evolved from this decomposing hydrate raised the stack pressure back to the control set point and the solenoid valve was closed. This cycle of operations was repeated at a frequency dependent on chlorine demand.

Section 16

SUBMODULE DESIGN, ASSEMBLY AND QUALIFICATION

INTRODUCTION

Six submodules of the bipolar, comb-type design were used in the construction of the Mark 4, 45kWh load-leveling module. These submodules represent the state-of-the-art technology in the assembly of zinc-chlorine hydrate batteries. Production of these units reflects some changes in design and indicates the areas where additional improvements could be made.

DESIGN

The 7.5kWh submodules shown in Figure 16-1, used to construct the Mark 4 module, are a refinement of the comb-type single cells developed at EDA under an internally funded program. Each unit cell contains 44 chlorine electrode substrates and 23 zinc electrode substrates, the zinc electrode substrates being plated on both sides. Ten cells are connected together in series to form a submodule as shown in Figure 16-2. Zinc and chlorine electrodes of adjacent cells are pressed into opposite faces of the same bus connector. A zinc and chlorine end bus, at the appropriate end of each series, completes the stack-up of cells.

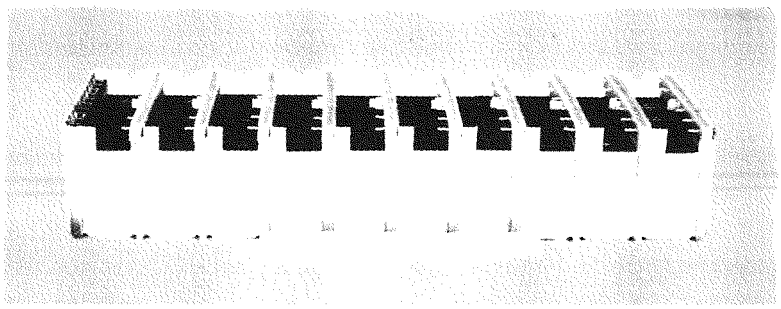

Figure 16-1. 7.5kWh Submodule

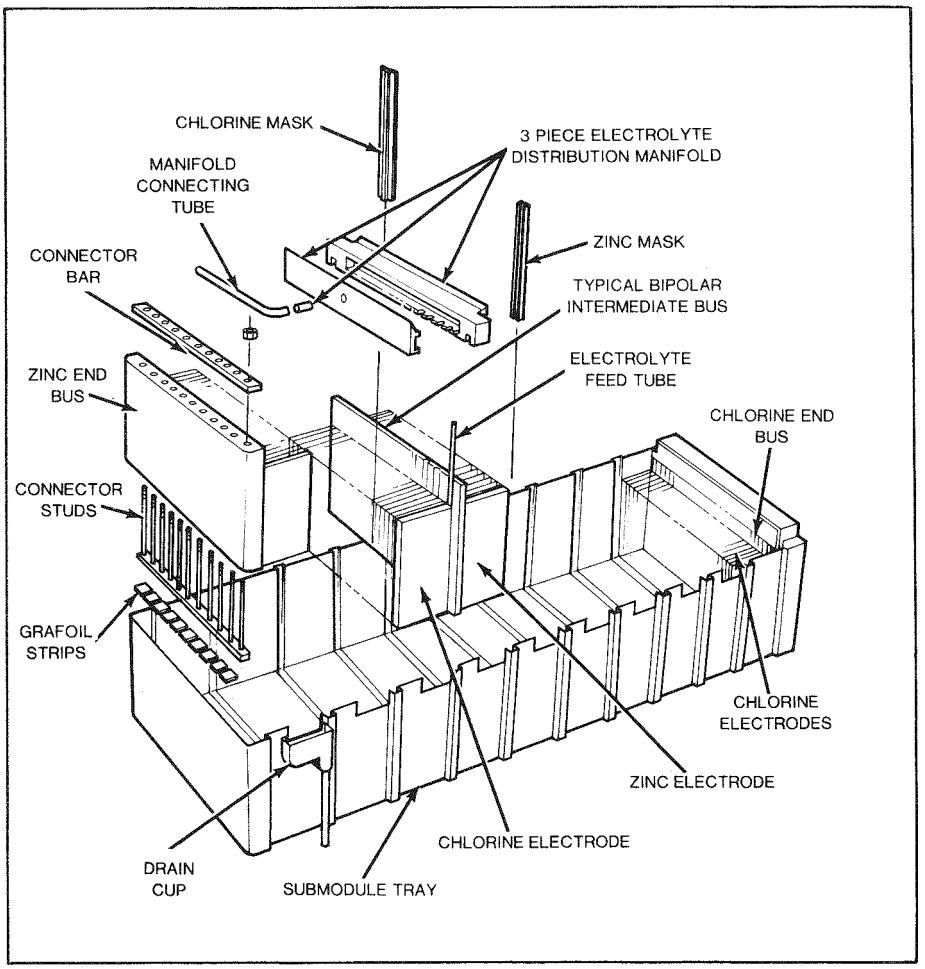

Figure 16-2. Basic Parts Used to Assemble 8.3kWh Submodules

The submodule is assembled into a pan designed to locate the buses relative to each other. Assembly is completed with the addition of zinc and chlorine masking and the cell manifold. A manifold is installed on each cell to feed electrolyte to the 22 porous graphite pairs that form the chlorine electrode substrate.

Each chlorine electrode pair shown in Figure 16-3 is a subassembly consisting of two mirror image profiled plates of porous graphite bonded together to create a cavity. During operation, electrolyte is pumped into the cavity in each electrode and flows through the pores of the electrode, into the interelectrode gap, and exits the cell over the submodule tray. Arrangement of ten cells in the above manner yields a submodule that will store 7.5kWh of energy. The submodule has an

open circuit voltage of ∿21.2 volts. Charge voltages are ∿2.28 volts per cell at 28mA/cm^2 and a discharge voltage of ∿1.88 per cell at 40mA/cm^2.

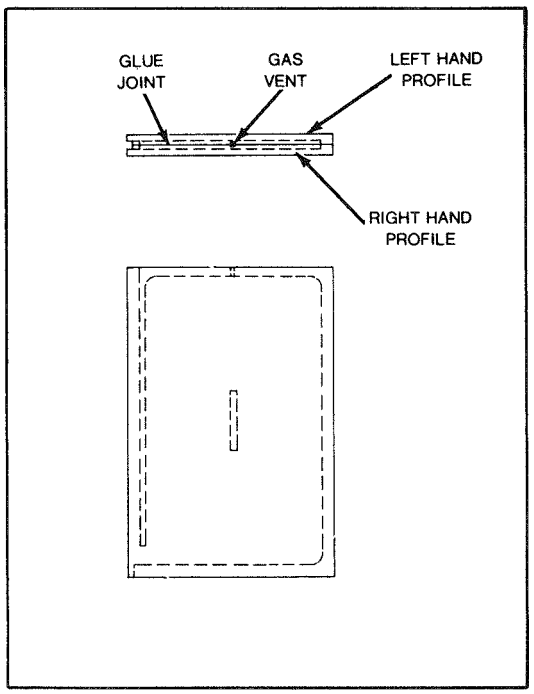

Figure 16-3. Typical Glued Chlorine Electrode Used in 8.3kWh Submodules. Note slot on left side to hold feeder tubes.

ASSEMBLY

Assembly of 7.5kWh submodules for the Mark 4 module was undertaken on a laboratory scale. Existing part designs and techniques were used in assembly of the Mark 4 submodules. Based on the experience gained from previous submodule construction, an assembly flow chart was prepared for the Mark 4 battery submodules. This flow chart is shown in Figure 16-4.

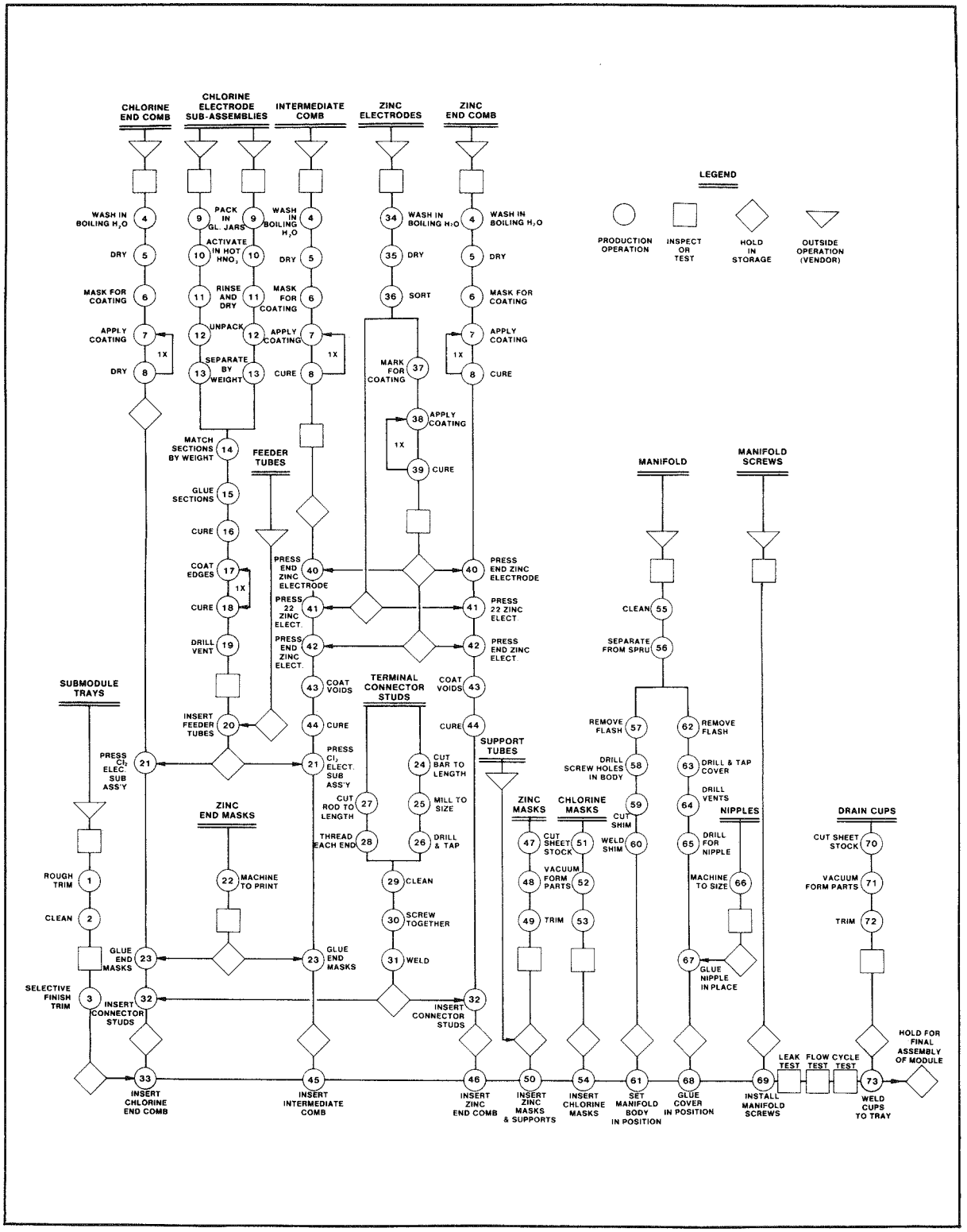

Figure 16-4. Submodule Assembly Flow Chart

Trays for the 7.5kWh submodules are vacuum formed from 1/8" x 45" x 25" extruded Kynar sheet. The trays are formed by a vendor and shipped to EDA. Mold release compounds are removed from the parts before inspection. Each tray is inspected for leaks and repaired when necessary. The individual pans are then trimmed for a particular location in the module stack-up. Chlorine end bus subassemblies are the first items assembled into the trays. These subassemblies consist of the bus, chlorine electrode subassemblies, feeder tubes and titanium contact posts.

The chlorine end buses are inspected when received from the vendor. As received they are drilled for the above-mentioned contact post, slotted to accept the chlorine electrode subassemblies and profiled to fit the radii of the submodule trays.

Accepted parts are cleaned in boiling water. After oven drying, areas of the buses to be insulated with Kynar are marked. A coating of Kynar resin, dissolved in an appropriate solvent, is applied to the buses in indicated areas, outside the active cell area illustrated in Figure 16-5. The coating is cured and the second coat applied. Chlorine electrode subassemblies are then pressed into the bus. The chlorine electrode subassemblies, as shown in Figure 16-3, are made from two mirror image profiled porous graphite (UCC PG-60) plates bonded together.

Individual porous graphite electrodes are inspected for dimensional errors and for physical defects on receipt from the machine shop. The electrodes are then activated by heating to $115^{\circ}C \pm 2^{\circ}C$ in nitric acid for 13 days. At the end of the activation period, the activation vessels are allowed to cool to room temperature, the nitric acid discarded, and the electrodes rinsed overnight by waterflow.

After a final rinsing operation, namely, filling with water and draining three times, the vessels are moved to an oven and heated to $\sim 120^{\circ}C$ for a minimum of 4 hours to dry the parts. The dried parts are then sorted by weight and the individual electrodes are matched to within ± 0.3 grams to form a chlorine electrode pair.

A film of Kynar resin and graphite suspended in a solvent is applied to one-half of the subassembly and the second half laid atop the first. A weight is applied

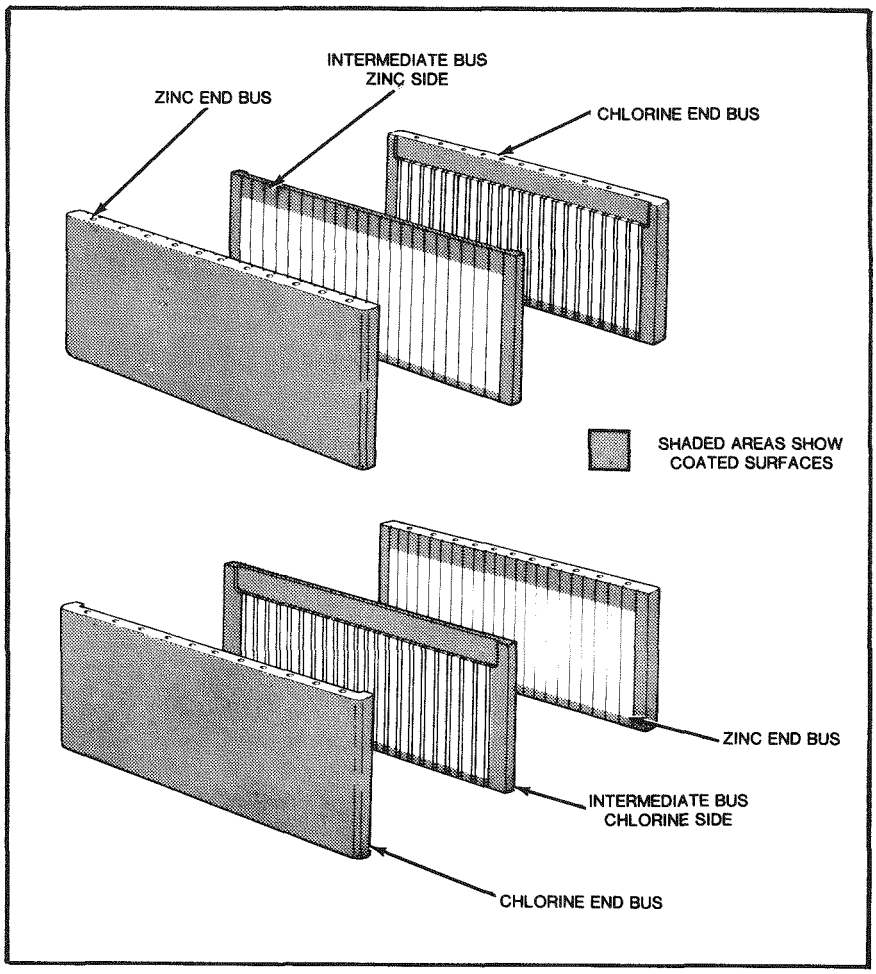

Figure 16-5. Coated Areas on Buses Used to Manufacture 8.3kWh Submodules

to the assembly or groups of assemblies. The weighted assemblies are placed in an oven and cured at 50°C overnight. A coat of Kynar glue is applied to the three flat edges of the electrode subassembly, cured overnight and recoated. The bonded electrode pairs are inspected for damage. A #14 lightweight FEP tube is positioned in the slot in the bonded electrode halves.

The completed subassembly (chlorine electrode) is stored until buses are ready to be assembled. The chlorine electrode subassemblies are then pressed into the machined slots in coated and chlorine buses.

A zinc electrode mask (a detailed part machined from Kynar) is glued to the bus and the outboard chlorine electrode on each end of a bus as shown in Figure 16-6. The titanium contact posts are pressed into the end chlorine bus and as the tray becomes available the buses positioned in the predetermined end of each pan.

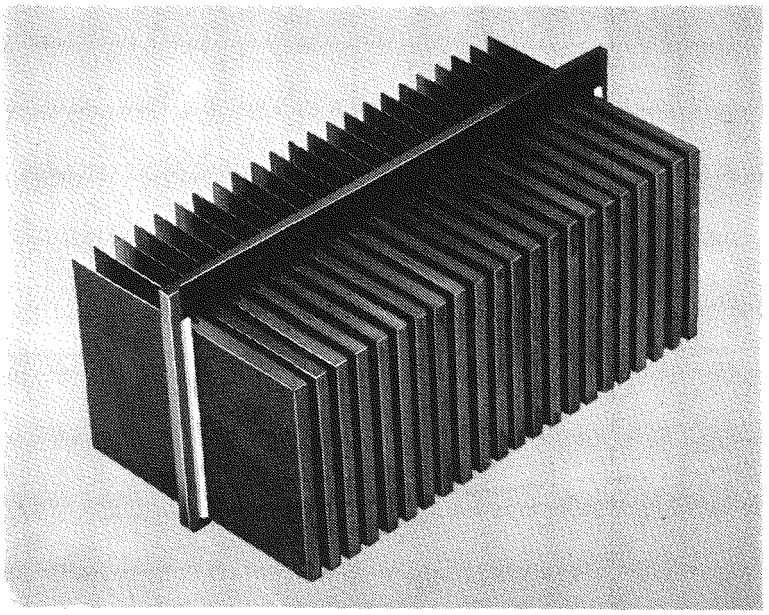

Figure 16-6. Intermediate Comb Showing Relationship of Zinc and Chlorine Electrodes Relative to the Bus. Note end zinc chlorine mask glued in corner of bus and chlorine electrode.

Both zinc end buses and intermediate buses are inspected for dimensional errors and physical defects upon receipt from the vendor. They are also cleaned and coated by the methods described in the preparation of the chlorine end electrodes. Some storage is necessary between preparation and assembly of individual buses.

Both intermediate and zinc end buses are assembled by first pressing the zinc substrates into position. The titanium contact posts are assembled into the zinc end buses, as described in chlorine end bus assembly, and this subassembly is stored.

Intermediate buses are set into a fixture and chlorine electrode subassemblies pressed into position on the opposite side of the bus from the zinc electrodes. Zinc masks are glued into the corner of the bus and the outboard chlorine electrode, at both ends of the bus as shown in Figure 16-6.

Finished intermediate bus subassemblies are positioned in the locating grooves in the submodule pan, beginning with the groove closest to the chlorine end bus, zinc electrodes toward the chlorine end bus. Eight additional intermediate buses are positioned and the zinc end bus inserted in the end groove.

Each partially assembled submodule is inspected to assure that the electrode tops are all at the same level and that buses have bottomed in the locating groove. Chlorine masks are then positioned between the end of each chlorine electrode and the bus opposite it and the zinc substrates protruding from that bus on either side of the chlorine electrode, as shown in Figure 16-7.

The 220 chlorine electrode masks needed per submodule are vacuum-formed in-house and trimmed. The parts are formed from 0.010" Kynar sheet stock.

The 210 zinc masks in the Mark 4 were formed from 0.007" thick Kynar sheet rather than 0.010 mil material the part was designed to be made from, due to a material shortage. Consequently, the zinc mask required the support from two #20 AWG FEP tubes between each mask and the chlorine electrode on either side of the mask, also shown in Figure 16-7.

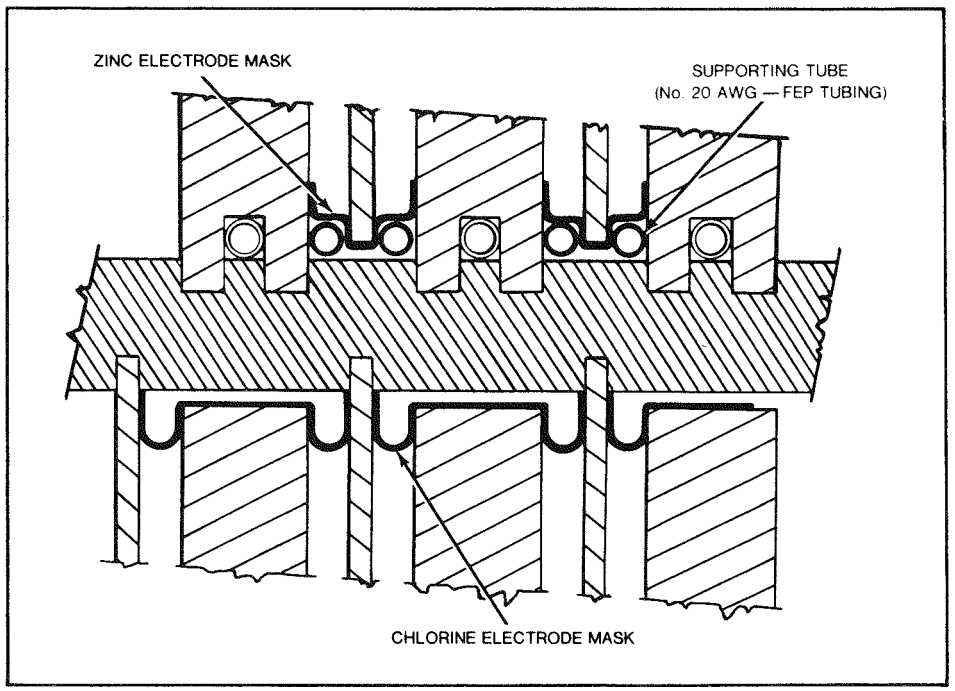

Figure 16-7. Relationship of Zinc and Chlorine Masking to Bus Bar

The zinc electrodes and support tubes are put into place on the end of each zinc electrode, between the electrode and the opposite bus and the chlorine electrodes protruding from it. Each cell is inspected to insure that both the zinc and chlorine masking are in their proper position.

After the zinc end chlorine masking is in place, manifolds are put in place on top of the intermediate buses. The distribution manifold for each cell directs electrolyte to each of the chlorine electrode assemblies pressed into the bus in that cell. Manifolds for the chlorine bus are machined to fit next to the end chlorine bus.

The manifolds are injection molded by a vendor in an EDA die. The parts are inspected, cleaned, deburred, and slightly modified in-house. Approximately 10% are modified for use with end chlorine buses. All manifold covers are drilled to accept a connector for tubing coming from the module manifold. Vent holes, are drilled through the manifold body. The machined connector is pushed into place in the cover. The manifold is now ready to be assembled onto a bus.

A slot along the bottom of the manifold slips over the top of a bus. The top of the feeder tubes protruding above each chlorine electrode aligns with half-round grooves in the main body of the manifold as shown in Figure 16-8.

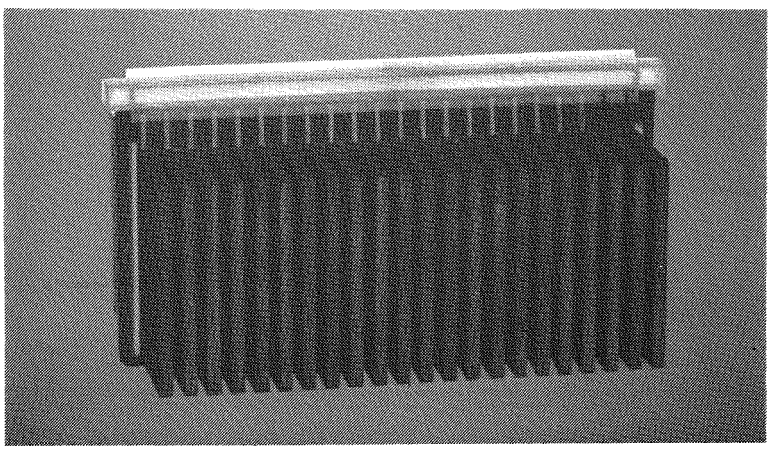

Figure 16-8. Bus, Chlorine Electrodes, and Manifold Body. Note feeder tubes extending into manifold from electrodes. Manifold cover snaps in place across tubes. Two electrodes at right do not have feeder tubes in place.

Glue is applied around the edge of the manifold cover and it is snapped into place on the main body with half-round grooves on the cover around the exposed half of the feeder tubes. Six 4-40 Teflon screws are threaded through the manifold, into the tapped holes in the cover. The Kynar glue is allowed to cure at room temperature overnight.

Excess material is trimmed from one in ten manifolds and it is assembled around the top of the feeder tubes on the end chlorine bus. This manifold is supported by the feeder tubes rather than the bus. This end chlorine bus manifold does present some problems during handling but is secured at assembly of the units.

The final part attached to the submodule before the stack-up of the submodules in the module is the discharge cup. This part is vacuum-formed (in-house) from Kynar. Each of the ten cells per submodule has a discharge cup welded over a notch cut at one side (Figure 16-2). This part collects the electrolyte overflowing a cell and funnels it into an electrolyte discharge manifold.

QUALIFICATION

Post-assembly testing of a submodule is carried out in two steps: fluid flow/leak testing and electrochemical testing. After the glue in the manifold joints has been cured each manifold is tested for leaks and each chlorine electrode is checked to assure that electrolyte is flowing through that electrode. Repairs, if necessary, are made before the submodule is tested for electrochemical performance.

Submodules are charged and discharged under conditions similar to those under which the unit would operate, except no supporting electrolyte is used. Each unit is charged @ 27mA/cm^2. The rate of electrolyte flow is 2cc/min-cm^2. Temperature is maintained at $\geq 30^{\circ}C$. Beginning pH is adjusted to 0.0-0.2. A beginning Sp.Gr. of 1.27 of the volume of electrolyte held by the test stand allows the unit to be charged for 8+ hours without going below a Sp.Gr. of 1.08. Dissolved chlorine is held between 2.0-2.5 grams per liter during charge.

During charge the unit is monitored for internal shorts and voltage readings. Voltage and the shape of the discharge curve, shown in Figure 16-9, are monitored during discharge as is the coulombic efficiency. Discharge is effected at a rate of 40mA/cm^2 and an electrolyte flow of 2cc/min-cm^2. Chlorine concentrations are maintained at 2.5-3.0 grams per liter.

The average charge voltage per cell over the six submodules used for the Mark 4 unit was 2.29 volts. The corresponding average discharge voltage was 1.83. The discharge curves have relatively sharp knees, illustrated in Figure 16-9. Two modules have a slight step in their discharge curve, below the knee, indicating a slightly uneven discharge of the cells.

Coulombic efficiencies of the six modules averaged 67%. The range of the efficiencies was 64.9 to 69.0%.

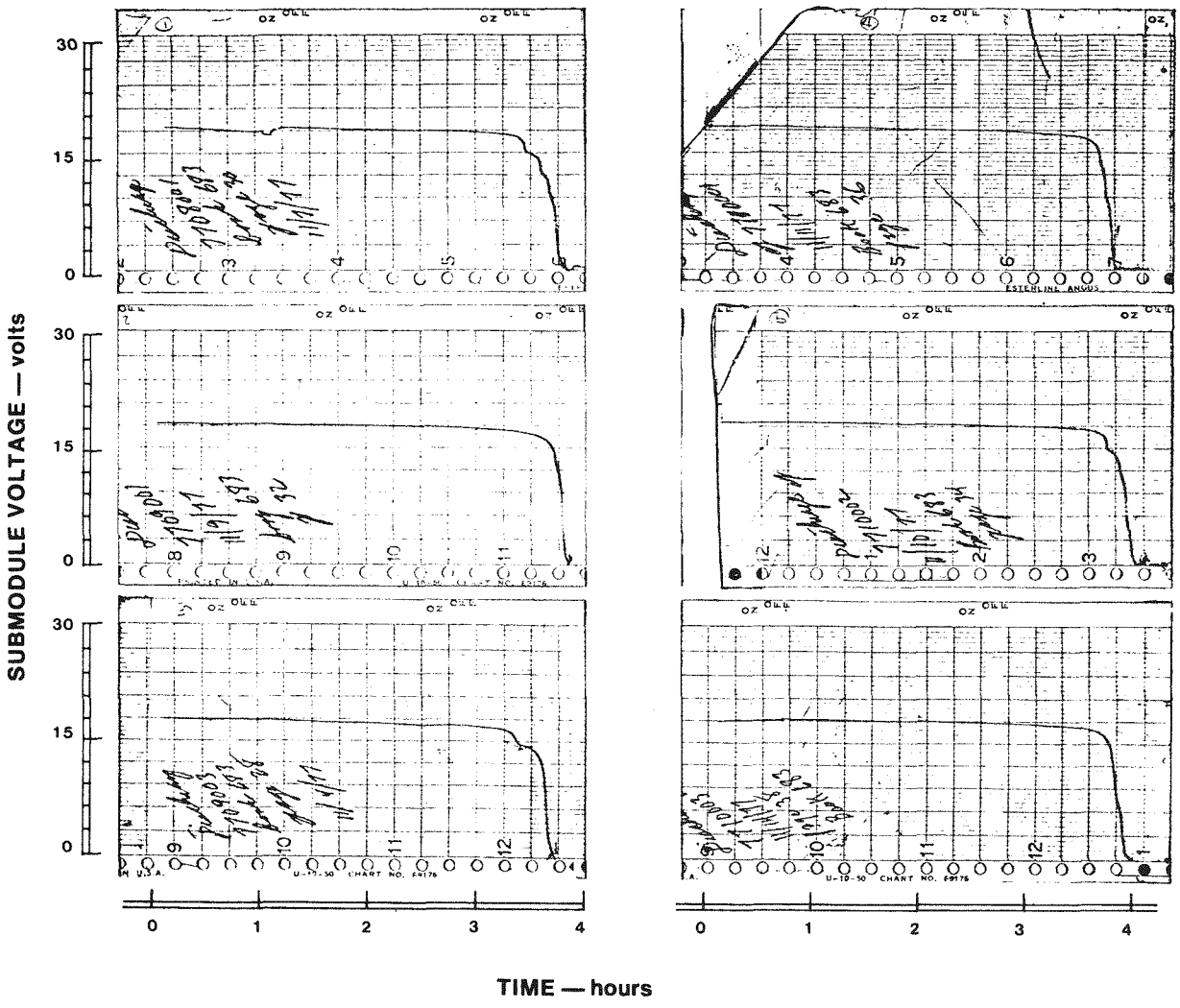

Figure 16-9. Discharge profiles of the six submodules for the 45kWh peak-shaving module. Discharged at current density, 40mA/cm^2, at 28°C.

DISCUSSION

There are many areas for improvement in the assembly process and in the components used. Manifold assembly, around the feeder tubes, will be accomplished as a subassembly, outside the submodule, followed by leak/flow testing of the subassembly on future submodules. The manifold subassembly will then be fitted to the bus assembly after the bus has been located in the tray and the masking inserted.

The vacuum formed submodule trays presented three problems: 1) uneven case thickness, 2) thin corners, to the point of ruptures, and 3) uneven shrinkage, because of uneven wall thickness. A portion of the physical problem with the case may be alleviated by finding a suitable substitute for Kynar. This material has a high shrink factor which is a function of the thickness of the material. Thus, parts such as the tray, that have uneven wall thicknesses, shrink at different rates in different areas. Kynar is also relatively expensive.

The contact post in each end has a relatively high contact resistance. Improvement in this contact will improve the overall performance of the submodules.

The tight tolerance required in the fit of the zinc electrodes into the zinc bus slots will require some specialized manufacturing techniques. Profiled chlorine electrodes are more expensive than flat plate electrodes 1) to machine and 2) for material cost. Machining flat plate electrodes would require slabbing off the electrode and minor finishing, while profiled electrodes require additional machine steps to complete the profile. Profiled chlorine electrode pairs represent ∿25% usable graphite (75% machined away) while flat plate electrodes represent 52% usable graphite. If the electrodes were wafer-sliced, as discussed in Part II, Section 7 of this report, graphite utilization would be further improved. An in-situ activation process for the chlorine electrodes in a submodule has been developed and is explained in Part V, Section 34 of this report. Incorporation of this process into the process/assembly routine for comb-type cells will reduce in-process time for the electrodes and reduce handling losses.

Section 17

PUMP TESTING AND EVALUATION

The present peak-shaving zinc-chlorine battery design requires two fluid handling systems; one to uniformly distribute the zinc chloride electrolyte throughout the cells of the stack, and one to pump the chlorine gas and form hydrate during battery charging. This report covers the performance testing and qualification of the pumps used to power these two systems.

BATTERY PUMPING REQUIREMENTS

Electrolyte

Electrochemical criteria defined the electrolyte flow rate at $2ml/cm^2$ of electrode area. For the six submodule battery stack with $165,000cm^2$ of effective electrode area, the electrolyte pumping system is sized at 332 liters/minute or 87 gpm.

The pump head required at this flow is determined by optimizing the hydraulic effects against the electrical considerations. For minimum parasitic current losses in the electrolyte distribution system (caused by the conducting fluid circulating between the cells) a long path with minimum cross-sectional area to maximize electrical resistance between cells is desired. From the hydraulic viewpoint the opposite is desired. To minimize the energy used by the electrolyte pumping system, low hydraulic losses are necessary. These losses are increased by using small cross-section, long-length piping resulting in higher fluid frictional losses, and thus, a higher pump pressure requirement. The optimization of these effects results in a 3.5 psi pressure needed at the entrance to the battery stack distribution manifold. An elevation difference between the electrolyte pump outlet and manifold entrance results in an additional 0.5 psi pressure requirement for a total of 4 psi at the pump discharge connection.

To minimize the concentration of dissolved chlorine in the electrolyte and thus to minimize corrosion losses, the stack pressure is reduced to 5 psi below atmospheric. Since the electrolyte collection sump is open directly to the battery stack, this results in a low absolute pressure at the electrolyte pump suction of 10 psia. For

the pump to operate without cavitation, the absolute pressure of the electrolyte being pumped must exceed the vapor pressure of the fluids handled by an amount sufficient to overcome any entrance frictional losses. Since the electrolyte is not only saturated with chlorine gas but also has additional entrained chlorine gas, the available suction pressure is further reduced. The amount of absolute suction pressure at the impeller required for the pump to operate at capacity is referred to as the Net Positive Suction Head (NPSH). The battery system electrolyte pump is designed for a minimum NPSH requirement and lowest possible suction losses.

Gas Pumping/Hydrate Formation

The specifications for the gas/hydrate-forming pump were determined by scaling up smaller battery systems and from additional store development work in the Phase I program. The specifications established require the transfer of 28 liters/min of chlorine gas on charge, from the stack to the hydrate store. Simultaneously, the pump circulates and mixes 10 liters/min of dilute zinc chlorine solution (Sp. Gr. 1.03) with the gas to form the chlorine hydrate. In order to form hydrate the temperature of the two-phase flow mixture of gas and dilute solution has to be maintained at $6^{\circ}C$ for the -5 psig inlet condition. The amount of chlorine formed into the hydrate is dependent on the pressure/temperature relationship of the gas/liquid mixture at the pump outlet. The optimum pump discharge pressure was determined to be 10 psig. During the charging process the gas pump has to transfer chlorine and form chlorine hydrate at a rate sufficient to maintain the below-atmospheric pressure desired in the stack. During discharge the pump circulates 3 liters/min of solution and 8 liters/min of gas through the hydrogen reactor with the suction pressure at atmospheric and the discharge pressure at 6 psig.

Additional Design Requirements

In addition to the hydraulic design requirements stated, the pumping system components must meet stringent durability and efficiency criteria consistent with power plant usage. Because of the nature of the internal fluids, the pumps must be absolutely free from leakage to the environment. To assure zero leakage, rotational seals are precluded and drive torque must be supplied through a positive static seal by means of magnetic drives or canned motors. Also, because of the nature of the fluids being pumped, the available materials of construction are very limited.

DESCRIPTION OF PUMPING EQUIPMENT

The electrolyte pump, shown in Figure 17-1, is of the end suction centrifugal type. The gas/hydrate-former pump is the positive displacement spur-gear unit illustrated in Figure 17-2. Both pumps are mounted through the battery-case wall and incorporate specially designed magnetic couplings.

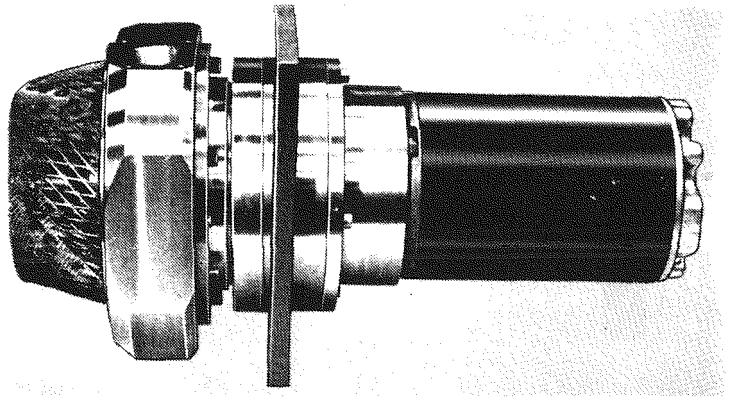

Figure 17-1. Electrolyte pump is end-suction centrifugal type mounted inside the sump with motor outside the case connected through the case wall with magnetic coupling.

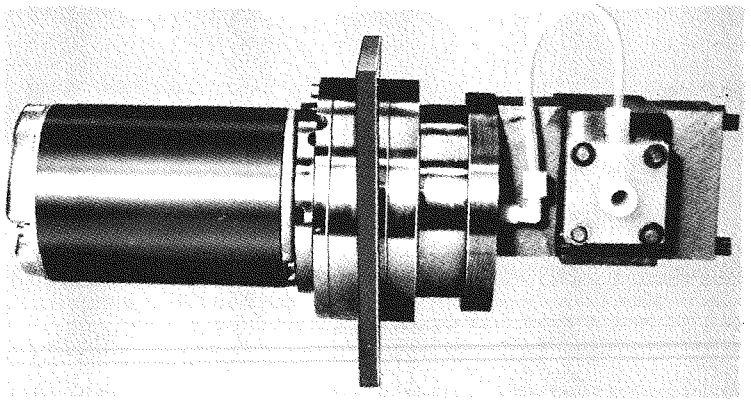

Figure 17-2. Spur Gear Pump Used to Pump Chlorine Gas and Form Hydrate. Pump is mounted inside the store and is connected by a magnetic coupling to a motor mounted outside the case.

Magnetic Coupling

The coupling design is unique and satisfies the conditions of zero leakage and high efficiency as well as being capable of transmitting the required high torque. Figure 17-3 is a cross-sectional drawing of this design. In order to obtain its maximum efficiency, the inner rotating portion must be physically small to minimize viscous drag caused by rotating submerged in the pumped fluid. The static seal separating the outer magnetic assembly from the inner driven rotor must be non-magnetic and non-conducting to eliminate eddy current losses. For the most effective coupling system, the magnetic gap separating the driver and driven units must be as small as possible. The static seal between the magnets is fabricated from Kynar material which has the chemical inertness and physical strength required for minimum section thickness. The magnets are rare earth (samarium-cobalt) with an

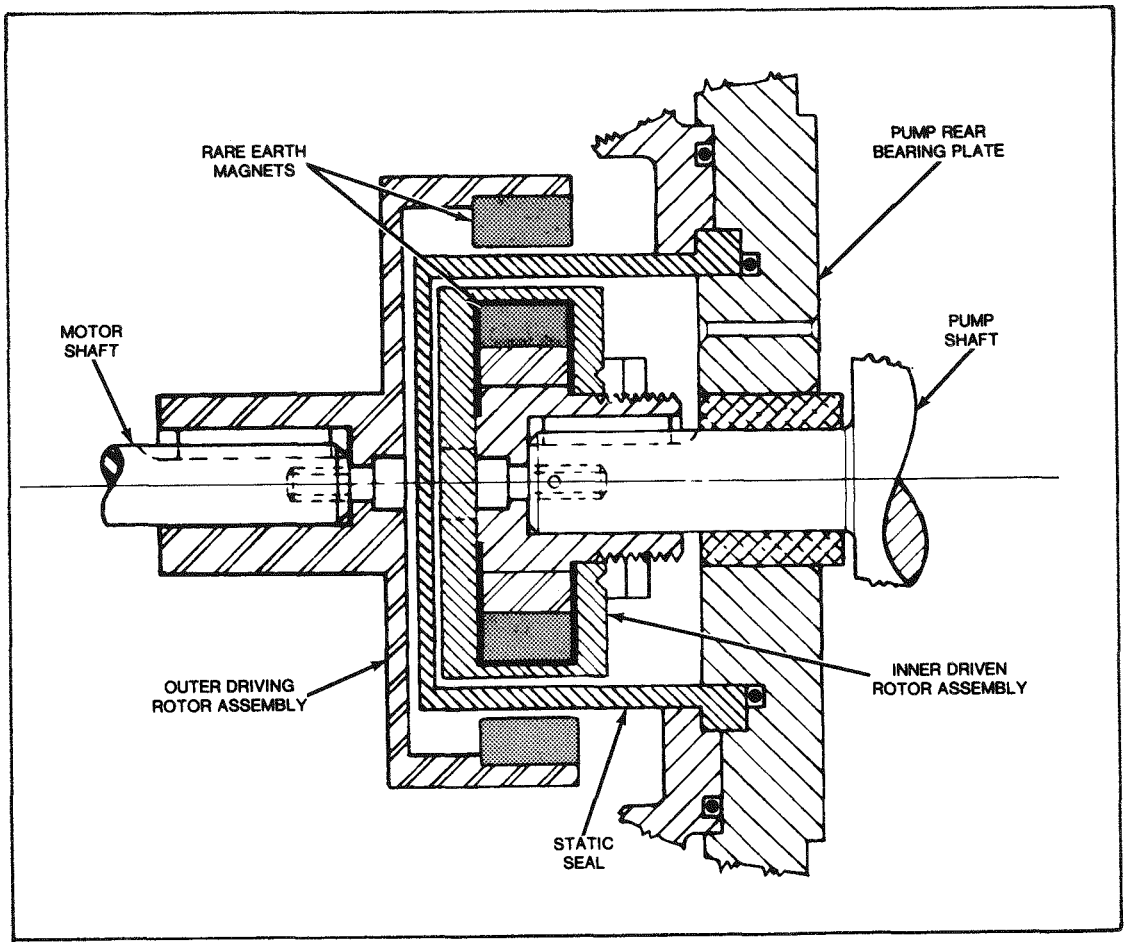

Figure 17-3. Detail of Magnetic Coupling Shown in Cross-Sectional Drawing

extremely high magnetic energy product of 16 MGOe. The inner magnetic rotor assembly has a titanium hub inside the iron core which carries the magnets. They are supported against centrifugal force by a thin titanium ring press-fitted over the rotor assembly. The entire rotor assembly is encapsulated in a Kynar cover to protect it from the chlorinated zinc chloride environment.

Mounting Flanges

In order to maintain the minimum gaps between the rotating inner and outer magnetic units and the static seal, a very close-tolerance motor mounting system is employed. As shown in Figure 17-4, the motor-mounting flange ring (detail 17) telescopes into the pilot bore on the mating-pump support flange (detail 14) and bottoms against the internal shoulder. This mounting method provides accurate centerline and position alignment assuring concentricity of the coupling assembly while facilitating easy removal and replacement of the drive motors.

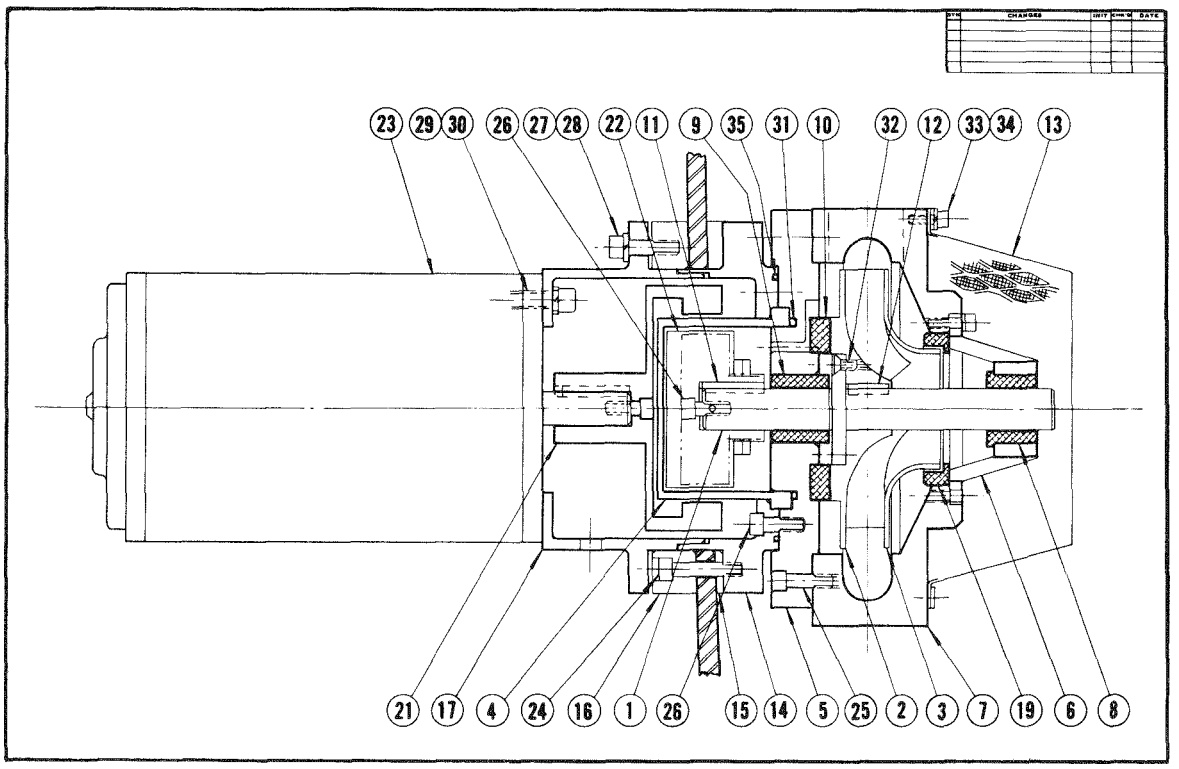

Figure 17-4. General Arrangement Drawing of Electrolyte Pump, Motor, and Coupling. Note that motor can be removed without disturbing the case-mounted pump.

Electrolyte Pump

An exploded view of the electrolyte pump components is shown in Figure 17-5. The motor, motor-support-flange outer-drive magnet assembly, and pump-support flange are shown disassembled, in order from right to left. The remaining components, in order, are the Kynar-cup static seal, inner rotor assembly, impeller/shaft/rear-bearing plate assembly, volute housing/front bearing assembly, and suction entrance screen.

This pump design incorporates several unique features. To reduce the suction hydraulic losses, the pump is through-case mounted with the inlet submerged directly into the electrolyte sump thus eliminating suction piping losses. This concept provides maximum suction entrance area and lowest fluid approach velocities minimizing the potential for cavitation. By submerging the entire pump inside the battery case, only one static seal is necessary. Any leakage from the pump itself is contained within the battery.

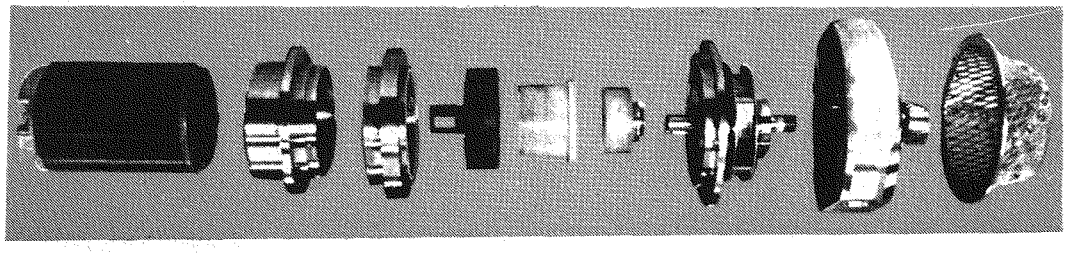

Figure 17-5. Electrolyte pump components include intake screen, pump body, impeller and rear-bearing plate, magnetic coupling parts with static seal between, inner and outer mounting flanges, and motor.

To satisfy the durability requirement with the limited material selection available, the bearing design is a key consideration. The graphite-shaft journal bearings have a very low pv factor (measure of bearing load). This velocity-pressure product is reduced by minimizing the bearing loads and impeller rotation speed. A speed of 1500 rpm was selected as the best compromise between bearing loads and hydraulic efficiency. Because of the submerged design, the front shaft bearing can be cantilevered through the suction, as there is no piping to contend with. By suspending the impeller between the bearings, the bending moment loads are much reduced. These radial loads were further reduced by hydraulically matching the three-radii volute impeller-housing with the desired flow velocity. By optimizing the housing design for a specific flow, maximum efficiency and minimum loads occur. To enhance the bearing capabilities a very hard, smooth bearing surface is used.

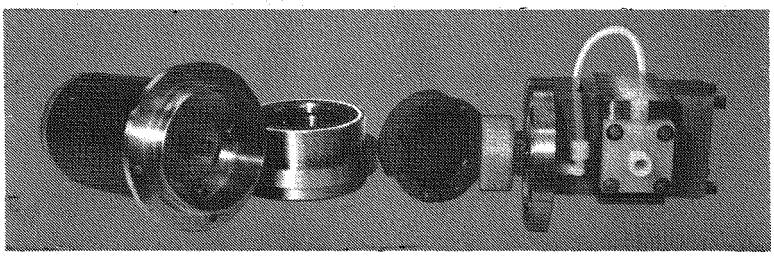

Figure 17-6. Gas/hydrate-former pump components include motor with mounting flange, inner flange, magnetic coupling parts, and gear pump assembly with mounting plate.

The impeller axial loads are reduced by hydraulically balancing the back face and front suction seal diameters. The back-face impeller seal also acts as a thrust bearing and is made of graphite. Details 8 and 9 of Figure 17-4 are the graphite front and rear impeller-shaft bearings. The back-face thrust bearing and front suction seal are details 10 and 19. Only a very slight running clearance exists between the front suction seal and the impeller shroud. The 90° lip configuration provides the best method of reducing suction leakage with the least drag.

Gas/Hydrate-Former Pump

The gas/hydrate-former pump, shown disassembled in Figure17-6, illustrates the similarity of the magnetic coupling and motor mounting components to those of the electrolyte pump described above. The bearings used are also graphite journals with titanium shafts as illustrated in Figure 17-7. The pump gears (detail 19) are of filled Teflon material with the lower gear and drive shaft (detail 5) driving

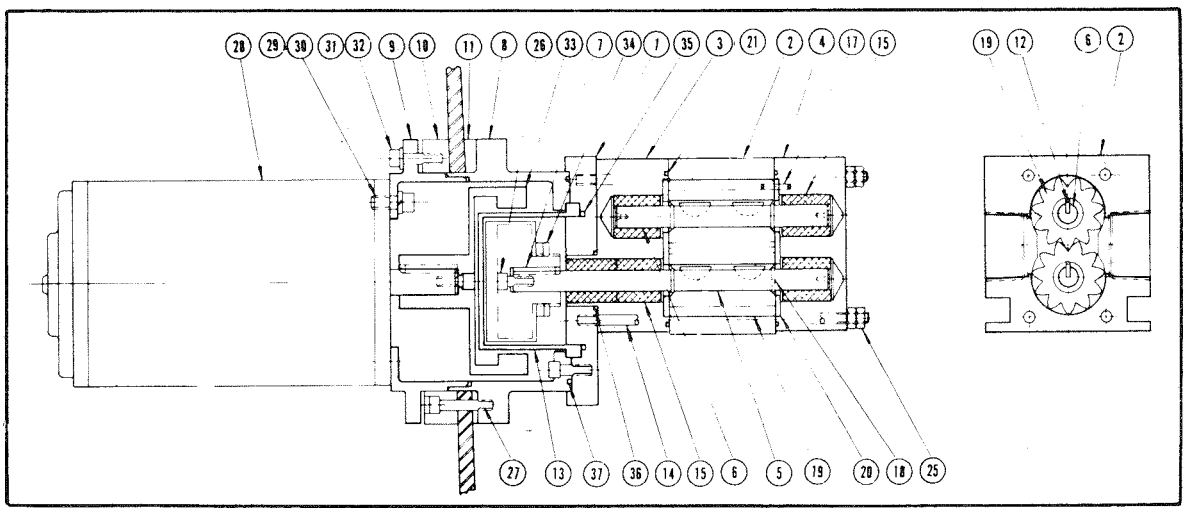

Figure 17-7. General arrangement drawing of spur-gear type gas/hydrate-former pump showing magnetic drive coupling with static seal (13) separating external motor from internal pump.

the upper idler gear and idler shaft (detail 6). The titanium pump assembly, consisting of gear housing (detail 2), front bearing block (detail 4), rear bearing block (detail 3), and rear mounting plate (detail 1), is held together by four tie-rods (detail 14). Specially designed Kynar inlet and outlet fittings are used to connect the pump to the battery system piping.

TESTING REQUIREMENTS

Hydraulic Performance Testing

Pump parameters of speed, head, and flow, as well as motor performance, must be known before the electrolyte and gas/hydrate-former pumps are sealed into the integrated battery system. Performance testing under conditions simulating those expected during battery operation provided the necessary flow/pressure/speed curves for interpretation of pump performance while operating within the system during cycle testing. During testing the pumps are preset to the operating conditions required of the battery system. The electrolyte and gas/hydrate-former pump operating specifications are outlined in Table 17-1. The hydraulic conditions listed were simulated and the pumps tested using water and air for the test fluids. The electrolyte pump pressure/flow characteristic curves for various constant pump speeds were plotted from data obtained during this testing (see Figure 17-10, page 17-15).

The test procedure followed was to operate the electrolyte pump at constant speed by controlling the dc motor voltage and varying the pump discharge pressure from the highest (shut-off head) to the lowest (run-out head) values obtainable with each of the pump speeds plotted. The pump head parameter was varied by adjusting the pressure drop through the discharge throttle valve. The gas/hydrate-former pump was used to establish the low pressure necessary to evaluate the electrolyte pump under negative suction conditions. Pump-drive motor-input wattage was also determined. The pump hydraulic output power was calculated from the flow and pressure data. The ratio of pump hydraulic output power to motor input power is the "wire to water" or overall efficiency for the pump and motor combination. This overall efficiency value can be used to derive the "pump only" efficiency by

Table 17-1

PERFORMANCE SPECIFICATIONS FOR PEAK-SHAVING BATTERY MODULE PUMPS

ELECTROLYTE PUMP

Pump Characteristics	Charge Cycle	Discharge Cycle
Flow Rate	332 ℓ/m (87 gpm)	332 ℓ/m (87 gpm)
Outlet Pressure	0 psig	+5 psig
Inlet Pressure	-4 psig	0 psig
Temperature	50°C	50°C
Pumped Fluid	Aqueous zinc chloride ∿1.3 S.G.	Aqueous zinc chloride ∿1.3 S.G.
Entrained Gas	Chlorine ∿5%	Chlorine ∿5%
Overall Efficiency	60%	60%

GAS/HYDRATE-FORMER PUMP

Pump Characteristics	Charge Cycle	Discharge Cycle
Flow Rate Gas	28 STP ℓ/min chlorine gas	8 STP ℓ/min chlorine gas
Liquid	10 ℓ/min dilute $ZnCl_2$ (∿1.03 S.G.)	3 ℓ/min dilute $ZnCl_2$ (∿1.03 S.G.)
Outlet Pressure	+15 psig	+10 psig
Inlet Pressure	-5 psig	0 psig
Temperature	6°C	11°C
Overall Efficiency	25%	25%

interpretation of the dc motor dynomometer curves to obtain the corresponding motor efficiency. This indirect method is used since there was no convenient way to install a torque reading system on the magnetic coupling between the driver and pump.

The gas/hydrate-former pump was also performance tested on air and water. A bench test evaluation of the pump and motor unit followed using a water store/hydrate-forming test rig duplicating the system actually installed in the peak-shaving battery assembly.

Endurance and Life Testing

In order to evaluate the electrolyte and gas/hydrate-former pumps against projected reliability and durability criteria, accelerated endurance/life cycle testing is necessary. The rate of bearing, gear, shaft, and seal wear are especially important for the long duration, high-efficiency pump operation required. Measurement of this wear parameter against accumulated running time will provide data for projecting the ultimate length of pump service life. The time-related effects of static seal and coupling encapsulation degradation can also be derived from accumulated pump test time. Similarly, the general performance of the materials of construction will be qualified by periodic observation during the tests.

Battery System Testing

Data for pump performance evaluation will be accumulated during the actual peak-shaving battery cycle testing. This phase of electrolyte and gas/hydrate-former performance qualification and evaluation testing is in reality the "proof of the pudding". The information obtained will be used to modify the pumping specifications, iterate the design, and thereby optimize pump performance.

DESCRIPTION OF TEST EQUIPMENT

Hydraulic Test Stand

The special stand for pump testing was developed and is shown in Figure 17-8. The test stand equipment is fabricated from materials compatible with the zinc chloride/chlorine gas environment. This pump test system provides a means of installing the electrolyte pump through the test tank wall with the inlet submerged inside and the motor flanged outside duplicating the battery installation. The motor can be seen projecting from the lower right-hand corner of the stand. In order to simulate the below-atmospheric pump suction condition, the tank is completely sealed. The one-inch thick clear acrylic top is removable to facilitate pump installation. The top is sealed to the fabricated PVC tank by means of a perimeter Gortex sealing gasket and cap screws tapped into the tank edge. The tank is supported by four internal dividers also acting as a baffle and weir system to "defoam" the aerated test liquid on its return to the pump suction. The inverted U-shaped 3" diameter schedule 40-CPVC and glass piping shown above the test tank is the pump discharge piping containing the throttling valve and sharp-edge orifice-plate flow meter. This piping is also removable and is sealed through the tank top with O-rings and flanges. The overall dimensions of the tank are 36 inches square

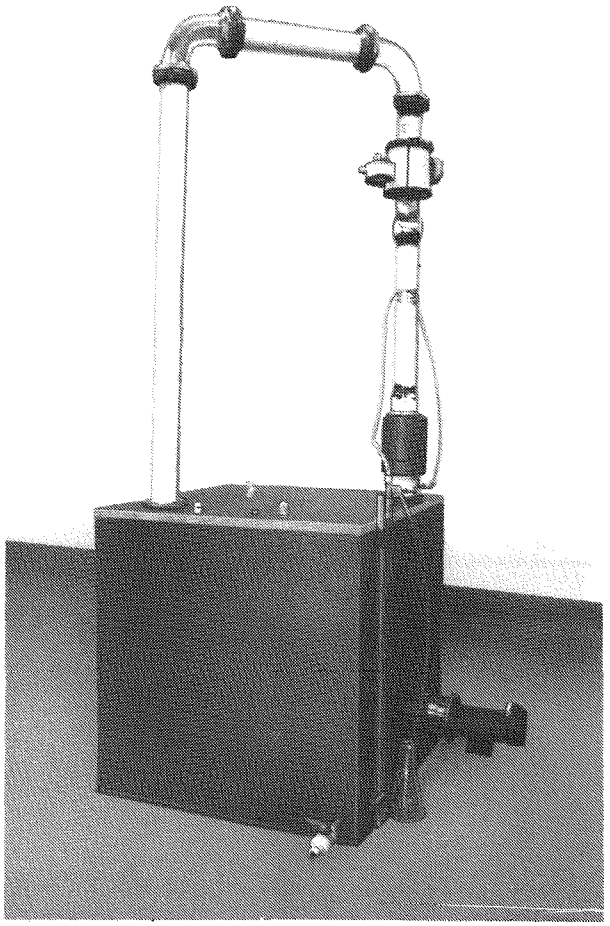

Figure 17-8. General View of Hydraulic Test Stand. Note test pump mounted through the tank wall in lower right-hand corner.

x 37 inches high. The test tank, 27.75 cubic feet in volume, holds approximately 637 liters of liquid at the 30" operating level.

Negative Suction Capability. Figure 17-9 is a schematic of the pump test system. As depicted in the illustration, the gas/hydrate-former pump is used to pump the air from the sealed tank to provide the negative suction conditions for the electrolyte pump testing. Water is drawn from the test tank in addition to the air being evacuated from the atmosphere above the liquid. This water serves to cool, lubricate, and seal the gas/hydrate-former gear pump. The liquid and gas are separated on the pump discharge side with the excess air vented and the water returned to the tank through a valve in the return line. With the addition of

motor control and monitoring equipment (not shown), this system is also used to hydraulically test the gas/hydrate-former pump on water and air.

Instrumentation. Figure 17-9 shows the pressure and flow reading equipment necessary to obtain the data for plotting the pump performance parameters. The pump motor operation is monitored by reading of the motor armature current and terminal voltage with the rpm indicated by a phototachometer. The motor terminal voltage values are obtained by direct readout using a Data Tech Model 3362-02, digital voltmeter with 10 millivolt resolution for the ±60 volt scale. The armature line current is obtained by reading the millivolt drop across a 25 amp/50mV shunt inserted in the line between the motor speed controller and motor. These mV readings

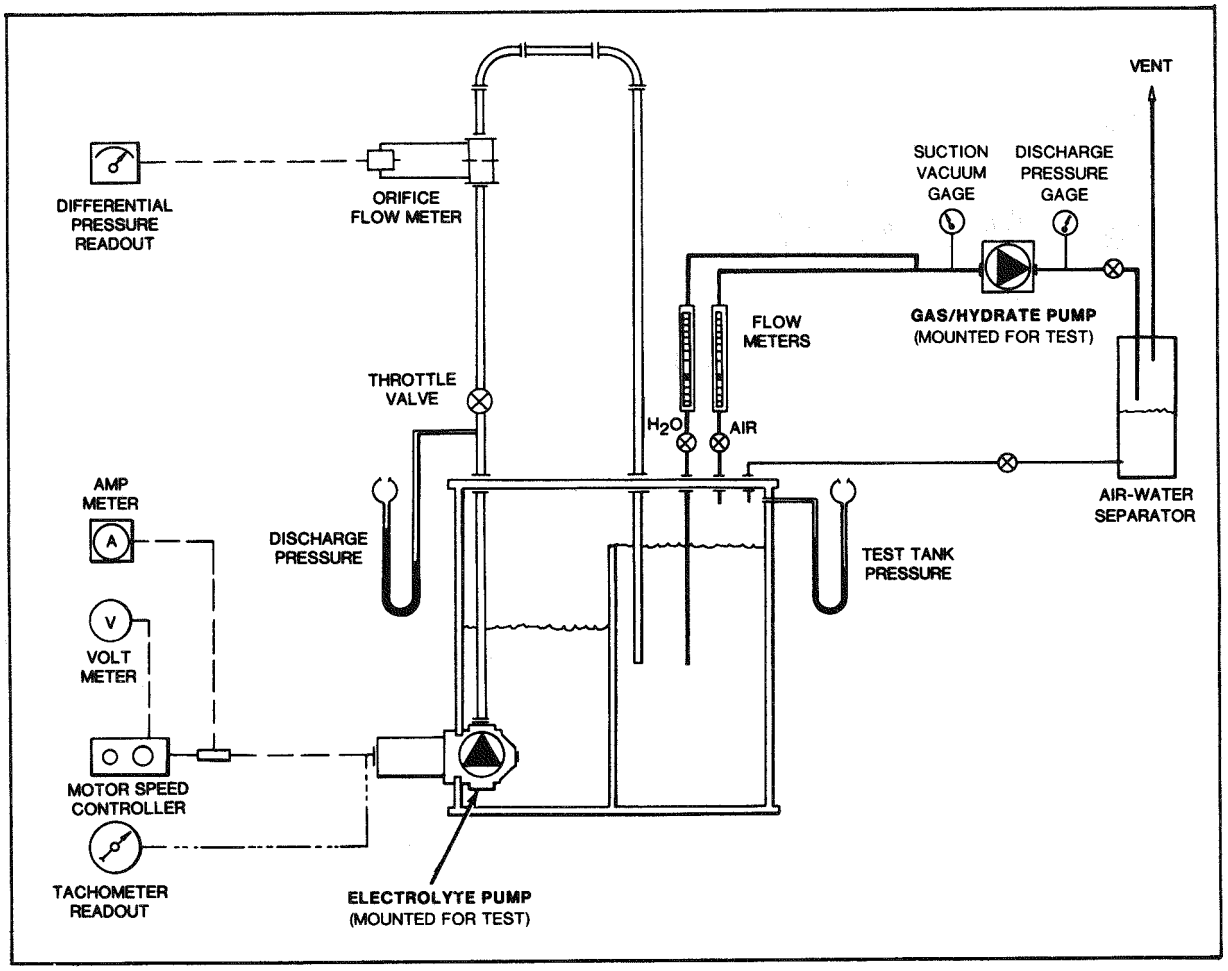

Figure 17-9. Schematic arrangement of hydraulic test stand including control and data gathering instrumentation.

are also taken with a Data Tech 3362 having a resolution of 100 microvolts for the ±600mV full scale reading. Pressure readings for the electrolyte pump discharge and inlet suction (tank pressure) are obtained by readings taken on mercury manometers tapped into the discharge pipe and tank wall.

The electrolyte pump flow data is obtained from a 1.8-inch diameter, sharp-edge orifice inserted in the 3-inch diameter pump discharge line. The titanium orifice is supported by machined Teflon flanges incorporating the differential pressure taps. The differential pressure is read-out on a Validyne Model CD12 variable-reluctance transducer indicator with a 5" taut band meter of ±1% accuracy. A DP15 variable reluctance differential ±5 psia pressure transducer with 0.5% full scale accuracy is installed across the orifice plate and is separated from the test fluid by Zavoda Teflon isolators with titanium diaphragms. A calibration curve for the flow meter system was plotted and used to translate the Validyne voltages to gpm flow rates.

The instrumentation used for testing the gas/hydrate-former pump is also shown in Figure 17-9. The same motor control and monitoring equipment (not shown) as described for the electrolyte pump motor is used for obtaining the motor data. The pressure gauges used are standard-dial type and the flow meters are Brooks tube type, size R-615-B with tantalum floats. The rate of flow values are read from the corresponding Brooks calibration curves for the fluids in use.

Endurance Test Stand

A test stand for endurance testing of the electrolyte pump was fabricated from 1/2-inch thick PVC sheet. The stand is approximately 18 inches in width x 12 inches in depth x 24 inches high. The stand has the electrolyte pump mounted through the wall similar to the test equipment described above. The pump discharge is piped internally within the tank and has a fixed orifice in the line to simulate the pump discharge pressure of 4 psig when operating at the 87-gpm rate. The tank has a single weir dividing the discharge side from the submerged pump suction section to partially reduce the turbulence thus simulating the conditions within the battery sump.

EXPERIMENTAL RESULTS

Electrolyte Pump

Figure 17-10 shows the characteristic curves for the electrolyte pump (serial no. 2) installed in the peak-shaving battery presently undergoing cycle testing. Curves

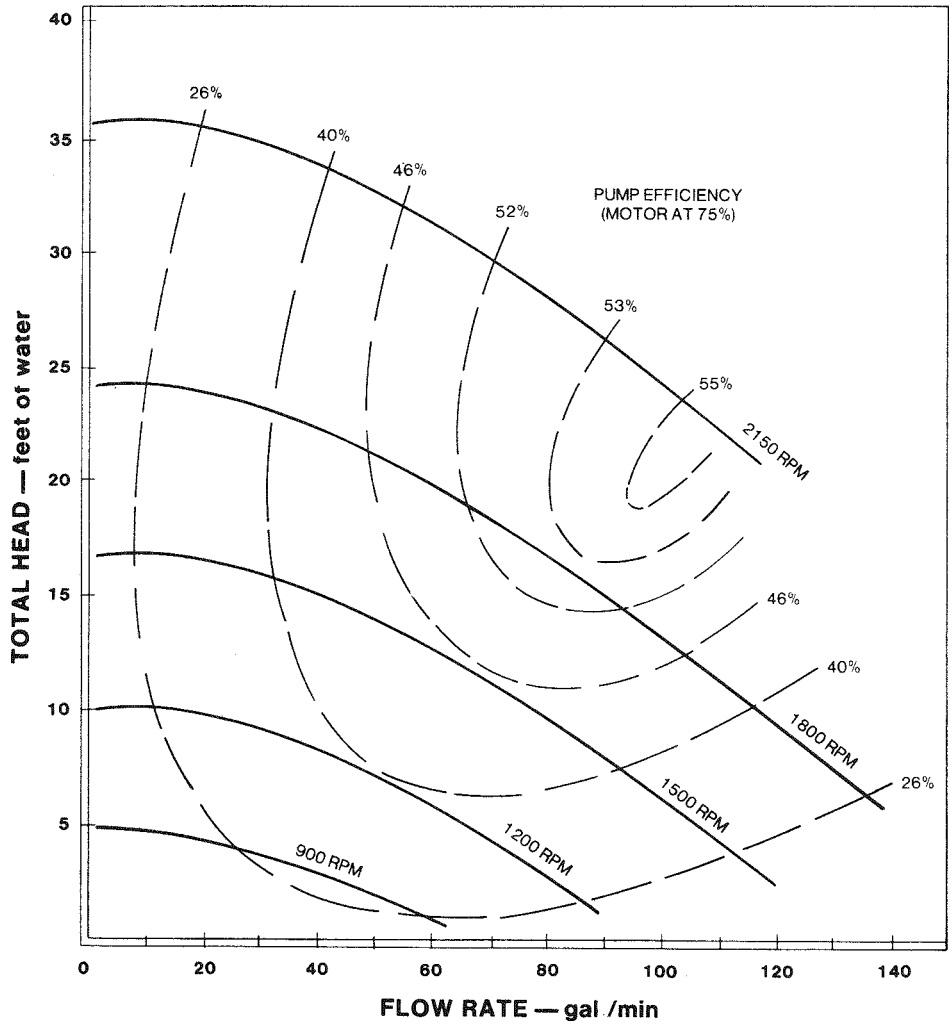

Figure 17-10. Characteristic performance curves for centrifugal-type electrolyte pump, serial number 2.

are plotted for five constant speed values from 900 to 2150 rpm. Table 17-2 is a typical data set for the 1500 rpm run. The data was obtained from water testing the electrolyte pump in the test stand described above. During this testing the pump suction had 2 feet of water coverage with the test tank at atmospheric pressure. The design operating point for the pump is approximately 1500 rpm at 87 gpm and 8 feet of water head corresponding to 4 psig when pumping zinc chloride. The pump characteristic curve for 1500 rpm indicates the actual pump performance was very close to the predicted design performance. Shown in Figure 17-11 are the Bosch dc motor performance curves supplied by the manufacturer. The motor curves indicate approximately 70 to 75% efficiency can be expected from the motor when

Table 17-2

ELECTROLYTE-PUMP DATA FOR WATER
AT A PUMP SPEED OF 1500 RPM

Validyne Reading (volts)	Pump Flow (gpm)	Disch. Manom. (cm Hg)	Disch. Head (ft H_2O)	Disch. Press. (psig)	Pump Hyd. Output (watts)	Motor Input (amps)	Motor Input (volts)	Motor Input (watts)	Overall Eff. (%)
0	0	37.6	16.8	7.3	0	5.7	29.4	166	0
0.2	21	37.2	16.6	7.2	66	7.6	30.0	228	29
0.5	33	32.5	14.5	6.3	90	9.9	30.5	302	30
1.4	56	29.0	12.9	5.6	137	12.1	32.1	387	35
2.2	72	24.4	10.9	4.7	148	12.9	32.1	413	36
3.4	92	17.0	7.6	3.3	132	13.5	32.0	430	31
4.5	105	11.3	5.0	2.2	100	13.8	32.0	442	23

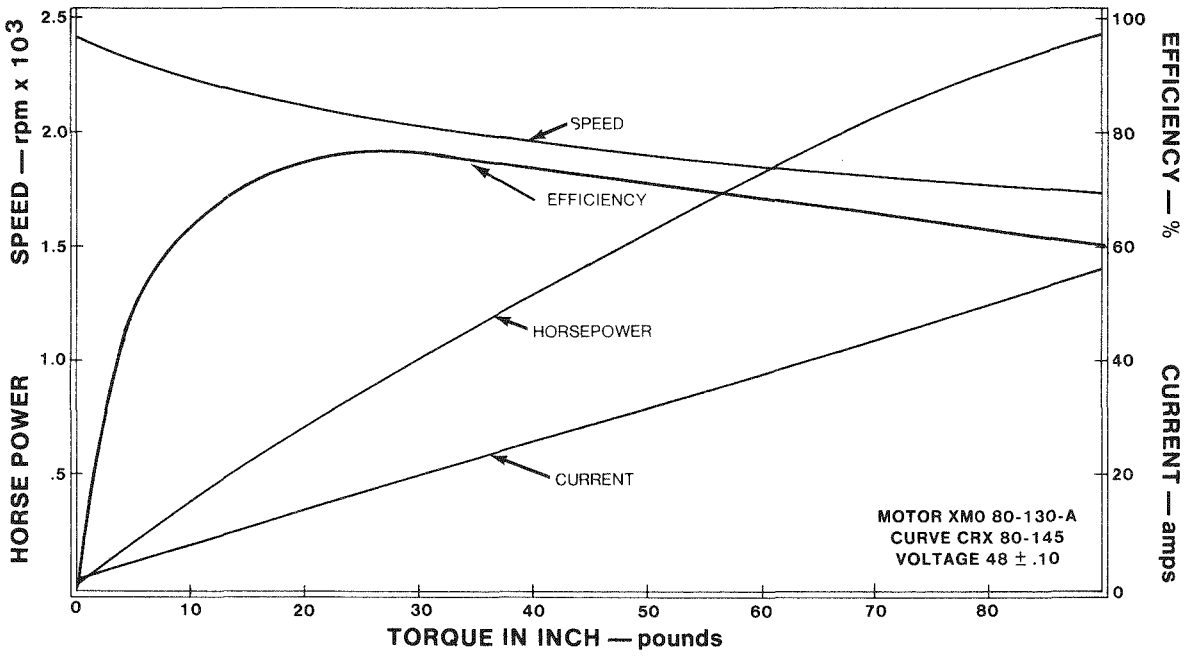

SOURCE: AMBAC INDUSTRIES, EPD DIV. COLUMBUS, MISS.

Figure 17-11. Manufacturers Performance Curves for Bosch XMO 80-130-A Motor

operating at the 1500-rpm pump speed. This estimated 75% motor efficiency value is used to determine the pump only efficiency values plotted in Figure 17-10.

Testing to confirm the electrolyte pump performance with reduced inlet pressure was aborted due to test tank failure when the tank corner failed at the weld. Other testing done at negative pressures (-4 psig) with similar pumps demonstrated this design is capable of delivering rated flow and pressure without cavitation.

A second electrolyte pump (serial no. 3) was water tested with almost identical water performance to that of serial no. 2 plotted above. This second electrolyte pump was recently installed in the endurance test tank and has accumulated approximately 81-hours running time.

Battery cycle testing to date indicates the electrolyte pump is performing satisfactorily. Typical pump data taken during the peak-shaving battery cycle testing is presented in Table 17-3.

Table 17-3
ELECTROLYTE PUMP DATA

Motor/Pump Characteristics	Charge Cycle	Discharge Cycle
Discharge Pressure	+14.6cm Hg	+23cm Hg
Inlet Pressure	-4.1cm Hg	+4.6cm Hg
Motor Voltage	30 volts	30 volts
Motor Current	13.2 amps	12.6 amps
Input Voltage	396 watts	378 watts

Gas/Hydrate-Former Pump

The gas/hydrate-former pump bench test data is tabulated in Table 17-4 and typical performance data obtained from the peak-shaving battery cycle testing is shown in Table 17-5. The gas/hydrate-former pump is also performing satisfactorily in the peak-shaving battery, but at higher speeds and lower gas flows than predicted.

Table 17-4

GAS/HYDRATE-FORMER PUMP BENCH TEST DATA FOR 5-HOUR RUN

Motor/Pump Characteristics	Beginning of Test	End of Test
Pump Speed	1970 rpm	1970 rpm
Outlet Pressure	47cm Hg	60cm Hg
Inlet Pressure	-25cm Hg	-22cm Hg
Outlet Temperature	10°C	11°C
Inlet Temperature	7°C	8°C
Liquid Flow	10 ℓ/min	10 ℓ/min
Cl_2 Gas Flow	28 ℓ/min @ STP	28 ℓ/min @ STP
Motor Volts	39.5 volts	39.3 volts
Motor Current	8.0 amps	8.7 amps
Motor Watts	316 watts	342 watts

Table 17-5

GAS/HYDRATE-FORMER PUMP PEAK-SHAVING BATTERY CYCLE TEST

Motor/Pump Characteristics	Charge Cycle	Discharge Cycle
Outlet Pressure	+46cm Hg	+34cm Hg
Inlet Pressure	-16cm Hg	+1cm Hg
Liquid Flow	11 ℓ/min	----
Cl_2 Gas Flow Rate	33 ℓ/min	----
Motor Voltage	41.4 volts	21.2 volts
Motor Current	11 amps	5 amps
Motor Watts	455 watts	106 watts

DISCUSSION AND FUTURE WORK

Electrolyte Pump Design

The characteristic performance curves for the electrolyte pump plotted in Figure 17-10 indicate a pump-only peak efficiency of ∿55% at 2150 rpm and 105 gpm at 23-feet water head. Under the 87-gpm flow rate used for the 45kWh module, the pump only efficiency was ∿42% at 1500 rpm and 8-feet water head. It is predictable that both these efficiencies will be somewhat lower when pumping gas-saturated zinc chloride. Optimization of this design for life and efficiency at the 87-gpm design point will be pursued during the second phase of this program. By slightly increasing the rotating speed and simultaneously reducing the impeller size, the peak-efficiency point can be shifted to a lower total head for the 87-gpm-only operating point. The smaller size impeller will also reduce the viscous disc-friction losses which are proportional to rotor size. This will slightly increase the magnitude of the peak-efficiency point. The reduction in impeller size will have a secondary effect of reducing the maximum torque required; therefore, the magnetic coupling size can be reduced, lessening the viscous friction losses associated with the inner rotor assembly. However, this increase in rotational speed must be balanced against bearing life and low absolute suction pressure effects where lower rotational speeds are desirable. This size-scaling of similar design pumps is common and the parameter used to estimate performance has been derived by dimensional analysis. The dimensionless group which relates pump speed, flow, and head is called specific speed, denoted N_s, and is expressed as:

$$N_s = \frac{NQ^{0.50}}{H^{0.75}}$$

In American centrifugal pump practice, the units used are rpm for pump speed (N), gpm for capacity (Q), and feet of liquid for the pump head (H). The specific speed of the pump tested at the design point of 87 gpm @ 8ft of H_2O and 1500 rpm is approximately 2900. For specific speeds of over 2000 and flows of approximately 100 gpm, the highest efficiency for a well-designed centrifugal pump has been shown to be slightly over 70% (5-1). To meet the 60% overall target efficiency for the ultimate pump/motor combination, the driver efficiency would have to be approximately 86% for matching with an optimum 70% efficient pump. The dc type motor selected for this test battery system for ease of speed variation and control requires some form of commutation. The brushes or solid-state switching for this introduces electrical losses that diminish overall efficiency. In peak-shaving applications

ac power will be readily available. Fractional-horsepower induction ac motors can be expected to deliver ∿80% efficiency.

Gas/Hydrate-Former Pump Performance

The data listed in Table 17-4 for the gas/hydrate-former pump bench test are typical values taken over a 5-hour running period -- one near the beginning of the test and one near the end. During the test run the pump speed was held constant. As the test progresses, the hydrate formed is stored in a fixed volume container, and thus the resistance of the accumulated stored hydrate increases the pressure at the pump outlet. At the start of the run the measured 28 liters/min of chlorine gas plus a calculated 8 liters/min of dissolved gas as standard conditons are equivalent to 50 liters/min at the pump inlet conditions of 7°C and -25cm Hg. This chlorine-gas mass flow corresponds to 21 liters/min at the outlet port conditions. There is an effective compression ratio of 2.4 for the compressible fluid within the gear pump. For an assumed isothermal compression, the power required equals 54.8 watts. At the same time, 10 liters/min of incompressible zinc chloride solution is pumped from -25cm Hg pressure to 47cm Hg pressure. The power required is 16 watts. By ignoring the energy for mixing the two-phase flow within the pump during hydrate formation, the overall pump efficiency determined is 22.5%. The Bosch speed-controlled driver efficiency is estimated at 75%. The pump only efficiency for the gas/hydrate-former pump is, therefore, approximately 30%.

The apparent fluid volume displaced by the pump per unit time is the sum of the liquid flow and gas flow volumes passing through the inlet port -- 10-ℓ/min and 40-ℓ/min gas. The 60-ℓ/min fluid throughout indicates a 68% volumetric efficiency of the pump since, at 1970 rpm, the calculated pump displacement volume is 88.5 ℓ/min.

The specified 40 ℓ/min of chlorine gas at standard conditions is approximately 55 ℓ/min at the pump inlet conditions. Added to this is the 10-ℓ/min of zinc chloride solution for a total inlet flow of approximately 65 ℓ/min required. Assuming the volumetric efficiency stays at 68% and the pump suction conditions are above cavitation suction pressure, the calculated pump speed for 65 ℓ/min is 2150 rpm -- too high for the long life requirement. A larger pitch diameter spur gear pump would increase the overall pump efficiency. The resulting lower pump speed would extend service life in addition to increasing the volumetric efficiency and providing more cavitation margin.

Additional Zinc Chloride/Chlorine Gas Testing

To optimize the design of both the electrolyte pump and the gas/hydrate-former pump additional testing on the actual working fluids -- saturated zinc chloride solution and chlorine gas -- should continue. All of the measured performance on the electrolyte pump has been obtained using water and air as a test fluid with the results projected to $ZnCl_2/Cl_2$ performance. To optimize the hydraulic performance, measurements will have to be obtained using the actual working media. Refinement of the hydraulic design requires more accurate data to obtain optimum efficiency. It is relatively easy to reach the first 45 to 50% pump efficiency but the remaining 20% is obtained with much greater difficulty. With this size pump, very small machining variations could easily account for several points of efficiency when in the 50 to 60% range. The hydraulic improvements are easily masked by small dimensional inaccuracies in the test model. These last few points in pump efficiency improvement require very exacting procedures -- both in securing accurate test data and representative test models. The same comments are applicable to the gas/hydrate-former pump but at the lower 20 to 25% pump efficiency value.

Continuance of Endurance Testing

Because of the uniqueness of the pumping application, very little published information relating to expected service life of the materials and bearing system used in these pumps is available. In order to project the long range performance of the peak-shaving battery pumping systems, a data base has to be developed. Continued life and endurance cycle tests are needed to accumulate this data. By periodic inspection, performance evaluation, and actual measurement of the wear surfaces for known intervals of running time under simulated conditions, an estimate of mean time before failure can be developed.

Cost and Reliability Improvement

Performance testing and evaluation of the current-design pumps reinforces the merit of the submerged pump/static seal concept. This concept could be developed one step further by also encapsulating and submerging the drive motor within the peak-shaving battery case. Encapsulated motor/pump combinations are commonly referred to as "canned rotor pumps". Figures 17-12 and 17-13 illustrate the canned pump design. The motor armature and bearing assembly are enclosed within a liquid-tight can and the can is sealed to the liquid end of the pump, thereby eliminating the rotating seal.

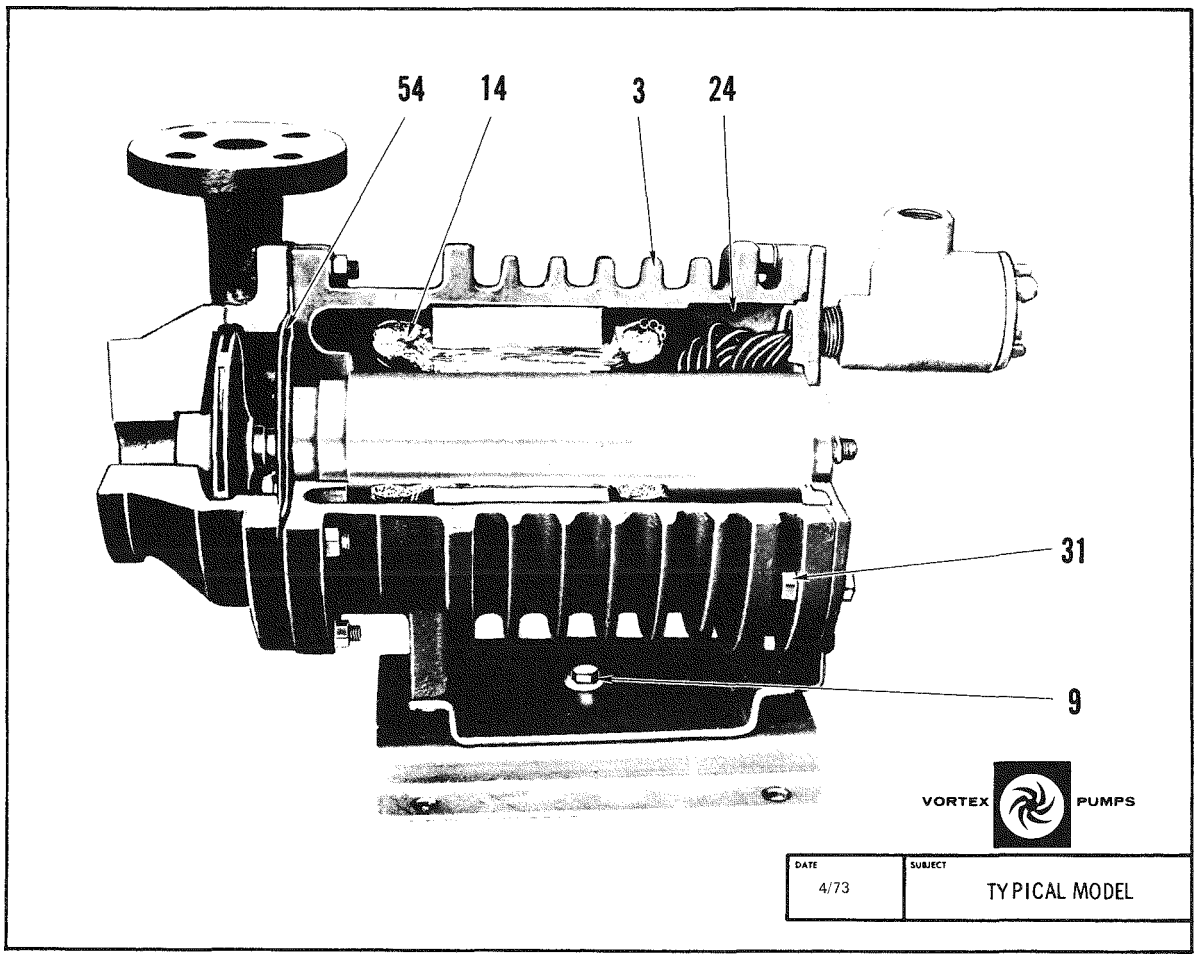

Figure 17-12. Cutaway of a Typical Canned-Rotor Pump and Motor Assembly

The encapsulating can-to-pump liquid-end seal (item 54) is shown in Figure 17-12. The Kynar static seal in the magnetic coupling serves the same purpose. The motor armature of the canned pump and the inner rotor of the magnetic coupling are also similar. Both rotate in the fluid being pumped. The common armature/impeller shaft rotates in a single set of submerged bearings (items 56 and 57) as illustrated in Figure 17-13. The motor stator is wound around the sealing can containing the armature assembly. The stator assembly is removable and is sealed into the pump assembly with a gasketed joint. The pump/motor assembly is essentially a hermetically/sealed unit preventing fluids from leaking out and contaminants from seeping in.

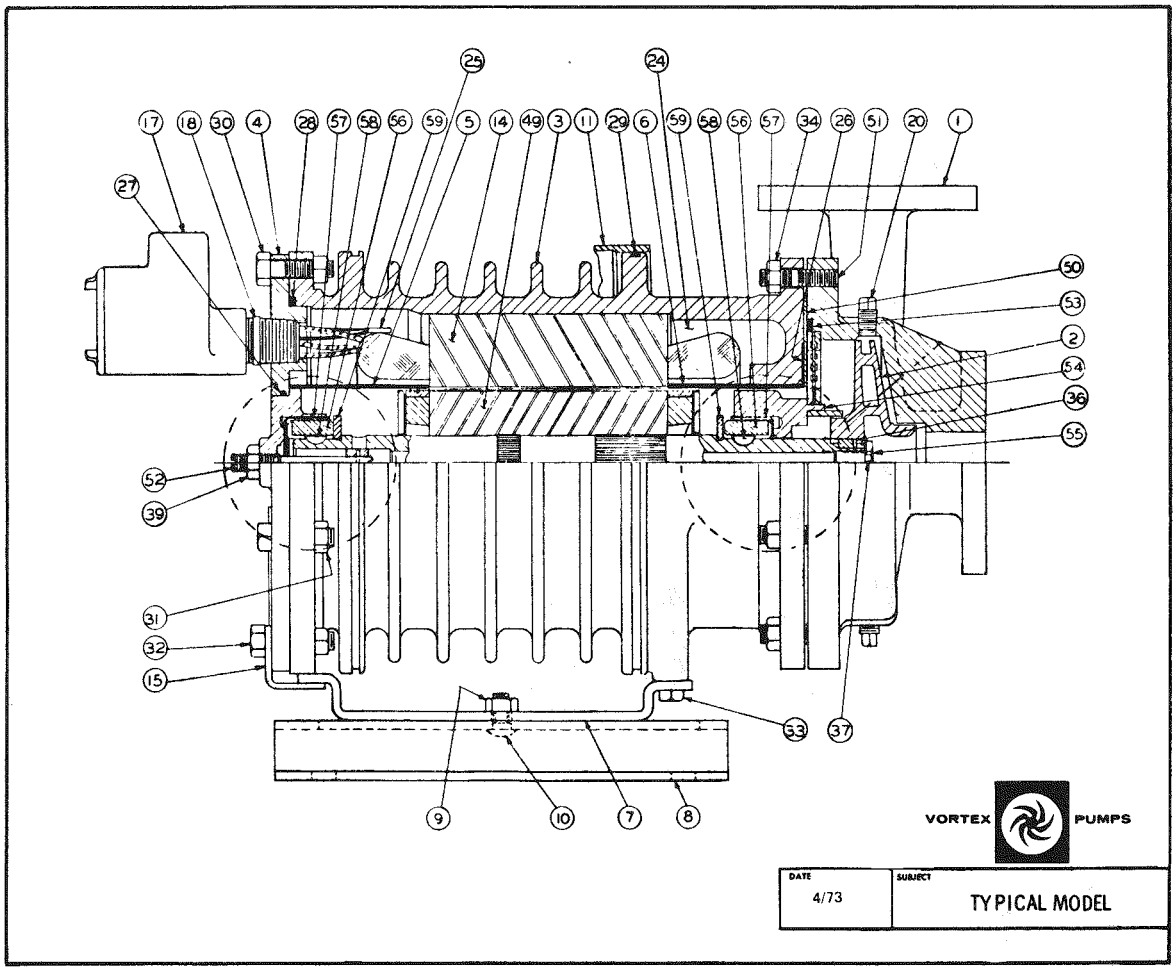

Figure 17-13. General Arrangement Drawing of One Style of Canned-Rotor Pump and Motor Assembly with Bearings Lubricated by Pumped Fluid

This concept is applicable to the zinc-chlorine peak-shaving battery where ac current is available and may be cost-effective by reducing the pump/motor part-count, as well as improving battery module manufacturing assembly and test time. The cost savings accrued with this design must be balanced against the reduced overall pump/motor efficiency that can be expected.

A search of the literature available indicates the efficiency of the "canned pump" will be less than an externally-mounted motor unit. The prime reason is the encapsulating material or "can" inserted in the magnetic gap between the stator and armature fields. Any increase in gap dimensions reduces the rotor efficiency appreciably. A secondary efficiency reduction would be due to eddy current and conductive losses within the material and fluid in the gap.

Since the armature is immersed in the pumped fluid contained in the encapsulating can, the viscous friction is also increased. An external motor armature has a "windage" friction loss that is much less than the submerged motor spinning "hydraulic" loss. The canned-rotor pump would eliminate the magnetic coupling with the motor armature taking the place of the coupling inner-rotor. A slight increase in losses would, therefore, be expected due to the increased surface area of the ac motor armature.

By combining the motor armature and pump impeller on the same shaft, a set of motor bearings is eliminated, and thus, part of the bearing losses. Since it is difficult to compute the exact magnitude of the losses, the amount of overall efficiency reduction expected with a canned-rotor-type design cannot be predicted. A prototype assembly would have to be produced and tested to obtain the required data.

Since the complete pump and motor are to be submerged in the zinc chloride/chlorine gas environment, additional engineering problems of materials and fabrication must be solved, especially those involved with protecting the stator and sealing the electrical leads.

REFERENCE

17-1 Karassik, Drutzsch, Faser, Messina. Pump Handbook, New York: McGraw-Hill, 1976, pp. 2-10, Figure 5.

Section 18

CHLORINE HYDRATE FORMATION AND DECOMPOSITION

INTRODUCTION

The selection of an approach to hydrate storage for the 45kWh system over other conceivable approaches was predicated on prior experience with hydrate formation and storage techniques. The approach selected and described in subsequent sections is believed to be that best suited to the modular 45kWh system size. The reduction to practice of this approach to give a functional design for the battery system has been an evolutionary process. Numerous tests to determine what can and cannot be done, with elucidation of the observed effects by the available data, have resulted in not only a functional design for the 45kWh modular system, but also a broader understanding of how the data can be applied to the design of future systems. The areas in which the evolutionary testing have been most useful and necessary have been those relating to the behavior of chlorine hydrate in solution as a fluidized-particulate matter. The range of concentrations and conditions during normal battery operation are so variable, and the published theory relating to this behavior sufficiently limited, that trial and error testing under simulated battery conditions was considered the most expeditious route to a final design.

The discussions in this section are intended to indicate the basis for the components and operating points selected and do not detail all comparisons between the method used and other conceivable methods. The discussion of testing has also been restricted principally to the significant developments and the test results of the final phases.

HYDRATE FORMATION AND DECOMPOSITION

Chlorine hydrate is a clathrate-type ice-like compound formed with water near its freezing point, by inclusion of the chlorine into cages or holes in the (ice) crystal lattice. The presence of chlorine in the lattice stabilizes the solid crystalline structure at a somewhat higher temperature (9.6^{o}C) than when the chlorine is not present due to the Van der Waals forces in the chlorine-water lattice.

There are, in the "crystalline water" of the chlorine hydrate, six "large" and two "small" cages in each repetitive unit of 48 molecules. The six large cages are readily filled by Cl_2 at ambient pressures, with the result that the chlorine hydrate is usually observed as $Cl_2 \cdot 8H_2O$ ($Cl_2 \cdot 7\text{-}2/3H_2O$ in the perfect continuous crystal). At higher pressures, the two smaller cages are filled as well with the result that the hydrate may be observed as $Cl_2 \cdot 6H_2O$ ($Cl_2 \cdot 5\text{-}2/3H_2O$ in a perfect structure). The formula of the hydrate can, therefore, be variable, depending upon formation conditions, with the consequence that heat of formation and quantity of chlorine stored per unit weight of water may also be slightly variable.

For processes used in the load-leveling battery system, the hydrate has been successfully treated as $Cl_2 \cdot 8H_2O$ and it is assumed that this ratio approximates what is found in existing systems.

Heats of formation for chlorine hydrate were estimated in 1973 by applying the Clausius-Clapeyron equation to vapor pressure data taken for chlorine over water and zinc chloride solutions of various concentrations. At atmospheric pressure in water this heat was estimated to be 18.6kCal/mol; this agrees with most heat of formation data reported in the literature which are no doubt based upon the same method of determination.

Density

The density of chlorine hydrate is reported in most sources as 1.23g/ml and given with the composition $Cl_2 \cdot 8H_2O$. The density has been reported as 1.29g/ml for $Cl_2 \cdot 6H_2O$. Direct measurements and densities derived from measurements of other parameters support these values.

When formed by turbulent contact with excess forming solution, the hydrate behaves as a finely divided particulate solid, but with a tendency to agglomerate or pack when formed in nearly pure water. This tendency is not as evident when formed from zinc chloride solutions, possibly due to the salt in the tightly bound water layer surrounding the individual particles.

Particle Size

In 1974, particle size estimates were made from flow rate-pressure drop data taken for hydrate beds. The hydrate beds were formed by sparging into zinc chloride or water at elevated pressure. The reduced data, given as permeability versus chlorine density is shown in Figure 18-1.

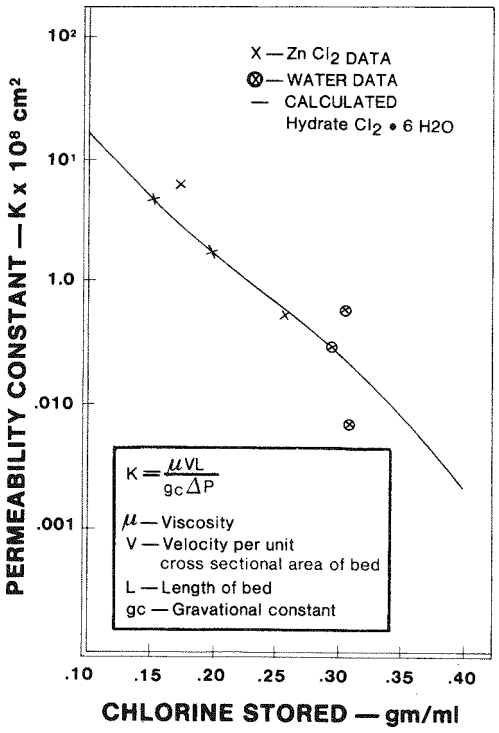

Figure 18-1. Permeability-concentration relationship for beds of particulate chlorine hydrate.

In this method of analysis, the particle information extracted was the product of particle diameter and shape factor, where shape factor is defined as volume of the particle divided by the volume of a sphere having the surface area of the particle. Values of shape factor cannot, therefore, be greater than 1. The particle diameter-shape factor product was 1.6×10^{-3}.

The range of probable shape factors was estimated by comparison with known materials to be between 0.28 (for mica flakes) and 0.65 (crushed glass). The corresponding range of probable particle sizes was 57μm to 25μm.

The particulate hydrate, when separated from the forming liquid by some variant of a simple filtration (without packing) and stored in this condition has been observed to range from 35% to 40% solids by volume indicating that the porosity or void fraction between solid particles ranges from 0.7 to 0.6, respectively. Comparison with reported void fractions for other materials indicates that the packing

density is similar to other particulate materials having a similar particle size. Activated carbon, for example, at 17 microns has been reported to exhibit a void fraction of 0.76 (6-1).

Temperature of Formation

The equilibrium line for the chlorine partial pressure over hydrate in water and over three concentrations of zinc chloride solution is given in Figure 18-2. For

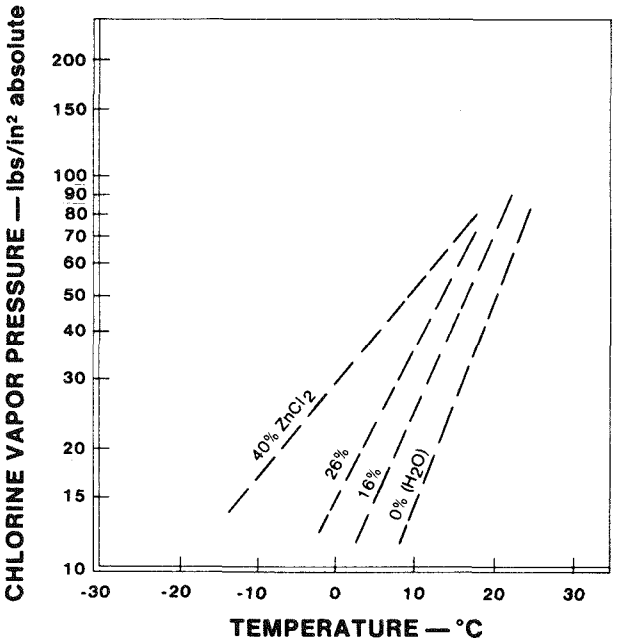

Figure 18-2. Vapor pressure of chlorine over chlorine hydrate.

pressures above the line at a given temperature, the hydrate is stable and tends to form. At pressures below the line the hydrate decomposes. The temperature at which the hydrate is stable for a given pressure is reduced as salt concentration is increased just as the freezing point of water solutions is reduced by increasing the salt concentration.

It is believed chlorine hydrate is formed under all circumstances from chlorine which is in solution. The chlorine from the gas phase first dissolves at the gas liquid interface and then releases the heat of formation to the surrounding "local" water that is then transmitted by conduction from the site of formation to the

surrounding water or to a heat transfer surface in the vicinity. Rates for the crystallization have not been measured but appear to be very high for chlorine in solution. In practice the formation rate is controlled by either the local rates of dissolution or by local heat removal, whichever is limiting.

The chlorine concentration remaining in solution in equilibrium with the hydrate at a given temperature is proportional to the partial pressure of chlorine over the hydrate at that temperature in approximate agreement with Henry's Law. Therefore, the ratio of partial pressure to weight of chlorine in solution at a starting temperature will approximately equal the ratio of partial pressure to chlorine concentration at a final temperature. More generally, the temperature and pressure conditions may be used to estimate the amount of chlorine in solution for application to design. Measured chlorine concentrations over zinc chloride solutions are shown in Figure 18-3a. The approximate chlorine concentrations parametric in pressure for water are shown in Figure 18-3b.

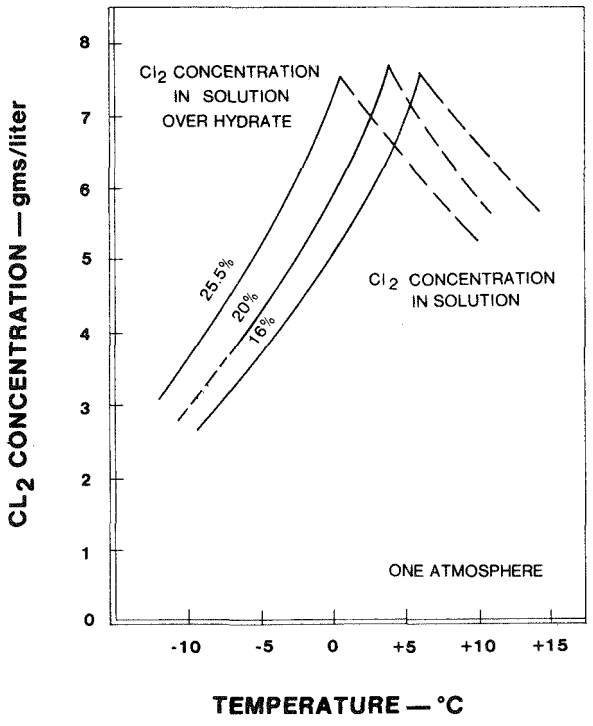

Figure 18-3a. Chlorine concentration in solution as a function of temperature.

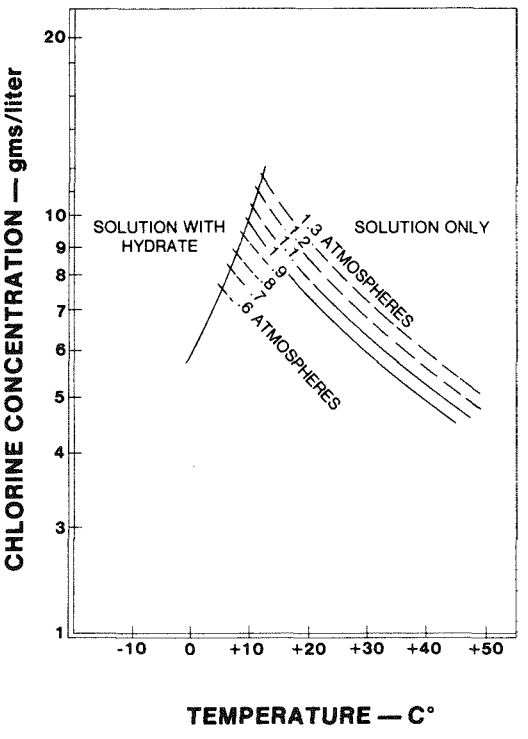

Figure 18-3b. Chlorine concentration in solution as a function of temperature.

Initiation of Crystallization

Some supercooling is required to initiate crystallization even in gently stirred systems, as shown in Figure 18-4. The degree of supercooling required has been

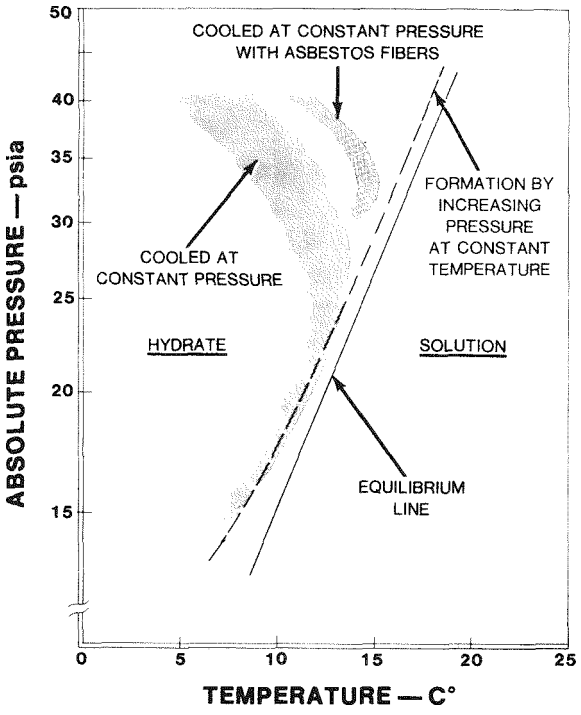

Figure 18-4. Supercooling requirement to initiate formation of chlorine hydrate.

experimentally observed to be dependent upon the path of approach to final conditions. If the solution is cooled at constant pressure, the supercooling is greater than if the solution is pressurized at constant temperature. Introduction of hydrate nuclei induces rapid crystallization and approach to equilibrium. Even foreign materials offering surface discontinuity to serve as nucleation sites (such as asbestos crystals or sharp metal edges) reduce the supercooling requirement.

Formation and Storage Requirements from the Data

The factors which must be considered, or may be used in the design of practical devices, are summarized as follows:

- Solid density of 1.23g/ml and formula $Cl_2 \cdot 8H_2O$
- Fine particle characteristics of hydrate with consequent bed formation characteristics and behavior
- Equilibrium curve
- Supercooling to initiate crystallization if no nucleation sites are available
- Heat removal of 18.6kCal/mole of chlorine
- Equilibrium concentrations of chlorine in solution for a given temperature and partial pressure

General Rules Derived from Experience

In addition to the factors which must be observed as an obvious consequence of the general data, there are several general rules which must be observed in device design.

- Hydrate adherence to surfaces -- When conditions for hydrate formation with adequate chlorine exist at a cooled surface such that the heat of formation is being released to the surface (such as a heat exchanger tube wall) the hydrate will be formed at the surface and will adhere. Even highly turbulent flow past the hydrate layer will not result in hydrate detachment and, because a hydrate nucleation site is present, the layer will usually build rapidly. Removal of hydrate from the inappropriate surface must be accomplished by decomposition.
- Hydrate crystals fluidized in a pipe will tend to impact and accumulate on discontinuities, eventually plugging the area of discontinuity. Even sharp corners or edges can serve as sites for accumulation. The tendency is most pronounced with hydrate in water, but will also sometimes occur when the fluidizing solution is zinc chloride. This tendency for particles to be deposited in flow shear zones is well known and serves as a basis for dust and mist separation in certain kinds of equipment design.
- The gas-liquid interface area generation requirement for high rate hydrate formation is relatively high. This is due to the combined requirement for rapid heat transfer from the local site to the bulk and the tendency for a formed hydrate film to impede diffusion from the gas phase into the bulk. Practical limits appear to be 3×10^4 cm/liter-sec ± 1 order of magnitude for bulk temperatures a few ^{o}C from equilibrium.
- Channeling in the hydrate bed in a hydrate storage device can occur if attention is not given to flow patterns. When the flow is either upward or downward through the bed and no gas is present, the channels become filled with hydrate and the condition is self-correcting. With flow downward and both gas and liquid present, the gas rises and single phase flow downward fills any channels. However, with two-phase flow upward (Reynolds 2000 or less) the gas

tends to collect in the channel to form large bubbles and the area requirement for rapid formation is not met. The rising gas will maintain the channel and the gas can pass through the bed without forming hydrate. This problem can be solved by satisfying the area requirement to form the hydrate at the entry zone to the bed.

- In decomposition, where heat is supplied from a surface, the gas will rise through the bed by means of the channeling mechanism even though the bulk temperature is below the equilibrium condition. This tendency can be utilized for rapid chlorine generation for charge-discharge turnaround by applying heat to the desired decomposition parts, but must also be considered in the location of warm surfaces within the hydrate storage space since decomposition can proceed even during the formation phase, with a consequent reduction in the net formation rate.

OPERATION CONSTRAINTS AND DESIGN POINTS

A schematic of the hydrate formation system within the overall battery system is shown in Figure 18-5. This system involved the mixing in a gear pump of chlorine

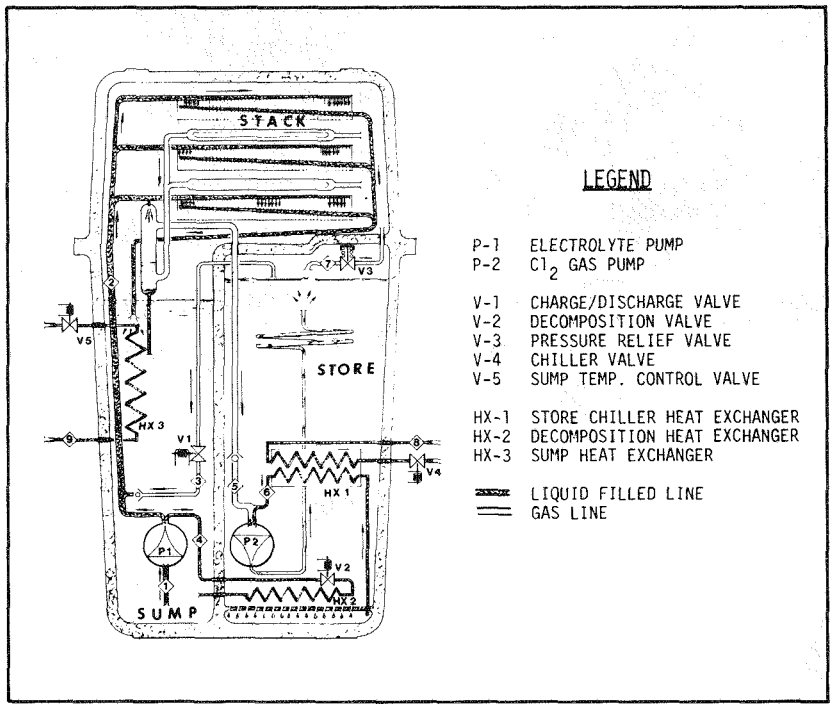

Figure 18-5. Positional and operational schematic of 45kWh zinc chlorine battery module.

gas from the battery gas space (line 5) with continuously recirculated chilled liquid from the store; the recirculating liquid having passed through the filter,

through the heat exchanger (HX1), and into the inlet of the pump (line 6). Gas and liquid mixed in the pump were expelled from the pump outlet at a pressure of 5 to 10 psi above store pressure. The mixture then passed through a coiled titanium tube of sufficient length to allow a residence time of 1 to 2 seconds at substantially above hydrate equilibrium pressure to maximize hydrate formation.

In addition, the maximum temperature required for decomposition supplying chlorine to pump P1 through line 4 at 4 psig was 12.5°C (see Figure 18-2), thereby requiring a minimum of cooling prior to the start of the next charge cycle. Due to the substantial mass of liquid in the store (293kg) with a specific heat of 0.96Cal/gm-°C, each degree of cooling requires 281kCal heat removal. Removal of this heat to the coolant during each cycle represents an additional parasitic power which can be minimized by utilizing an operating temperature on charge that more closely approaches the decomposition temperature on discharge.

The minimum temperatures for operation of the heat exchanger were determined by the equilibrium temperatures for hydrate stability at a given pressure, taking into account the supercooling required for initiation of hydrate formation in the absence of nucleation sites. The limiting condition was that which existed at the tube wall. The temperatures prevailing in the counter current flow heat exchanger are represented in Figure 18-6. For estimates of temperatures at the wall, the assumptions were made that the temperature drop in the wall is very

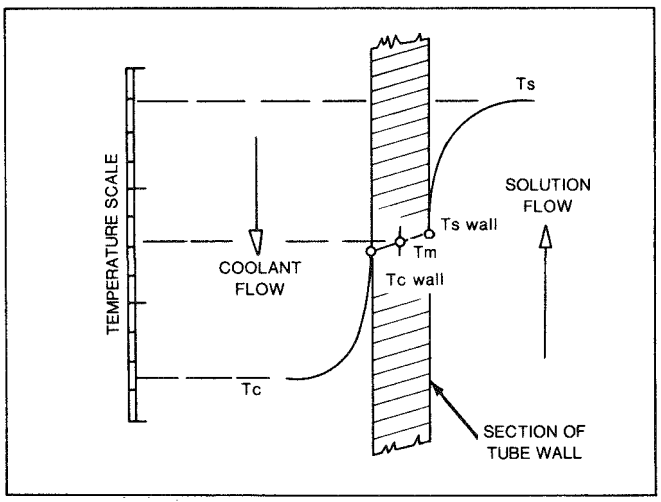

Figure 18-6. Temperature profile at heat exchanger tube wall.

small compared to those in the boundary layer at the wall, that the temperature drops in the two boundary layers are approximately equal, and that the pressure drop through the heat exchanger is small. From these assumptions the limiting conditions exist at the coolant inlet end of the heat exchanger.

At a pressure of -5 psig the equilibrium temperature for chlorine hydrate is 6.5°C. This represents a "safe" median temperature for coolant and solution since an additional 2 to 3° subcooling is required to start hydrate formation.

The flow of gas to the pump, and as a result of battery charge, was to be 28.5 standard liters per minute of Cl_2 at a pressure of -5 psig to give a chlorine volumetric flow rate of 43.2 liters per minute. The total pumping requirement was the sum of this electrochemically-generated chlorine, whatever chlorine was bypassed from the store through valve V3 (Figure 6-5), and chlorine which was removed from solution due to the difference in chlorine solubility at the conditions at the bottom of the store and those found in the liquid at the inlet of the pump.

Total Heat Load

Rates of heat removal from the hydrate storage system during charge were determined by total from 6 sources:

- Heat of formation of hydrate amounting to 18.6kCal/mol and a function of charge rate.
- Heat input from the gas pump P-2 estimated to be 80% to 85% of the total power input to the pump due to the fact that the pump head was totally immersed and some of the motor heat would be transmitted through the mounting to the head.
- Heat transmitted from the battery sump walls to the hydrate storage as a result of temperature difference between battery sump and hydrate liquid. This value was experimentally determined.
- Heat transmitted through the separator plate between battery and store at the top of the store.
- Heat transmitted through the walls of the store from the environment.
- Heat carried over from stack to store as heat of vaporization of water vapor.

The estimated contributions of each of these factors to the total heat load is given in Table 18-1 for the collection of assumptions leading to the maximum and minimum heat load for each item.

Table 18-1

HYDRATE STORAGE SYSTEM HEAT LOAD

7 Hr Charge - 38.4kg Cl_2 Stored

	Assumptions Leading to Maximum Heat Load watts	Assumptions Leading to Minimum Heat Load watts
Hydrate Formation	1675	1675
Pump Heat	380	340
Transmitted from Sump	180 ($40^{o}C$)*	114 ($30^{o}C$)*
Transmitted to Gas Space from Battery Store Separator	50 ($40^{o}C$)*	33 ($30^{o}C$)*
Transmitted from Environment	40	26
Carried over as Heat of Vaporization with Water Vapor from Battery	101 ($40^{o}C$)	49 ($30^{o}C$)
Totals	2426 (34.8KCal/min)	2237 (32.1KCal/min)

*Battery Temperature

DESIGN BASIS FOR WATER STORE SYSTEM

Storage Requirements

The design basis weights and volumes for the 45kWh hydrate storage system are given in Table 18-2. The chlorine storage requirement for the battery system was 38.4 kilograms. Due to the fact that this system was a completely different shape, with many component locations not previously tested, a conservative approach was used. A 5% excess was provided to insure adequate chlorine in the system near the end of discharge. Because a rectangular store cross-section was specified and the filtration means was to be within the storage space rather than along the walls and covering the corners, sizing was based upon a conservative 32% solids by volume (void fraction of 0.68). It was to be expected that corners, spaces around the pump, or behind pipes would be only partially filled with the hydrate.

A 5% zinc chloride solution was preliminary choice as the forming liquid to reduce the tendency toward agglomeration at various points in the system.

Table 18-2

SPECIFICATION OF WEIGHTS AND VOLUMES FOR 45kWh-MODULE HYDRATE-STORAGE SUBSYSTEM

Cl_2 Stored*	40.3 kg
8 H_2O	81.8 kg
Cl_2 Hydrate	122.1 kg
Cl_2 Hydrate Volume (Sp.Gr.=1.23)	99.3 liters
Excess Liquid (32% Solids by Vol)	210.4 kg
Fluid (without Cl_2)	
Volume	280.4 liters
Weight**	292.7 kg
Fluid (with Cl_2)	
Volume	298.3 liters
Weight	333.0 kg
10% Gas Space	28.0 liters
TOTAL VOLUME	308.4 liters

* 5% Excess Cl_2

** 5% $ZnCl_2$

A gas space of 10% above the theoretical fill line was provided to allow room for rapid gas movement without liquid entrainment when switching from charge to discharge. Because the battery operates at below atmospheric pressures during charge with the store at positive pressure, and is immediately brought to ambient pressure for discharge by opening valve V1, the gas velocity during the transient associated with the valve opening is sufficiently high for liquid entrainment. In addition, piling or peaking of the hydrate mass toward the vent valve during the latter parts of charge had been observed in the test system.

Operating Constraints

The desired performance for the system was:

Hydrate Formation Rate: 91.4 gm/min
28.5 std. liters Cl_2/min

Maximum Allowable Store Pressure: 10 psig

Desired Normal Operating Pressure: 5 psig

Desired Vacuum Maintained in Stack: -5 psig

The flow rate and the temperature of solution passing through line 6 were established by three considerations:

- The total heat load for the store which was:
  equal to $\dot{W}C_p\Delta T$ of the liquid
  where $\dot{W}$ = weight rate of flow
  C_p = heat capacity of liquid
  ΔT = temperature drop between bulk temperature and inlet temperature to pump P2

- The quantity of gas released from solution under the reduced pressure at the inlet of pump P2. Since this was an additional gas pumping requirement for the pump, the liquid flow rate should be minimized.

- The minimum temperature which could be allowed in the heat exchanger (HX1) without forming hydrate on the tube walls with consequent reduction in heat transfer coefficient and eventual plugging.

The optimum condition for operation of this portion of the system was considered to be that which resulted in minimum gas evolution since pump capacity was limiting. This optimization is given in Figure 18-7, showing that for most anticipated conditions the optimum was near 10 liters/minute.

TESTING

Background

The general store concept (basic flow schematic) was established prior to the beginning of the test phase. The elements of this concept were:

Charge:

- Hydrate formation by mixing Cl_2 gas with aqueous-forming liquid in a gear pump; gas was to be drawn from the stack under vacuum approaching -5 psig, the liquid from the store, and the hydrate-liquid mixture with any unreacted gas into the store.

- The forming liquid in the store was not to be mixed with stack electrolyte, so that water or dilute salt solutions could be used, thereby allowing the formation to proceed at the highest possible temperature.

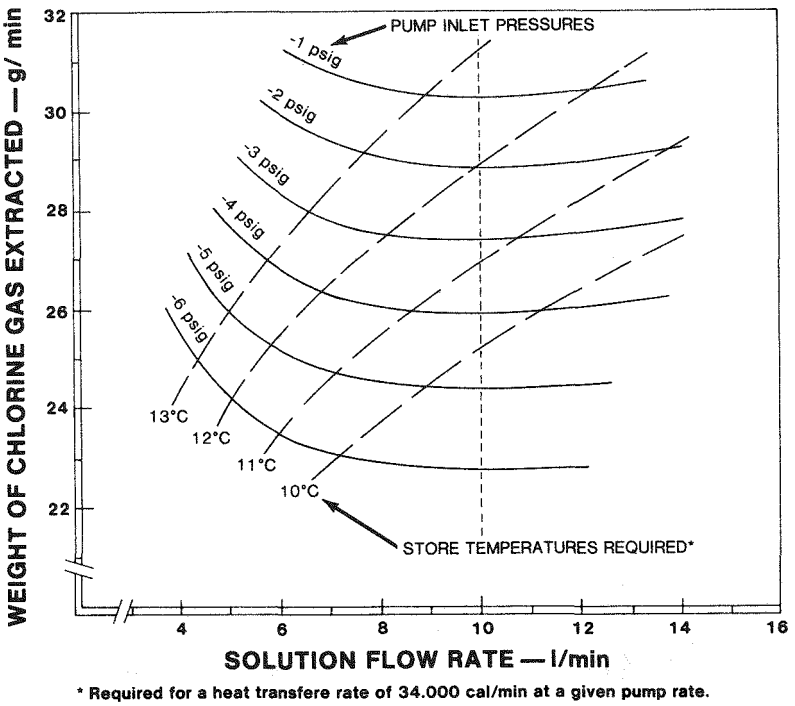

Figure 18-7. Chlorine extracted from recirculating forming solution at various operating conditions showing minimum at 10 liters/minute.

- Removal of heat of formation was to be by subcooling the water from the store at near the gear pump inlet vacuum to provide pressures low enough to prevent hydrate formation in the heat exchanger under all expected modes of operation.

- Separation of forming liquid from the hydrate after expulsion into the store areas to be downward through the hydrate bed, through a filter, with driving force provided by pressure difference between store and pump suction pressure.

- Unreacted gas was to pass to a gas space at the top of the store, be relieved back to the battery gas space for recycle to the pump suction with chlorine being produced by the battery.

- The 6.2% volume expansion occurring in the storage space as a result of addition of 39kg of chlorine as hydrate was to be compensated by allowing room in the gas space at the top of the store.

Discharge:

- Decomposition was to be by circulating battery electrolyte through separate heating coils located within the store.

Other parameters of the design such as line sizes, area and exact location of filters, flow rates, operating temperatures, and features of design necessary to assume uniform and reliable operating during charge and discharge were established by test. The testing was divided into five periods having somewhat different objectives as described in pages 18-17 through 18-19. The schematic depicting arrangement of components with location of temperature, flow and pressure measurement points in the test setup used in the final periods (4 and 5) of testing in the test setup is shown in Figure 18-8. Variations of this arrangement were used in the earlier periods. The temperatures and pressures as a function of time during the final simulated charge cycle in the test series are shown in Figure 18-11.

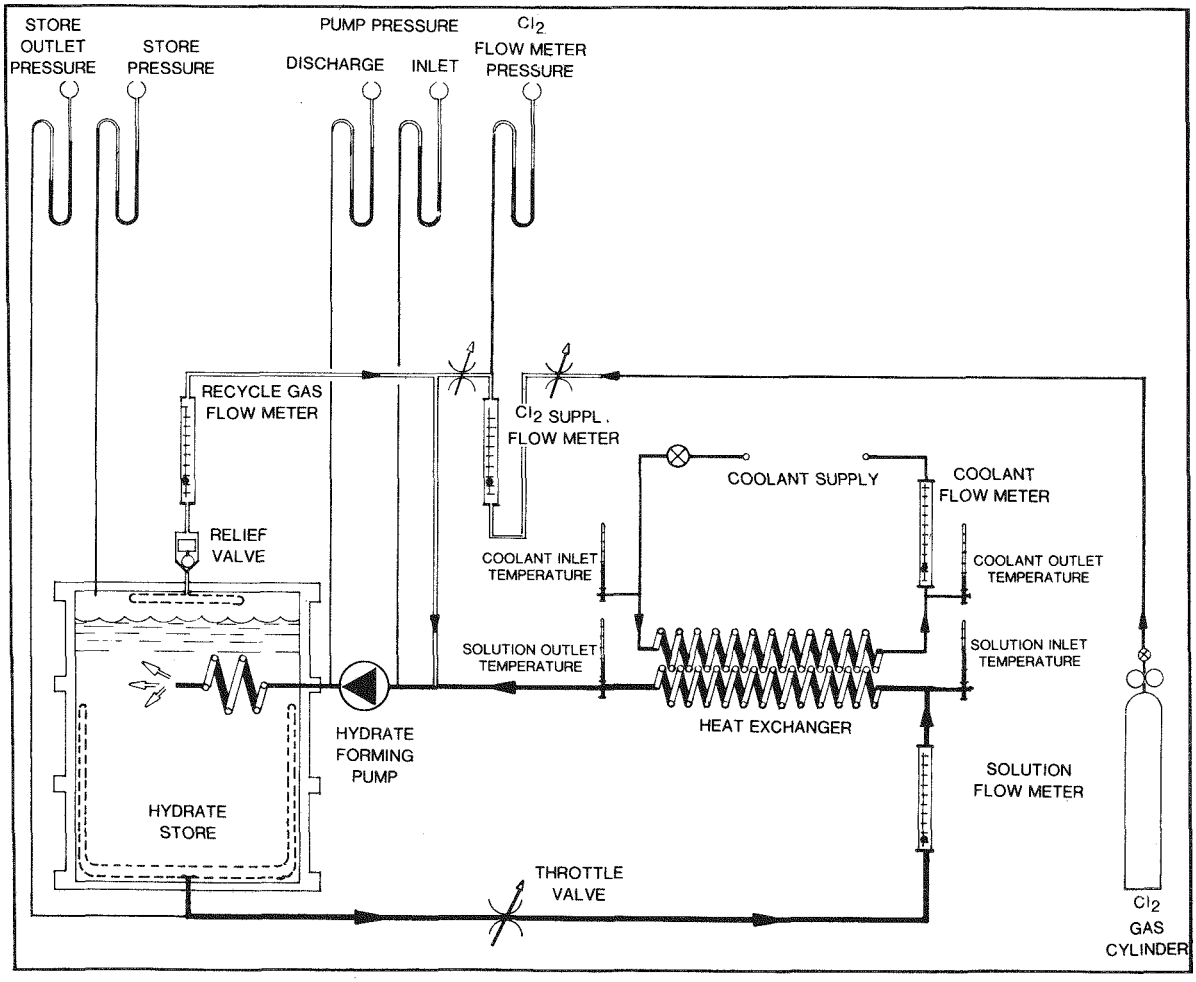

Figure 18-8. Hydrate Store Test System Schematic

Testing leading to the specification of operating procedures and of components other than the pump and heat exchanger was carried out with a cylindrical store container which was 5/7 of the volume of the final 45kWh system. The "charge cycle" for this store at full rates was therefore 5 hours rather than 7 hours. The dimensions and cross-section are shown in Figure 18-9. The similar unit was used because it was immediately available, and was close enough to the final design size to accurately establish the chlorine hydrate bed behavior and chlorine storage density. Limits of absorption rate and factors which would impact the components, the pump and the heat exchanger, were fixed prior to testing.

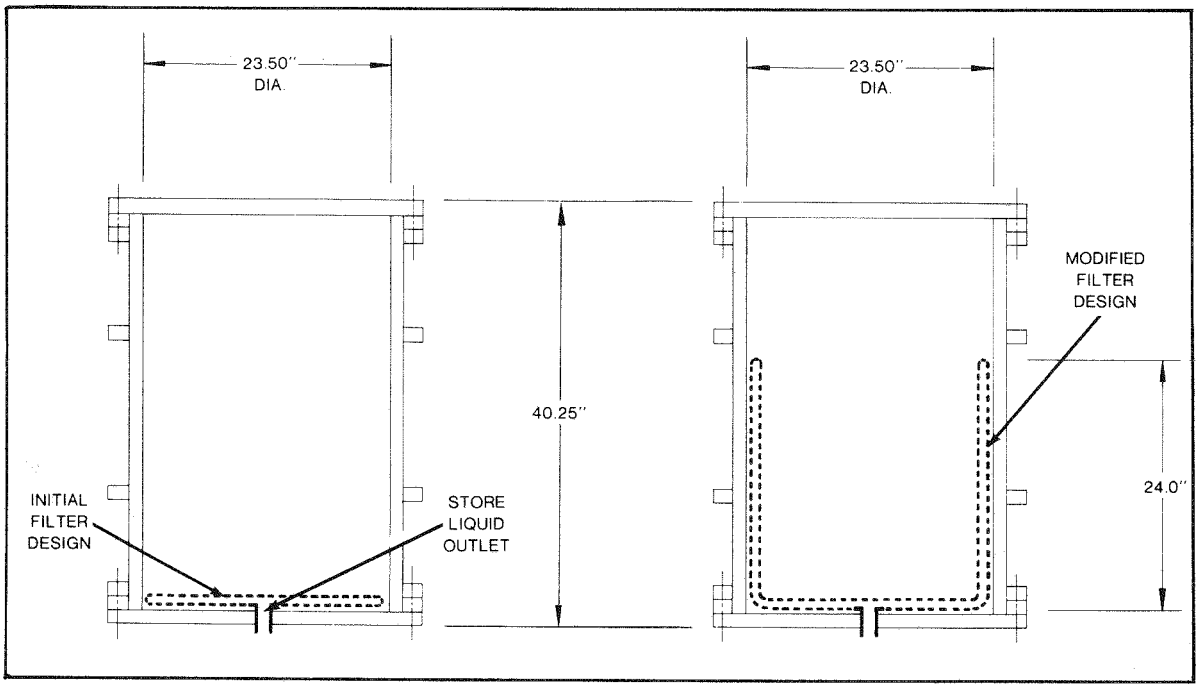

Figure 18-9. Test Hydrate Store with Modified Filter Location

The pump was a G-10 Titanium gear pump upon which substantial experience in design and operation had been obtained in other laboratory uses. The heat exchanger was a shell-and-tube type having 5.37 ft^2 of heat transfer surface designed earlier to offer sufficient flexibility for multiple battery uses. It is described in Part V.

Testing of the store system was conducted in five periods, with somewhat different objectives, as follows:

Period #1 - Exploratory Testing. Ten short tests were conducted to identify possible problems, the temperature limits for continuous high rate operation, and the general behavioral dependence of the particulate hydrate in this type of system upon changes in inlet conditions to the pump and changes in the zinc chloride concentration in the electrolyte.

The pump for these tests was a titanium G-10 having a direct drive (shaft seal) from a 3/4-hp Dayton Model 2Z846 variable speed, reversible motor. The heat exchanger was as subsequently used in the 45kWh battery system with one modification. The 3/8" pipe thread inlet and outlet connections were subsequently enlarged to 3/4" pipe for reasons discussed below.

Problems identified as a result of this testing were:

- Plugging of the outlet tube from the pump into the store by the particulate hydrate formed by compression in the pump. It was established that this plugging was physical in origin due to discontinuities in the line and could not be alleviated by changing the temperature or liquid flow rate. Adding some zinc chloride to the water initially used in forming reduced the problem but increases above 3% did not have a significant effect in these tests. The problem was eventually solved in the short runs by removing an offending connector between the pump and tubing inlet.
- Pressure drops on the low pressure side of the pump were slightly higher than calculated from two-phase flow analogies.
- Definite out-gassing of the forming solution on the low pressure side of the pump as might have been predicted by careful application of the available pressure-chlorine solubility data.
- Pump capacity limits resulting from the above.

It was further established that the solution flowing through the heat exchanger could be subcooled by 2° to 3°C below the equilibrium without forming hydrate on the tube walls of the exchanger.

Period #2 - Verification of Expected Cl_2 Storage Density. Four runs were completed following a) reworking of the pump outlet to remove discontinuities and a 90° bend between the pump outlet block and the tubing entering the store, and b) reworking of the lines on the low pressure side of the pump. The final run of the series, for 8 hours at a Cl_2 inlet rate of 17.6 liters/min, gave a storage density of 0.15gms chlorine/cc of volume.

Pump capacity remained a problem due to excessive out-gassing of the solution on the low pressure side of the pump. This problem was substantially reduced by replacing the 3/8" pipefitting with a 3/4" pipefitting at the heat exchanger inlet and outlet.

The problem was solved temporarily by switching the pump off momentarily on the incidence of current above 20 amps. It was determined by disassembly and inspection of the pump that the plugging was originating on the outlet port block. This problem was solved by reworking the block to provide a smoother flow transition

Period #3 - Verification of Rate. Two runs were completed at the design gas inlet rate of 28.5 STP liters/minute. A problem was identified at these rates with high pressure drop through the hydrate bed at the filter. The solution to this problem was to increase the filter area such that the side walls of the store were covered with filter in the bottom 2/3 of the store. This modification is shown in Figure 18-9.

Period #4 - Verification Testing at Desired Storage Density and Chlorine Rate. Seventeen runs were completed in which the chlorine storage rate was verified and storage density was verified for the 45kWh system. A single run was substantially shorter than expected due to failure of supporting equipment (Cl_2 supply). During this period the size for the gas space in the top of the store, necessary due to volume expansion during charge as chlorine mass was added to the store, was established. The sensitivity of the system performance to changes in the liquid flow rate and minimum heat exchanger operating temperature (coolant temperature) was established. In addition, minor problems were identified and modifications made.

Period #5 - Verification with Magnetically Coupled Pump. The final phase of testing began when the magnetically coupled G-10 titanium pump to be used on the 45kWh system became available. This was to be verification tested but a final problem emerged, in that plugging of the outlet recurred. This was marked by an increase in the pump motor current to above 20 amps (normal current 9 amps) as the pump was loaded by the high outlet pressure.

The problem was solved temporarily by switching the pump off momentarily on the incidence of current above 20 amps. It was determined by disassembly and inspection of the pump that the plugging was originating on the outlet port block. This problem was solved by reworking the block to provide a smoother flow transition between the pump housing cavity and the outlet tube inlet.

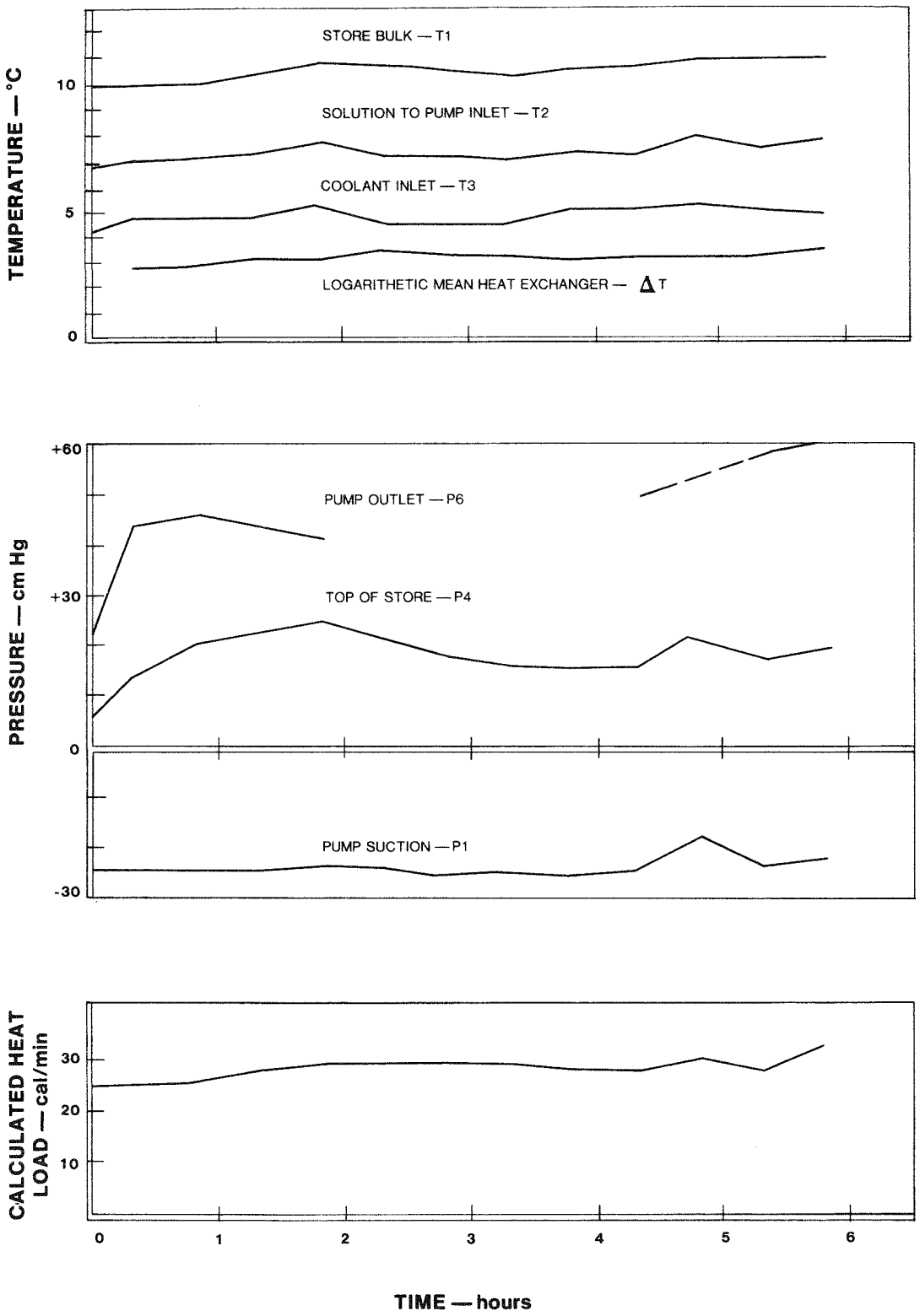

Figure 18-10. Test Hydrate Store Operating Characteristics

FINAL TEST RESULTS

The variation of the principal variables for the final run in the test series with the test hydrate store is shown as a function of time in Figure 18-11. Several characteristics are evident, representative of the general behavior of the store during normal operation in all runs. The temperature of store bulk was 10°C at beginning of run and had increased to 11° by the end of the run. This range is considered within the norm for the store operation.

The "damped" response of store bulk temperature, indicated by T1, to excursions of ±0.4°C in coolant temperature, T3, was indicative of the thermal inertia of the system. The temperature of solution exiting the heat exchanger and going into the pump follows the coolant temperature more closely.

The behavior of the pressure readings at the top of the store (P4) is of interest in that the observed pressure in the gas space is 3 to 4 psig (16 to 20 cm of mercury) higher than the equilibrium pressure for the observed bulk temperature. This is believed to occur because heat transmitted from the surroundings through the side walls from the valves and pump decomposes a small amount of hydrate, releasing Cl_2 which passes up the walls into the gas space. A small amount of gas may also be passing through the bed, unreacted during the initial two hours of operation. This gas does not react at the surface because the uppermost layer of liquid (a film) is relatively warm, and the small amount of heat entering from the environment and transported to the surface by convection tends to keep the uppermost layer warm. The slight drop in store pressure after approximately two hours was due in part to the reduction in solution temperature following a slight downward excursion in coolant temperature. Due to thermal inertia, the store bulk follows more slowly. However, the tendency for the store gas-space pressure to remain low until the final 1-1/2 hours of operation is typical, possibly because the abundance of hydrate in the store serves to aid nucleation and close approach to equilibrium at all points. The pump outlet pressure typically followed store pressure until the final hour of run when the store is well filled with hydrate and the work required to move the relatively "stiff" crystal mass by expulsion of liquid from the outlet is significant.

REFERENCE

18-1 R.H. Perry. Chemical Engineers Handbook. 4th ed. New York: McGraw-Hill, 1963, pp. 5-52.

Section 19

MODULE ASSEMBLY

INTRODUCTION

The manufacture and assembly of the battery module was planned and executed as a one-of-a-kind operation. With the exception of the submodule, the major components such as the case, pumps, heat exchangers, filter, electrolyte manifold, and channel plate were designed and processed on the basis of manufacturing a single unit with minimal tooling and no restrictions in regard to interchangeability of components. For example, the pump flange and the sump were trimmed to suit the as-built condition of the lower case. No attempt was made to design or process the above components with the required tolerance that would allow the components to be assembled without trimming. The cost of tooling to meet the required tolerances would be prohibitive for manufacturing one module.

MODULE PROCESS AND ASSEMBLY

The basic materials in the battery module are graphite, titanium, Kynar, and fiberglas/polyester. These materials are processed by machining, vacuum forming, injection molding, welding, and hand assembly. Table 19-1 shows the primary materials and manufacturing process for the major components.

The module illustration, Figure 19-1, identifies and shows the location of the major components within the module structure. The actual process sequence used for the module assembly was as follows:

- The lower case is received from quality control, with size variance specifications indicated, and pressure-tested.
- The location of the pumps is specified in relation to size variance in the case and the pump-mounting hole patterns and surfaces are prepared.

Table 19-1

PRIMARY MATERIALS AND MANUFACTURING PROCESS FOR MAJOR COMPONENTS

COMPONENT	PRIMARY MATERIALS	PRIMARY MANUFACTURING PROCESS
Case	Kynar Shelf Polyester/Fiberglass	Vacuum-Formed Kynar Liner with Hand Lay Up RFP
Electrolyte Pump	Titanium Bar	Machining Operator
Gas Pump	Titanium Bar	Machining Operator
Filter	Expanded Titanium Sheet & Teflon Cloth	Welded Titanium Frame with Sewed Teflon Cloth Filter Media
Electrolyte Heat Exchanger	Titanium Tube & Plate	Machining & Welding
Decomposition Heat Exchanger	Titanium Tube	Forming
Electrolyte Pump Outlet Manifold	Titanium Plate & Tube	Machining & Welding
Main Manifold	Kynar	Machining & Welding
Intercell Connector	Titanium	Sheet Metal Forming, Machining, & Welding
Channel Plate	Kynar	Machining
Submodule	Graphite, Kynar, Titanium	Machining, Vacuum-Forming, Injection-Molding, Welding, Bonding

- Gas pump is tested for performance specifications.
- Gas pump is mounted on the lower-case hydrate-store wall.
- Sump assembly with HX1 (the main electrolyte heat exchanger) is mounted to the lower case.
- 85-gpm main electrolyte pump is tested for performance specifications.
- The 85-gpm pump is mounted to the lower-case sump wall. The lower main manifold expansion joint and manifold transition are fastened to the pump outlet flange.
- The hydrate filter is located in the bottom of the hydrate store (lower case), HX3 (the chiller heat exchanger), and HX2 (the

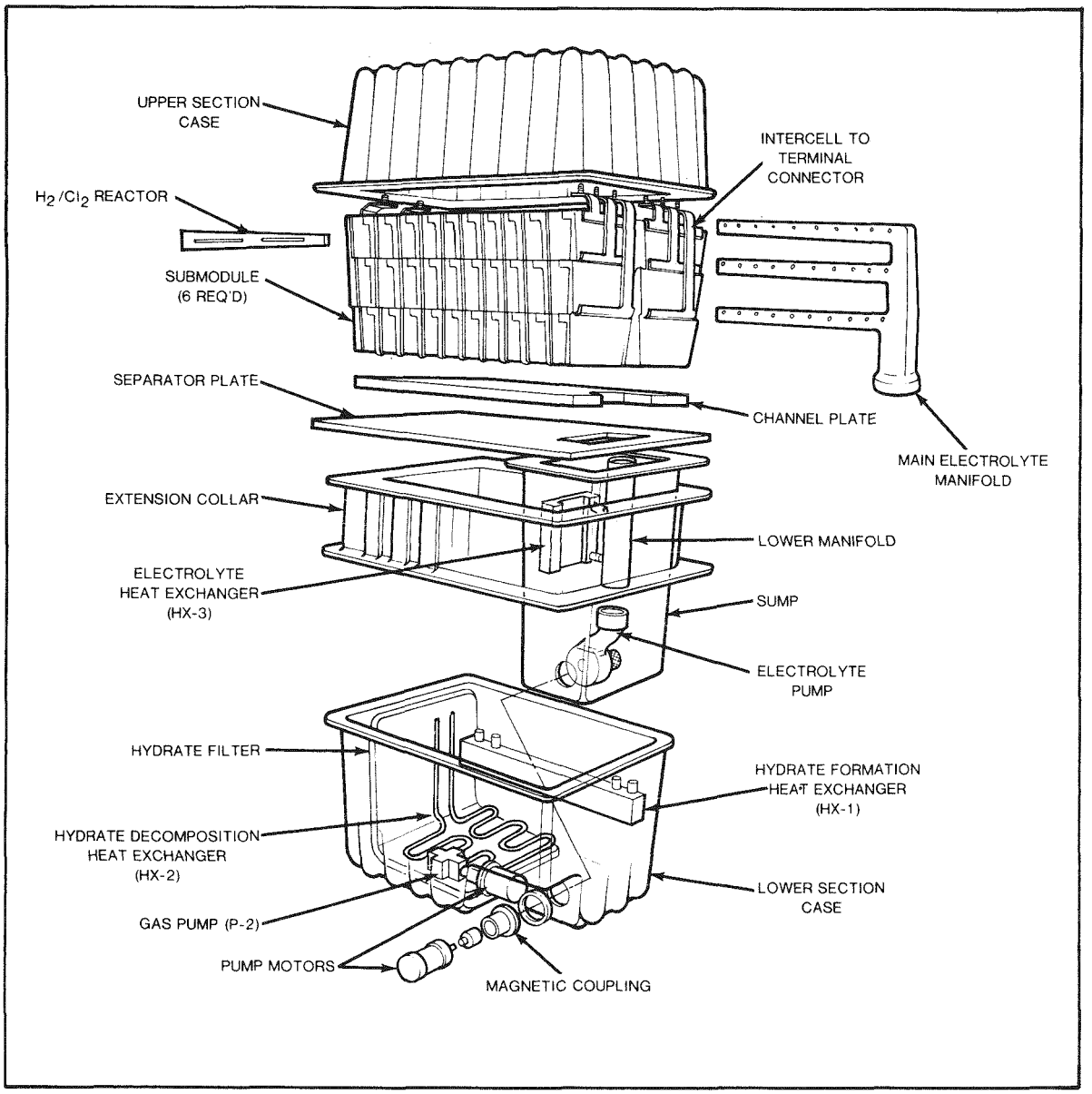

Figure 19-1. 45kWh Battery Module Perspective

decomposition heat exchanger) is located atop the filter. These components are plumbed and the hydrate forming coil and pressure probes are assembled to the gas pump.

- Solenoid valve assemblies are tested for operational functions.

- Solenoid valve assemblies are mounted to the lower-case (hydrate store) access wall, and store piping is completed.
- Intermediate plate is located on the lower-case flange, sealed and clamped.
- The hydrate store area and sump are tested for pressure and leaks.
- Channel plates are located on the intermediate plate.
- Stack assembly is located on channel plates.
- The H_2 reactor, upper main manifold, manifold clamps, manifold cell tubes, intercell connectors, long connectors, and short connectors are assembled into the existing completed assembly.
- The internal module assembly is finalized by fastening all the terminals, sealing the H_2 reactor tube, locating the flange gasket, and resting the upper case assembly onto the intermediate plate.
- Bolt ring is clamped onto the case flange and the holes transferred. Flange bolts are tightened for final pressure-testing of the case.
- Module assembly is tested for operability.

An assembly diagram sheet describing the sequence of operations, the operations, and material flow for the module process is shown in Figure 19-2.

DISCUSSION

The peak-shaving module was first of a kind and as such posed a number of often small but irritating assembly problems. Paramount among these problems was the extensive use of Kynar throughout the battery system. Kynar is a fluoroplastic material that can be vacuum-formed, can be welded, can be solvent bonded, can be injection molded, etc., but all with considerably more difficulty than the more common plastics (some of this difficulty is undoubtedly due to lack of experience with the material). For example, the Kynar vacuum-forms used for the case liner and for the submodule trays generally showed physical defects such as holes, thin sections, and a rough surface finish; the latter making sealing difficult. The vacuum-formed parts also showed differential shrinking effects which made toleranc-ing difficult. The move towards the more common plastics, PVC, polyester, etc. as they become qualified, will alleviate these problems. Other problems such as porosity in the fiberglas-reinforced polyester module case, the location of twelve terminals (for individual submodule monitoring) rather than two terminals through the case, and the basic sealing of a disassemblable system were minor in nature but time-consuming during actual assembly.

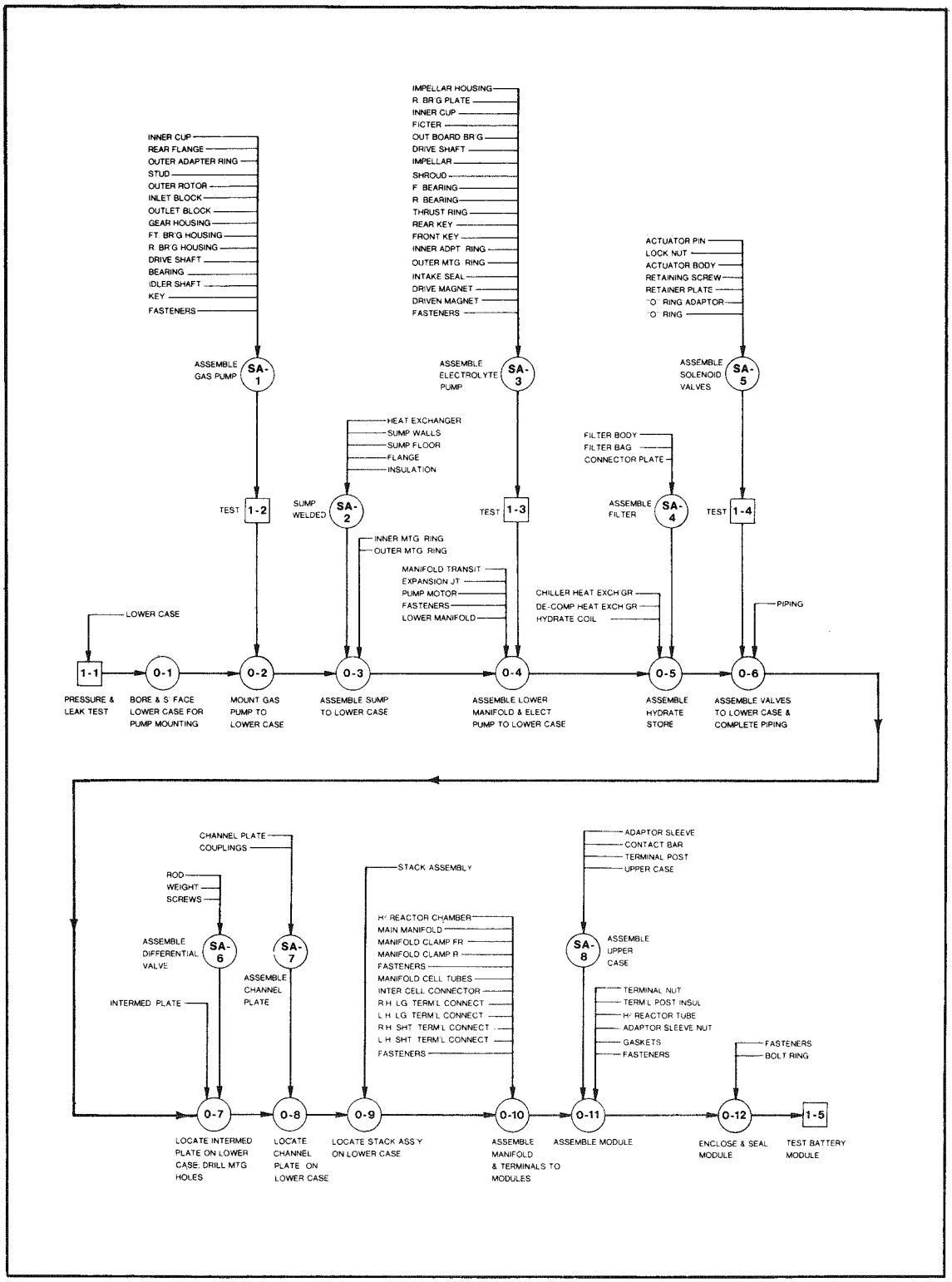

Figure 19-2. Module Assembly Diagram

Section 20

INITIAL TESTING

INTRODUCTION

This section describes the system debugging during the initial testing of the 45kWh battery. Included are details of the system modifications necessary to attain the 45kWh delivered energy for this battery. Discussions of the stack and store performance are also included together with the results of a 10-cycle test performance verification.

SYSTEM DEBUGGING

The first charge of the 45kWh load-leveling module was made on December 5, 1977 (Figure 20-1). This charge was limited to two hours because of rectifier overheating. After repairing the rectifier, six more runs were made in the following two weeks. Generally, the module worked well on these runs, especially from a battery control standpoint. However, some unexpected problems did show up. They were:

- Rate of hydrate formation. The maximum rate of hydrate formation that could be sustained corresponded to a charging current density of 25mA/cm^2 instead of the designed 28mA/cm^2. This indicated a higher heat flux into the hydrate system than anticipated.

- Gas pump blockage. Blockage of the gas pump outlet by chlorine-hydrate occurred during the initial tests. The problem was slightly improved by substituting ∿3% zinc chloride solution for the water in the store. From our past experience, hydrate formed from zinc chloride solutions was less inclined to agglomerate than that formed from water. Removal of discontinuities in the pump outlet was also necessary to prevent hydrate build-up at these sites.

- Mechanical valve blockage. The mechanical relief valve in the battery allows unreacted chlorine gas in the hydrate store to recirculate back to the stack space when the pressure gradient between the stack and the store reaches the design point of 10 psi. However, this valve blocked up with hydrate during the latter stage of the charge when the store was almost filled with hydrate. As a result of this blockage, the store pressure built up and the charge had to be terminated.

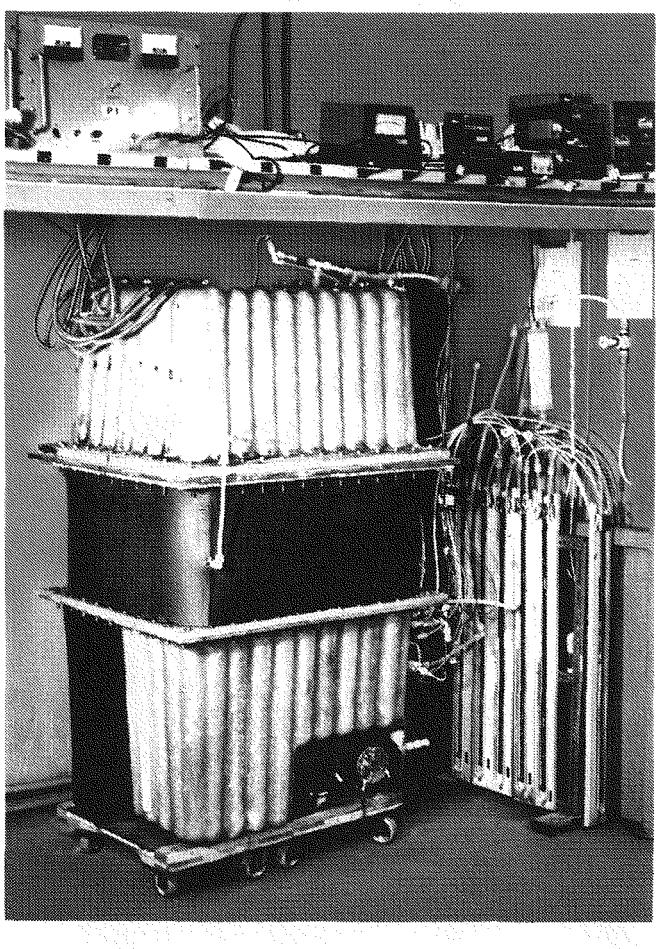

Figure 20-1. The 45kWh Peak-Shaving Module Under Test

- Store fluid transfer. A significant amount of liquid transfer from the store to the stack was observed. Most of the transfer occurred during the early part of discharge when the store was filled with hydrate and the gas was being rapidly evolved. The gas carried over the store liquid into the gas return line leading to the sump. This not only resulted in loss of liquid in the store for the subsequent cycles, but also diluted the electrolyte in the stack.

- Utilization of store liquid. Near the end of charge, when the store is filled with hydrate, the gas pump started gas-locking. This indicated the amount of liquid flow into the inlet of the gas pump was too low. Since the total liquid volume in the store was at the design point, this indicated that a better utilization of the store liquid was required, i.e., to improve the filter arrangement.

- Low vacuum in the stack. One purpose of the gas pump is to maintain the stack pressure at -4 to -5 psi during charge. This serves to reduce the chlorine concentration in the battery electrolyte and thereby decrease the corrosion current and increase the charge coulombic efficiency. During testing, the stack pressure ranged

between -1 to -2 psi rather than the -4 to -5 psi desired. There was also a pressure drop of 1 to 2 psi in the line between the battery stack and the gas pump inlet (including the check valve). It is believed that this pressure drop can be reduced by increasing the line size and replacing the check valve with a valve having a larger valve opening.

- Bus and contact losses. An average of more than 0.6 volts of voltage drop per submodule was observed; this was due to the bus work and a higher than anticipated graphite to terminal contact resistance. As this loss occurs in both charge and discharge, the voltaic efficiency penalty amounts to approximately 6%.

During January and February, work was mainly devoted to disassembly and reassembly of the battery system in order to accomplish the following major modifications:

- Installed 1" thick foam rubber around the lower store case to reduce the heat transfer from the surroundings to the store and, consequently, decrease the heat load to the hydrate chiller.

- Installed partitions along the cavity on the two sides of the sump adjacent to the store wall. This closure stops free circulation of liquid into this cavity and, therefore, reduces heat transfer from these two sides of the sump wall.

- Replaced the small secondary filter with a large "L" shaped filter to improve filtration in the hydrate bed toward the end of charge.

- Installed a filter at the inlet of the mechanical relief valve to prevent the access of hydrate to this valve and subsequent blockage.

- A modified outlet block was installed to provide a smoother transition between the pump housing and the outlet tube coil in the store compartment.

- Relocated the gas return line into the cavity behind the sump wall. This is to avoid the liquid carryover from the store to the stack during the early part of the discharge. Because of the warm sump wall, no hydrate can be stored inside this narrow cavity; thus, this stagnant liquid zone will not be disturbed by the chlorine evolution on discharge.

- Six sets of voltage probes to monitor the bus voltage of each submodule were installed because of the high terminal contact resistance existing in the module. The development of an improved graphite-titanium contact technique, which reduced the voltaic inefficiency from 6% to less than 1%, arrived too late for inclusion in module fabrication.

The implementation of these changes led to a successful run on February 28, 1978, when the module accepted a full charge and delivered 45.2kWh of energy on discharge.

STACK PERFORMANCE

The usable round-trip coulombic efficiency of this 45kWh module was in the low 60%'s instead of the 70% plus of the design target. Therefore, to deliver 45kWh usable energy, a charge current capacity density of 240mAh/cm^2 (charge current density of 30mA/cm^2 for 8 hours) was used instead of the design capacity density of 196mAh/cm^2 (7 hours at 28mA/cm^2). This high coulombic inefficiency was mainly attributed to the corrosion of electroplated zinc with the dissolved chlorine in the electrolyte. Optimizing the electrolyte composition and maintaining higher vacuum in the stack compartment would improve the coulombic efficiency. For the majority of measurements, probe-voltages were used instead of the module terminal voltages due to high contact resistances (∿0.009 ohms) between the submodule bus and the terminal post.

Figure 20-2 shows a typical 8-hour charge and 5-hour discharge profile of this 45kWh module. The average charge probe-voltage is 22.55 voltage (23.3 volts at external terminal) per submodule at 495 amps (30mA/cm^2). The initial electrolyte

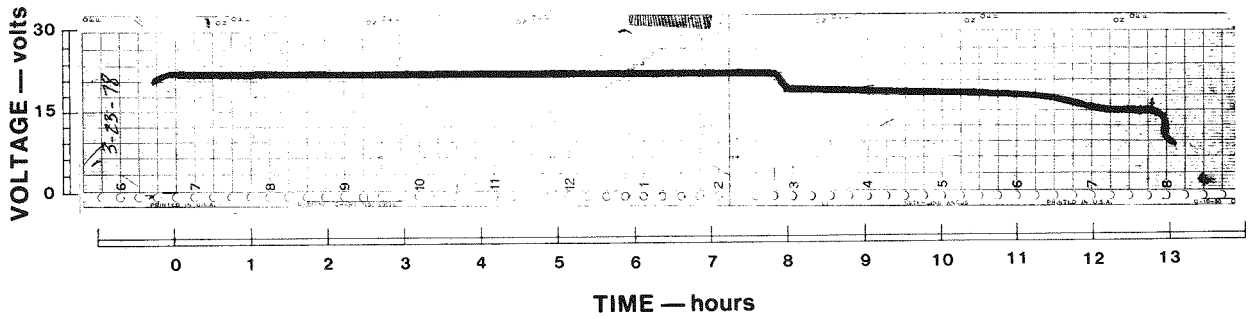

Figure 20-2. A Typical 8-Hour Charge and 5-Hour Discharge of the 45kWh Module

composition was 3M $ZnCl_2$ + 1.25M KCl at pH=0.1 at room temperature. At the end of charge, the zinc chloride concentration was reduced to 0.5M. The stack was operated at -1 to -3 psig rather than the designed -4 to -5 psig. The reason for this "off specification" operation will be discussed in the following subsection on the performance of the hydrate store.

The typical discharge voltage was 18.5 volts at the full discharge current of 540 amps (33mA/cm^2). Discharge was continued at full current until the voltage fell to 16 volts; the amp-hour capacity at this point was termed the full power coulombic. The current was then slowly reduced to hold the module voltage at 16 volts.

When the current had been lowered to 88 amps ($5mA/cm^2$), the amp-hour capacity was again recorded and termed the usable coulombic. The remaining capacity to the complete discharge stage was defined as unusable coulombic. According to the tests, the unusable coulombic was in the range of 7% to 8% of the total coulombic. This number was much higher than the 4% of the design point. Apparently, the degree of cell imbalance was greater than anticipated.

STORE PERFORMANCE

The hydrate storage system operated as designed and was readily controllable in overall operation, in cooldown, charge, turn-around between charge and discharge, and control during discharge. However, several component problems were encountered which will require system modification. These problem areas are described below together with the aspects of operation that were on design. Those aspects of system operation which were on design were:

1. Total storage capacity was sufficient when the store was properly filled to deliver 45kWh of energy. Reduction of liquid level to alleviate a water carryover; from store to stack, as discussed below, reduced the store capacity in the final two runs of the series to approximately 40kWh.

2. General operation during charge -- The cooldown and charge were readily controllable. The store liquid was cooled to approximately 11.5°C with pump P2 operating at 1/2 voltage (20 volts) to circulate gas through the stack hydrogen reactor and liquid through the heat exchanger. Pump voltage was then increased to full voltage for maintenance of vacuum on the heat exchanger HX1 (to prevent hydrate formation) and the system was further cooled to 10.5 to 11°C for start of charge. Control during charge was maintained by controlling coolant inlet temperature at 5.2°C ± 0.2°C with the gas pump operating at approximately 2000 rpm at 42 volts.

3. Turnaround between charge and discharge was controlled by turning off coolant, opening solenoid valve V2 between store and pump P1, and activating the automatic controller for solution to HX2 which operated valve V1 on-off controlling on pressure in the stack gas space. The pump P2 also remained at 1/2 voltage (20 volts) to circulate gas through the battery hydrogen reactor.

4. Discharge -- Proceeded as described under automatic control of valve V1 on stack gas space pressure. Warm battery electrolyte flow through HX1 provided heat to decompose hydrate wherever stack pressure dropped below 1 atmosphere.

The problem areas were:

1. Carryover of water from store to stack at beginning of discharge. This apparently occurred because the location of the gas outlet from store to stack through V2, which was behind the sump and two inches below the top, allowed substantial entrained liquid to be carried into the open line. Displacement and lifting of the liquid from the hydrate mass by gas evolved around HX2 at the bottom of the store may also have contributed by forcing liquid into close proximity to the outlet.

   It is believed that this problem can be resolved by establishing a 1-inch liquid separation zone above the filter located at the top of the store and locating the outlet in the separator plate.

2. Plugging of the gas pump P2 at the outlet due to buildup of hydrate on the discontinuities in the outlet block or connection between outlet block and outlet tubing (line 6) occurred occasionally during the runs. This occurrence was marked by an increase in pump current from 9 amps to 20 amps. To solve this problem, a careful redesign of the outlet block to insure no discontinuities in the outlet zone will be necessary.

3. Capacity of the Gas Pump -- The desired suction pressure of -5 psig in the stack compartment was not achieved during the course of testing. Pressures ranged from -1 to -3 psig. This occurred because the actual gas pumping was the sum from three principal sources: 1) the gas electrochemically generated in the stack amounting to approximately 28 standard liters per minute, 2) gas drawn out of solution from the recirculating liquid stream, amounting to 7 to 9 standard liters per minute, and 3) gas liberated by hydrate decomposition along the warm walls of the sump or in the vicinity of other warm components within the store, which passed to the top of the store and was vented back to the battery gas space through valve V3. This rate was estimated from heat transfer considerations to be approximately 4 standard liters per minute. The total gas pumping requirement from these three sources was approximately 40 standard liters per minute. Previous testing of P2 had indicated that the total displacement was approximately 60 liters per minute with 10 to 11 liters per minute allotted for the liquid flow. The remaining displacement of 49 to 50 liters per minute was available for gas flow. The expansion of the 40 liters per minute of gas under reduced pressure to the 49 to 50 liters per minute of available displacement would result in a calculated inlet pump pressure of -2.8 psig.

4. Relief valve malfunction -- The gas relief valve V3 malfunctioned in the closed position, assumed to be due to "sticking" during the latter phases of the testing. An improved valve is available for installation in future systems.

10 CYCLE TEST

A series of ten cycles to complete the initial qualification of the 45kWh battery was started on March 6, 1978. The tests were conducted on the basis of one cycle per day, the cycle consisting of an 8-hour charge, a 5-hour discharge, and, finally, a cleanup period. The conditions which were used for the tests are shown in the following table.

Table 20-1

10 CYCLE TEST CONDITIONS FOR 45kWh MODULE

	Charge	Discharge
Current Density (mA/cm^2)	30	33
Temperature (°C)	30	30 to 40
Electrolyte Flow Rate (cm^3/cm^2-min)	2	2
Stack Pressure (cm Hg)	-13	0

The charge time was 8 hours instead of the 7-hour charge because of the lower coulombic efficiency discussed previously. All the discharges were made at 33mA/cm^2 to 1.6 volts per cell as full power coulombic efficiency and then at 16 volts/cell to 5mA/cm^2 as usable coulombic efficiency. After obtaining the usable coulombic efficiency, the battery was self-discharged by circulating the chlorinated electrolyte overnight to clean up the stack before the next cycle test. Data from the ten cycle tests are summarized in Table 20-2. A plot of the delivered energy vs. the cycle number is shown in Figure 20-3. The average delivered energy was 43kWh, the average usable coulombic efficiency was 59%, and the average voltaic efficiency was 82.5%. The overall electrochemical energy efficiency was 48.7% for the ten runs.

This 45kWh battery system exhibited very good operational characteristics during the cycle tests and required very little attention during each cycle. Control on charge was maintained by simply controlling the glycol inlet temperature at 5.2 ± 0.2°C, while stack pressure was used as the control parameter for automatic discharge control.

Table 20-2

DATA FOR 10 CYCLE TEST OF 45kWh MODULE

RUN #	1	2	3	4	5	6	7	8	9	10
DATE	3/6	3/7	3/8	3/13	3/15	3/16	3/17	3/20	3/21	3/23
CURRENT DENSITY (mA/cm^2)										
Charge	30	30	30	30	30	30	30	30	30	30
Discharge	31	33	33	33	33	33	33	33	33	33
STARTING CONDITIONS										
Specific Gravity	1.350	1.352	1.360	1.330	1.327	1.325	1.325	1.325	1.350	1.340
pH	.13	.07	0	.07	.13	.10	0	.08	0	.08
Cl_2 CONCENTRATION										
Charge	2.40	2.49	2.27	2.87	2.66	2.72	3.03	3.19	2.89	3.18
Discharge	2.08	1.75	1.62	1.97	1.68	1.78	1.64	1.77	1.63	1.65
TEMPERATURE (^oC)										
Charge	27.6	28	30	29	29.4	27.	25.7	25.2	22	22
Discharge	22.4	31.9	37.5	32.4	35.7	32.5	34.6	30.2	30.7	31.7
H_2 CONCENTRATION PEAK (%)										
Charge	.70	.70	.45	.38	.50	.27	.30	.20	1.09	.22
Discharge	.30	.55	.98	.75	1.35	1.05	1.20	.60	.70	.75
CAPACITY (Amp hr)										
Charge	3940	3930	3940	3960	3960	3960	3960	3960	3960	4000
Full Power Discharge	2208	1992	1960	2244	2160	2160	2111	2160	2160	2224
Useable Discharge	2358	2186	2293	2396	2332	2315	2300	2319	2312	2430
COULOMBIC EFFICIENCY (%)										
Full Power	56.04	50.69	49.75	56.67	54.55	54.55	53.31	55.55	53.03	55.60
Useable	59.85	55.62	58.20	60.51	58.89	58.46	58.08	58.57	58.38	60.75
MODULE VOLTAGE (volts)										
Charge	22.5	22.5	22.5	22.5	22.5	22.5	22.5	22.5	22.6	22.6
Discharge	17.91	18.33	18.36	18.85	18.78	18.82	18.72	18.71	18.59	18.62
VOLTAIC EFFICIENCY (%)	79.6	81.46	81.58	83.80	83.45	83.61	83.19	83.15	82.25	82.38
USEABLE ENERGY DELIVERED (kWh)	42.24	40.62	42.09	45.18	43.79	43.55	43.05	43.39	42.98	45.24
ENERGY INPUT (kWh)	88.65	88.42	88.65	89.10	89.10	89.10	89.10	89.10	89.50	90.40
USEABLE ENERGY EFFICIENCY (%)	47.65	45.31	47.48	50.71	49.15	48.88	48.32	48.70	48.02	50.04

The problem of the liquid carried over from the store compartment to the stack compartment during the early part of the discharge was evidenced on all runs where the store was filled to its designed liquid capacity at the start of the run. As a result of this liquid transfer, adjustment of the zinc chloride concentration in the stack and the addition of more dilute zinc chloride to the store was necessary at the start of each cycle. A minor problem was also encountered with the mechanical relief valve; the valve had a tendency to stick in the closed position.

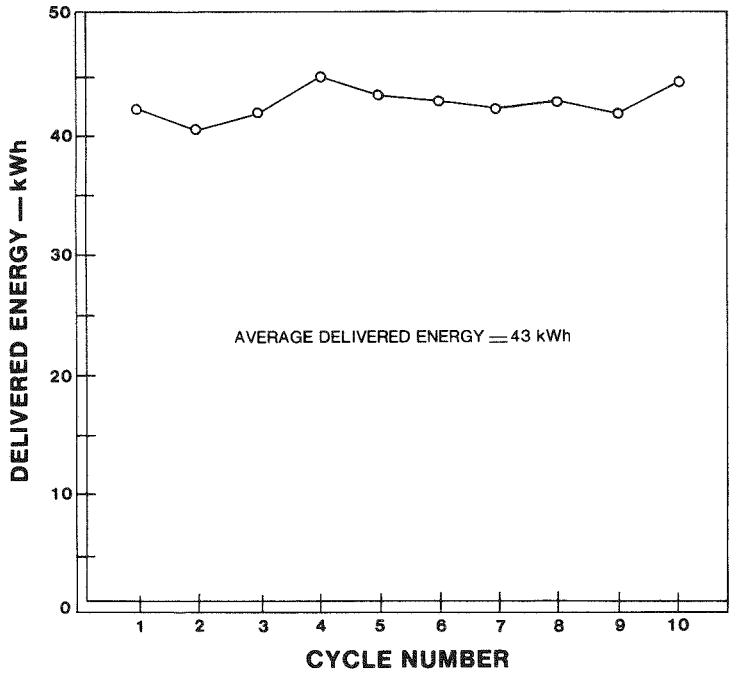

Figure 20-3. Delivered energy for the 10-cycle test of the 45kWh peak-shaving module.

The average 59% usable coulombic was substantially lower than the design goal of 73%. Part of this inefficiency was due to the stack operating under higher pressure than anticipated. Instead of a vacuum of -5 psig, the stack was charged at -1 to -3 psig. A vacuum in the stack compartment reduces the dissolved chlorine concentration in the solution and thus decreases the corrosion current. Submodule testing had shown low capacity and high cell-to-cell variability with heavily salted electrolytes which would lead to higher efficiency. Improvement of the coulombic efficiency will be achieved once the formulation of the electrolyte is optimized.

Probe voltages rather than terminal voltages were used in this report. This was due to the high contact resistance between the graphite bus and the titanium current collector. A reduction of almost 6% in the voltaic efficiency was calculated if the contact resistances wre included. As mentioned in the previous section, an improved contact technique has been developed and has shown a reduction in the terminal voltaic inefficiency to less than 1%.

In addition to the voltaic penalty due to the high graphite to titanium contact resistance, variations in contact resistance between submodules created an im-

balance of the current flow through each submodule when the submodules were connected in parallel. One of the six submodules in the 45kWh battery showed a 10% lower than average current because of this effect. Instead of a normal charging current of 82.5 amps, this submodule capacity was lower on this submodule than the average and, since each submodule has approximately the same capacity loss due to corrosion currents, this submodule also showed a lower amp-hour efficiency.

Section 21

DISCUSSION OF PART III

An integrated battery module, complete with hydrate-formation and storage capabilities, was chosen in early 1977 as the basic concept for the Mark 4 design under the EPRI-EDA zinc-chlorine battery program. A one-year development program to design, assemble, and test the prototype module for this conceptual design was completed in March, 1978.

The design goal for delivered energy, 45kWh, was achieved. The battery system exhibited good operational characteristics and required little attention during the operation. This module also gave satisfactory performance repeatability as demonstrated by testing over ten consecutive charge-discharge cycles. However, two major problem areas did exist in this module -- firstly, the excessive voltage losses due to the high contact resistance between the graphite bus and the titanium current collector; and secondly, the substantially lower coulombic efficiency.

The high contact resistance between the graphite bus and the titanium current collector introduced a reduction of voltaic efficiency of almost 6%. In addition to this reduction of voltaic performance, the variation in contact resistance between submodules created an imbalance of current flow through each submodule when the submodules were connected in parallel.

An average of 59% usable coulombic efficiency was substantially lower than the design goal of 73%. The low coulombic efficiency was mainly due to the battery stack operating under less vacuum than the design conditions of -5 psig. The lower stack pressure serves to reduce the concentration of chlorine dissolved in the electrolyte, decreases the corrosion of electroplated zinc by dissolved chlorine, and thereby raises the coulombic efficiency.

To improve module performance and to upgrade the delivered energy to 50kWh, a refurbishing program will be initiated during Phase II of the EPRI-EDA Program. This refurbishing will involve improving the graphite-titanium contacts, achieving the design level of vacuum in the stack compartment, increasing the hydrate density

in the store compartment, and minimizing the heat transfer from the warm sump to the cold store.

The stack operated under less vacuum than anticipated due to the limited pumping capacity of the present gas pump. The present gas pump may be adequate in size if the hydraulic system can be adjusted to prevent an extra nine liters of chlorine gas recirculating into the gas pump besides the gas generated from the stack compartment. This nine liters of gas is drawn from the chlorine-saturated liquid stream in the store compartment as the liquid pressure changes from the positive store pressure to the suction pressure of the gas pump. An alternative solution may involve the use of a larger gas pump.

The store section will be designed to have a hydrate-storage capacity of at least 54kg of chlorine. This hydrate-storage capability would allow the delivered energy to be increased to 60kWh if the performance of the battery stack were further upgraded. A filter of greater area will be incorporated into the store design to ensure the adequate liquid flow rate for hydrate formation. The sump will be located above the store compartment so that a layer of gas provides very good insulation between the warm sump and the cold store. Also, this rearrangement prevents the possibility of liquid being carried over from the store to the stack compartment even at the beginning of discharge when the store is full. This store section can be pre-checked for performance before system assembly.

To increase the voltaic performance, an improved method for making electrical connections has been developed and has shown a reduction of the terminal voltaic inefficiency to less than 1% instead of the existing inefficiency of 6%. This technique will be applied in the refurbishing of the 45kWh module.

With this refurbishment, the module is expected to deliver 50kWh at an electrochemical energy efficiency of 65%. It is important to note that no further scale-up of this module will be required. Further increases in delivered energy will be realized only by improvement of the voltaic and coulombic efficiencies.